Synthesis, Characterization, and Reactivity Studies of Pyridine Bis(anilide) Iron Complexes

Thesis by
Edward Charles Weintrob

In Partial Fulfillment of the Requirements for the
Degree of Doctor of Philosophy

California Institute of Technology
Pasadena, California
2012

(Defended July 28, 2011)

Acknowledgements

Looking back on my time at Caltech, there were many ups and downs. Helping me through it all were some very special people, and they deserve to be acknowledged. First and foremost, John Bercaw has been a wonderful mentor to me. I have learned quite a lot from you, and I enjoyed our many discussions about my science. I always appreciated your laid-back attitude and enthusiasm for research. Jay Labinger, it seems whenever we speak, you come up with some suggestion for me that completely changes the way I think about a problem. Your keen insights have been extraordinarily helpful over the years. I would also like to thank my other committee members, Bob Grubbs, Brian Stoltz, and Jonas Peters for their helpful comments.

A variety of Caltech staff have been important to the work herein. Larry Henling and Mike Day did all of the crystallography for my complexes. I'm quite indebted to their persistence, despite the many failed attempts we had to make for every successful one. Larry, I always enjoyed our talks during down time. Thanks also to Jens Kaiser for his help with getting diffraction data at the synchrotron source. Rick Gerhart has made for me ridiculous amounts of custom glassware that was necessary for work on the high vac. line. Thanks Rick. No matter how complicated and/or convoluted the sketch, you were always up for the challenge. I am indebted to David VanderVelde and Scott Ross for their tremendous help with NMR experiments, and for generally being willing to chat about NMR. I'm happy I got the opportunity to work with you as a GLA all these years. David,

you've been such an asset to the NMR facility, and I know it will continue to grow and improve under your guidance.

I was very fortunate to work in a group containing so many interesting and talented people. Theo Agapie and Dan Tofan started the NNN project. I ended up writing my thesis using the ligand, so thanks! Theo and Paul Elowe also deserve my gratitude for training me to use the high vac. line. Thanks also to Steve Baldwin for help in that vein. Travis Williams was my first baymate in Bercaw group. He has one of the best senses of humor of anyone I've ever met, and I still miss his quirkiness. Good luck at USC, Travis! Aaron Wilson trained me to do electrochemistry, and we've had many a good conversation. George Chen had a desk near me, and I always appreciated his interest in diverse areas of science. Thanks for teaching me about biology and economics, and for your enthusiasm for science. Your optimism was nice to have when the results weren't coming. Bolin Lin, it was great getting to know you. It was nice talking chemistry with you, and learning about China from you. We were all surprised when you came back from vacation married. Good luck to you and Lu. Alex Miller, you were a great leader in the group in many ways, and we all gained from having you around. Thanks for organizing the basketball team; it was a lot of fun. Good luck to you and Jill at UNC. Yan-Choi Lam, I have enjoyed our conversations about history and politics; good luck on the new project. David Weinberg, what a joy to have you in the group. I think you contributed to a jovial, social and friendly atmosphere as much as any have in the group. You are a man of many interests and talents, and were always fun to have a conversation with. I still fondly look

back at playing poker and going to parties at your place. There are too many people to thank without rambling on too long: Rachel Klet, Emmanuelle Despagnet-Ayoub, Amaruka Hazari, Nilay Hazari, Ned West, Melanie Zimmermann, Koyel Bhattacharyya, Carl Laskowski, Jeff Byers, Alexandra Velian, Josef Meier and Valerie Scott. Thanks to you all, and the best of luck to you in the future.

Certain people have had a particular impact on life, personally and professionally, and thus deserve special mention. Paul Oblad, we both started out in the Peters group, and we've had a somewhat similar experience here at Caltech. It was nice to have another Bercaw group member as a fellow GLA. We were baymates for awhile, and we sat next to each other in the office for pretty much all five years. As a result of my spot next to you in the office, I have benefited from a lot of good advice over the years. You've been a valuable colleague and a wonderful friend. I still smile when I think of our video game breaks in first year. All of the happiness in the world to you, Stephanie, and Liam.

Ian Tonks, we've been through quite a lot together. Not only did we go to Columbia together, we even worked in Parkin group together! And then we ended up in the same group again at Caltech. I have been very lucky to have you as a labmate and friend. I have learned quite a lot from our many discussions, and your enthusiasm for research often motivated me to run into lab to try some new idea we had just talked about. It was a nice break playing softball, so thanks for organizing the team. I'm quite confident that you will succeed in whatever you endeavor. Best of luck to you!

Matt Winston, you joined us from the Stoltz group, and their loss was our gain. Your knowledge of organic transformations was a huge boon to me personally, and to the group as a whole. You got me started seriously working out, and were a good workout buddy. "Mattflix" has kept me entertained many a time, and you've introduced me to some of my favorite movies and tv shows; my favorite, Battlestar Galactica, deserves special mention. I've loved our talks about gaming, movies, music, chemistry, and pretty much anything I can think of. You've been a good friend, and I've always been able to count on you when the going got tough. Good luck in the MacMillan group!

Taylor Lenton, you were a great addition to the group, and our last metallocene chemist. You've been a great baymate, blue box mate, and high vac. line mate; I hope I was able to teach you a thing or two along the way. I can leave Caltech happy knowing that HgBI will be in good hands. Since you joined the group, we've had lunch most days and I always found that time as a great way to relax from the stress of chemistry. Good luck in your science; I'm sure you'll go far.

There are also a number of non-Bercaw group people that deserve special mention. Greg Kimball, we were both in Columbia chemistry together, but we didn't know each other too well. Luckily, we ended up on the same floor of Noyes and I got a second chance. You have the unique gift of always having something interesting to say. Your curiosity and enthusiasm for life are a joy to experience. Thanks to you and Pia for all of the good food over the years. Thanks also to Pia for the good fashion advice. Good luck to you both! Young-In Oh was always a

source of good conversation. Thanks also for throwing me a Karaoke party for my birthday and taking me shopping for work clothing. Chris Gilmore and Pam Tadross were excellent bowling buddies and were always fun to have a drink with. Congrats on the engagement! Justin Chartron was a great lunch buddy, and I was happy I got a chance to learn a little about biology and crystallography. I think you are the hardest worker at Caltech, and I'm sure that such a work ethic will take you far.

There a number of people who contributed to my early scientific training. Paul Cohen was my high school chemistry teacher, and it was he who first introduced me to chemistry and sparked my interest in science. Without you, I wouldn't be here. Robert Fine gave me my first experience in a research lab working with Tammy Do in oncology. Thanks for a great opportunity to try my hands at real research for the first time.

Mikhail "Misha" Barybin deserves more praise than is possible in this acknowledgements section. I worked in his lab in the University of Kansas over a summer on an REU program. It was in his lab that I was first exposed to organometallic chemistry, and I've been hooked ever since. Misha, you were always there for me, and I am forever indebted to you. Thank you. In Misha's lab, I worked with both Randy Robinson and Tom Holovics, who were both great and patient mentors to me.

I worked in Ged Parkin's group at Columbia for almost two years, and it was a great way to build on the skills I had acquired in Misha's group. Thanks Ged. I

worked closely with Bryte Kelly and Josh Figueroa in Ged's group. Thanks to both of you for your patience and advise.

Finally, I would like to thank members of my family. First, my older sister Liz has always been a wonderful source of wisdom, and I continue to benefit from her advice. Thanks for being "good at life" and passing on some of that to your younger brother. I certainly would not be in this PhD program at all without my parents, Neil and Susan. My father has always encouraged me to try my hardest at what I do, and I believe that notion influenced my decision to embark on a simultaneously difficult and rewarding career path. My mother home-schooled me until 8th grade, so I am indebted to her for so much that to make a comprehensive list is precluded in the given space. Suffice it to say, however, that she imbued me with the ability and confidence that I could learn to do anything to which I set my mind. Thanks also go to my grandmother Rita Haber and my late grandfather Karl Haber.

Abstract

The unifying concept within this thesis is the investigation of pyridine bis(anilide) (NNN) iron complexes. Within this topic, chapter 1 speaks to the motivation behind studying these complexes, and how they relate to problems within iron catalysis in general. Chapter 2 introduces the general ligand design and the features which are thought to give unique and desirable properties to the complexes derived from it. The mesityl susbstituted ligand [^{Mes}NNN]H_2 and subsequently ferrous ([^{Mes}NNN]Fe(THF)) and ferric ([^{Mes}NNN]FeI and ([^{Mes}NNN]Fe)$_2$O) complexes are synthesized. The properties of the complexes are investigated using a variety of characterization techniques. Such techniques include paramagnetic ^{1}H NMR spectroscopy, X-ray crystallography, Evans method, cyclic voltammetry, DFT calculations, and UV-vis spectrscopy. A detailed explanation of the challenges and solutions involved in using paramagnetic NMR are discussed. Crystallographic data indicate that the ligand framework confers a quite unusual geometry about the iron center, especially for the ferrous derivative [^{Mes}NNN]Fe(THF). The factors involved in this geometry are discussed, and DFT calculations supplement this discussion. Chapter 3 focuses on the reactivity of the iron complexes. Various oxidants and reductants were employed which interconvert the iron derivatives in chapter 2. Organometallic derivatives [^{Mes}NNN]FeR (R = hydride, alkyl, aryl) were not accessible, likely due to homolytic processes. L ligand exchange for [^{Mes}NNN]Fe(THF) was investigated. Ethylene reversibly binds, while cyclohexene does not. Trimethylphosphonium methylidene displaces THF to generate [^{Mes}NNN]FeCH_2PMe_3. Although the I oxidation state was accessible for [^{Mes}NNN]Fe(THF) electrochemically, attempts to chemically produce Fe^I complexes based on the NNN led to multiple products. Chapter 4 focuses on the intramolecular C-H activation of [^{Mes}NNN]Fe(THF) with RN_3 to afford [^{Mes}NNN-NHR]Fe (R = $SiMe_3$, adamantyl). The kinetics of the reaction with Me_3SiN_3 was

investigated in detail, and a mechanism was proposed. Iron complexes based on the pincer ligands [^{tBu}NNN] and [ONO] were investigated.

Table of Contents

List of Figures

Chapter 2

Chapter 3

Chapter 4

Appendix A

List of Tables

Chapter 1
General Introduction

The text in this chapter was taken in part from
Weintrob, E. C.; Tofan, D.; Bercaw, J. E. *Inorg. Chem.* **2009**, *48*, 3808–3813.

Noble metals have been dominant in many areas of catalytic organic transformations: a fact that may be partially due to their readily accessible two electron redox couples, as well as their oxygen, water, and functional group tolerance.[1] These abilities are counterbalanced, however, by those same metals' cost, and in some cases by environmental or toxicological considerations. By comparison, iron is cheap, relatively nontoxic and environmentally benign.[2] For these reasons, this decade has seen an emergence of research in areas not historically associated with iron,[3–6] including hydrogenation,[7–13] hydrosilation,[8]

(1) Fürstner, A.; Majima, K.; Martin, R.; Krause, H.; Kattnig, E.; Goddard, R.; Lehmann, C. W. *J. Am. Chem. Soc.* **2008**, *130*, 1992–2004.

(2) Enthaler, S.; Junge, K.; Beller, M. *Angew. Chem. Int. Ed.* **2008**, *47*, 3317–3321.

(3) Bolm, C.; Legros, J.; Le Paih, J.; Zani, L. *Chem Rev*, **2004**, *104*, 6217–6254.

(4) Correa, A.; Mancheño, O.; Bolm, C. *Chem. Soc. Rev.* **2008**, *37*, 1108–1117.

(5) Buschhorn, D.; Pink, M.; Fan, H.; Caulton, K. G. *Inorg. Chem.* **2008**, *47*, 5129–5135.

(6) Fryzuk, M. D.; Leznoff, D. B.; Ma, E. S. F.; Rettig, S. J.; Young Jr., V. G. *Organometallics* **1998**, *17*, 2313–2323.

(7) Daida, E. J.; Peters, J. C. *Inorg. Chem.* **2004**, *43*, 7474–7485.

(8) Bart, S. C.; Lobkovsky, E.; Chirik, P. J. *J. Am. Chem. Soc.* **2004**, *126*, 13794–13807.

(9) Trovitch, R. J.; Lobkovsky, E.; Chirik, P. J. *Inorg. Chem.* **2006**, *45*, 7252–7260.

(10) Bart, S. C.; Hawrelak, E. J.; Lobkovsky, E.; Chirik, P. J. *Organometallics* **2005**, *24,* 5518–5527.

(11) Enthaler, S.; Hagemann, B.; Erre, G.; Junge, K.; Beller, M. *Chem. Asian. J.* **2006**, *1*, 598–604.

(12) Casey, C. P.; Guan, H. *J. Am. Chem. Soc.* **2007**, *129*, 5816–5817.

(13) Mikhailine, A.; Lough, A. J.; Morris, R. H. *J. Am. Chem. Soc.* **2009**, *131*, 1394–1395.

hydrodefluorination,[14] and cross-coupling (Scheme 1.1).[15–17] Additionally, the well-studied area of oxidation chemistry with iron complexes has made great strides in mechanistic understanding, substrate scope, chemo-, regio-, and enantioselectivity, and pertinence to industrial applications.[18–22]

One issue that has been the object of much study is the accessibility of two-electron chemistry for iron complexes, in order to mimic much of the chemistry available to late metals. In particular, oxidative addition and reductive elimination are vital steps in many catalytic cycles. Additionally, group transfer sometimes exploits two-electron redox cycles. The two classical oxidation states for iron complexes are II and III, thus enabling a variety of radical-based reactions but not two-electron reactivity. One strategy to circumvent this problem is the use of redox active ligands, such as the pyridine diimine (PDI) iron complexes employed by

---

(14) Vela, J.; Smith, J. M.; Yu, Y.; Ketterer, N. A.; Flaschenriem, C. J.; Lachicotte, R. J.; Holland, P. L. *J. Am. Chem. Soc.* **2005**, *127*, 7857–7870.

(15) Fürstner, A.; Martin, R. *Chem. Lett.* **2005**, *34*, 624–629.

(16) Fürstner, A.; Martin, R.; Krause, H.; Seidel, G.; Goddard, R.; Lehmann, C. W. *J. Am. Chem. Soc.* **2008**, *130*, 8773–8787.

(17) Czaplik, W. M.; Mayer, M.; von Wangelin, A. J. *Angew. Chem. Int. Ed.*, **2009**, *48*, 607–610.

(18) White, M. C.; Doyle, A. G.; Jacobsen, E. N. *J. Am. Chem. Soc*. **2001**, *123*, 7194–7195.

(19) Chen, J.; Woo, L. K. *J. Organomet. Chem.* **2000**, *601*, 57–68.

(20) Chen, M. S.; White, M. C. *Science* **2007**, *318*, 783–787.

(21) Suzuki, K.; Oldenburg, P. D. and Que Jr., L. *Angew. Chem. Int. Ed.* **2008**, *47*, 1887–1889.

(22) Gedalcha, F. G.; Bitterlich, B.; Anilkumar, G.; Tse, M. K.; Beller, M. *Angew. Chem. Int. Ed.* **2007**, *46*, 7293–7296.

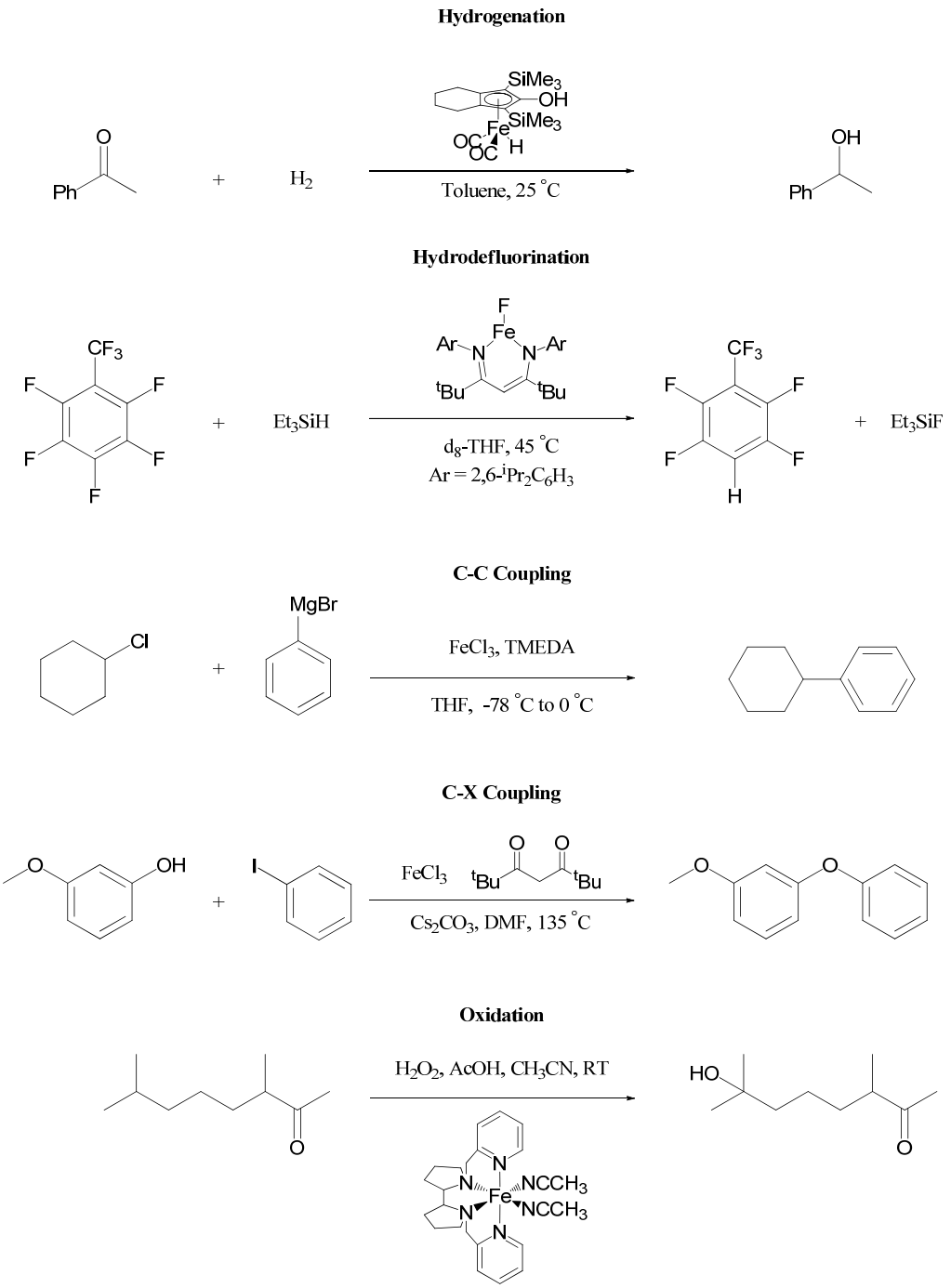

Scheme 1.1. Examples of the increased versatility of modern iron catalysis: Hydrogenation,[12] hydrodefluorination,[14] C-C coupling,[23] C-X coupling,[24] and oxidation.[20]

(23) Nakamura, M.; Matsuo, K.; Ito, S.; Nakamura, E. *J. Am. Chem. Soc.* **2004**, *126*, 3686–3687.

(24) Bistri, O.; Correa, A.; Bolm, C. *Angew. Chem. Int. Ed.* **2008**, *47*, 586–588.

Chirik (Scheme 1.2).[25] Chirik has shown that PDI iron systems mediate a variety of two-electron processes via oxidative addition/reductive elimination pathways. For instance, PDI iron complexes catalyze the hydrogenation of a variety of alkenes.8

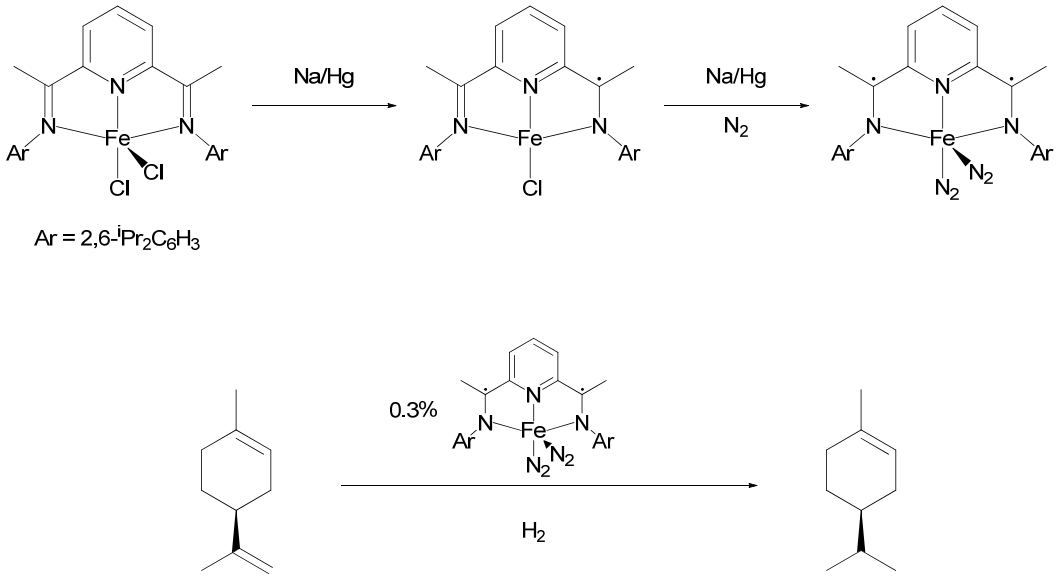

Scheme 1.2. Storing of reducing equivalents on the PDI ligand framework (top). Alkene hydrogenation catalyzed by [PDI]Fe(N_2)$_2$.

Use of tailored ligand architectures has enabled the accessibility of low and high oxidation states of iron. Peters has employed tris(phosphine) ligands to access a wide range of iron redox states. For example, he has demonstrated catalytic hydrogenation via a likely Fe^{II}/Fe^{IV} couple.7 Che has employed a likely Fe^{III}/Fe^{V}

(25) Bart, S. C.; Chłopek, K.; Bill, E.; Bouwkamp, M. W.; Lobkovsky, E.; Neese, F.; Wieghardt, K.; Chirik, P. J. *J. Am. Chem. Soc.* **2006**, *128,* 13901–13912.

couple for the catalytic aziridination of olefins with organic azides.[26] Finally, Fürstner demonstrated that enyne cyclization may be mediated by a formally Fe^{I} complex.1

The following chapter discusses the features of a pyridine bis(anilide) ligand scaffold. It was hypothesized that the highly electron-rich, π-donating ligand may support highly oxidized iron centers, and thus facilitate unique and valuable transformations.

(26) Liu, Y.; Che, C.-M. *Chem. Eur. J.* **2010**, *16*, 10494–10501.

Chapter 2
Synthesis, Characterization, and Computational Studies of Iron Derivatives Having a Pyridine-Linked Bis(anilide) Pincer Ligand

The text in this chapter was taken in part from:
Weintrob, E. C.; Tofan, D.; Bercaw, J. E. *Inorg. Chem.* **2009**, *48*, 3808–3813.

All computational work performed by:
Dr. Robert Smith Nielsen, Goddard Group, California Institute of Technology

Introduction

The new ligand investigated herein, [^{Mes}NNN]H_2 ([^{Mes}NNN]H_2 = (2,6-NC_5H_3(2-(2,4,6-$Me_3C_6H_2$)-NHC_6H_4)$_2$) possesses two features that may engender unique properties upon complexation with iron. First, the ligand forms two *six*-membered chelate rings with the metal center. This ring size is less common than the five-membered rings found in many iron chelates. Second, the deprotonated ligand [^{Mes}NNN]$^{2-}$ is dianionic, unlike the neutral or monoanionic ligands more common to iron chemistry. The relative rarity of the two aforementioned motifs is surprising in light of the rich and diverse chemistry available to iron porphyrins (Figure 2.1),[27] which are dianionic and form six-membered rings upon chelation. One important difference between [^{Mes}NNN]

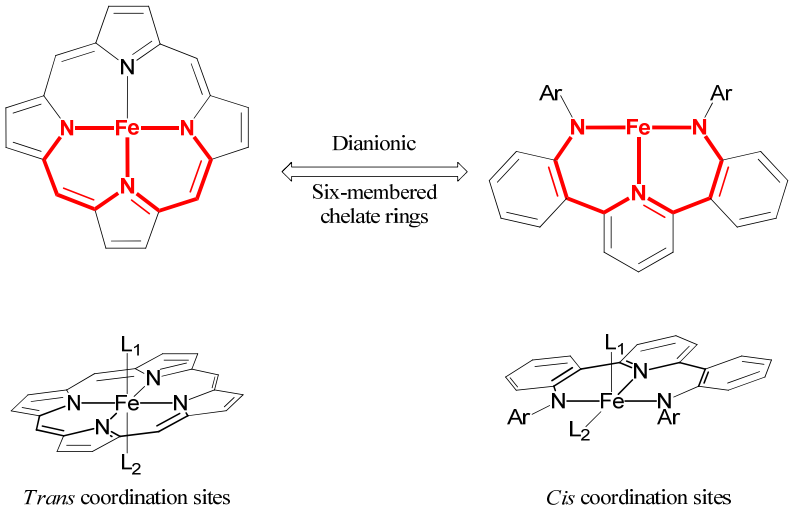

Figure 2.1. Some similarities (top) and differences (bottom) between iron porphyrins and the iron pincer complexes herein.

(27) Simonneaux, G.; Tagliatesta, P. *J. Porphyrins Phthalocyanines* **2004**, *8*, 1166–1171.

and porphyrin complexes, however, is the potential for *cis*-coordination sites at iron for the former. We report herein a chelating pyridine-linked bis(aniline) ligand and iron complexes derived therefrom.

Results and Discussion

The original synthesis of the ligand precursor **1** was accomplished via *in situ* borylation of 2-bromoaniline, followed by a two fold Suzuki coupling with 2,6-dibromopyridine. It was found, however, that use of the *preformed* borylated precursor (commercially available) led to approximate doubling of the yield of **1** (35% vs. 69%), and significantly simplified purification. The arylation of **1** with an excess of mesityl bromide was accomplished with Buchwald-Hartwig coupling,

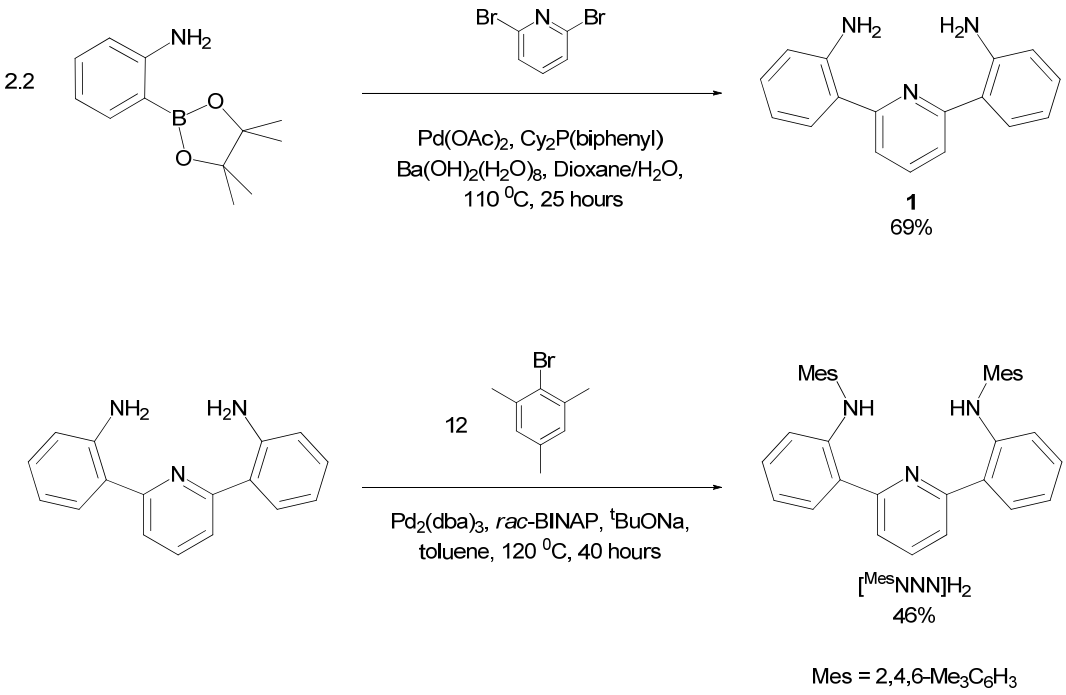

Scheme 2.1. Synthesis of $[^{Mes}NNN]H_2$.

yielding the ligand [^{Mes}NNN]H_2 (Scheme 2.1). X-ray quality crystals of the ligand were obtained by slow evaporation of a diethyl ether solution (see appendix C). Attempts to employ [^{Mes}NNN]H_2 as an L_3 ligand with either $FeCl_2$ or $FeCl_3$ did not lead to any reaction. Thus, [^{Mes}NNN]H_2 was deprotonated with two equivalents of trimethylsilylmethyllithium in toluene, giving the dilithium salt [^{Mes}NNN]Li_2 as a bright yellow solid (Scheme 2.2). Use of the weaker base $LiNMe_2$ led to

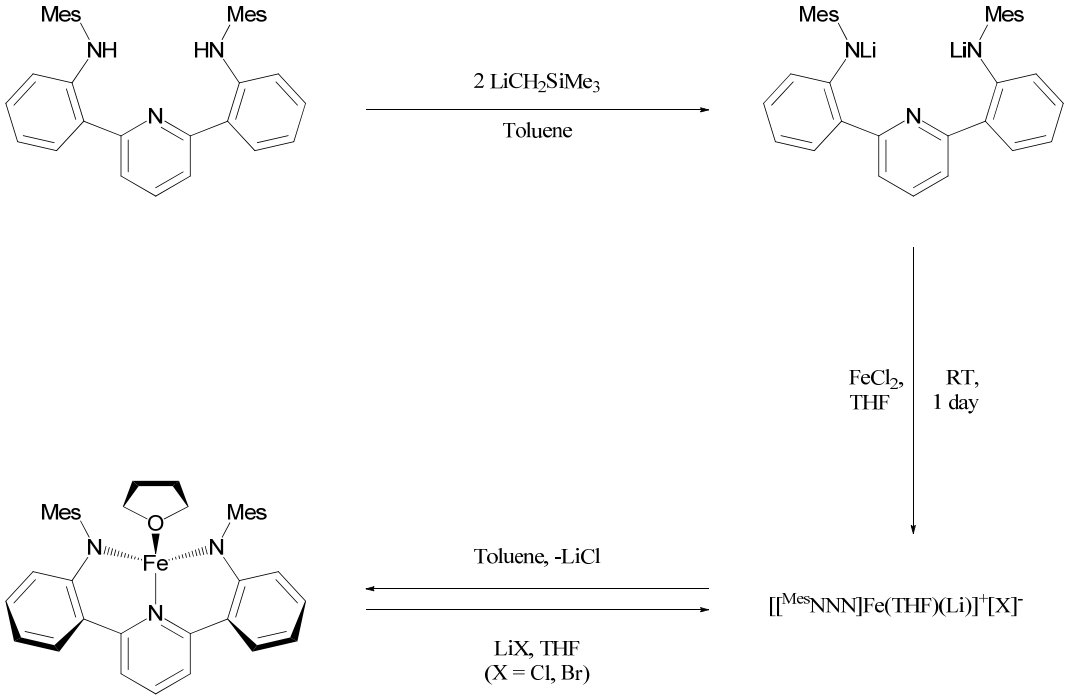

Scheme 2.2. Synthesis of [^{Mes}NNN]Fe(THF).

decomposition instead of the dilithium salt. [^{Mes}NNN]Li_2 was subsequently allowed to react with anhydrous ferrous chloride in tetrahydrofuran for one day, yielding a lithium chloride adduct of [^{Mes}NNN]Fe. Lithium chloride-free [^{Mes}NNN]Fe(THF) may be obtained by repeated filtration using toluene and a fine frit. Alternatively,

addition of thallium hexafluorophosphate or crystallization from arene/pentane solutions at -30 °C also removes the lithium chloride. Reaction of [^{Mes}NNN]Fe(THF) with lithium chloride or lithium bromide in THF regenerates the ^{1}H NMR spectrum of the lithium chloride adduct, thus it is likely a cationic complex with an outer sphere halide. Additionally, potassium chloride does not react with [^{Mes}NNN]Fe(THF).

The magnetic moment of [^{Mes}NNN]Fe(THF) was measured via Evans method in benzene-d_6,[28] giving μ_{eff} = 4.8 μ_B, which is close to the spin-only value of 4.9 μ_B for a quintet ground state. X-ray quality crystals were obtained by cooling a saturated toluene/petroleum ether solution at -30 ºC overnight (Figure 2.2). [^{Mes}NNN]Fe(THF) does not closely resemble any regular polyhedron, but can best be described as having a distorted trigonal monopyramidal geometry, with the THF and the anilide nitrogens forming the basal plane and the pyridine nitrogen at the apex. Tetrahedral, and to a lesser extent square planar, are the dominant geometries for four-coordinate iron. In contrast, there are only a handful of structurally characterized iron complexes with a trigonal monopyramidal geometry.[29–32] Although the sum of the angles in the basal plane is close to 360º,

(28) Evans, D. F. *J. Chem. Soc.* **1959**, 2003–2005.

(29) Hung, C.-H.; Chang, F.-C.; Lin, C.-Y.; Rachlewicz, K.; Stępień, M.; Latos-Grażyński, L.; Lee, G.-S.; Peng, S.-M. *Inorg. Chem.* **2004**, *43*, 4118–4120.

(30) Cotton, F. A.; Daniels, L. M.; Falvello, L. R.; Matonic, J. H.; Murillo, C. A. *Inorg. Chim. Acta* **1997**, *256*, 269–275.

the individual angles are all quite different from 120º (approx. 140º, 110º, 107º). The binding pocket of the ligand is too small to accommodate a C_{2v}-type ligand geometry, which is partially a result of the two six-membered chelate rings that are formed upon metallation. Chirik has reported several iron compounds from a

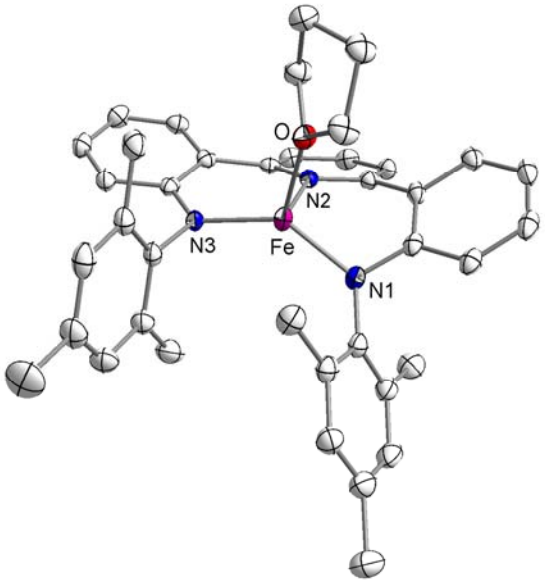

Figure 2.2. Structure of [^{Mes}NNN]Fe(THF) with displacement ellipsoids at the 50% probability level. Hydrogen atoms were omitted for clarity. Selected bond lengths (Å) and angles(deg): Fe-N3, 1.928(1); Fe-N1, 1.932(1); Fe-N2, 2.036(1); Fe-O, 2.113(1); N3-Fe-N1, 139.52(4); N3-Fe-N2, 94.97(4); N1-Fe-N2, 96.44(4); N3-Fe-O, 110.45(4); N1-Fe-O, 106.54(4); N2-Fe-O, 96.85(4); Sum of angles N3-Fe-N1, N3-Fe-O, and N1-Fe-O = 356.5°.

bis(enamide)pyridine ligand with two five-membered chelate rings;[33] these complexes comprise the only other crystallographically characterized iron pincer

(31) Govindaswamy, N.; Quarless. Jr., D. A.; Koch, S. A. *J. Am. Chem. Soc.* **1995**, *117*, 8468–8469.

(32) Ray, M.; Golombek, A. P.; Hendrich, M. P.; Young, Jr., V. G.; Borovik, A. S. *J. Am. Chem. Soc.* **1996**, *118*, 6084–6085.

(33) Bouwkamp, M. W.; Lobkovsky, E.; Chirik, P. J. *Inorg. Chem.* **2006**, *45*, 2–4.

compounds with anilide arms. The most useful comparison may be made with his pyridinebis(anilide) iron (II) amine adduct **A** (Figure 2.3). In contrast to [^{Mes}NNN]Fe(THF), **A** supports a slightly distorted square planar configuration (the sum of the four angles about iron is ~361º).

Given the unusual geometry of [^{Mes}NNN]Fe(THF), unrestricted DFT calculations were performed to investigate the effect of the steric bulk of the anilide nitrogens on the overall complex geometry (Figure 2.4). The calculated and experimental geometries of [^{Mes}NNN]Fe(THF) were in good agreement.

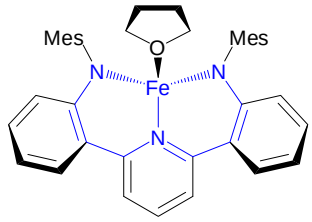

[^{Mes}NNN]Fe(THF)

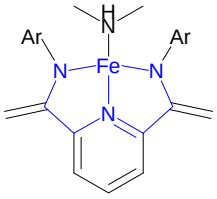

A

Ar = 2,6-^{i}Pr$_2$C$_6$H$_3$

Figure 2.3. Comparison between five- and six-membered chelate rings in pyridine bis(anilide) iron complexes.

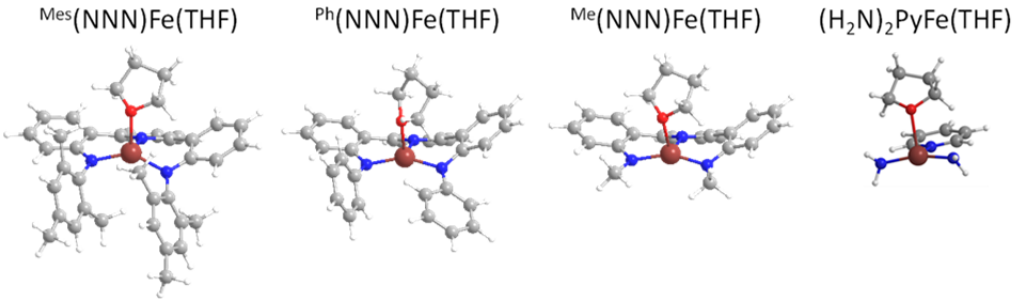

N Substitution	Mesityl	Phenyl	Methyl	Proton
N_{Amide}-Fe-N_{Amide}	141°	153°	154°	160°
N_{Py}-Fe-O	99°	104°	107°	88°

Figure 2.4. Calculated geometries of (Py)(R$_2$N)$_2$Fe(THF) complexes.

Geometries were also calculated for phenyl and methyl substituted NNN ligands ([^{Ph}NNN]Fe(THF) and [^{Me}NNN]Fe(THF)), as well as the non-chelated complex $(H_2N)_2$PyFe(THF). The bite angle of the ligand increases with decreasing bulk of the substituent. The $N_{pyridine}$-Fe-O variation exhibits a less discernable pattern, as it increases with decreasing bulk, but then decreases to the lowest observed value for $(H_2N)_2$PyFe(THF). The two steric extremes, [^{Mes}NNN]Fe(THF) and $(H_2N)_2$PyFe(THF), seem to lie on a continuum between a trigonal monopyramid and a *cis*-divacant octahedron.

Additional calculations were performed to determine the extent of spin delocalization onto the ligand framework (Figure 2.5). Of the four unpaired spins, almost all of the spin density is localized on iron (3.61994). The remainder is essentially found only on the immediate coordination sphere and not on the ligand periphery.

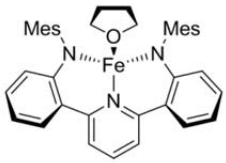

Atom	Spin Density
Fe	3.61994
$N_{anilide}$	0.10972
$N_{anilide}$	0.11039
$N_{pyridine}$	0.06470
O	0.01094

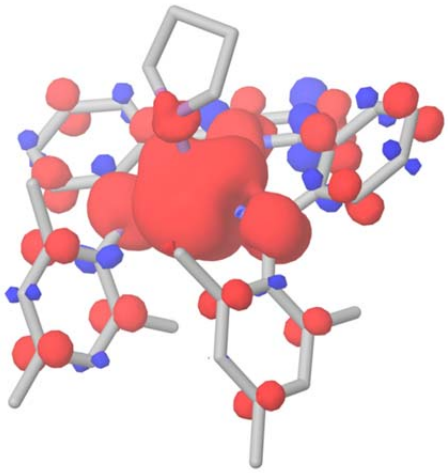

Figure 2.5. Calculated spin density of [^{Mes}NNN]Fe(THF).

Given the paramagnetism of the iron complexes herein, the NMR experiments performed require some explanation. Paramagnetism has several often disadvantageous effects on the spectral properties of molecules. Signal to noise is often reduced to the point where detection of peaks is impossible in a reasonable amount of time. The signal to noise problem causes experiments with low abundance nuclei, such as ^{13}C, to be impractical. Additionally, any pulse sequence requiring multiple pulses, such as 2D experiments, are precluded because of prohibitively fast paramagnetic relaxation. For instance, the longest ^{1}H T_1 relaxation in [^{Mes}NNN]Fe(THF) is 0.05 sec. Broadening of peaks is frequently of sufficient magnitude to obscure all coupling information. The broadening also renders integration unreliable, given the amount of signal intensity which is left in the baseline. Finally, chemical shift values are not straightforward to interpret. The rule of thumb for diamagnetic molecules–electron rich shifts upfield and electron poor shifts downfield–simply does not apply to paramagnetic systems. The shift can be approximated as the sum of two terms: the dipolar shift and the Fermi-contact shift.[34] The former is dependent on the distance of the paramagnetic center and the nucleus, while the latter depends on a through-bond interaction. Via crystallographic characterization, the dipolar term may be obtained, but there is not an *a priori* way to predict the contact term. Thus peak assignment on the basis of chemical shift for paramagnetic complexes is not feasible in most cases. The high

[34] Roquette, P.; Moranna, A.; Reinmuth, M.; Kaifer, E.; Enders, M.; Himmel, H.-J. *Inorg. Chem.* **2011**, *50*, 1942–1955.

variability for the dipolar and Fermi-contact shift terms contributes to a lack of generality concerning the spectral behavior of paramagnetic species, where certain species permit a variety of NMR experiments of quality and characteristics approaching that of diamagnetic compounds. On the other extreme, many paramagnetic compounds do not produce any discernable peaks even for simple 1D ^{1}H experiments. Thus, a lack of general methodology exists, and the NMR behavior of paramagnetic species must be examined on a case-by-case basis.

What remains information-wise in many paramagnetic NMR spectra is a number of peaks, and at worst a fingerprint of the molecule in question. For [^{Mes}NNN]Fe complexes, the number of peaks usually reflects the number expected for a C_s symmetric species (Figure 2.6). Empirically, two ligand resonances appear

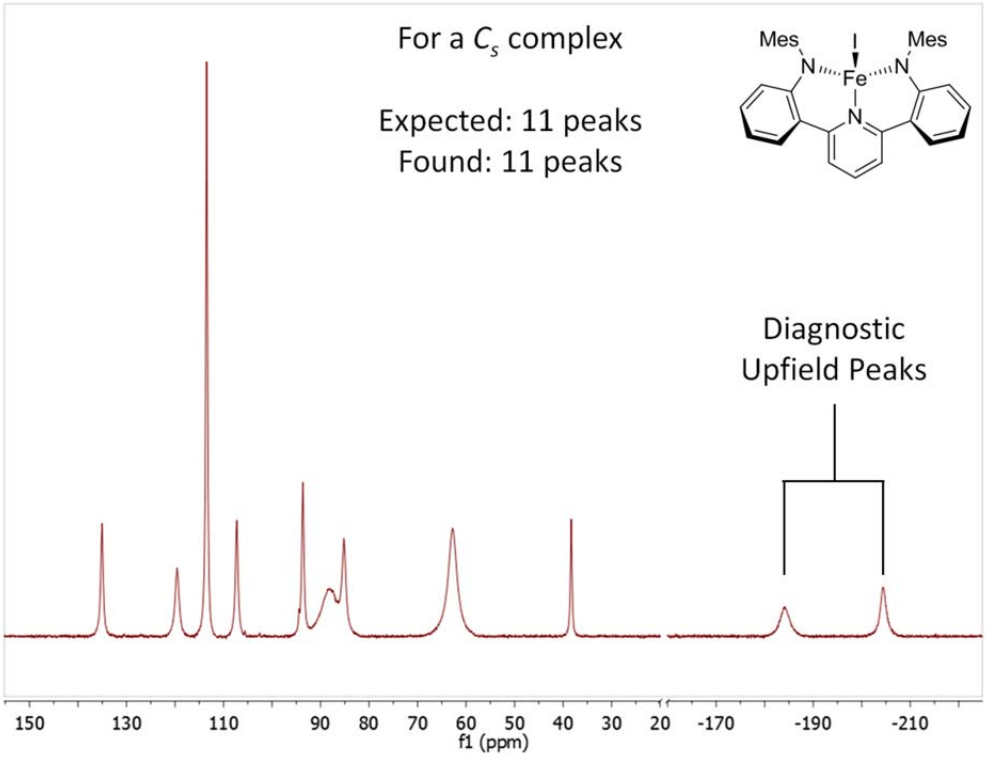

Figure 2.6. ^{1}H NMR spectrum of [^{Mes}NNN]FeI in d_8-toluene (20 to -160 ppm truncated for clarity).

upfield of the diamagnetic region for C_s symmetric complexes. This observation provides a good NMR handle for determining the number of products in a reaction or the complex symmetry. The signal to noise problem, at least for ^{1}H NMR, may be mitigated significantly (Figure 2.7). As stated above, there is no general pulse

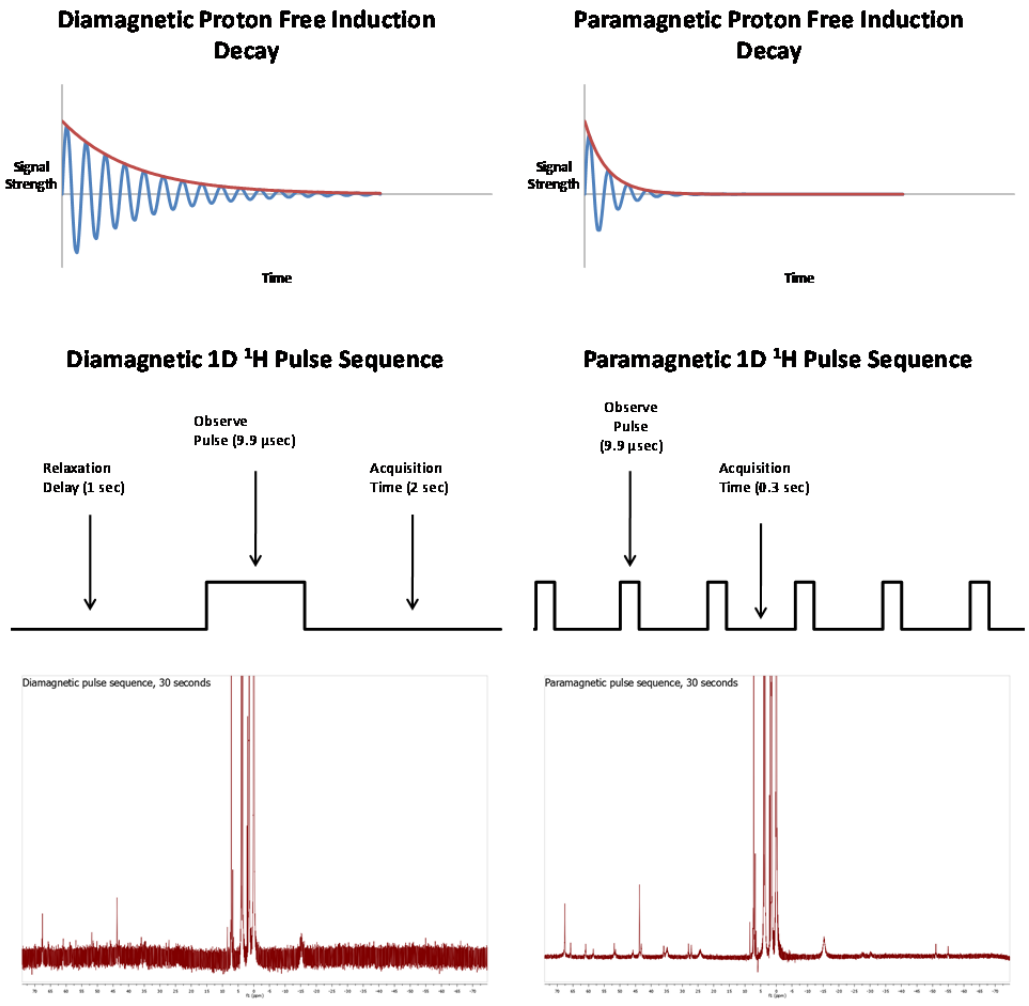

Figure 2.7. Comparison of diagmagnetic (left) and paramagnetic (right) ^{1}H NMR characteristics. Top: Relative comparison of FIDs for diamagnetic and paramagnetic protons. Middle: Comparison of a standard pulse sequence for a 1D diamagnetic proton NMR experiment, and a sequence for obtaining superior results with the paramagnetic complexes herein. Bottom: Example of spectra obtained at 30 seconds of the same solution of [^{Mes}NNN-NHSiMe$_3$]Fe using the pulse sequences shown above.

sequence for paramagnetic molecules. The sequence shown (Figure 2.7, middle right) gave superior results for the molecules examined in this work, however.Because paramagnetic protons decay so quickly (Figure 2.7, top right), most of the time in a standard pulse sequence is spent acquiring when all discernable signal has decayed. Thus elimination of the relaxation delay time, and severe shortening of the acquisition time leads to significantly better spectra (Figure 2.7, bottom). The short acquisition times allow for many pulses to be accomplished in a very short period of time. The absolute heights of the paramagnetic peaks are drastically enhanced, and the diamagnetic to paramagnetic signal ratio is lower. It should be noted that the truncation error of the residual protio impurity peaks begins to interfere with other peaks at very low acquisition times (<0.15 seconds). Additionally, when attempting to get high quality ^{1}H spectra of mixtures with both diamagnetic and paramagnetic species, it was found that sometimes two acquisitions were necessary whose pulse sequences were tailored to either paramagnetic or diamagnetic protons. Attempts to obtain ^{1}H NOESY, ROESY, COSY, NOE difference, ^{13}C, and natural abundance ^{2}H spectra were unsuccessful. In one case, however, a paramagnetic ^{29}Si spectrum was successfully obtained (see chapter 4).

Cyclic voltammetry studies were performed on [^{Mes}NNN]Fe(THF) (Figure 2.8). A quasireversible, diffusion controlled[35] reduction occurs at $E_{1/2}$ = -0.96 V (vs. the ferrocene/ferrocenium couple), and an irreversible, diffusion controlled oxidation is also observed at -0.37 V (Figure 2.9). Two new reduction waves (-0.92, -1.14 V) are coupled to the irreversible oxidation event, which are observed addition to the original reversible reduction wave. The electrochemical data suggest that the [^{Mes}NNN]Fe framework is capable of supporting either reduced or oxidized

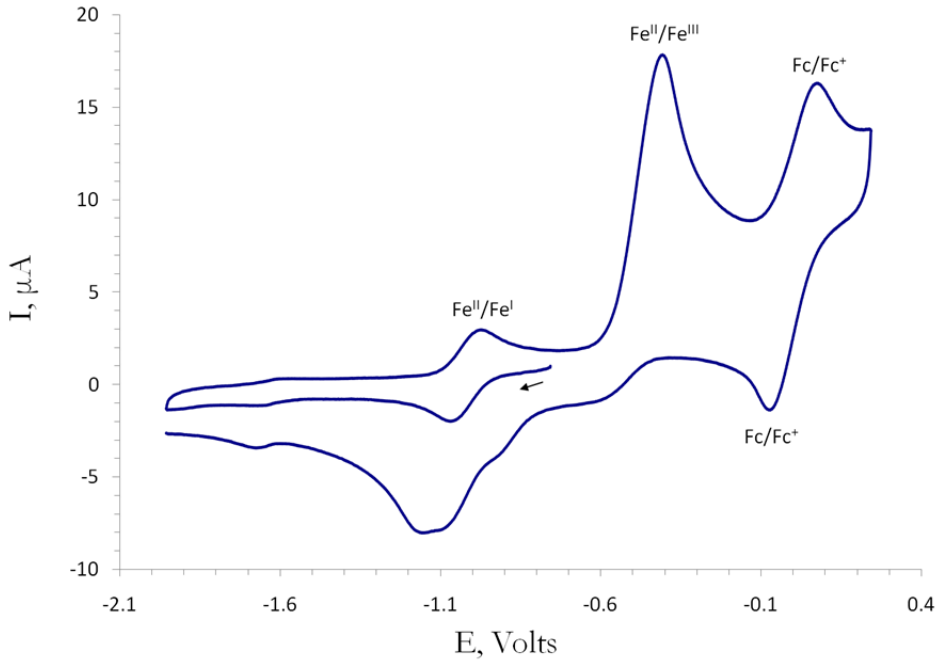

Figure 2.8. Voltammogram of 0.003 M [^{Mes}NNN]Fe(THF) in THF with 0.3 M $^{n}Bu_4NBF_4$ as supporting electrolyte. Data were recorded at 150 mV/s, and peaks were referenced to the ferrocene/ferrocenium couple.

(35) The peak current is inversely proportional to the root of the scan rate, which is consistent with the Cottrell equation for diffusion controlled waves. Bard, A. J.; Faulkner, L. R. *Electrochemical Methods. Fundamentals and Applications*, 2nd ed.; Wiley, New York, 2001.

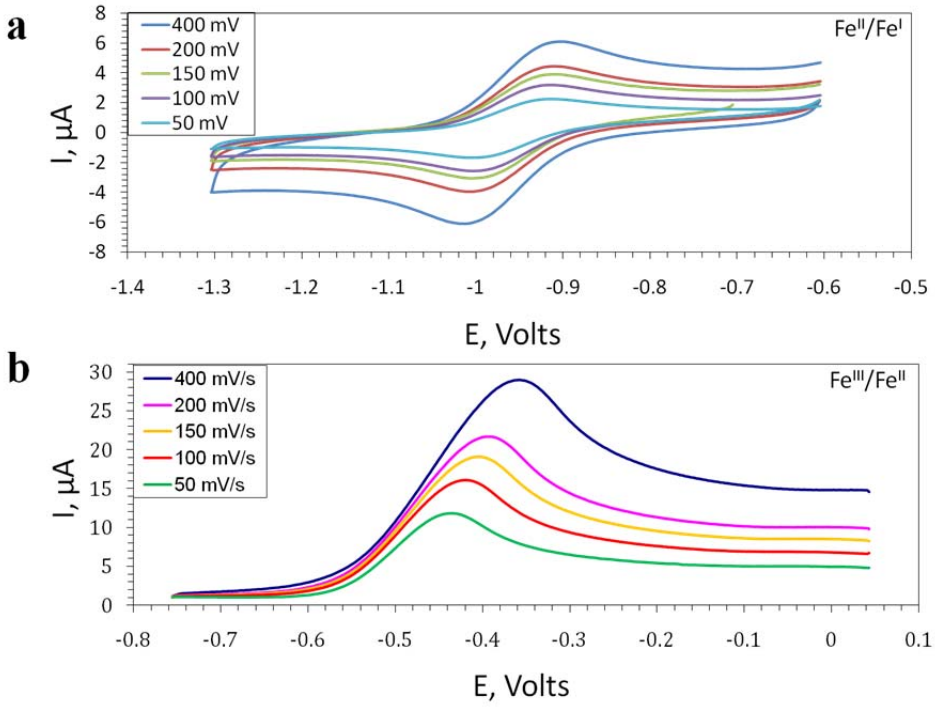

Figure 2.9. Scan rate study of the Fe^{II}/Fe^{I} couple (a) and the Fe^{III}/Fe^{II} couple (b).

species.

In light of the electrochemical data, chemical oxidation of [^{Mes}NNN]Fe(THF) was attempted. Oxidation using molecular iodine generates [^{Mes}NNN]FeI, which resembles a chelated version of a previously reported complex (Scheme 2.3).[36]

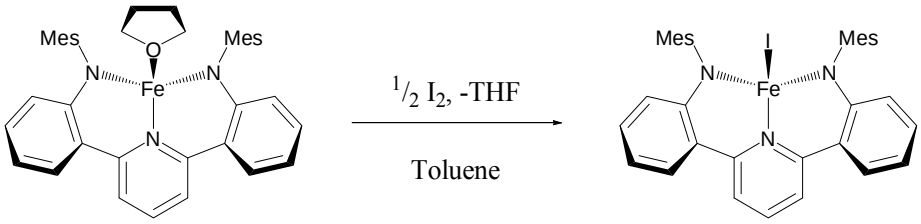

Scheme 2.3. Synthesis of [^{Mes}NNN]FeI.

(36) Stokes, S. L; Davis, W. M.; Odom, A. L.; Cummins, C. C. *Organometallics* **1996**, *15*, 4521–4530.

[^{Mes}NNN]FeI exhibits a solution magnetic moment of 5.8 μ_B in benzene-d_6, consistent with a sextet ground state. The solid state structure of [^{Mes}NNN]FeI (Figure 2.10) reveals a more tetrahedral, but still quite distorted geometry about the iron center, in contrast to the more trigonal monopyramidal geometry observed for [^{Mes}NNN]Fe(THF).

Oxidation of [^{Mes}NNN]Fe(THF) via dioxygen generates a bridging oxo dimer, ([^{Mes}NNN]Fe)$_2$O (Scheme 2.4, Figure 2.11). Bridging-oxo diiron complexes are well-known.[37,38] The magnetic moment of ([^{Mes}NNN]Fe)$_2$O is 3.6 μ_B in deuterated

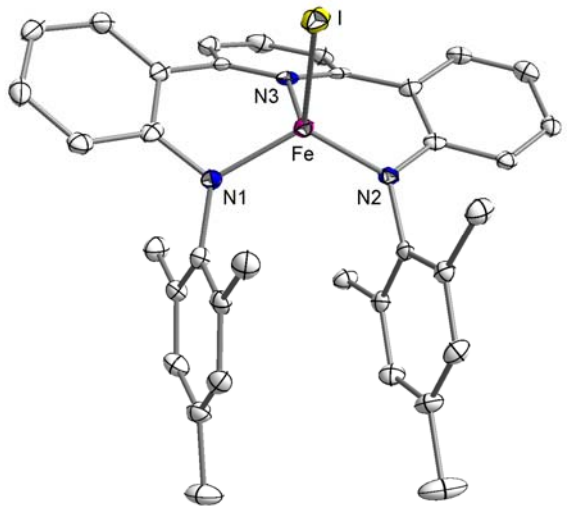

Figure 2.10. Structure of [^{Mes}NNN]FeI with displacement ellipsoids at the 50% probability level. Two virtually identical [^{Mes}NNN]FeI molecules were present in the asymmetric unit. Hydrogen atoms, solvent molecules, and the other [^{Mes}NNN]FeI molecule were omitted for clarity. Selected bond lengths (Å) and angles (deg): Fe-N1, 1.8993(1); Fe-N2, 1.8834(1); Fe-N3, 2.0274(1); Fe-I, 2.5784(1); N1-Fe-N2, 118.297(5); N1-Fe-N3, 93.436(4); N2-Fe-N3, 94.660(4); N1-Fe-I, 115.771(4); N2-Fe-I, 118.771(4); N3-Fe-I, 108.740(4).

(37) Kurtz, Jr., D. M. *Chem. Rev.* **1990**, *90*, 585–606.

(38) Fontecave, M.; Ménage, S.; Duboc-Toia, C. *Coord. Chem. Rev.* **1998**, *178–180*, 1555–1572.

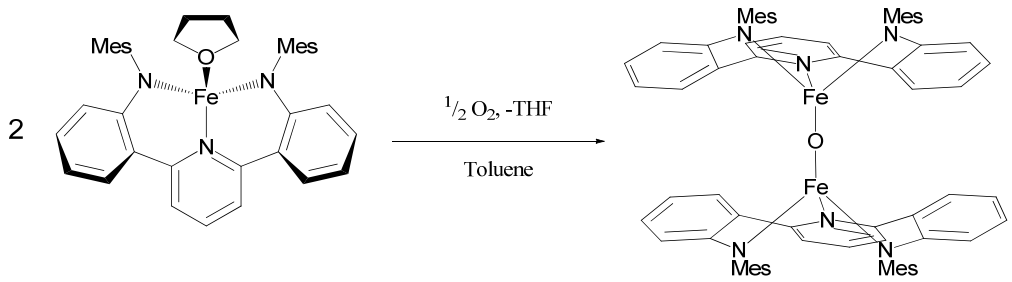

Scheme 2.4. Synthesis of ([^{Mes}NNN]Fe)$_2$O.

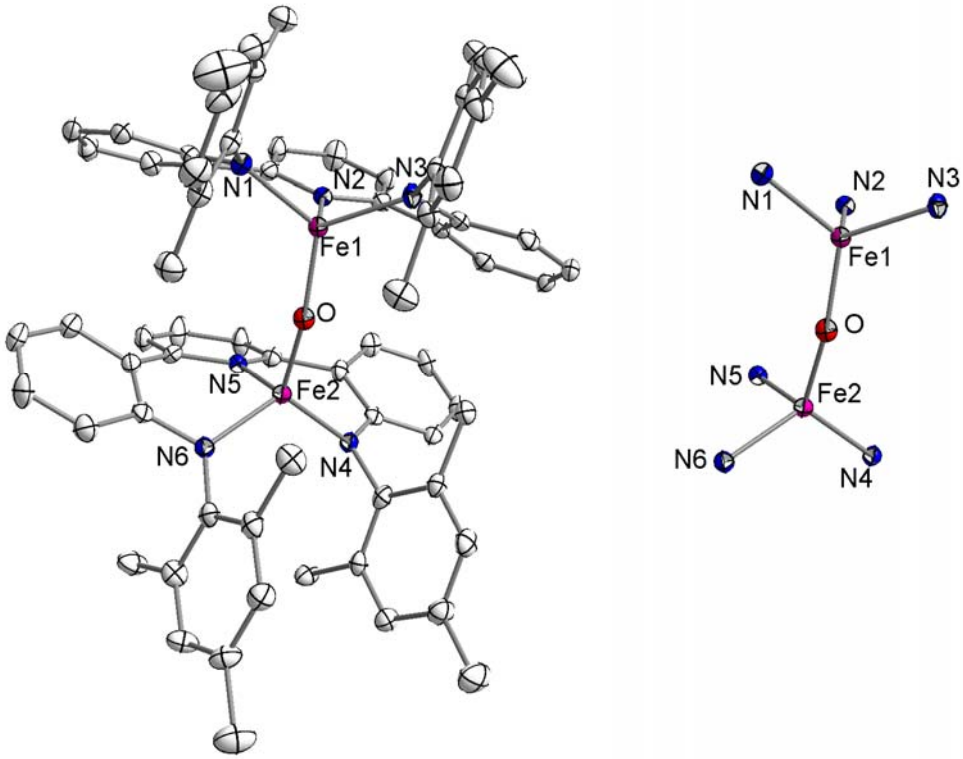

Figure 2.11. Structure of ([^{Mes}NNN]Fe)$_2$O (left) and iron coordination sphere (right) with displacement ellipsoids at the 50% probability level. Hydrogen atoms and solvent were omitted for clarity. Selected bond lengths (Å) and angles (deg): Fe1-N1, 1.9174(1); Fe1-N2, 2.0161(1); Fe1-N3, 1.9262(1); Fe1-O, 1.7802(1); Fe2-N4, 1.9263(1); Fe2-N5, 2.0154(1); Fe2-N6, 1.9234(1); Fe2-O, 1.7761(1); Fe1-O-Fe2, 156.601(3); N1-Fe1-N3, 117.501(2); N1-Fe1-N2, 92.864(2); N2-Fe1-N3, 95.140(2); N1-Fe1-O, 120.084(3); N3-Fe1-O, 116.843(3); N2-Fe1-O, 104.570; N6-Fe2-N4, 116.394(2); N6-Fe2-N5, 95.056(2); N5-Fe2-N4, 93.669; N6-Fe2-O, 117.267(3); N4-Fe2-O, 119.968(3); N5-Fe2-O, 106.367(2).

arene solvents. This value is between the predicted, spin-only values for a net triplet (μ_{eff} = 2.8 μ_B) and a net quintet (μ_{eff} = 4.9 μ_B). The triplet case would indicate both iron are doublets, while the latter denotes one iron as a doublet and the other as a quartet. Thus the value of 3.6 μ_B suggests an admixture of states at 25 °C. [^{Mes}NNN]FeI and ([^{Mes}NNN]Fe)$_2$O possess significantly smaller anilide nitrogen iron anilide nitrogen angles (118.13° and 117.50°, respectively) than does [^{Mes}NNN]Fe(THF) (139.52°); the reasons for this distortion are not immediately apparent.

The complexes as well as the protonated ligand were characterized by UV-vis spectroscopy in THF (Figure 2.12). The spectrum of the ligand exhibits a peak at 354 nm which is likely a π to π^* transition. The complexes each show absorbances slightly red-shifted from that value (371–381 nm), which have extinction coefficients similar to that of the ligand (10^3–10^4 M^{-1} cm^{-1}); therefore, the origin of the transitions is likely ligand based. In conclusion, the synthesis and characterization of iron complexes based on the new ligand [^{Mes}NNN]$^{2-}$ has been accomplished.

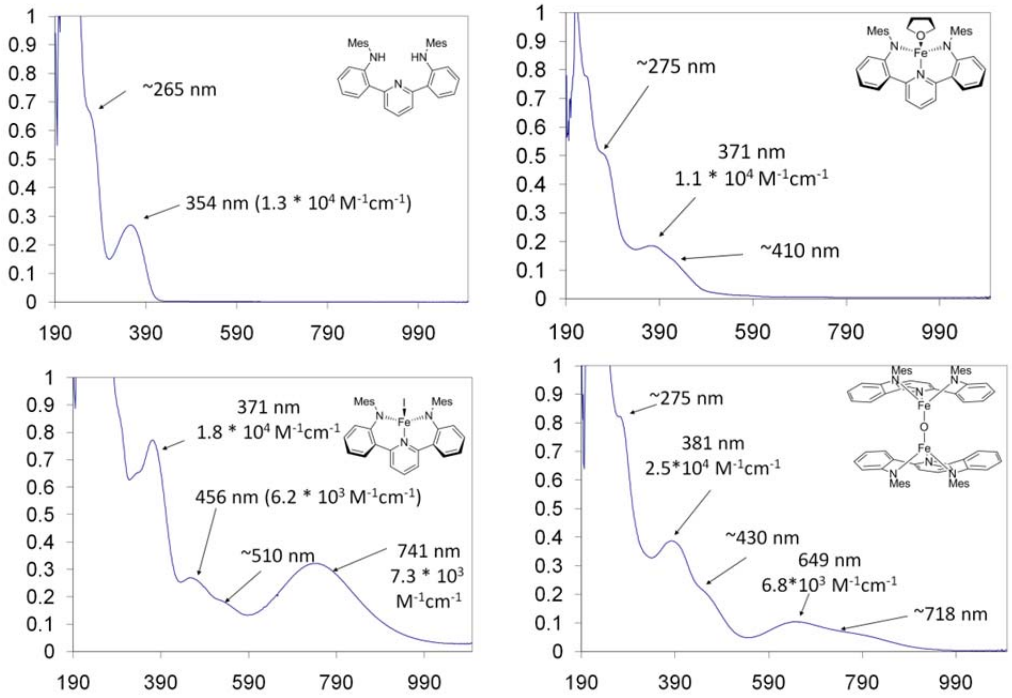

Figure 2.12. UV-vis spectra of [^{Mes}NNN]H_2 and its iron complexes.

Experimental

General Methods: Unless otherwise specified, air exposed solids were dried under vacuum prior to use, liquids were degassed or bubbled with argon, protio solvents were dried via Grubbs' method,[39] reagents were used as received from the supplier, and reactions were performed under an inert atmosphere or vacuum. All air and moisture sensitive compounds were handled using standard glovebox, Schlenk, and high-vacuum line techniques.

(39) Pangborn, A. B.; Giardello, M. A.; Grubbs, R. H.; Rosen, R. K.; Timmers, F. J. *Organometallics* **1996**, *15*, 1518–1520.

Deuterated chloroform, benzene, and tetrahydrofuran were obtained from Cambridge Isotope Laboratories. Deuterated chloroform was used as received and not stored under inert atmosphere. Deuterated benzene and tetrahydrofuran were dried with disodium benzophenone. Deuterated benzene was subsequently dried using titanocene dihydride. 2-bromoaniline was obtained from Avocado. 2-aminobenzeneboronic acid pinacol ester was obtained from Alfa Aesar. 2-(dicyclohexylphosphino)biphenyl, tris(dibenzylideneacetone) dipalladium (0), and thallium hexafluorophosphate were obtained from Strem. Palladium (II) acetate, racemic 2,2'-bis(diphenylphosphino)-1,1'-binaphthyl (BINAP), sodium tert-butoxide, mesityl bromide, triethylamine, 2,6-dibromopyridine, 3 Å Linde type molecular sieves, and calcium hydride were obtained from Aldrich. Sodium and benzophenone were obtained from Lancaster and MCB reagents, respectively. Mesityl bromide was dried on 3 Å Linde type molecular sieves for six days prior to use. Triethylamine was stirred on calcium hydride for several days, then vacuum transferred onto 3 Å Linde type molecular sieves prior to use. 1,4-dioxane was obtained from EMD, dried sequentially with 3 Å Linde type molecular sieves and disodium benzophenone, then vacuum transferred before use. Pinacolborane was obtained from Aldrich or Alfa Aesar, and stored at -30º C. Barium hydroxide octahydrate was obtained from Mallinckrodt, and stored open to the atmosphere. Trimethylsilylmethyllithium was sublimed before use. Ferrous chloride 99.99% was obtained from Aldrich as anhydrous beads.

NMR spectra were recorded on Varian Mercury 300 Megahertz NMR spectrometers, and referenced according to the solvent residual peak.[40] Solution magnetic moments were determined via Evans Method.[24] The paramagnetism of the iron complexes precluded assignment of peaks in their ^{1}H NMR spectra. The paramagnetism also implies that the integrations must only be regarded as rough estimations. Electrochemical measurements were performed using a glassy carbon rod as a working electrode, a platinum wire as auxiliary electrode, and partitioned Ag/AgCl wire as a pseudoreference electrode. Data were obtained using BAS100W software, on a BAS100A Electrochemical Analyzer. 0.3 M $^{n}Bu_4NBF_4$ THF solutions were employed, with 0.003 M concentration for the analyte. Ferrocene was employed as the internal standard, and all potentials were reference to the ferrocene/ferrocenium couple. All data were obtained in an inert atmosphere glovebox. X-ray diffraction data were obtained on a Bruker SMART 1000 or Bruker KAPPA APEXII. UV-Vis spectra were recorded on an Agilent 8453 UV-Vis spectrometer. High resolution mass spectra (HRMS) were obtained at the California Institute of Technology Mass Spectral Facility using a JEOL JMS-600H magnetic sector mass spectrometer. Elemental analyses were carried out by Desert Analytics, Tucson, AZ, 85714. DFT computational details are as follows. The M06L functional was employed. The basis sets employed were Los Alamos 2- ζ for iron and 6-31G** and for the light atoms. Orbitals were unrestricted, and spin densities were based on Mulliken populations.

---

(40) Gottlieb, H. E.; Vadim Kotlyar, V.; Nudelman, A. *J. Org. Chem.* (**1997**) *62*, 7512–7515

Original synthesis of Bis(aniline) 1.[41] In a glovebox, 2-bromoaniline (34.48 g, 200.5 mmol), palladium (II) acetate (2.33 g, 10.4 mmol), and 2-(dicyclohexylphosphino) biphenyl (13.80, 19.36 mmol) were added to a 2-liter, 3-neck roundbottom flask, and the flask was sealed. Under an argon purge, the flask was equipped with a reflux condenser and an addition funnel. Triethylamine (112 mL, 803 mmol) and 425 mL of dioxane were added via cannula. Pinacolborane (88 mL, 610 mmol) was cannulated into the addition funnel, and added dropwise to the stirring solution over 43 minutes. Upon addition, vigorous bubbling occurred and the solution turned olive green. After addition was complete, the reaction mixture was heated to 80 ºC for 2.5 hours, then allowed to cool to room temperature. Under an argon purge, solid barium hydroxide octahydrate (195.2 g, 618.7 mmol) was slowly added until the bubbling ceased, then the remainder was added. Subsequently a solution of 2,6-dibromopyridine (21.58 g, 91.11 mmol) in 140 mL of dioxane was added via cannula. Finally, 97 mL of deionized water was bubbled with argon for approximately 10 minutes, then cannulated into the reaction mixture. The reaction was heated to 101 ºC for approximately 24 hours, then allowed to cool to room temperature. The solvent was removed *in vacuo*. The remaining solid was repeatedly pulverized then washed with methylene chloride (1.7 L) to remove trapped product from insoluble barium hydroxide, as indicated by the washings no longer darkening. The solution was extracted with an equal amount of water, then

(41) The borylation and Suzuki coupling were based on a similar procedure found in Rebstock, A. S.; Mongin, F.; Trécourt, F.; Quéguiner, G. *Org. Biomol. Chem.*. **2003**, *1*, 3064–3068.

concentrated in vacuo. The crude black sludge was purified by column chromatography using methylene chloride and ethyl acetate. After chromatography, the resulting yellow solid was washed repeatedly with large amounts of diethyl ether until the ether lost most of its yellow color (though the pure compound is very faintly yellow). After the washings, the solid was dried *in vacuo*, giving 7.91 g of **1** as an off-white solid in 33% yield. ^{1}H NMR ($CDCl_3$): δ 5.38 (s(broad), 2H, N<u>H</u>), 6.76 (dd, J_{H-H}=8 Hz, 1 Hz, 2H, C<u>H</u>), 6.82 (td, J_{H-H}=8 Hz, 1 Hz, 2H, C<u>H</u>), 7.19 (dd, J_{H-H} = 12 Hz, 7 Hz, C<u>H</u>), 7.52 (s(broad), 2H, C<u>H</u>), 7.54 (s(broad), 2H, C<u>H</u>), 7.86 (t, J_{H-H}=8.0 Hz, 1H, *p*-$NC_5\underline{H}_3$). ^{13}C NMR ($CDCl_3$): δ 117.1, 117.8, 120.2, 123.0, 129.9, 130.0, 138.1, 146.1, 157.7. HRMS (FAB+) m/z calcd. for $C_{17}H_{16}N_3$: 262.1344. Found: 262.1348 (M + H), 245.0991 (M-NH_2). Sublimation point (130 °C, high vacuum).

Improved synthesis of Bis(aniline) 1. In a glovebox, 2-aminobenzeneboronic acid pinacol ester (4.6798 g, 21.360 mmol), palladium (II) acetate (247.3 mg, 1.102 mmol), and 2-(dicyclohexylphosphino)-biphenyl (717.2 mg, 2.046 mmol) were added to a reaction bomb. On the bench, a sidearm-roundbottom flask was charged with 2,6-dibromopyridine (2.3076 g, 9.7412 mmol). The solid was dissolved in 40 mL of wet dioxane. The dioxane solution was bubbled with argon then transferred to the reaction bomb via syringe. 20 mL of dioxane and 10 mL of deionized water were combined, bubbled with argon, and transferred to the reaction bomb via syringe. Under an argon purge, solid barium hydroxide octahydrate (20.8803 g, 66.1900 mmol) was added. The solution was heated to 110 °C. After 25 hours, the reaction was cooled to room temperature. The solution was poured away from the

remaining solid into a roundbottom flask and concentrated in vacuo. The remaining solid was washed with large amounts of CH_2Cl_2 then dissolved in boiling water. The CH_2Cl_2 washings were added to the roundbottom. The roundbottom solution was extracted with water, then the aqueous layer back-extracted. The solution derived from boiling water was washed with CH_2Cl_2. The combined organic layers were concentrated in vacuo. The crude black solid was solid loaded onto a silica gel (~600 mL) column packed with hexanes, and run using 8:2 hexanes:ethyl acetate as eluent. The yellow solid obtained was washed with 20 mL of diethyl ether. 1.7392 g of off-white **1** were obtained in 69% yield.

Synthesis of ligand [^{Mes}NNN]H$_2$.[42] In a glovebox, **1** (7.91 g, 30.3 mmol), tris(dibenzylideneacetone)-dipalladium (0) (1.39 g, 1.51 mmol), *rac*-2,2'-bis(diphenylphosphino)-1,1'-binaphthyl (2.34 g, 3.75 mmol), sodium tert-butoxide (8.82 g, 91.7 mmol), 300 mL of toluene, and mesityl bromide (56 mL, 360 mmol) were combined in a 3-neck, 1 liter roundbottom flask. The solution was refluxed under an argon atmosphere for approximately 41 hours. Under an argon purge, the reaction was quenched with 20 mL of water, and then concentrated *in vacuo*. Excess mesityl bromide was distilled away by heating the solid at 70º C under high vacuum. The solid was washed with 50 mL of petroleum ether, then dissolved in 250 mL of methylene chloride. The solution was extracted with an equal amount of water, filtered, and concentrated *in vacuo*, giving a yellow solid.

(42) The Buchwald-Hartwig coupling was based on a similar procedure found in Wolfe, J. P.; Tomori, H., Sadighi, J. P.; Yin, J.; Buchwald, S. L. *J. Org. Chem.* **2000**, *65*, 1158–1174.

Any palladium-containing species were removed by passing a methylene chloride solution of the product through 1 liter of silica gel packed with methylene chloride. The solution was concentrated to a yellow solid. The solid was washed repeatedly with methanol until the solid appeared off-white. [^{Mes}NNN]H_2 was obtained in 46% yield (6.93 g). ^{1}H NMR (C_6D_6): δ 2.01 (s, 12H, *o*-C$\underline{H}_3$), 2.15 (s, 6H, *p*-C$\underline{H}_3$), 6.50 (d, J_{H-H}=8 Hz, 2H, C$\underline{H}$), 6.74 (s, 4H, mesityl-C$\underline{H}$, t, 2H, J_{H-H}=7 Hz, C$\underline{H}$), 7.03 (t, J_{H-H}=8 Hz, 2H, C$\underline{H}$), 7.2-7.4 (m, 3H, C$\underline{H}$), 7.55 (d, J_{H-H}=8 Hz, 2H, C$\underline{H}$), 8.53 (s, 2H, N$\underline{H}$). ^{1}H NMR (d_8-THF): δ 1.97 (s, 12H, *o*-C$\underline{H}_3$), 2.23 (s, 6H, *p*-C$\underline{H}_3$), 6.20 (d, J_{H-H}=8 Hz, 2H, C$\underline{H}$), 6.69 (t, J_{H-H}=8 Hz, 2H, C$\underline{H}$), 6.82 (s, 4H, C$\underline{H}$), 7.02 (t, J_{H-H}=8 Hz, 2H, C$\underline{H}$), 7.59 (d, J_{H-H}=8 Hz, 2H, C$\underline{H}$), 7.76 (d, J_{H-H}=8 Hz, 2H, C$\underline{H}$), 7.97 (t, J_{H-H}=8 Hz, 1H, *p*-N$C_5\underline{H}_3$), 8.42 (s, 2H, N$\underline{H}$). ^{1}H NMR ($CDCl_3$): δ 2.01 (s, 12H, *o*-C$\underline{H}_3$), 2.27 (s, 6H, *p*-CH_3), 6.27 (d, J_{H-H}=8 Hz, 2H, C$\underline{H}$), 6.76 (t, J_{H-H}=7 Hz, 2H, C$\underline{H}$), 6.85 (s, 4H, mesityl-C$\underline{H}$), 7.09 (t, J_{H-H}=8 Hz, 2H, C$\underline{H}$), 7.57 (d, J_{H-H}=8 Hz, 2H, C$\underline{H}$), 7.66 (d, J_{H-H}=8 Hz, 2H, C$\underline{H}$), 7.91 (t, J_{H-H}=8 Hz, 1H, *p*-N$C_5\underline{H}_3$), 8.14 (s, 2H, N$\underline{H}$). ^{13}C NMR ($CDCl_3$): δ 18.5, 21.0, 113.2, 117.1, 120.8, 123.3, 129.1, 130.0, 130.1, 135.1, 136.0, 136.1, 137.9, 145.4, 158.1. HRMS (FAB+) m/z calcd. for $C_{35}H_{35}N_3$: 497.2831. Found: 497.2849 (M^+), 482.2596 (M-CH_3). UV-Vis (THF, nm ($M^{-1}cm^{-1}$)): 275 (sh), 354 ($1.3*10^4$). X-ray quality crystals were obtained by slow evaporation of a saturated diethyl ether solution. The crystal data are summarized as follows: formula, $C_{35}H_{35}N_3$; formula weight, 497.66; lattice system, monoclinic; space group $P2_1/n$ (#14); temperature 100 K; lattice parameters a= 12.1774(12) Å, b = 8.3901(8) Å, c = 27.039 (3) Å, β = 93.803(2)°; unit cell volume V = 2756.5(5) Å^3; calculated density D_{calc} = 1.199 g/cm^3; number of molecules in the unit cell Z = 4;

linear absorption coefficient μ = 0.070 mm^{-1}; no empirical absorption correction; MoKα radiation recorded on a Bruker SMART 1000 diffractometer; 34841 reflections collected, 6476 unique reflections (4122 with I > 2σ(I)); θ_{max} = 28.41°; 349 parameters; 0 restraints; H atoms were placed in calculated positions; all other atoms were refined anisotropically, full matrix least-squares on F^2 refinement method; reliability factor *R* for all data = 0.0900 (for data I > 2σ(I) = 0.0554), weighted reliability factor R_w = 0.0939 (for data I > 2σ(I) = 0.0907), goodness-of-fit on F^2, 1.579. Crystallographic data have been deposited at the CCDC, 12 Union Road, Cambridge CB2 1EZ, UK. Copies can be obtained on request, free of charge, by quoting the publication citation and the deposition number 65353 or by visiting www.ccdc.cam.ac.uk/data_request/cif.

Synthesis of [^{Mes}NNN]Li$_2$. In a glovebox, [^{Mes}NNN]H$_2$ (2.222 g, 4.465 mmol) and trimethylsilylmethyllithium (0.943 g, 10.01 mmol) were combined as solids. On the high vacuum line, ~100 mL of toluene were vacuum transferred from a titanocene dihydride pot onto the solids at -78° C. After transfer was complete, the mixture was stirred and allowed to warm to room temperature. Upon warming, the solids dissolved. After two hours, the orange solution was concentrated *in vacuo*. In the glovebox, the orange solid was suspended in 30 mL pentane (obtained by vacuum transfer from a disodium benzophenone/tetraglyme pot). The orange suspension was cooled via a liquid nitrogen-cooled cold well, then filtered. The aforementioned procedure was repeated with an additional 30 mL of pentane. The remaining solid was dried *in vacuo*, giving 2.256 g of [^{Mes}NNN]Li$_2$ as a bright yellow solid in 99% yield. ^{1}H NMR (d_8-THF): δ 1.65 (s, 12H, *o*-C$\underline{H}_3$), 2.20 (s, 6H, *p*-C$\underline{H}_3$), 5.99 (d, $J_{H\text{-}H}$

=8 Hz, 2H, *o*-anilide C<u>H</u>), 6.14 (t, J_{H-H} =7 Hz, 2H, *p*-anilide C<u>H</u>), 6.58 (s, 4H, mesityl aryl-C<u>H</u>), 6.70 (t, J_{H-H} =7 Hz, 2H, *m*-anilide C<u>H</u> *para* to pyridine ring), 7.54 (d, J_{H-H} = 8 Hz, 2H, *m*-anilide C<u>H</u> *ortho* to pyridine ring), 7.64 (d, J_{H-H} =8 Hz, 2H, *m*-$NC_5\underline{H}_3$), 7.84 (t, J_{H-H} =8 Hz, *p*-$NC_5\underline{H}_3$). ^{13}C NMR (C_6D_6) δ 18.54, 20.91, 112.34, 116.36, 119.56, 120.74, 129.52, 130.53, 131.44, 131.92, 131.97, 139.62, 147.51, 156.84, 160.77. Anal. Calcd. for $C_{35}H_{33}Li_2N_3$: C, 82.50; H, 6.53; N, 8.25. Found1: C, 81.25; H, 6.14; N, 7.34. Found2: C, 80.85; H, 5.93; N, 7.33.

Synthesis of [^{Mes}NNN]Fe(THF). Ferrous chloride (199 mg, 1.57 mmol**)** and [^{Mes}NNN]Li_2 (800 mg, 1.57 mmol) were combined as solids, then dissolved in 20 mL of tetrahydrofuran. The reaction mixture was stirred for 25 hours, then concentrated *in vacuo* to give the lithium chloride adduct [^{Mes}NNN]Fe(THF)$_x$(LiCl)$_y$. ^{1}H NMR (d_8-THF): δ -51.32 (s, 2H, C<u>H</u>), -38.59 (s, 2H, C<u>H</u>), 18.25 (s, 4H), 19.82 (s, 2H, C<u>H</u>), 28.43 (s, 2H, C<u>H</u>), 41.07 (s, 6H), 44.42 (s, 2H, CH), 47.59 (s, 2H, C<u>H</u>), 66.06 (s, 2H, C<u>H</u>), 73.51 (s, 1H, *p*-$NC_5\underline{H}_3$), 77.72 (s, 4H). The lithium chloride adduct was dissolved in 55 mL of toluene, filtered, diluted with 100 mL of petroleum ether, and left at -30 ºC overnight. 531 mg of black crystalline [^{Mes}NNN]Fe(THF) were obtained after drying *in vacuo* in 54% yield. ^{1}H NMR (C_6D_6): δ -52.03 (s, 2H, C<u>H</u>), -27.83 (s, 2H, C<u>H</u>), 2.85 (s, 4H), 33.41 (s, 4H), 47.42 (s, 2H, C<u>H</u>), 52.78 (s, 6H, *p*-$C\underline{H}_3$), 54.28 (s, 2H, C<u>H</u>), 55.40 (s, 2H, C<u>H</u>) 63.46 (s, 1H, *p*-NC_5H_3). ^{1}H NMR (d_8-THF): δ -52.39 (s, 2H, C<u>H</u>), -31.47 (s, 2H, C<u>H</u>), 33.04 (s, 4H), 44.15 (s, 10H), 46.66 (s, 2H, CH), 52.35 (s, 2H, CH), 52.78 (s, 6H, $C\underline{H}_3$), 56.97 (s, 2H, C<u>H</u>), 66.25 (s, 1H, *p*-NC_5H_3). Anal. Calcd. for $C_{39}H_{41}FeN_3O$: C, 75.11; H, 6.63; N, 6.74. Found1: C, 74.90; H, 6.74; N, 6.67.

Found2: C, 73.72; H, 6.50; N, 6.64. CV (THF): $E_{1/2}$, V vs. Ferrocene at 100 mV/s (ΔE_p, i_{pa}/i_{pc}): -0.96 V (90 mV, 0.88) and -0.37 V (irreversible). UV-Vis (THF, nm ($M^{-1}cm^{-1}$)): 275 (sh), 371 ($1.1*10^4$), 410 (sh). X-ray quality crystals were obtained from a toluene/petroleum ether solution at -30º C. The crystal data are summarized as follows: formula, $C_{39}H_{41}N_3OFe$; formula weight, 623.60; lattice system, monoclinic; space group $P2_1/c$ (#14); temperature 100 K; lattice parameters a = 14.5396(6) Å, b = 13.5644(6) Å, c = 16.6014(7) Å, β = 98.247(2)˚; unit cell volume V = 3240.3(2) $Å^3$; calculated density D_{calc} = 1.278 g/cm^3; number of molecules in the unit cell Z = 4; linear absorption coefficient μ = 0.501 mm^{-1}; no empirical absorption correction; MoKα radiation recorded on a Bruker KAPPA APEX II diffractometer; 97719 reflections collected, 14879 unique reflections (10317 with I > 2σ(I)); θ_{max} = 36.53˚; 403 parameters; 0 restraints; H atoms were placed in calculated positions; all other atoms were refined anisotropically, full matrix least-squares on F^2 refinement method; reliability factor R for all data = 0.0792 (for data I > 2σ(I) = 0.0501), weighted reliability factor R_w = 0.0860 (for data I > 2σ(I) = 0.0848), goodness-of-fit on F^2, 2.823. Crystallographic data have been deposited at the CCDC, 12 Union Road, Cambridge CB2 1EZ, UK. Copies can be obtained on request, free of charge, by quoting the publication citation and the deposition number 678268 or by visiting www.ccdc.cam.ac.uk/data_request/cif.

Synthesis of [^{Mes}NNN]FeI. [^{Mes}NNN]Fe(THF) (116.8 mg, 187.3 μmol) and iodine (23.8 mg, 93.6 μmol) were combined as solids, dissolved in 10 mL of toluene, and left stirring for 15 minutes. The solution was then concentrated *in vacuo*. 126 mg of [^{Mes}NNN]FeI were isolated in 77% yield. X-ray quality crystals were obtained by

dissolution with benzene, dilution in an equal quantity of petroleum ether, and cooling to -30 °C. The crystal data are summarized as follows: formula, $2(C_{35}H_{33}N_3FeI)$ $1.5(C_6H_6)$; formula weight, 1473.98; lattice system, triclinic; space group P-1(#2); temperature 100 K; lattice parameters a = 14.8740(7) Å, b = 14.9489(7) Å, c = 16.9750(8) Å, α = 69.528(3)˚, β = 72.061(3)˚, γ = 76.207(3)˚; unit cell volume V = 3327.7(3) $Å^3$; calculated density D_{calc} = 1.471 g/cm^3; number of molecules in the unit cell Z = 4; linear absorption coefficient μ = 1.413 mm^{-1}; semi-empirical absorption correction from equivalents; MoKα radiation recorded on a Bruker KAPPA APEX II diffractometer; 85468 reflections collected, 22141 unique reflections (13476 with I > 2σ(I)); θ_{max} = 32.13˚; 1102 parameters; 0 restraints; H atoms were located via a Difference Fourier map; all other atoms were refined anisotropically, full matrix least-squares on F^2 refinement method; reliability factor R for all data = 0.1132 (for data I > 2σ(I) = 0.0507), weighted reliability factor R_w = 0.0647 (for data I > 2σ(I) = 0.0602), goodness-of-fit on F^2, 1.524. Crystallographic data have been deposited at the CCDC, 12 Union Road, Cambridge CB2 1EZ, UK. Copies can be obtained on request, free of charge, by quoting the publication citation and the deposition number 695390 or by visiting www.ccdc.cam.ac.uk/data_request/cif. ^{1}H NMR (d_8-THF): δ -208.67 (s), -187.22 (s), 38.38 (s, 1H), 64.06 (s, 4H), 88.58 (2 overlapping peaks, s, 6H) 96.40 (s, 2H), 109.64 (s, 2H), 115.71 (s, 6H), 121.91 (s, 2H), 124.74 (s, 1H), 137.74 (s, 2H), 144.48 (s, 1H). Anal. Calcd. for $C_{35}H_3FeN_3I$: C, 61.97; H, 4.90; N, 6.19. Found1: C, 62.25; H, 4.46; N, 6.15. Found2: C, 62.42; H, 4.47; N, 5.95. UV-Vis (THF, nm ($M^{-1}cm^{-1}$)): 371 ($1.8*10^4$), 456 ($6.2*10^3$), 510 (sh), 741 ($7.3*10^3$).

Synthesis of ([^{Mes}NNN]Fe)$_2$O. In the glovebox, [^{Mes}NNN]Fe(THF) (167.9 mg, 269 μmol) was dissolved in 25 mL of toluene. On the high vacuum line, the solution was degassed. ~1 atm of dioxygen was dried via a dry-ice/acetone trap for one hour, then exposed to the solution. The solution immediately turned from dark red to dark green. After 30 minutes, the solution was concentrated *in vacuo* to an intractable sludge. The sludge was treated with petroleum ether, stirred briefly, then concentrated *in vacuo* to a green powder and isolated in 85% yield. X-ray quality crystals were obtained by vapor diffusion of petroleum ether into a saturated toluene solution. The crystal data are summarized as follows: formula, $C_{70}H_{66}N_6OFe_2 \bullet 0.5(C_7H_8)$; formula weight, 1165.05; lattice system, orthorhombic; space group Iba2 (#45); temperature 100 K; lattice parameters a = 19.8707(9) Å, b = 39.4031(19) Å, c = 15.1038(6) Å; unit cell volume V = 11825.8(9) Å^3; calculated density D_{calc} = 1.309 g/cm^3; number of molecules in the unit cell Z = 8; linear absorption coefficient μ = 0.542 mm^{-1}; no empirical absorption correction; MoKα radiation recorded on a Bruker KAPPA APEX II diffractometer; 121688 reflections collected, 18216 unique reflections (14462 with I > 2σ(I)); θ_{max} = 32.23˚; 757 parameters; 10 restraints; H atoms were placed in calculated positions; all other atoms were refined anisotropically, full matrix least-squares on F^2 refinement method; reliability factor R for all data = 0.0600 (for data I > 2σ(I) = 0.0416), weighted reliability factor R_w = 0.0567 (for data I > 2σ(I) = 0.0558), goodness-of-fit on F^2, 1.792. Crystallographic data have been deposited at the CCDC, 12 Union Road, Cambridge CB2 1EZ, UK. Copies can be obtained on request, free of charge, by quoting the publication citation and the deposition number 697910 or by visiting

www.ccdc.cam.ac.uk/data_request/cif. ^{1}H NMR (C_6D_6): δ -10.59 (s), δ -8.66 (s), δ 10.35 (s), δ 11.24 (s), δ 12.86 (s), δ 13.64 (s), δ 15.99 (s), δ 16.67 (s) (the overlap of peaks precluded integration). Anal. Calcd. for $C_{70}H_{66}N_6OFe_2$ (and 0.5 eq. C_7H_8): C, 75.77; H, 6.06; N, 7.21. Found1: C, 75.40; H, 5.81; N, 5.71. Found2: C, 75.32; H, 5.90; N, 6.32.

Chapter 3
Reactivity of Pyridine Bis(anilide) Ferrous and Ferric Complexes

Introduction

A prerequisite for the improvement of reaction scope and efficiency in iron catalysis is a detailed understanding of individual stoichiometric steps that interconvert different oxidation states and ligands on well-defined metal centers. Basic reactions such as insertion, oxidation, reduction, and transmetallation are vital to many catalytic cycles. The study of structure-reactivity correlation may suggest what kind of reactions are possible to catalyze with iron complexes. Thus, the reactivity profile of the [^{Mes}NNN]Fe series was canvassed to assess its reaction capabilities and potential for catalysis.

Results and Discussion

The ability to interconvert between different oxidation states and coordination environments is considered critical to catalysis. Thus, [^{Mes}NNN]Fe(THF), [^{Mes}NNN]FeI, and ([^{Mes}NNN]Fe)$_2$O were subjected to various reagents in an attempt to convert between each other or generate new complexes that may have desirable reactivity.

Access to Fe^{III} organometallic derivatives may have important uses with respect to C-X bond formation reactions, or olefin polymerization. Thus, both electrophilic and nucleophilic routes to iron carbon or iron hydrogen bonds were sought (Scheme 3.1). Generation of the iron methyl derivative [^{Mes}NNN]FeCH$_3$ (along with [^{Mes}NNN]FeI as a byproduct) was attempted by mixing [^{Mes}NNN]Fe(THF) and CH$_3$I. Instead, only [^{Mes}NNN]FeI was observed, along with ethane, in the ^{1}H NMR spectrum. Similarly, treatment of [^{Mes}NNN]FeI with CH$_3$Li

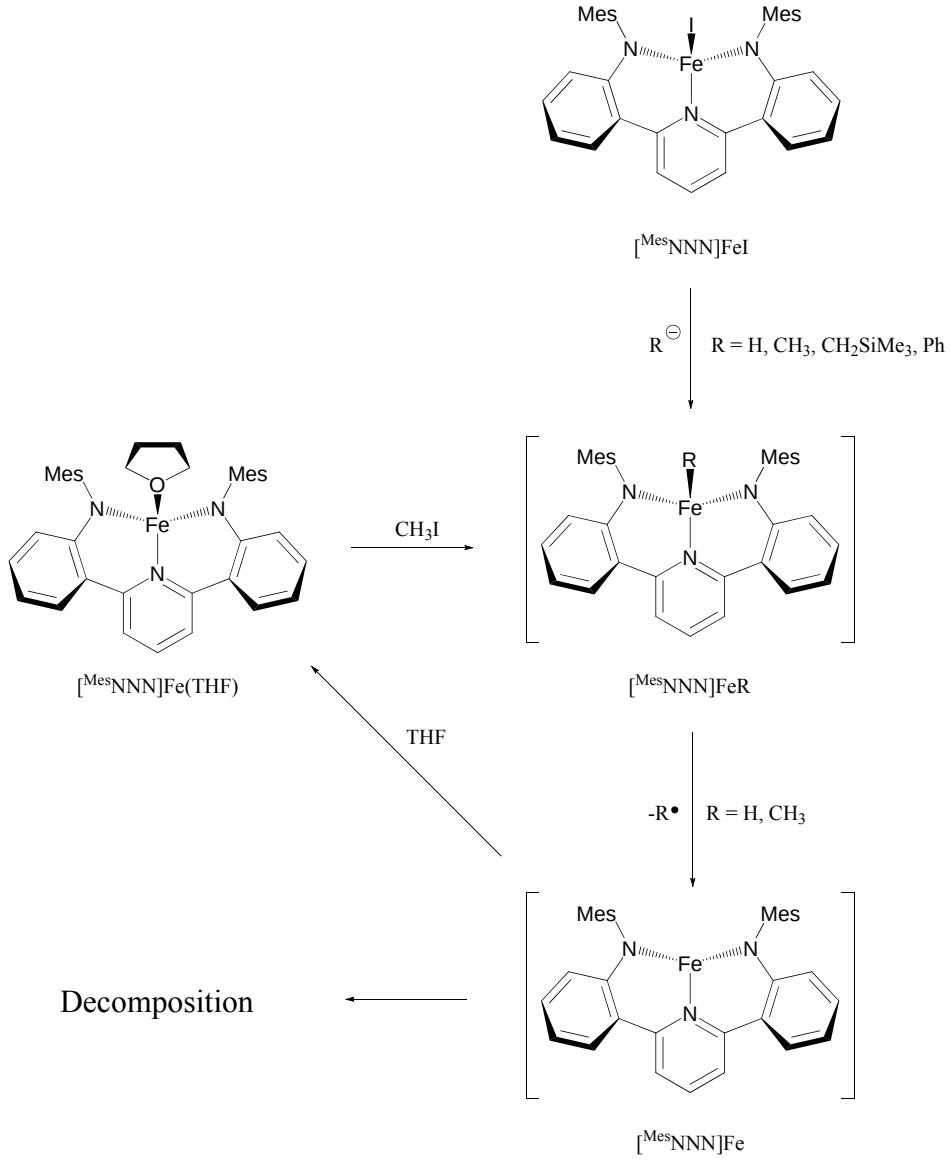

Scheme 3.1. Organometallic reactivity with the [^{Mes}NNN]Fe scaffold.

resulted in the appearance of a new species in the ^{1}H NMR spectrum, (potentially [^{Mes}NNN]FeCH$_3$), which decomposes to ethane and a mixture of products over the course of days. There is precedent for iron(III)-carbon bond homolysis, which may explain the above results with CH_3I and CH_3Li.[1,2] Additionally, the softer $Zn(CH_3)_2$

(1) Floriani, C.; Calderazzo, F. *J. Chem. Soc. A* **1971**, 3665–3669.

fails to react with [^{Mes}NNN]FeI. If the Fe-C bond in putative [^{Mes}NNN]FeCH$_3$ undergoes homolysis, then a reactive, low-coordinate Fe^{II} species "[^{Mes}NNN]Fe" might result; such a complex would likely be liable to various decomposition pathways.

Attempts to synthesize [^{Mes}NNN]FeH led to results similar to those above. Both [Et$_3$BH]$^-$ and [(MeO)$_3$BH]$^-$ decompose [^{Mes}NNN]FeI, though the latter cleanly produces [^{Mes}NNN]Fe(THF) when the reaction is performed in the presence of THF. This result lends credence to the intermediacy of an unstable "[^{Mes}NNN]Fe" complex, which may be trapped with a fourth ligand (THF) or decompose. A solution of [^{Mes}NNN]Fe(THF) in C_6D_6 fails to react with 1 atm of dihydrogen. The failure to produce either [^{Mes}NNN]FeCH$_3$ or [^{Mes}NNN]FeH via the above electrophilic and nucleophilic routes may suggest some fundamental instability regarding ferric organometallic complexes of this ligand.

It was hypothesized that if the decomposition of complexes [^{Mes}NNN]FeR were bimolecular, then the use of bulkier organometallic groups would prevent such a decomposition. The reaction of PhLi with [^{Mes}NNN]FeI seemed to produce one major product based on the ^{1}H NMR spectrum, though the spectroscopy was not definitive. Numerous efforts to obtain X-ray quality crystals failed, and the synthesis of [^{Mes}NNN]FePh was not attempted further. The reaction of LiCH$_2$SiMe$_3$ with [^{Mes}NNN]FeI in toluene seemed to proceed cleanly to one product (tentatively assigned as [^{Mes}NNN]FeCH$_2$SiMe$_3$) as judged by the ^{1}H NMR spectrum.

---

(2) Balch, A. L.; Olmstead, M. M.; Nasser, S.; St. Claire, T. N. *Inorg. Chem.* **1994**, *33*, 2815–2822.

Unfortunately, crystalline material of this complex was not obtained despite significant effort. Homolytic processes may also be possible for [^{Mes}NNN]FeCH$_2$SiMe$_3$. For instance, attempted crystallization of the product from THF gave crystals of [^{Mes}NNN]Fe(THF), and carrying out the synthesis in d_8-THF instead of toluene gave a mixture of [^{Mes}NNN]FeCH$_2$SiMe$_3$ and [^{Mes}NNN]Fe(THF). A solution of [^{Mes}NNN]FeCH$_2$SiMe$_3$ in d_8-toluene reacts with an atmosphere of ethylene to generate multiple paramagnetic species. No consumption of ethylene beyond stoichiometric reactions was apparent, however, and no polymeric material was visually perceptible. Additionally, no reaction of [^{Mes}NNN]FeCH$_2$SiMe$_3$ with H_2 was observed even upon heating to 90 °C for several hours.

Given the reduction of [^{Mes}NNN]FeI to [^{Mes}NNN]Fe(THF) using [(MeO)$_3$BH]$^-$, one-electron reductants were investigated for this transformation as well. Fe(C_5Me_5)$_2$ did not reduce [^{Mes}NNN]FeI, while Co(C_5H_5)$_2$ gave minor side products in addition to [^{Mes}NNN]Fe(THF). The use of Cr(C_6H_6)$_2$, however, allowed the reduction to proceed cleanly (Scheme 3.2). The reduction of [^{Mes}NNN]Fe(THF)

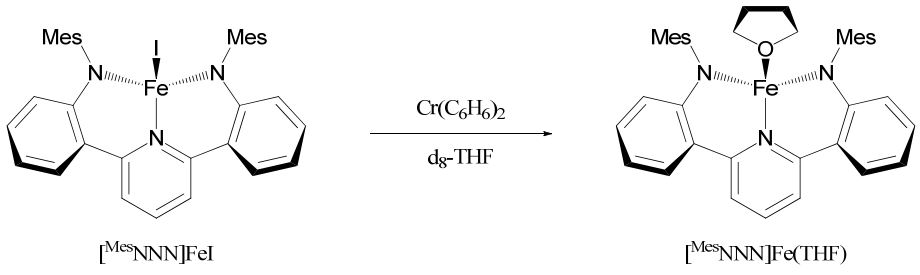

[^{Mes}NNN]FeI [^{Mes}NNN]Fe(THF)

Scheme 3.2. Reduction of [^{Mes}NNN]FeI to [^{Mes}NNN]Fe(THF).

was attempted, based on the quasireversible Fe^{II}/Fe^{I} couple observed electrochemically at -0.96 V in THF. $Co(C_5H_5)_2$ failed to reduce [^{Mes}NNN]Fe(THF), while sodium metal led to two products (1 + 2) under N_2 or vacuum (Scheme 3.3). $Co(C_5Me_5)_2$ gave two products under N_2 (1 + 3) or under vacuum (1 + 4).

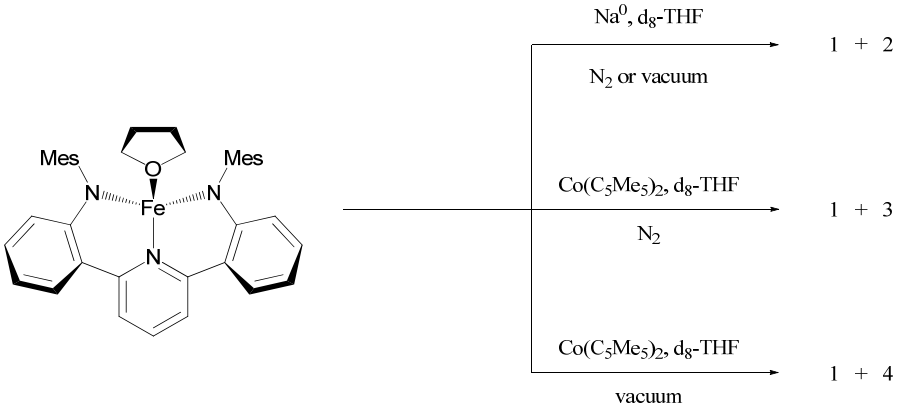

Scheme 3.3. Attempted reductions of [^{Mes}NNN]Fe(THF).

Given the facile interconversion of [^{Mes}NNN]Fe(THF) and [^{Mes}NNN]FeI, attempts to explore the reactivity of the oxo dimer ([^{Mes}NNN]Fe)$_2$O were made as well (Scheme 3.4). In addition to O_2, pyridine-N-oxide generates ([^{Mes}NNN]Fe)$_2$O at room temperature from [^{Mes}NNN]Fe(THF). ([^{Mes}NNN]Fe)$_2$O may also be generated from [^{Mes}NNN]FeI by either KO_2 at room temperature or Ag_2O at 80 °C . Na_2O_2 failed to react, however, even for extended periods in refluxing d_8-THF. Attempts to cleave the dimer with either triphenylphosphine or excess pyridine N-oxide failed even with vigorous heating. Methyl iodide, however, successfully generated [^{Mes}NNN]FeI and dimethyl ether from the dimer. Unfortunately, the reaction is not clean, as free ligand grows in over time as well. Methylation of the

arene solvent and subsequent H^+ expulsion may explain this side reaction, given the long reaction times at 100 °C. Nevertheless, the reaction is, to the best of our

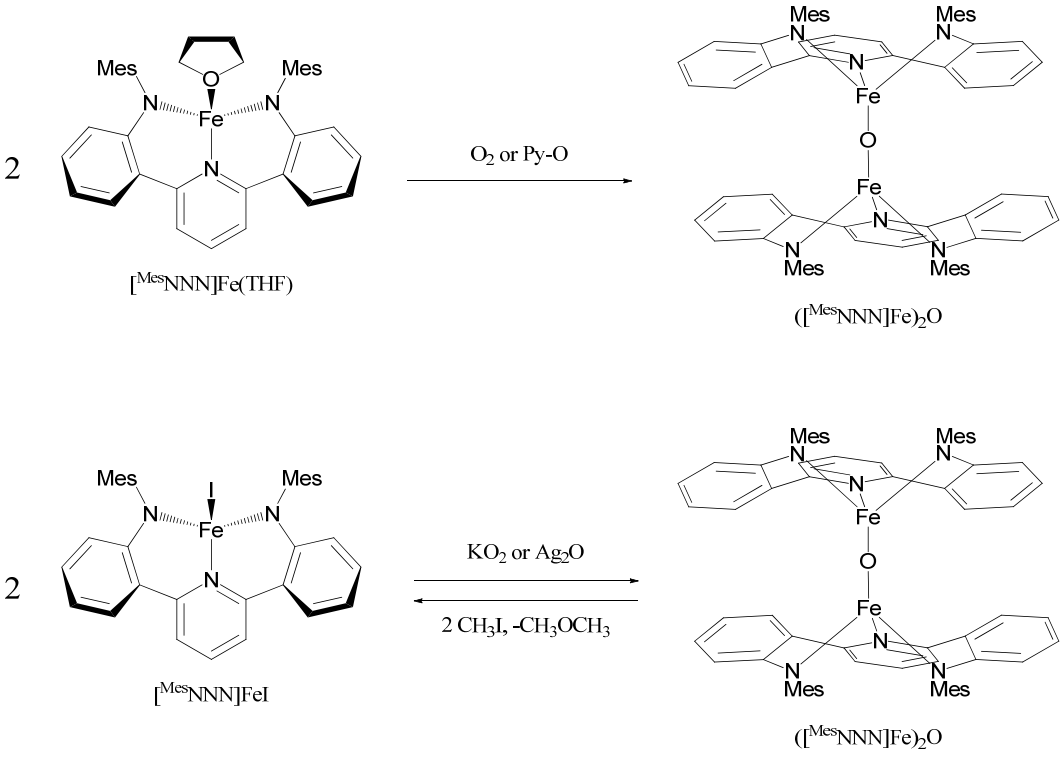

Scheme 3.4. Formation and reactions of $([^{Mes}NNN]Fe)_2O$.

knowledge, an unprecedented example of a C-O bond formation from a Fe^{III}-O-Fe^{III} dimer. This lack of precedence is somewhat surprising given the ubiquity of such dimers in iron chemistry. It is notable, however, that Holland has also observed C-O formation from an Fe^{II}-O-Fe^{II} dimer.[3]

THF displacement was attempted with several L-type ligands. THF self-exchange is apparent by broadening and shifting of the free THF peaks in a C_6D_6 solution of $[^{Mes}NNN]Fe(THF)$ and excess THF (Scheme 3.5). Exposure to an

(3) Sadique, A. R.; Brennessel, W. W.; Holland, P. L. *Inorg. Chem.* **2008**, *47*, 784–786.

atmosphere of ethylene results in the disappearance of the ^{1}H NMR of [^{Mes}NNN]Fe(THF) and the appearance of new peaks. Neither free ethylene nor free

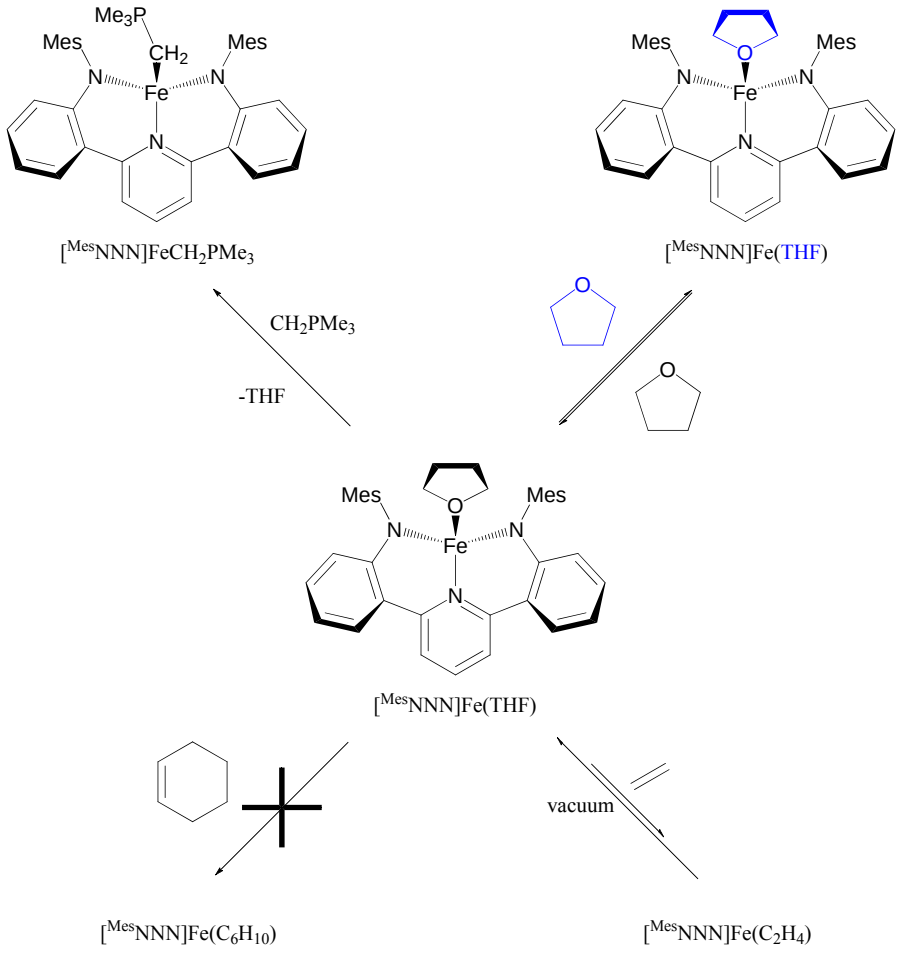

Scheme 3.5. Ligand exchange reactions of [^{Mes}NNN]Fe(THF).

THF are detected, possibly due to paramagnetic broadening resulting from fast ligand exchange processes. Concerning the latter observation, it is also possible that the THF remains bound. Carrying out three freeze-pump-thaw cycles results in the reappearance of the starting material. In contrast, excess cyclohexene fails to react with [^{Mes}NNN]Fe(THF). The reaction of [^{Mes}NNN]Fe(THF) with an excess of the

phosphorus ylide CH_2PMe_3 produces the adduct, [^{Mes}NNN]FeCH_2PMe_3. [^{Mes}NNN]FeCH_2PMe_3 exhibits 11 ^{1}H resonances and 1 ^{31}P resonance, as predicted for a C_s symmetric structure. X-ray quality crystals were grown by layering pentane on a benzene solution (Figure 3.1). The Fe-C bond distance of 2.137(3) is comparable to those in triphenylphosphonium methylidene adducts of iron.[4,5] The structure of [^{Mes}NNN]FeCH_2PMe_3 differs significantly from that of [^{Mes}NNN]Fe(THF) (Figure 3.2). The anilide nitrogen-iron-anilide nitrogen angle for

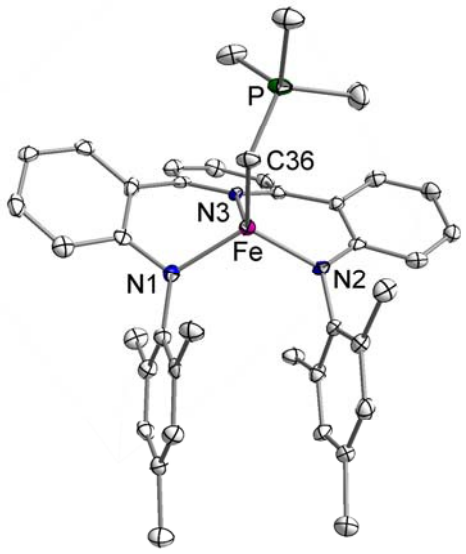

Figure 3.1. Structure of [^{Mes}NNN]FeCH_2PMe_3 with displacement ellipsoids at the 50% probability level. Hydrogen atoms and solvent were omitted for clarity. Selected bond lengths (Å) and angles(deg): Fe-N2, 1.964(2); Fe-N1, 1.974(2); Fe-N3, 2.062(2); Fe-C36, 2.137(3); N2-Fe-N1, 116.38(9); N2-Fe-N3, 92.16(10); N1-Fe-N3, 89.71(10); N2-Fe-C36, 120.06(11); N1-Fe-C36, 114.93(11); N3-Fe-C36, 116.94(10).

(4) Guerchais, V.; Astruc, D.; Nunn, C. M.; Cowley, A. L. *Organometallics* **1990**, *9*, 1036–1041.

(5) Nakazawa, H.; Yamaguchi, Y.; Mizuta, T.; Ichimura, S.; Miyoshi, K. *Organometallics* **1995**, *14*, 4635–4643.

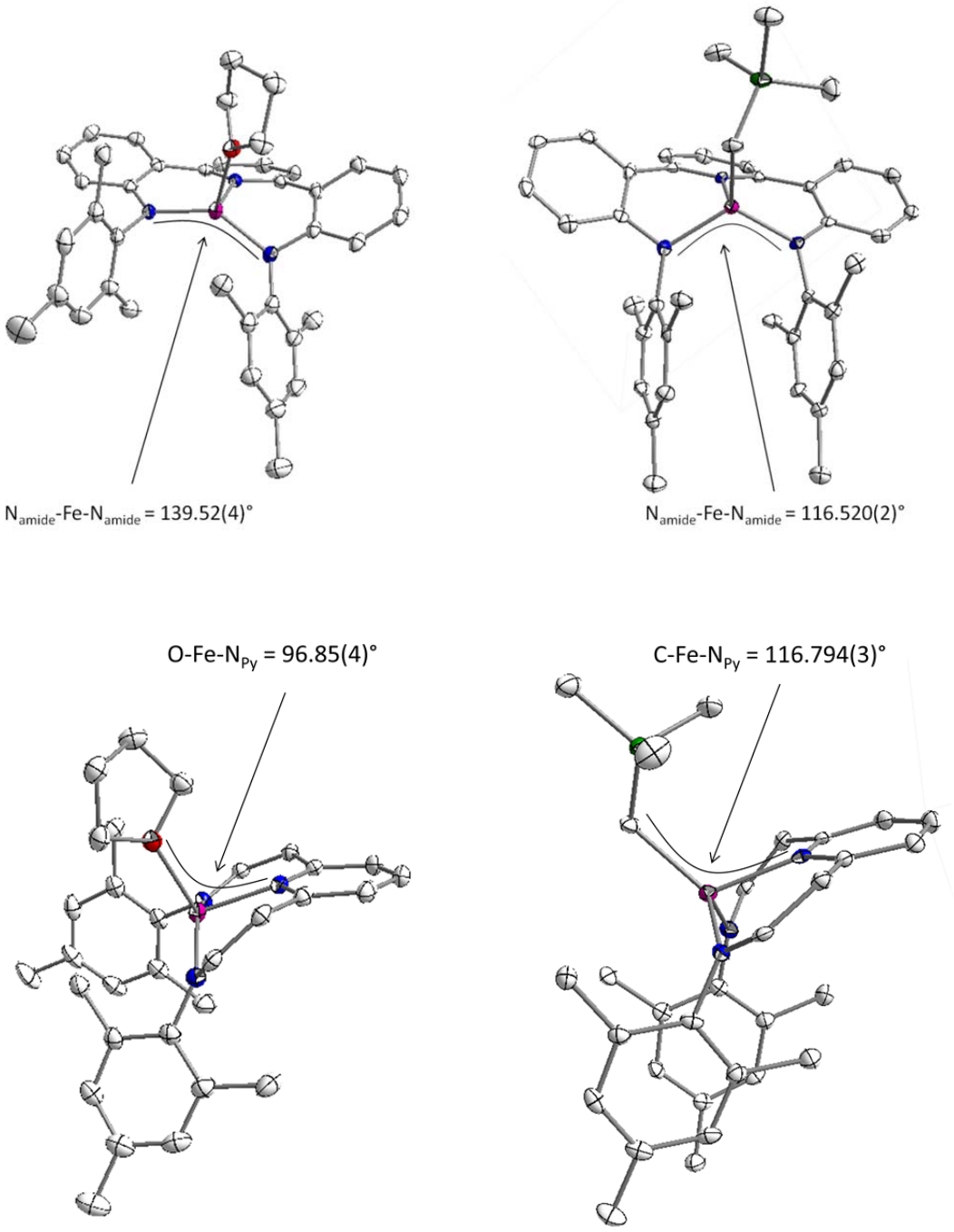

Figure 3.2 Contrasting iron geometries in [^{Mes}NNN]Fe(THF) (left) and [^{Mes}NNN]FeCH_2PMe_3 (right). Top: Different N_{amide}-Fe-N_{amide} bond angles. Bottom: Different N_{Py}-Fe-X (X = O or C) angles, with part of the benzene rings in the ligand cut away for clarity.

former is ~23° smaller than in the latter (116.38°(9) and 139.52°(4), respectively). Additionally, the pyridine nitrogen-iron-carbon angle in [^{Mes}NNN]FeCH$_2$PMe$_3$ (116.94°(10)) is ~20° larger than the pyridine nitrogen-iron oxygen angle in [^{Mes}NNN]Fe(THF) (96.85°(4)). This effect may be due to greater steric repulsion between the larger THF and the *o*-methyls of the aryl rings in [^{Mes}NNN]Fe(THF). [^{Mes}NNN]FeCH$_2$PMe$_3$ was sought in part to access a transient Fe=CH$_2$ species, possibly stabilized by the PMe$_3$ byproduct (Scheme 3.6). The methylidene could

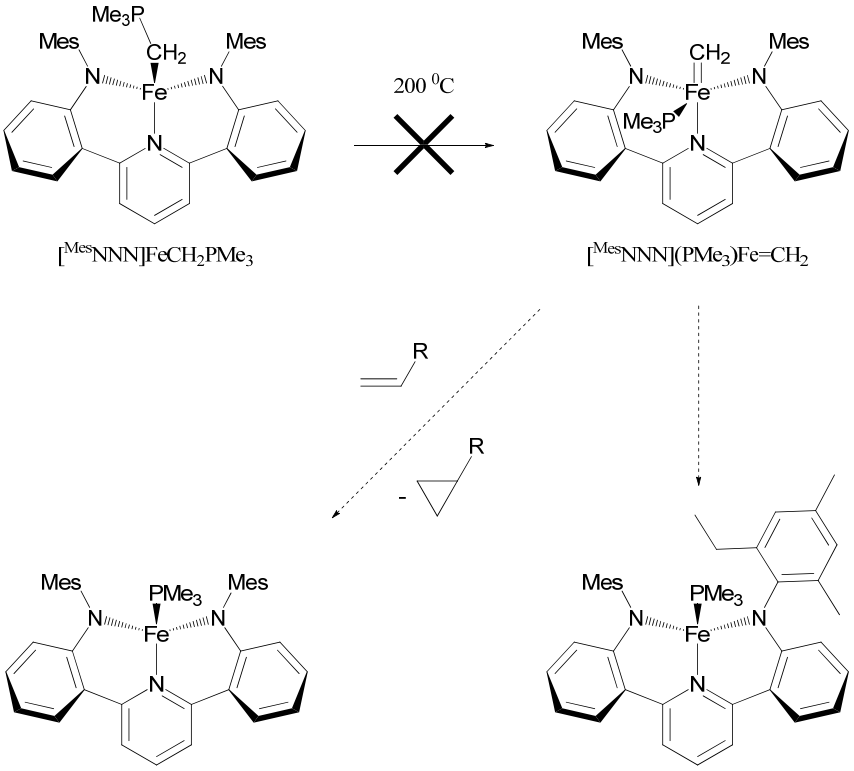

Scheme 3.6. Attempted reactivity with [^{Mes}NNN]FeCH$_2$PMe$_3$.

then undergo intramolecular C-H activation, as seen for organic azides (see chapter 4). Alternatively, methylene transfer would be possible if

"[^{Mes}NNN](PMe$_3$)Fe=CH$_2$" is long lived enough to prevent decomposition. Unfortunately, attempted thermolysis of [^{Mes}NNN]FeCH$_2$PMe$_3$ in d$_{10}$-*o*-xylene at 200 °C did not give any reaction after ~13 days. Heating in the presence of ethylene (90 °C) or norbornene (200 °C) did not lead to any reaction, so it is unlikely that the intermediate methylidene is present in any significant concentration. It should be noted that a more convenient method for the preparation of the free ylide CH$_2$PMe$_3$ has been found (see experimental).

Experimental

General Methods: Unless otherwise specified, air exposed solids were dried under vacuum prior to use, liquids were degassed or bubbled with argon, reagents were used as received from the supplier, and reactions were performed under an inert atmosphere or vacuum. All air and moisture sensitive compounds were handled using standard glovebox and high-vacuum line techniques. Argon and ethylene were purified by passage over MnO on vermiculite then 4 Å molecular sieves. Toluene was dried via Grubbs' method,[6] vac. transferred onto sodium/benzophenone, then vac. transferred and stored on titanocene dihydride. Benzene and pentane were dried via Grubbs' method, dried with 3 Å molecular sieves, then vac. transferred and stored on titanocene dihydride. THF was dried via Grubbs' method, then vac. transferred and stored on sodium/benzophenone.

(6) Pangborn, A. B.; Giardello, M. A.; Grubbs, R. H.; Rosen, R. K.; Timmers, F. J. *Organometallics* **1996**, *15*, 1518–1520.

Deuterated benzene and tetrahydrofuran were obtained from Cambridge Isotope Laboratories. Deuterated benzene, toluene, and tetrahydrofuran were dried with disodium benzophenone, then subsequently dried using titanocene dihydride. Methyl iodide was obtained from Aldrich, vac. transferred and stored on 3 Å molecular sieves and copper metal under vacuum at 0° C and shielded from light. Copper metal was obtained from Fisher. Sodium and benzophenone were obtained from Lancaster and MCB reagents, respectively. 3 Å molecular sieves were obtained from Aldrich, and dried at ~200° C under high vacuum for 1 day. Trimethylsilylmethyllithium was sublimed before use. Tetramethylphosphonium bromide was obtained from Strem. CH_2PMe_3 was prepared from Me_4PBr and KH using a slightly modified version of the published procedure (see below).[7] [^{Mes}NNN]Fe(THF), [^{Mes}NNN]FeI, and ([^{Mes}NNN]Fe)$_2$O were prepared as described above. NMR spectra were recorded on Varian Mercury 300 Megahertz NMR or Varian Inova 500 Megahertz spectrometers. ^{1}H and ^{13}C spectra were referenced according to the solvent residual peak.[8] The ^{31}P spectrum was referenced to an 85% H_3PO_4 solution = 0 ppm. Solution magnetic moments were determined via Evans Method. The paramagnetism of the iron complexes precluded assignment of peaks in their ^{1}H NMR spectra. The paramagnetism also implies that the integrations must

(7) Although the preparation in this paper calls for $NaNH_2$, a footnote by the checker recommends KH. This substitution allows the reaction to proceed at room temperature. Schmidbaur, H. *Inorg. Synth.* **1978**, *18*, 135–140.

(8) Fulmer, G. R.; Miller, A. J. M.; Sherden, N. H.; Gottlieb, H. E.; Nudelman, A.; Stoltz, B. M.; Bercaw, J. E.; Goldberg, K. I. *Organometallics* **2010**, *29*, 2176–2179.

only be regarded as rough estimations. X-ray diffraction data were obtained on a Bruker KAPPA APEXII. Elemental analyses were carried out by Robertson Microlit Laboratories, Madison, N.J. 07940. Data from elemental analyses are reported as the average of two runs.

Modified synthesis of CH_2PMe_3. Tetramethylphosphonium bromide (1.5379 g, 8.9925 mmol) and potassium hydride (422.7 mg, 10.54 mmol) were combined in a 100 mL roundbottom flask equipped with an 180° teflon valve. On a high vacuum line, 20 mL of diethyl ether were vac. transferred from a Cp_2TiH_2 pot onto the solids at -60 °C, then stirred and allowed to warm to ambient temperature. Most of the solid remained undissolved. The reaction was monitored by observing the pressure increase using a mercury bubbler. Stirring is vital to the reaction, as pressure change ceased upon stopping the stirbar. After 17 hours, no further pressure increase was observed. The solution was cooled to -78 °C and degassed. The solution was warmed to ambient temperature and the volatiles (diethyl ether and CH_2PMe_3) were vac. transferred to a new vessel cooled to -78 °C. This vessel contained a clear solution and white solid. The vessel was warmed to -45 °C using a dry-ice acetonitrile bath. The diethyl ether was removed by vac. transfer from the donor vessel (-45 °C) to the receiving vessel (-78 °C) for 40 minutes, leaving a white solid that melted to a clear liquid at room temperature. 460.5 mg of the product were obtained in 57% yield, with a small diethyl ether impurity.

Reaction of [^{Mes}NNN]Fe(THF) with CH_3I. ~0.5 mL of C_6D_6 was vac. transferred onto the iron complex (4.7 mg, 7.5 μmol) and the NMR tube was shielded from light. Methyl iodide (0.01 mL, 0.2 mmol) was vac. transferred onto the frozen

solution, then allowed to thaw. After ~2 hours, ^{1}H NMR indicated that [^{Mes}NNN]FeI was the only iron containing product, and that ethane was present.

Reaction of [^{Mes}NNN]FeI with CH_3Li. [^{Mes}NNN]FeI (9.3 mg, 0.014 mmol) and methyllithium (0.3 mg, 0.01 mmol) were combined as solids in a J-Young NMR tube, then treated with ~0.5 mL of C_6D_6. After ~13 hours, no [^{Mes}NNN]FeI remained, and some ethane was detected. A new species was also present, with the following peaks. ^{1}H NMR (300 MHz, C_6D_6): δ 35.84 (1H), 71.59 (5H), 82.19 (1H), 94.17 (3H), 107.68, 112.31 (overlap, 8H total), 128.94 (1H). Over the course of days, decomposition to a mixture of compounds occurred and ethane continued to grow in.

Reaction of [^{Mes}NNN]FeI with $Na(MeO)_3BH$. In a glovebox, ~1 mL solutions of [^{Mes}NNN]FeI (12 mg, 18 μmol) and sodium trimethoxyborohydride (2.3 mg, 18 μmol) were cooled to -30° C, then combined. After 75 minutes, the solution was concentrated in vacuo. A ^{1}H NMR spectrum of the residue in C_6D_6 revealed [^{Mes}NNN]Fe(THF) as the sole iron containing product.

Reaction of [^{Mes}NNN]FeI with $Cr(C_6H_6)_2$. [^{Mes}NNN]FeI (6.0 mg, 8.8 μmol) and bis(benzene) chromium (1.8 mg, 8.8 μmol) were combined as solids in a J-Young NMR tube. d_8-THF was vac. transferred onto the solids. Upon warming, solid precipate was observed. After 15 minutes, the conversion to [^{Mes}NNN]Fe(THF) as the only product was observed.

Reaction of [^{Mes}NNN]FeI with Ag_2O. [^{Mes}NNN]FeI (4.8 mg, 7.1 μmol) and silver I oxide (6.8 mg, 29 μmol) were combined as solids in a J-Young NMR tube. The tube was shielded from light. d_8-THF was vac. transferred onto the solids, and the

headspace was filled with argon. The solution was heated at 80 °C. After 29 hours, conversion to ([^{Mes}NNN]Fe)$_2$O was complete.

Reaction of ([^{Mes}NNN]Fe)$_2$O with Excess CH_3I. In a glovebox, ([^{Mes}NNN]Fe)$_2$O (8.1 mg, 7.2 μmol) was dissolved in 500 μL of d_8-toluene and transferred to a J-Young tube. The NMR tube was shielded from light. Methyl iodide (0.01 mL, 0.2 mmol) was vac. transferred onto the solution, and the tube was filled with ~1 atmosphere of argon. The solution was heated to 120 °C. ^{1}H peaks for [^{Mes}NNN]FeI and dimethyl ether gradually appeared, and after 20 hours, no resonances for ([^{Mes}NNN]Fe)$_2$O remained. Some [^{Mes}NNN]H$_2$ gradually appeared over the course of the reaction, indicating some decomoposition as well.

Reaction of [^{Mes}NNN]FeI with KO_2. [^{Mes}NNN]FeI (5.0 mg, 7.4 μmol) and potassium superoxide (1.0 mg, 15 μmol) were combined as solids in a J-Young NMR tube. ~0.5 mL of d_8-THF was vac. transferred onto the solids. After ~86 hours, ^{1}H resonances due to [^{Mes}NNN]FeI had completely disappeared and new peaks due to ([^{Mes}NNN]Fe)$_2$O had appeared.

Reaction of [^{Mes}NNN]Fe(THF) with C_2H_4. [^{Mes}NNN]Fe(THF) (4.8 mg, 7.7 μmol) was added to a J-Young NMR tube. ~0.5 mL of C_6D_6 was vac. transferred onto the solid, and the solution was put under an atmosphere of ethylene. The following spectrum was observed. ^{1}H NMR (300 MHz, C_6D_6): δ -65.73, -48.89, 6.42, 15.52, 40.84, 53.06, 54.95, 60.14, 61.86. Carrying out three freeze-pump-thaw cycles resulted in the reappearance of [^{Mes}NNN]Fe(THF).

Synthesis of [^{Mes}NNN]FeCH_2PMe_3. [^{Mes}NNN]Fe(THF) (233.2 mg, 0.3740 mmol) was loaded into a 100 mL roundbottom flask, which was equipped with a 180°

teflon valve. ~25 mL of benzene were vac. transferred onto the solid. Trimethylphosphonium methylidene (0.1 mL, 1 mmol) was vac. transferred onto the solution, and the solution was stirred for 3 hours. The volatiles were removed in vacuo. The flask was attached to a swivel frit apparatus, and ~50 mL of benzene were vac. transferred onto the solid. The solution was filtered, and the filtrate was concentrated to a solid. [^{Mes}NNN]FeCH$_2$PMe$_3$ was isolated in 69% yield. ^{1}H NMR (C_6D_6): δ -53.28, -38.61, -1.84, 22.57, 27.02, 39.83, 44.77, 45.96, 64.69, 70.52, 79.64. ^{31}P NMR (d_8-toluene): δ -13.92. Anal. Calcd. for $C_{39}H_{44}FeN_3P$: C, 73.01; H, 6.91; N, 6.55. Found: C, 71.58; H, 6.59; N, 6.71. X-ray quality crystals were grown by layering pentane on a saturated benzene solution. The crystal data is summarized as follows: formula, $C_{39}H_{44}FeN_3P \cdot 1.5(C_6H_6)$; formula weight, 758.75; lattice system, monoclinic; space group $P2_1/n$ (No. 14); temperature 100(2) K; lattice parameters a = 10.0318(4) Å, b = 37.7399(15) Å, c = 10.8356(4) Å, β = 98.561(2)°; unit cell volume V = 4056.6(3) Å^3; calculated density D_{calc} = 1.242 g/cm^3; number of molecules in the unit cell Z = 4; linear absorption coefficient μ = 0.448 mm^{-1}; no empirical absorption correction; MoKα radiation recorded on a Bruker KAPPA APEX II diffractometer; 32506 reflections collected, 9557 unique reflections, 6045 unique reflections used with I > 2σ(I); θ_{max} = 28.31°; 9557 parameter; 0 restraints; H atoms were placed in calculated positions; all other atoms were refined anisotropically, full matrix least-squares on F^2 refinement method; reliability factor R for all data = 0.1102 (for data $I > 2\sigma(I)$ = 0.0630), weighted reliability factor R_w = 0.1148 (for data $I > 2\sigma(I)$ = 0.1094), goodness-of-fit on F^2, 1.292. Crystallographic data have been deposited at the CCDC, 12 Union Road,

Cambridge CB2 1EZ, UK. Copies can be obtained on request, free of charge, by quoting the publication citation and the deposition number 785426 or by visiting http://www.ccdc.cam.ac.uk/data_request/cif.

Chapter 4
Iron Promoted C-H Bond Activation via Organic Azides

Introduction

Nitrene transfer is a synthetic strategy for the production of amines or aziridines (Scheme 4.1). This strategy has the potential for efficient routes to these desirable compounds, and minimal waste. Much of the early work in this field focused on tosyliminoiodinanes and related reagents.[1] Uncatalyzed nitrene transfer by thermolysis or photolysis of organic azides has been known since the 19th century.[2] The use of organic azides as nitrene sources for iron catalysis, however, is a new direction for the field. Azides possess the advantage that the only byproduct is N_2, rather than stoichiometric iodoarene for iminoiodinane-type reagents.

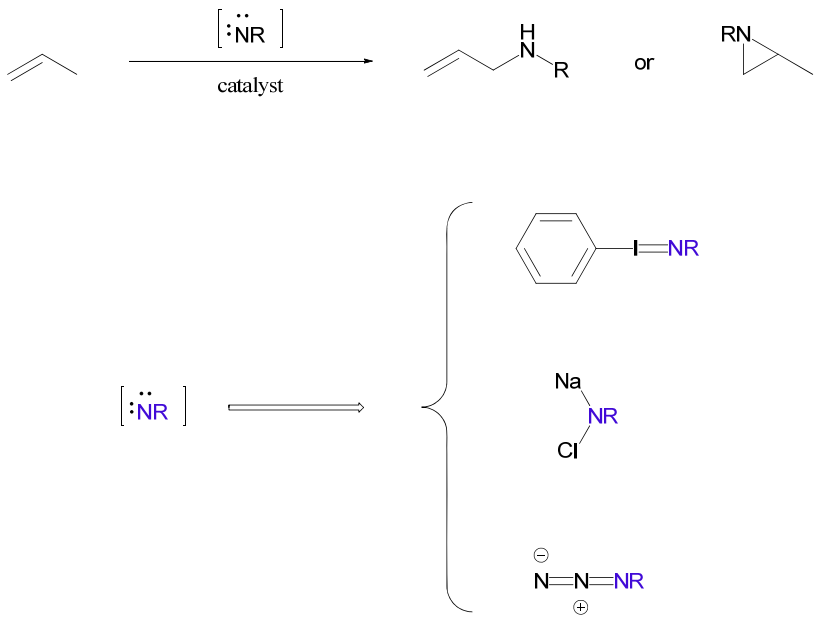

Scheme 4.1. Nitrene transfer as a synthetic strategy and common nitrene precursors.

(1) Collet, F.; Dodd, R. H.; Dauban, P. *Chem. Commun.* **2009**, 5061–5074.

(2) Bräse, S.; Gil, C.; Knepper, K.; Zimmermann, V. *Angew. Chem. Int. Ed.* **2005**, *44*, 5188–5240.

In the past five years significant progress has been made in this arena. Nacnac and dipyrrolemethane iron complexes initially exhibited stoichiometric ligand activations with organic azides, from the groups of Holland[3] and Betley[4] respectively (Scheme 4.2). Through rational ligand modification, they discovered catalytic systems (Scheme 4.3).[5,6] Additionally, Che observed nitrene catalysis

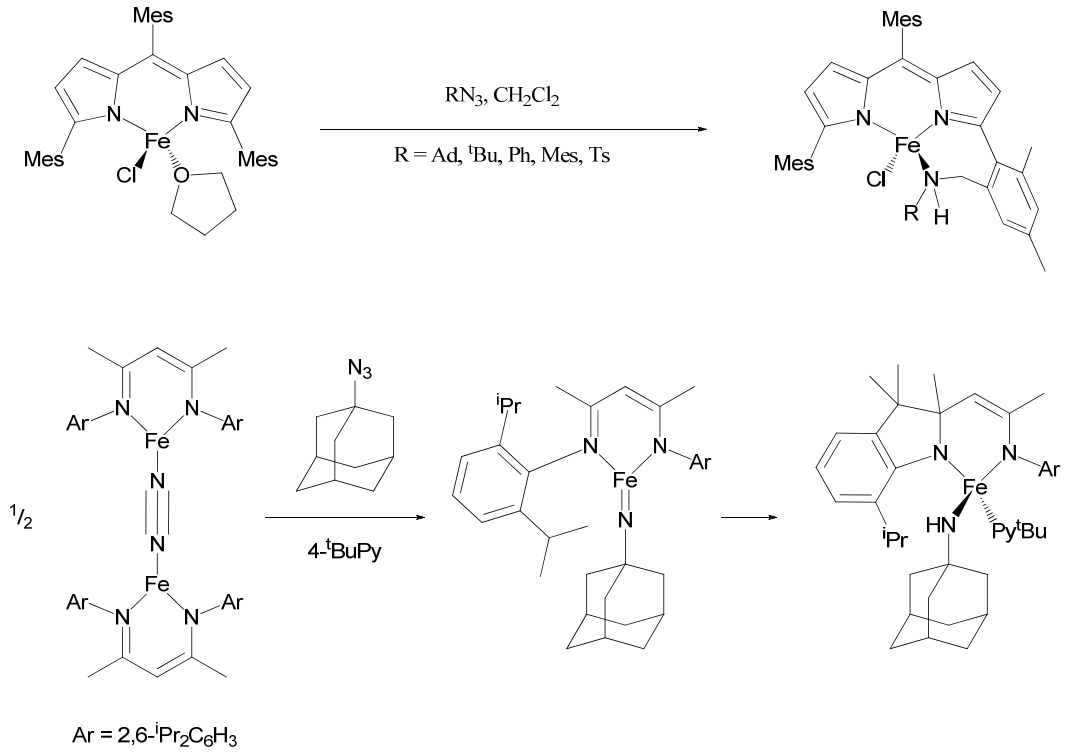

Scheme 4.2. Intramolecular C-H activation of iron complexes with organic azides.

(3) Eckert, N. A.; Vaddadi, S.; Stoian, S.; Lachicotte, R. J.; Cundari, T. R.; Holland, P. L. *Angew. Chem. Int. Ed.* **2006**, *45*, 6868–6871.

(4) King, E. R.; Betley, T. A. *Inorg. Chem.* **2009**, *48*, 2361–2363.

(5) Cowley, R. E.; Eckert, N. A.; Elhaïk, J.; Holland, P. L. *Chem. Commun.*, **2009**, 1760–1762.

(6) King, E. R.; Hennessy, E. T.; Betley, T. A. *J. Am. Chem. Soc.* **2011**, *133*, 4917–4923.

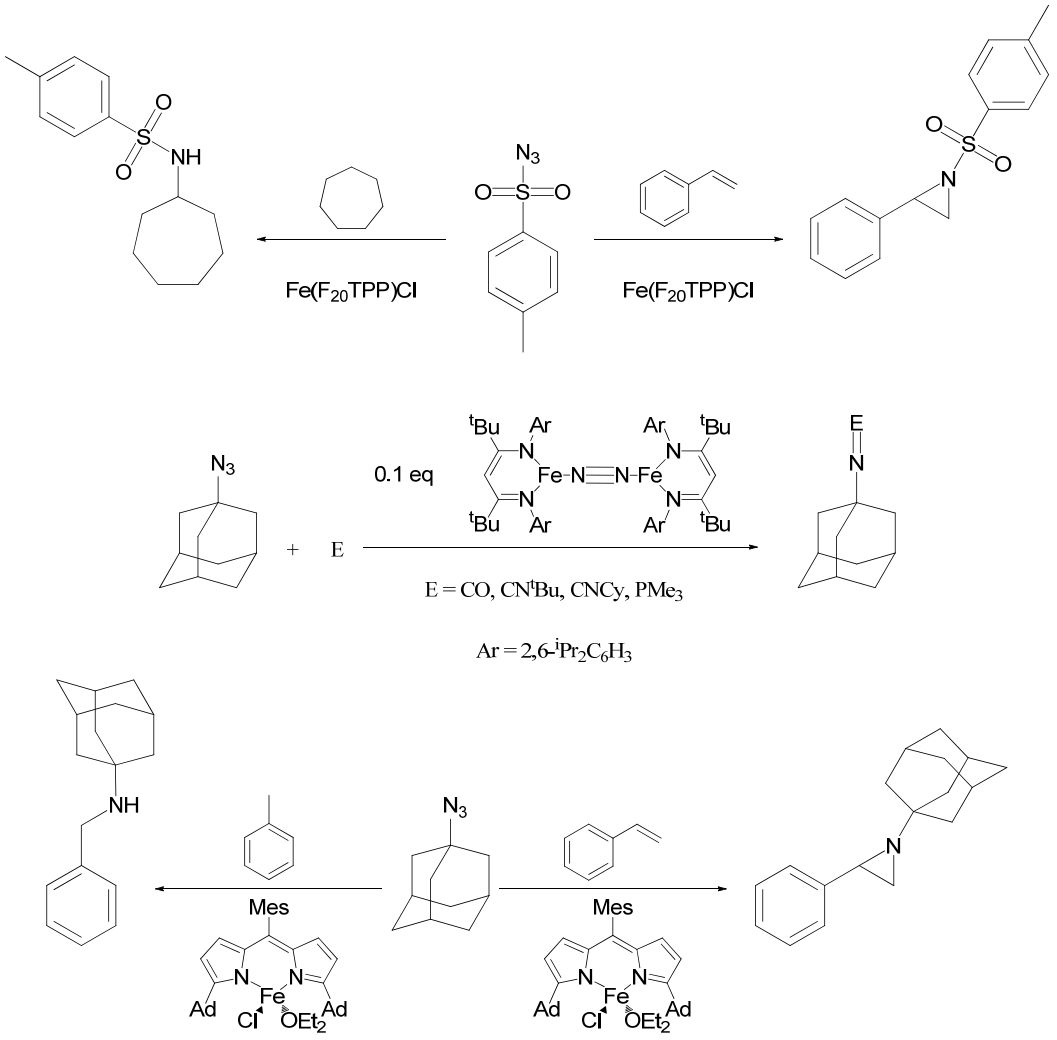

Scheme 4.3.: Iron-catalyzed nitrene transfer.

using a fluorinated porphyrin iron chloride.[7] Although the mechanism of azide interaction with iron catalysts has not been elucidated for most systems, the similarities to better-understood iron oxo systems suggest possible mechanistic overlap.

(7) Liu , Y.; Che, C. *Chem. Eur. J.* **2010**, *16*, 10494–10501.

Based on the above motivation, organic azide activation with [^{Mes}NNN]Fe complexes was considered. The reaction of [^{Mes}NNN]Fe(THF) with pyridine N-oxide or O_2 yields the bridging oxo dimer ([^{Mes}NNN]Fe)$_2$O. It is reasonable that the mechanism of this transformation involves a terminal iron oxo intermediate (Scheme 4.4). Thus there was some reason to believe that [^{Mes}NNN]Fe complexes could at least transiently support high valent RN=Fe^{IV} species. It was hypothesized that an isolobal iron imido species might not dimerize, due to the steric bulk of the R group on the imide. The long-term motivation for accessing iron imido species is

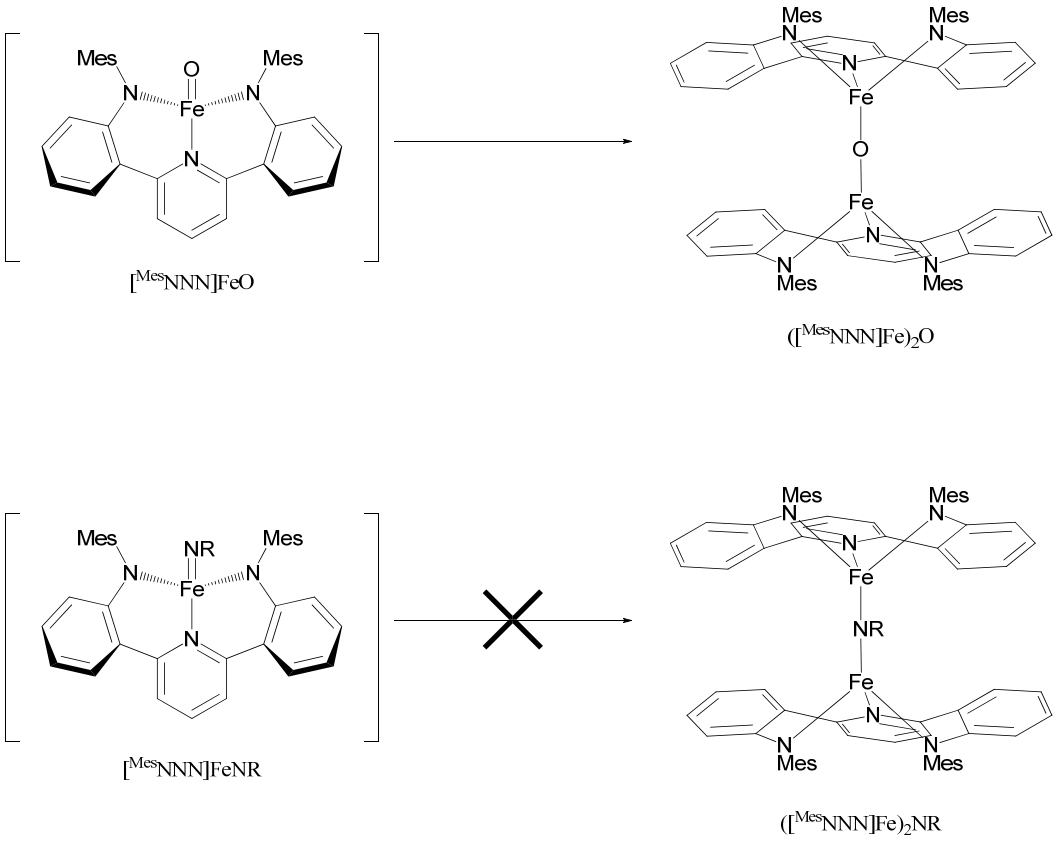

Scheme 4.4. Analogy between Fe oxo and Fe imido species, and possible preclusion of dimerization by using a sufficiently bulky R group on the imide.

their use in catalytic group transfer (Scheme 4.5).

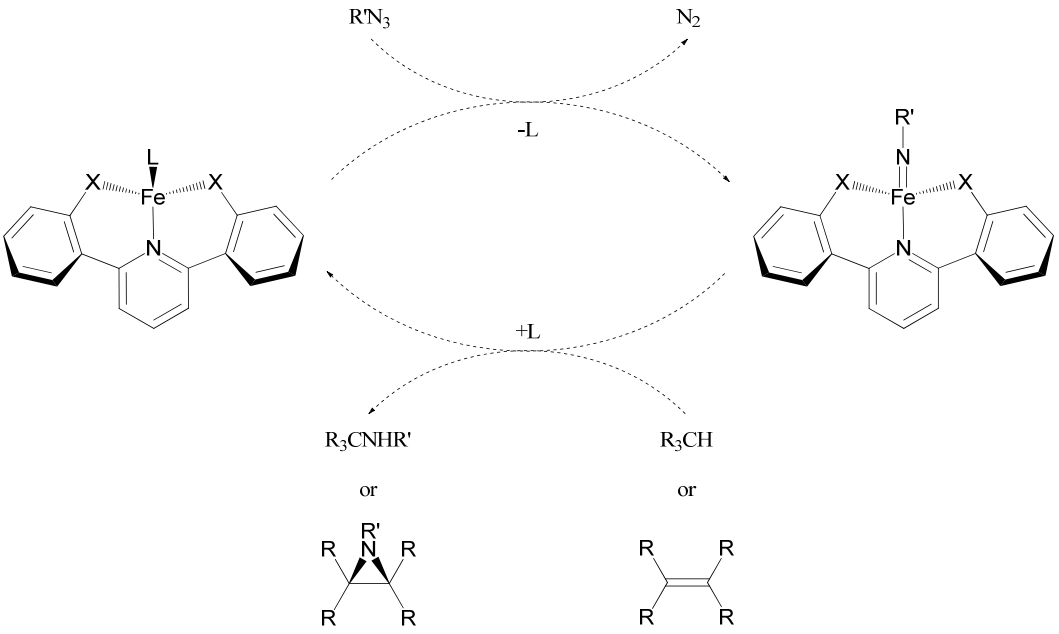

Scheme 4.5. Hypothetical catalytic cycle for nitrene transfer using iron pincer complexes.

Results and Discussion

Treatment of [^{Mes}NNN]Fe(THF) with either trimethylsilyl or 1-adamantyl azide led to complete consumption of the starting material peaks in the ^{1}H NMR spectrum (Scheme 4.6). A substantial increase in the number of product peaks was starting material. No further reactivity was observed in the presence of excess azide in either case. A crystal structure of the adamantyl substituted complex [^{Mes}NNN-NHAd]Fe was obtained (Figure 4.1). Although of poor quality, it confirms the identity of the complex.

To further confirm the above assignments, addition of water to the products produced the aminated free ligands (Scheme 4.7). The protonated ligands

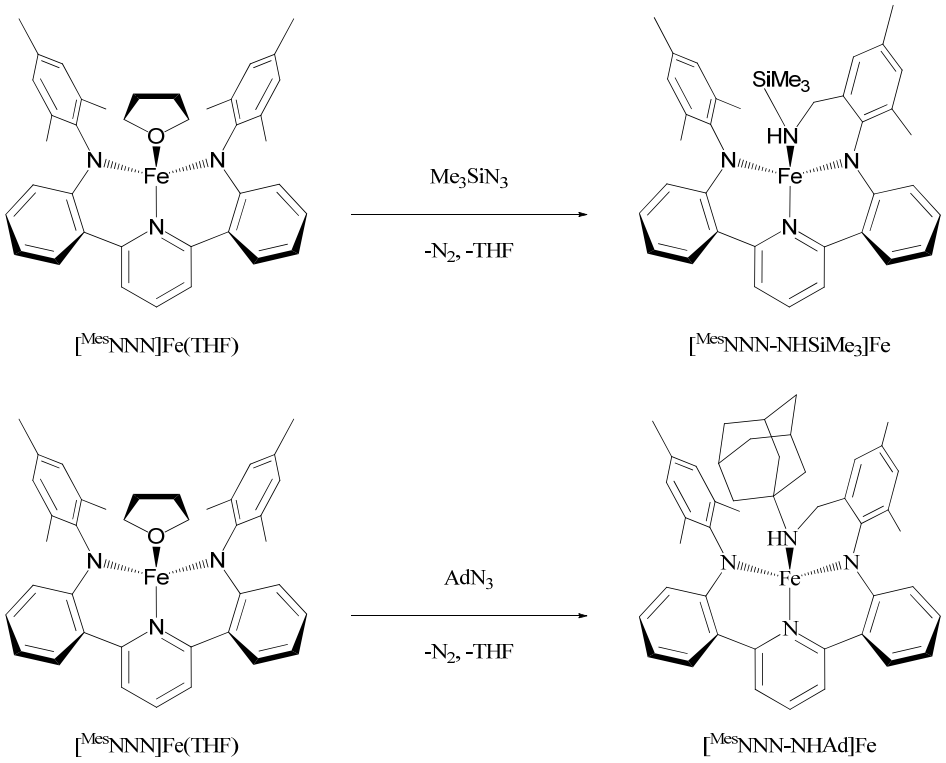

Scheme 4.6. Intramolecular C-H activation of [^{Mes}NNN]Fe(THF) with organic azides.

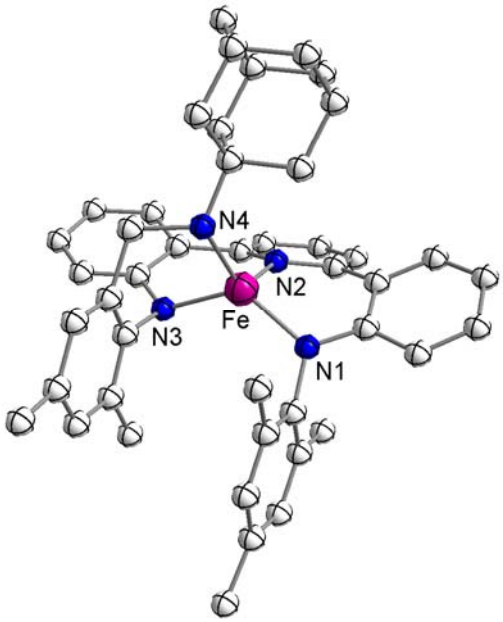

Figure 4.1. Isotropic structure of [^{Mes}NNN-NHAd]Fe.

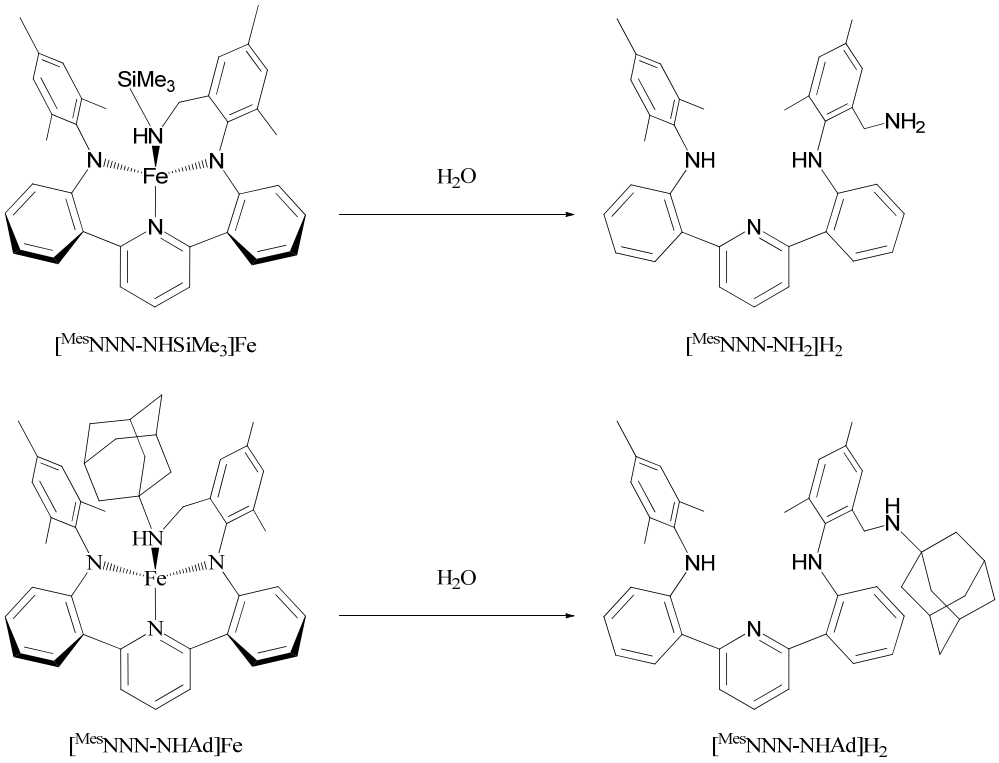

Scheme 4.7. Protonation of [^{Mes}NNN-NHR]Fe (R = $SiMe_3$, Ad).

[^{Mes}NNN-NHAd]H_2 and [^{Mes}NNN-NH_2]H_2 were characterized by ^{1}H, ^{13}C, and mass spectrometry. Addition of water to [^{Mes}NNN-$NHSiMe_3$]Fe not only protonates observed for both products, consistent with loss of C_s symmetry found in the the ligand, but also desilylates the pendant amine. Many peaks in the ^{1}H spectra of the protonated ligands were isochronous; however, the ^{13}C spectra unambiguously gave the expected number of peaks for the desymmetrized ligands. Both ligands gave the expected parent ion in fast atom bombardment (FAB^+) mass spectrometry. [^{Mes}NNN-NH_2]H_2 was characterized crystallographically (see appendix C). In order to confirm the presence of the trimethylsilyl group in the iron complex, a ^{29}Si NMR

spectrum was obtained (Figure 4.2). Indeed, a single resonance is observed, consistent with the assignment.

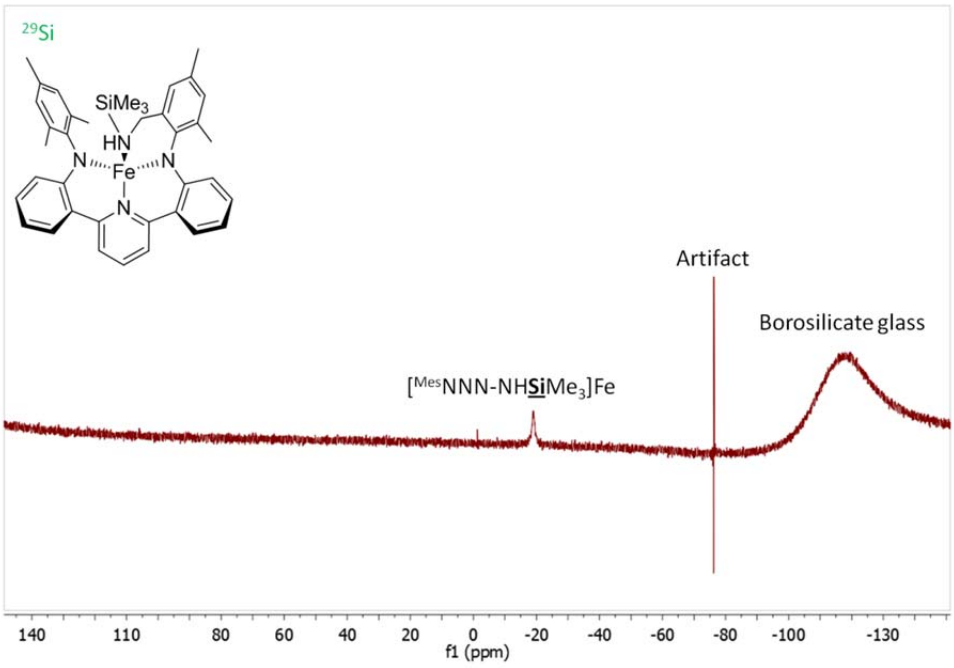

Figure 4.2. ^{29}Si NMR spectrum of [^{Mes}NNN-NHSiMe$_3$]Fe.

Given the interest in C-H amination, the reaction of [^{Mes}NNN]Fe(THF) with trimethylsilyl azide was explored in detail. The reaction was followed by observing the appearance of the product by ^{1}H NMR (Figure 4.3). The reaction was carried out under pseudo-first order conditions, with large excesses of trimethylsilyl azide and THF. The natural log of the concentration of [^{Mes}NNN]Fe(THF) decreases linearly with time, thus indicating that it is first order in the rate law (Figure 4.4). The effect of azide concentration on the reaction rate was also investigated. The pseudo-first order rate constant is linearly dependent on the concentration of trimethylsilyl azide (Figure 4.5). A plot of ln(k_{obs}) vs. ln([Me_3SiN_3]) has slope of

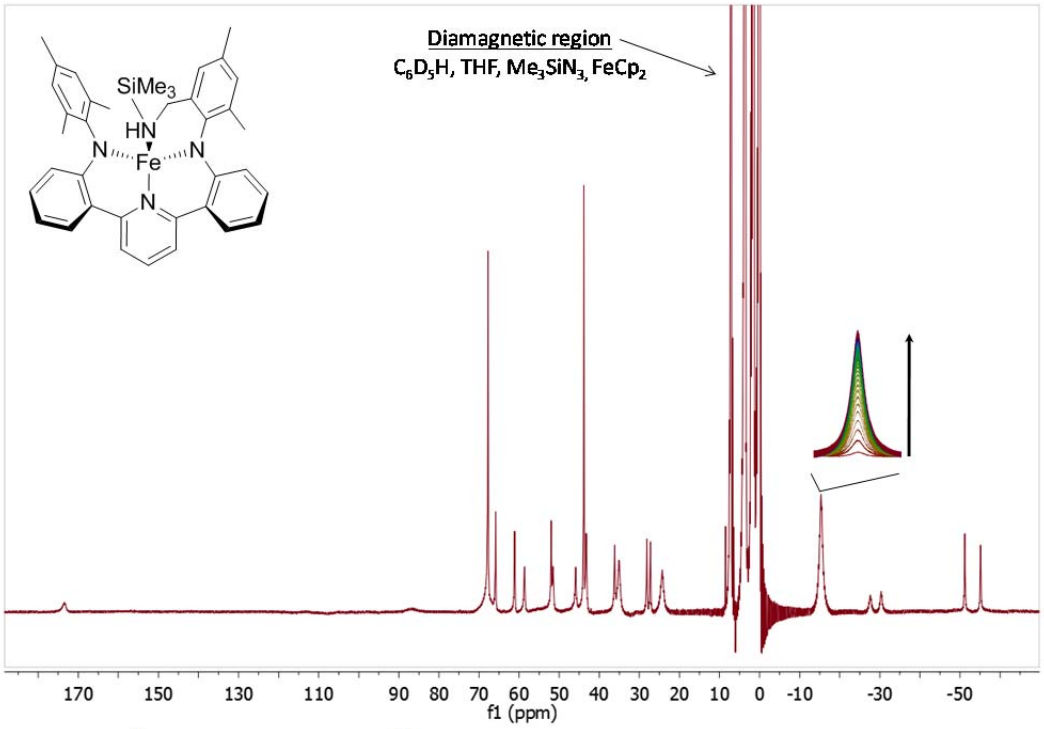

Figure 4.3. ^{1}H NMR spectrum of [^{Mes}NNN-NHSiMe$_3$]Fe, showing the peak monitored during kinetic runs.

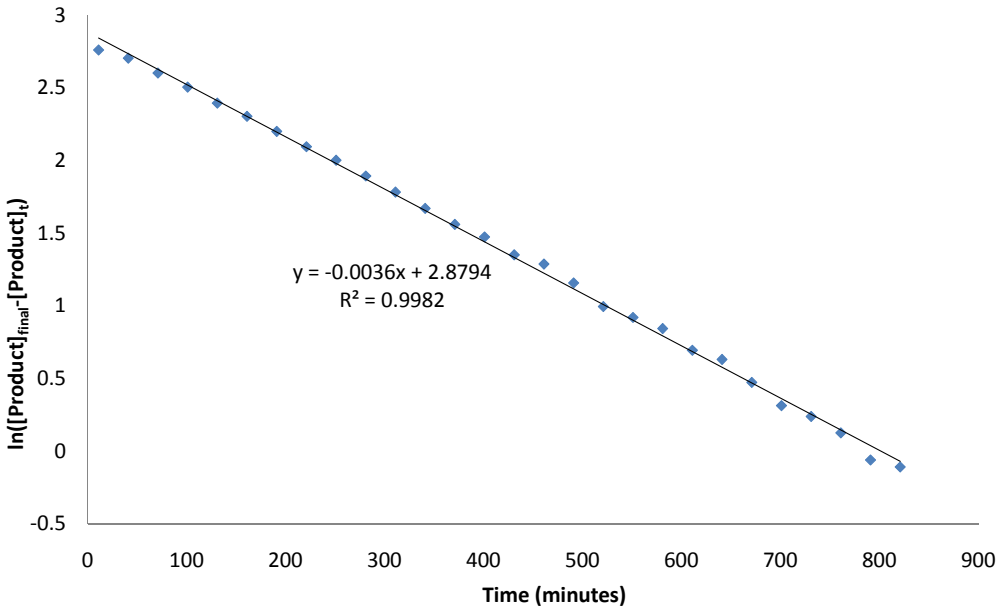

Figure 4.4. Pseudo-first order plot of [^{Mes}NNN]Fe(THF) consumption over time.

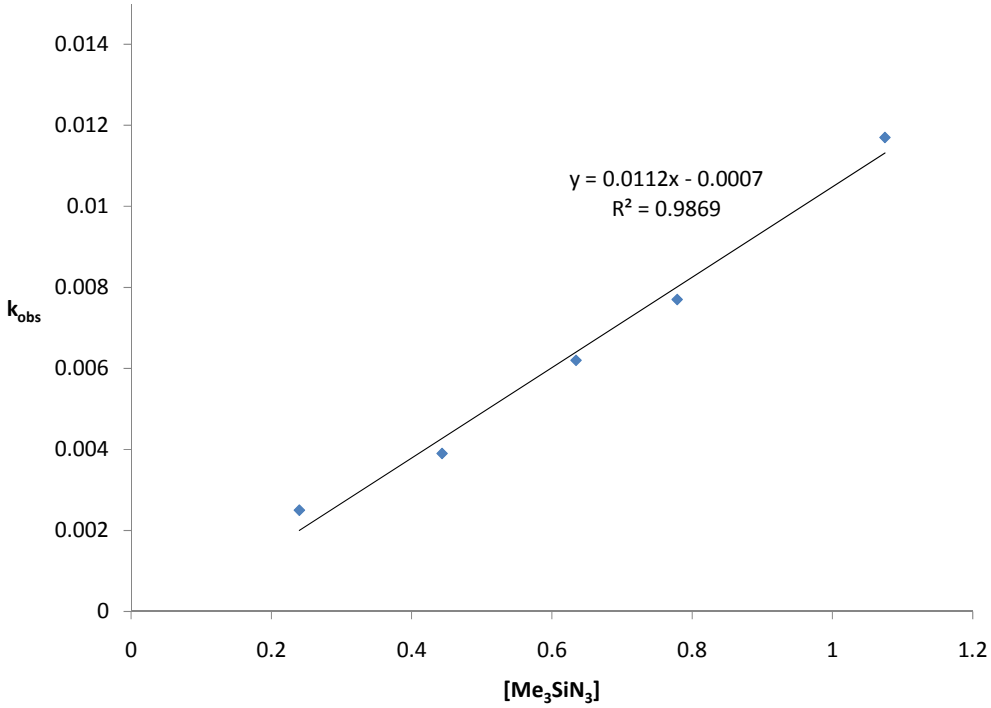

Figure 4.5. Plot of trimethylsilyl azide vs. pseudo-first order rate constant (min^{-1}).

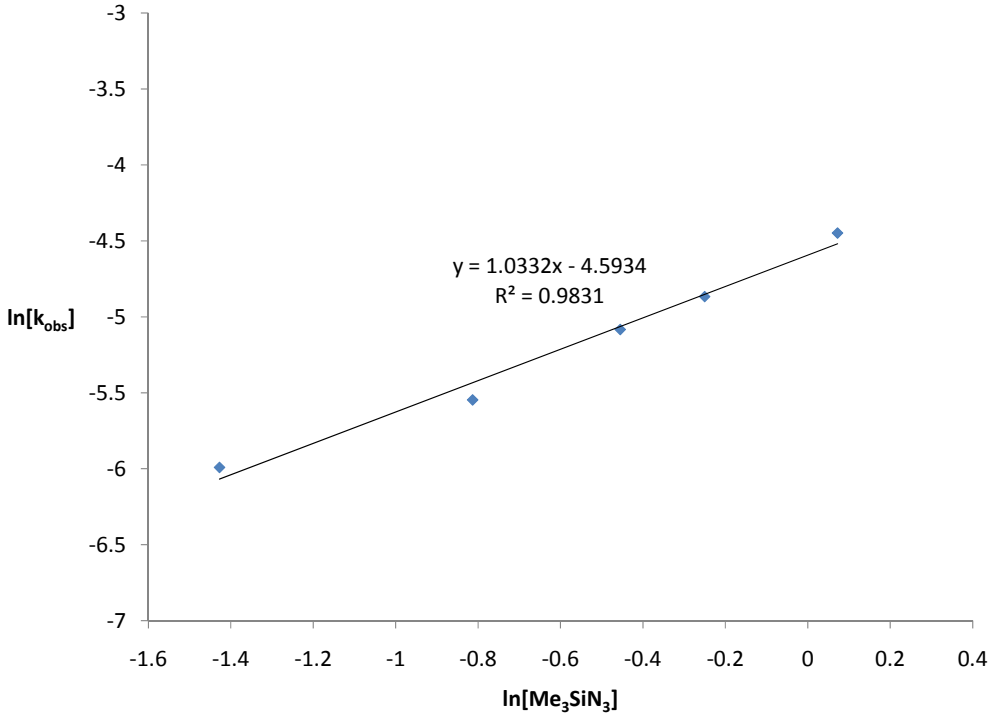

Figure 4.6. Plot of $ln([Me_3SiN_3])$ vs. $ln(k_{obs})$.

1.0, confirming that the azide is also first order in the rate law (Figure 4.6). Taking the quotient $(k_{obs})(THF)/(Fe)(Me_3SiN_3)$ for the five runs gives an average value of $8.0 \cdot 10^{-3}$ s^{-1} with a standard deviation of $6.3 \cdot 10^{-4}$.

Unfortunately, a more definitive study concerning the order of THF was unsuccessful. Decomposition and irreproducibility occur and at moderate to high THF concentrations such that a reasonable range of concentrations is not possible. Certain qualitative observations, however, indicate that THF is an inhibitor for the reaction. For identical concentrations of [^{Mes}NNN]Fe(THF) and azidotrimethylsilane, doubling the THF concentration gives a k_{obs} of half the value ([THF] = 1 M, $k_{obs} = 4 \cdot 10^{-3}$ min^{-1}, [THF] = 0.5 M, $k_{obs} = 8 \cdot 10^{-3}$ min^{-1}). While [^{Mes}NNN]Fe(THF) reacts with one equivalent of trimethylsilyl azide in ~13 hours in C_6D_6 at ambient temperature, it is unreactive in d_8-THF. Upon heating to 70 °C, the reaction goes to completion in ~66 hours with side products. The above observations concerning excess azide and THF inhibition suggest that ligand dissociation likely occurs either before or during the rate limiting step. Because THF is a monodentate ligand, it is reasonable from an entropic standpoint (i.e. the chelate effect) that its dissociation should be more facile than that the pendent amine donor in the product; thus the product is unreactive to additional azide. The reaction was run also run at -78 °C, in d_8-toluene with excess azidotrimethylsilane and no added THF. No reaction of [^{Mes}NNN]Fe(THF) was observed. The reaction was warmed by 10 degrees every hour. At -21 °C product began appearing. No intermediates were observed.

A tentative mechanism is proposed given the above observations (Scheme 4.8). THF inhibition is consistent with either a dissociative or associative mechanism. The latter is favored given the strained nature of a [^{Mes}NNN]Fe fragment, and the rarity of three-coordination for iron. As mentioned above, no intermediates are observed. This observation indicates that the equilibrium to form the azide adduct [^{Mes}NNN]FeN_3SiMe_3 may be unfavorable, or that the ligand exchange step may be rate-determining. N_2 extrusion to form [^{Mes}NNN]Fe=$NSiMe_3$ may also be rate-determining, and is very likely irreversible. Given the latter assumption, the last C-H activation step cannot be rate-determining or the imide intermediate would be a detectable intermediate.

Because [^{Mes}NNN]Fe(THF) reacts with organic azides intramolecularly, a new system was sought in order to bring about *intermolecular* imide transfer. The [^{tBu}NNN] ligand[8] was selected because it possesses similar electronic and steric properties to [^{Mes}NNN], but no reactive benzylic C-H bonds. X-ray quality crystals could grown by slow evaporation of either hexanes or acetonitrile solutions (see appendix C). Access to [^{tBu}NNN]Fe(THF) was attempted by the same metathetical route used to make the original [^{Mes}NNN]Fe(THF) complex (Scheme 4.9). By ^{1}H NMR one clean complex is formed in d_8-THF. Regrettably, attempts to scale up the synthesis have led to decomposition. This result may be a consequence of LiCl byproduct removal in the large scale reaction. The reaction of the *in situ* generated, putative [^{tBu}NNN]Fe(THF) was investigated for catalytic nitrene transfere with

(8) Tonks, I. A.; Tofan, D.; Weintrob, E. C.; Agapie, T.; Bercaw, J. E. *In preparation.*

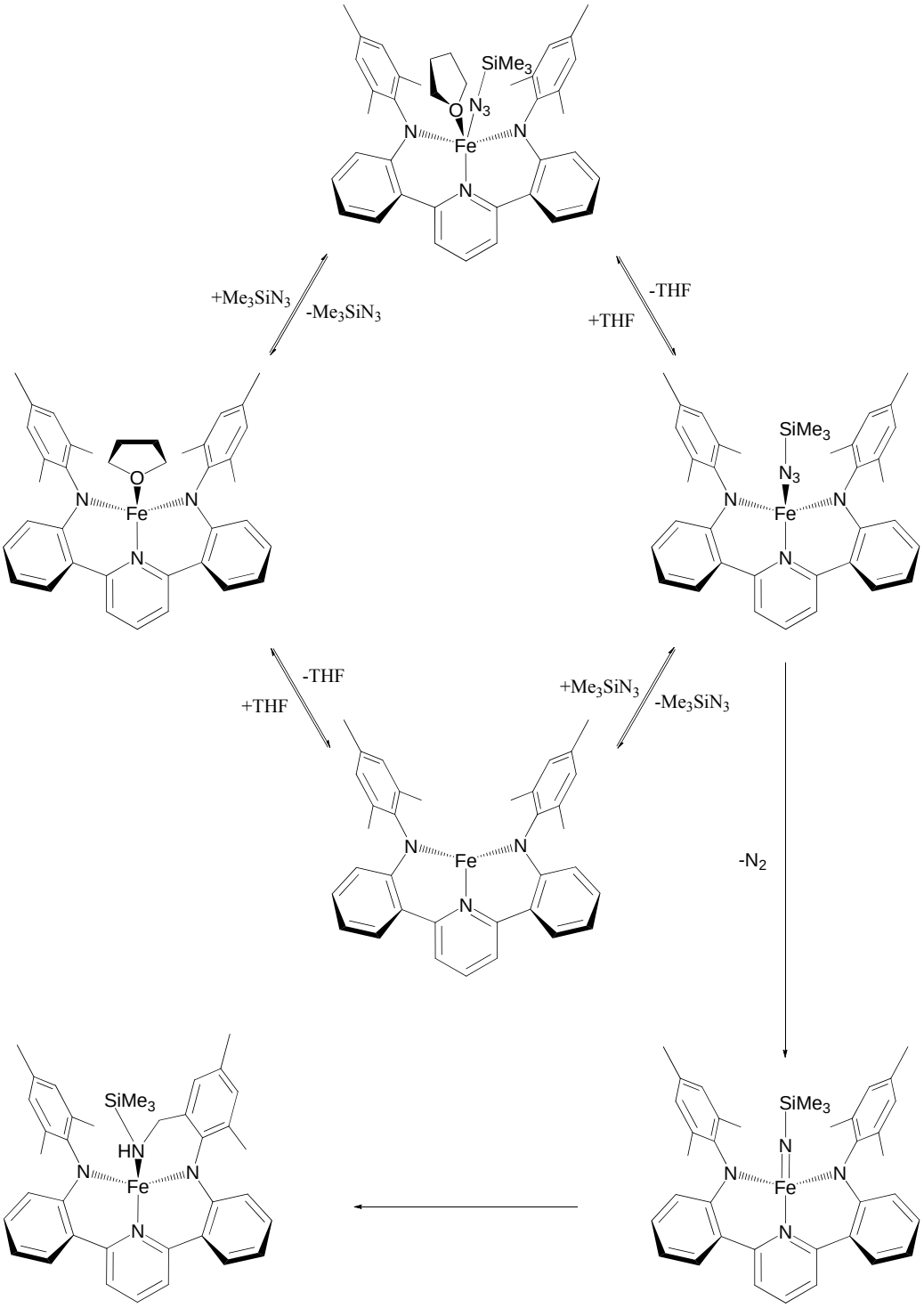

Scheme 4.8. Proposed reaction mechanism for the conversion of [^{Mes}NNN]Fe(THF) to [^{Mes}NNN-NHSiMe$_3$]Fe.

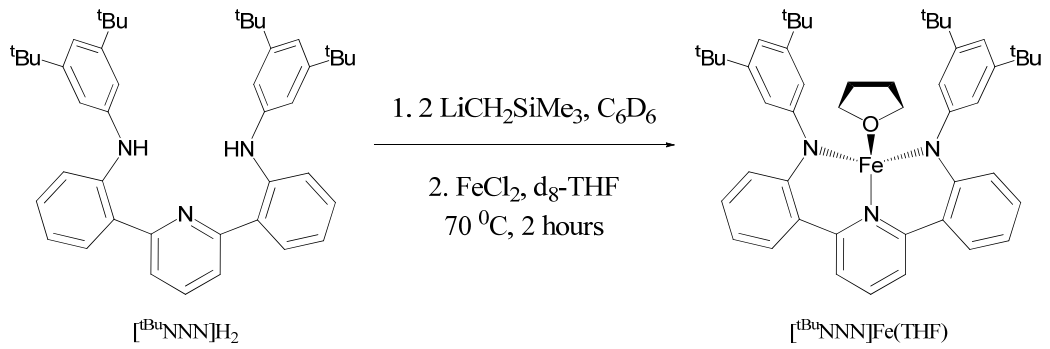

Scheme 4.9. Generation of [^{tBu}NNN]Fe(THF).

cyclohexene and trimethylsilylazide. Like its mesityl analog, [^{tBu}NNN]Fe(THF) does not react with excess cyclohexene. Unlike [^{Mes}NNN]Fe(THF) however, [^{tBu}NNN]Fe(THF) does not quickly react with trimethylsilylazide. After 5 days in C_6D_6, the complex slowly decomposes to a dark, insoluble precipitate (Scheme 4.10). This decomposition occurs more quickly in the presence of *both* excess cyclohexene and trimethylsilylazide. No consumption of either reagent was observed though. The non-volatiles from this reaction mixture were treated with aqueous HCl under argon. The mixture was extracted with CH_2Cl_2. The residue from the organic layer showed only [^{tBu}NNN]H_2 by ^{1}H NMR. Thus, an intramolecular C-H amination as observed for [^{Mes}NNN]Fe(THF) seems unlikely. Given the difficulty in isolating [^{tBu}NNN]Fe(THF) and its lack of productive reactivity with trimethylsilylazide, an alternative system was sought. The

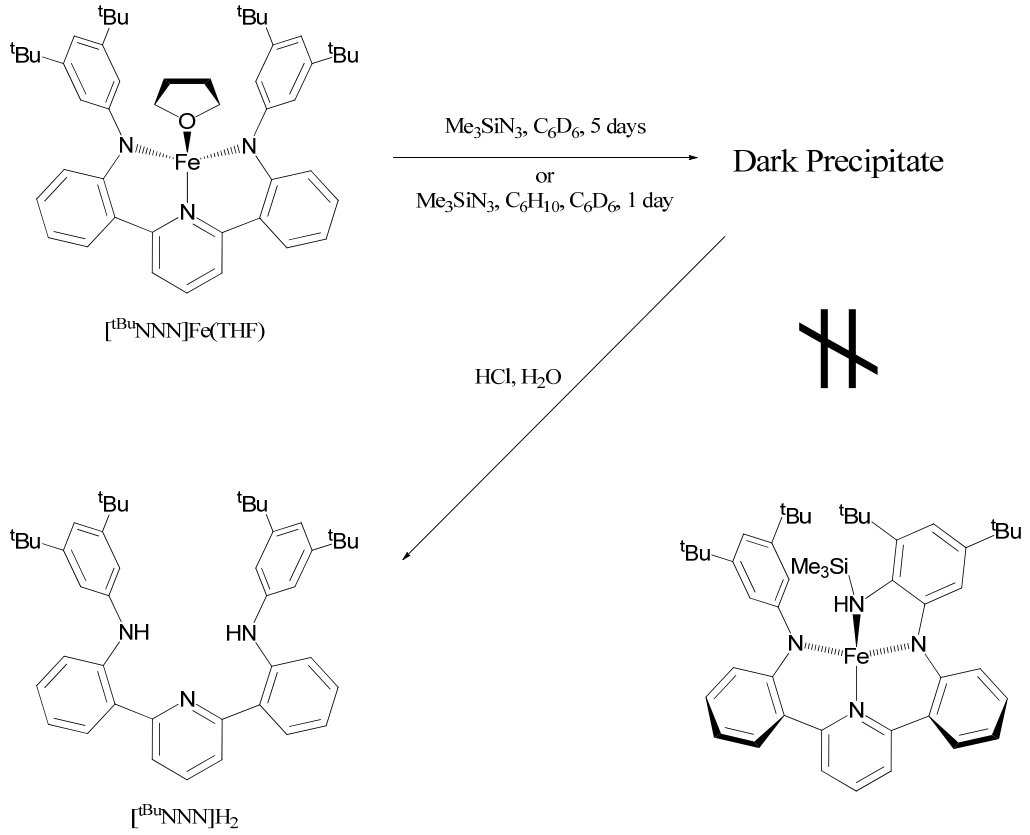

Scheme 4.10. Reactivity of [^{tBu}NNN]Fe(THF) with trimethylsilylazide.

previously synthesized pyridine bis(phenoxide) ligand[9] (abbreviated herein as [ONO]) was explored as a ligand for iron. It was hypothesized that the hard nature of the oxygen donors might stabilize high-valent iron to a greater extent than the nitrogen donors found in the NNN series. Additionally, no C-H bonds of ONO are in close proximity to the metal center, so intramolecular C-H amination is less

(9) Agapie, T. Synthetic, Reactivity, and Mechanistic Studies Relevant to Olefin Oligomerization and Polymerization. PhD Thesis, California Institute of Technology, Pasadena, CA, January 2007.

likely. Notably, a bis(ligand) complex ($[^{H}ONO]_2Fe)^-$ of a related non-t-butyl substituted ligand has been prepared previously.[10]

Initial attempts to ligate Fe focused on making the THF adduct, for a direct comparison to the NNN complexes. Formation of such a complex was likely observed by mixing $[ONO]Li_2$ and $FeCl_2$ in THF. Decomposition was observed upon removal of the volatiles in vacuo. Given the possibility of THF loss leading to decomposition, the less labile pyridine was employed. Gratifyingly, the bis(pyridine) adduct $[ONO]Fe(NC_5H_5)_2$ was obtained in high yield by doubly deprotonating $[ONO]H_2$ with trimethylsilylmethyllithium, then mixing with ferrous chloride and excess pyridine in THF (Scheme 4.11). The complex is stable to vacuum for extended periods.

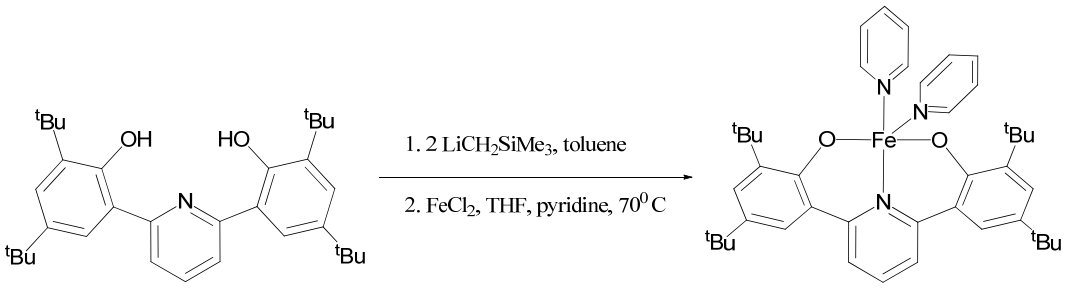

Scheme 4.11. The synthesis of $[ONO]Fe(NC_5H_5)_2$.

Evans method[11] of $[ONO]Fe(NC_5H_5)_2$ in C_6D_6 gives $\mu_{eff} = 4.6\ \mu_B$, which is close to the spin only value of 4.9 for a high spin d^6 metal center. X-ray quality

(10) Steinhauser, S.; Heinz, U.; Sander, J.; Hegetschweiler, K. *Z. Anorg. Allg. Chem.* **2004**, *630*, 1829–1838.

(11) Evans, D. F. *J. Chem. Soc.* **1959**, 2003–2005.

crystals were grown by vapor diffusion of heptane into a saturated toluene solution (Figure 4.7). The iron exhibits a distorted square pyramidal geometry, with N3 in the apical position. The distortion from an ideal square pyramid is significant, with the iron lying 0.4298 Å above the O1-N1-O2-N2 plane. The axial N3-Fe distance is significantly shorter than the equatorial N2-Fe distance (2.1450(12) and 2.2433(12), respectively), as expected for a square pyramidal geometry. Both benzene rings twist in the same direction, giving ONO an approximate C_s symmetry; a pyridine bis(phenoxide) copper bis(pyridine) complex has been reported which distorts in a C_2 fashion (Figure 4.8).[12]

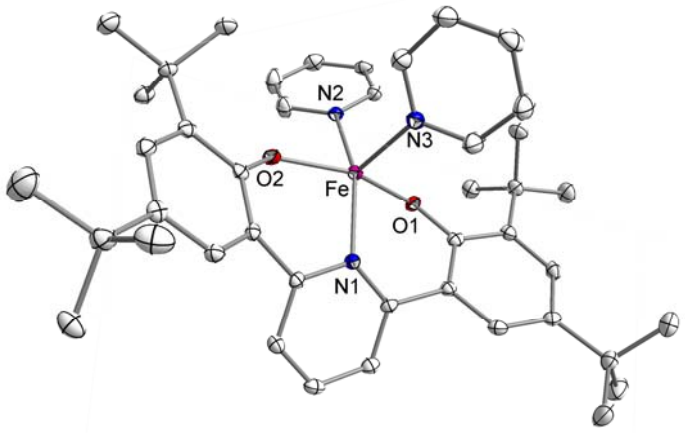

Figure 4.7. Structure of [ONO]Fe(NC_5H_5)$_2$ with displacement ellipsoids at the 50% probability level. Hydrogen atoms and solvent were omitted for clarity. Selected bond lengths (Å) and angles(deg): Fe-O2, 1.9413(10); Fe-O1, 1.9490(9); Fe-N3, 2.1450(12); Fe-N1, 2.2091(12); Fe-N2, 2.2433(12); O2-Fe-O1, 155.92(4); O2-Fe-N3, 105.65(4); O1-Fe-N3, 98.40(4); O2-Fe-N1, 88.36(4); O1-Fe-N1, 89.26(4); N3-Fe-N1, 98.64(4); O2-Fe-N2, 85.82(4); O1-Fe-N2, 86.82(4); N3-Fe-N2, 105.02(4); N1-Fe-N2, 156.33(4).

(12) Ludwig, E.; Schilde, U.; Uhlemann, E.; Hartl, H.; Brüdgam, I. *Z. Anorg. Allg. Chem.* **1996**, *622*, 701–706.

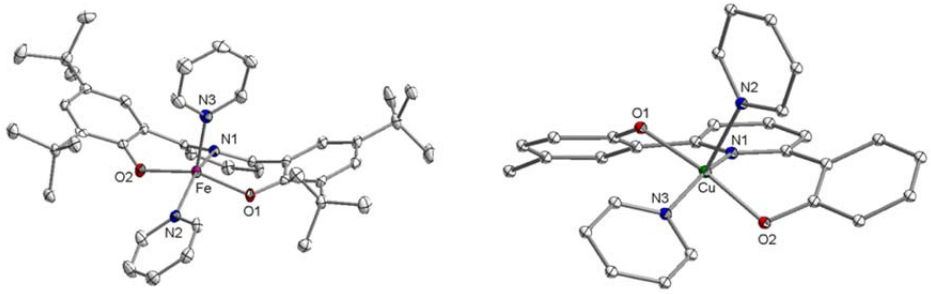

Figure 4.8. Comparison of Tonksomeric[13] ligand geometries: C_s for the Fe complex (left) and C_2 for Uhlemann's Cu complex (right).

The chemical shifts of the ^{1}H resonances for [ONO]Fe(NC_5H_5)$_2$ in deuterated arene solvents exhibit a dependence on concentration, and also change upon addition of excess pyridine. One possible explanation for these observations is an equilibrium between mono and bis(pyridine) adducts (Scheme 4.12). Unfortunately, [ONO]Fe(NC_5H_5)$_2$ does not react productively with either trimethylsilyl or 1-adamantyl azide. Additionally, cyclohexene is unreactive in the presence of trimethylsilyl azide and [ONO]Fe(NC_5H_5)$_2$.

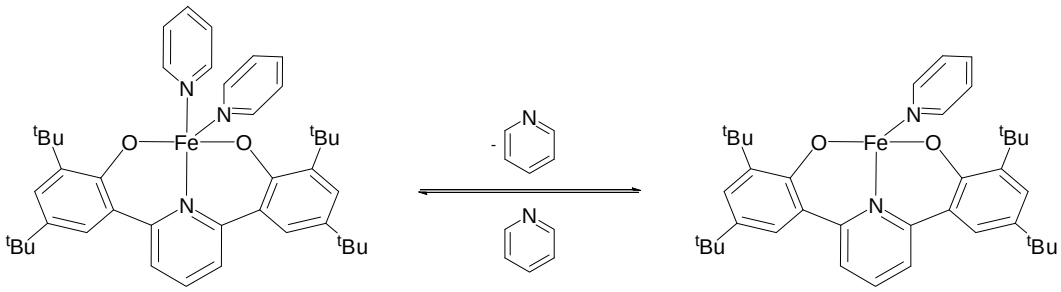

[ONO]Fe(NC_5H_5)$_2$ [ONO]Fe(NC_5H_5)

Scheme 4.12. Equilibrium between bis and mono pyridine adducts of [ONO]Fe.

(13) Tonks, I. A.; Henling, L. M.; Day, M. W.; Bercaw, J. E. *Inorg. Chem.* **2009** *48*, 5096–5105.

Experimental

General Methods: Unless otherwise specified, air exposed solids were dried under vacuum prior to use, liquids were degassed or bubbled with argon, reagents were used as received from the supplier, and reactions were performed under an inert atmosphere or vacuum. All air and moisture sensitive compounds were handled using standard glovebox and high-vacuum line techniques. Argon was purified by passage over MnO on vermiculite then 4 Å molecular sieves. Toluene was dried via Grubbs' method,[14] vac. transferred onto sodium/benzophenone, then vac. transferred and stored on titanocene dihydride. Benzene and pentane were dried via Grubbs' method, dried with 3 Å molecular sieves, then vac. transferred and stored on titanocene dihydride. N-heptane was dried on 3 Å molecular sieves, then vac. transferred and stored on titanocene dihydride. THF was dried via Grubbs' method, then vac. transferred and stored on sodium/benzophenone. Pyridine was dried using sodium metal. Deuterated solvents were obtained from Cambridge Isotope Laboratories. Deuterated benzene and toluene were dried on sodium/benzophenone, and then titanocene dihydride. Trimethylsilylmethyllithium was sublimed before use. Ferrous chloride 99.99% was obtained from Aldrich as anhydrous beads. Azidotrimethylsilane 95% and 1-azidoadamantane were obtained from Aldrich. Azidotrimethylsilane was vac. transferred onto 3 Å molecular sieves, and stored under vacuum and at 0° C. The azidotrimethylsilane was left on the sieves for at

(6) Pangborn, A. B.; Giardello, M. A.; Grubbs, R. H.; Rosen, R. K.; Timmers, F. J. *Organometallics* **1996**, *15*, 1518–1520.

least 5 days before use. 1-azidoadamantane was sublimed under high vacuum with the sublimator at ambient temperature and the probe at 10° C. The solid was stored at -30° C under an N_2 atmosphere and shielded from light.

NMR spectra were recorded on Varian Mercury 300 Megahertz NMR or Varian Inova 500 Megahertz spectrometers. ^{1}H and ^{13}C spectra were referenced according to the solvent residual peak,[15] and the ^{29}Si spectrum was referenced using the lock signal of C_6D_6. Solution magnetic moments were determined via Evans Method. The paramagnetism of the iron complexes precluded assignment of peaks in their ^{1}H NMR spectra. X-ray diffraction data were obtained on a Bruker KAPPA APEXII. High resolution mass spectra (HRMS) were obtained at the California Institute of Technology Mass Spectral Facility using a JEOL JMS-600H magnetic sector mass spectrometer. Elemental analyses were carried out by Robertson Microlit Laboratories, Madison, N.J. 07940. Data from elemental analyses are reported as the average of two runs.

Synthesis of [^{Mes}NNN-NHSiMe$_3$]Fe. In a glovebox, [^{Mes}NNN]Fe(THF) (450.0 mg, 0.7261 mmol) was loaded into a 250 mL roundbottom flask. 35 mL of toluene were vac. transferred onto the solid. Trimethylsilyl azide (0.24 mL, 1.8 mmol) was vac. transferred onto the solution at -78° C. The reaction was stirred and allowed to warm to room temperature. Upon warming, bubbling was observed; the reaction was periodically exposed to dynamic vacuum to vent the pressure. After ~3 hours,

(15) Fulmer, G. R.; Miller, A. J. M.; Sherden, N. H.; Gottlieb, H. E.; Nudelman, A.; Stoltz, B. M.; Bercaw, J. E.; Goldberg, K. I. *Organometallics* **2010**, *29*, 2176–2179.

the solvent concentrated in vacuo to a goo. Pentane was vac. transferred onto the product, stirred, and removed in vacuo. 439.4 mg of [^{Mes}NNN-NHSiMe$_3$]Fe were obtained as a powder in 95% yield. ^{1}H NMR (500 MHz, C_6D_6): δ -55.11, -51.24, -30.28, -27.61, -15.34, 23.86, 27.32, 28.05, 35.24, 36.41, 43.30, 43.51, 43.94, 45.74, 51.50, 52.17, 58.61, 61.18, 65.88, 67.77 (two overlapping peaks, one sharp and one broad), 174.12. ^{29}Si NMR (500 MHz, C_6D_6): -19.12 (s). Anal. Calcd. for $C_{38}H_{42}FeN_4Si$: C, 71.46; H, 6.63; N, 8.77. Found: C, 70.94; H, 6.43; N, 7.81.

Synthesis of [^{Mes}NNN-NHAd]Fe. In a glovebox, [^{Mes}NNN]Fe(THF) (499.5 mg, 0.8010 mmol) and 1-azidoadamantane (142.5 mg, 0.8039 mmol) were combined as solids in a 100 mL roundbottom flask, which was attached to a 180° teflon valve. The entire apparatus was shielded from light. The roundbottom was cooled to -78 °C (to prevent sublimation of the azide), then put under high vacuum. 50 mL of toluene were vac. transferred onto the solids, and the mixture was stirred and allowed to warm to room temperature. As the red solution warmed, bubbling was observed (the reaction was open to a mercury bubbler to prevent buildup of pressure). After ~6 hours, the solvent was removed in vacuo. The residue was pumped on overnight to remove any residual 1-azidoadamantane. Pentane was vac. transferred onto the solid, stirred, then removed in vacuo. 474.2 mg of [^{Mes}NNN-NHAd]Fe were isolated in 84% yield as a green powder. ^{1}H NMR (300 MHz, C_6D_6): δ -56.81, -48.39, -32.94, -28.67, -24.80, -11.71, -6.65, -6.09, 26.72, 29.52, 31.21, 33.70, 34.82, 40.03, 41.71, 42.99, 49.28, 50.10, 54.37, 60.50, 63.02, 63.68, 72.25, 76.53, 164.18. Anal. Calcd. for $C_{45}H_{48}FeN_4$: C, 77.13; H, 6.90; N, 8.00. Found: C, 76.75; H, 7.02; N, 7.76. X-ray quality crystals may be grown by vapor

diffusion of heptane into a saturated toluene solution or vapor diffusion of pentane into a benzene solution. A note on the color of [^{Mes}NNN-NHAd]Fe. In arene solvents the solution is red, while in alkane solvents the solution is green. This process is reversible, indicating that the color change is not a result of simple decomposition. Additionally, if the complex is concentrated from an arene solvent then it appears red, and similarly solid appears green when concentrated from alkanes. Crystals grown for X-ray diffraction were dichroic.

Synthesis of [^{Mes}NNN-NH$_2$]H$_2$. In a glovebox, [^{Mes}NNN-NHSiMe$_3$]Fe (100.0 mg, 0.1566 mmol) was dissolved in 2 mL of benzene and transferred to a reaction bomb. Several milliliters of water were vac. transferred onto the benzene solution and left stirring for 6.5 hours. The reaction was then exposed to the atmosphere. Benzene and water were then added until both layers contained ~50 mL. The layers were separated, and the aqueous layer was extracted with 50 mL of benzene. The combined organic layers were concentrated in vacuo to give 91 mg of crude product. The compound was purified column chromatography using ~1 mL of silica gel and methylene chloride as eluent. 20 mL were collected, containing chiefly [^{Mes}NNN]H$_2$. The eluent was then changed to ethyl acetate, and 25 mL were collected. The ethyl acetate fraction gave 56.3 mg of [^{Mes}NNN-NH$_2$]H$_2$ in 70% yield. ^{1}H NMR (CD_2Cl_2, 500 MHz): δ 1.01 (s(broad), 2H, NH$_2$), 2.03 (2 peaks overlapping) (s, 9H, CH$_3$), 2.29 (s, 3H, C<u>H</u>$_3$), 2.32 (s, 3H, CH$_3$), 3.57 (s, 2H, CH$_2$), 6.30 (t, J_{H-H} = 10 Hz, 2H, CH), 6.80 (q, J_{H-H} = 8 Hz, 2H), 6.89 (s, 2H, CH), 6.96 (s, 2H, CH), 7.12 (t, J_{H-H} = 7 Hz, 2H, CH), 7.58 (d, J_{H-H} = 7 Hz, 1H, CH), 7.64 (d, J_{H-H} = 7 Hz, 1H, CH), 7.72 (d, J_{H-H} = 8 Hz, 2H, CH), 7.95 (t, J_{H-H} = 8 Hz, 1H, CH), 8.46

(s, 1H, NH), 8.71 (s, 1H, NH). ^{13}C NMR (CD_2Cl_2, 126 MHz): 18.42, 18.47, 21.02, 21.08, 44.28, 113.32, 113.61, 117.27, 117.77, 121.00, 121.38, 123.21, 125.00, 127.41, 129.35, 130.09, 130.11, 130.29, 130.32, 130.55, 135.10, 135.41, 136.02, 136.12, 136.34, 136.63, 138.21, 139.51, 145.47, 146.01, 157.94, 158.81. FAB$^+$ m/z calcd. for $C_{35}H_{36}N_4$: 512.29. Found: 512.2915 (M^+), 496.2749 (M-NH_2).

X-ray quality crystals were grown by vapor diffusion of pentane into a CH_2Cl_2 solution. The crystal data is summarized as follows: formula, $C_{35}H_{36}N_4$; formula weight, 512.68; lattice system, monoclinic; space group P $2_1/n$ (No. 14); temperature 100(2) K; lattice parameters a = 12.1803(6) Å, b = 8.3648(4) Å, c = 27.4592(14) Å, β = 94.852(3)°; unit cell volume V = 2787.7(2) Å^3; calculated density D_{calc} = 1.222 g/cm^3; number of molecules in the unit cell Z = 4; linear absorption coefficient μ = 0.072 mm^{-1}; no empirical absorption correction; MoKα radiation recorded on a Bruker KAPPA APEX II diffractometer; 29589 reflections collected, 4775 unique reflections, 3224 unique reflections used with I > 2σ(I); θ_{max} = 25.56°; 361 parameters; 1 restraint; H atoms were placed in calculated positions; all other atoms were refined anisotropically, full matrix least-squares on F^2 refinement method; reliability factor R for all data = 0.0897 (for data I > 2σ(I) = 0.0574), weighted reliability factor R_w = 0.0748 (for data I > 2σ(I) = 0.0734); goodness-of-fit on F^2, 2.495. Crystallographic data have been deposited at the CCDC, 12 Union Road, Cambridge CB2 1EZ, UK. Copies can be obtained on request, free of charge, by quoting the publication citation and the deposition number 793154 or by visiting http://www.ccdc.cam.ac.uk/data_request/cif.

Synthesis of [^{Mes}NNN-NHAd]H$_2$. A solution of [^{Mes}NNN-NHAd]Fe (7.7 mg, 11 μmol) in ~0.5 mL of C_6D_6 was prepared in a J-Young tube. Water was added of the J-Young cap, and purged with argon. The cap was opened. The layers were then exposed to the atmosphere, and separated. The aqueous layer was washed with benzene, and the combined organic layers were concentrated in vacuo. The crude product was purified by column chromatography. 4 mL fractions were collected. The column was initially eluted with 1:4 CH_2Cl_2: hexanes for fractions 1–6. The CH_2Cl_2: hexanes ratio was changed to 1:1 for fractions 7–9. Subsequently, the column was eluted with large amounts of ethyl acetate into a jar. The ethyl acetate solution was concentrated in vacuo, giving 5 mg of [^{Mes}NNN-NHAd]H$_2$ in 70% yield. ^{1}H NMR ($ClCD_2CD_2Cl$, 500 MHz): δ 0.64 (s(broad), 1H, NHAd), 1.16 (d, J_{H-H} = 23 Hz, 6H, CH_2), 1.38 (dd, J_{H-H} = 40 Hz, 12 Hz, 6H, CH_2), 1.77 (s, 3H, CH), 2.04–2.07 (2 peaks overlapping) (s, 9H, CH_3), 2.27 (s, 3H, CH_3), 2.28 (s, 3H, CH_3), 3.41 (s, 2H, CH_2), 6.21 (d, J_{H-H} = 8 Hz, 1H, CH), 6.30 (d, J_{H-H} = 8 Hz, 1H, CH), 6.70 (t, J_{H-H} = 7 Hz, 1H, CH), 6.77 (t, J_{H-H} = 7 Hz, 1H, CH), 6.87 (s, 3H, CH), 6.93 (s, 1H, CH), 7.06 (q, J_{H-H} = 8 Hz, 2H, CH), 7.60 (d, J_{H-H} = 8 Hz, 1H, CH), 7.74 (d, J_{H-H} = 8 Hz, 1H, CH), 7.81 (d, J_{H-H} = 8 Hz, 1H, CH), 7.86 (t, J_{H-H} = 8 Hz, 1H, CH), 7.94 (d, J_{H-H} = 8 Hz, 1H, CH), 8.34 (s, 1H, NH), 10.20 (s, 1H, NH). ^{13}C NMR (CD_2Cl_2, 126 MHz): 18.49, 18.67, 20.93, 21.01, 29.88, 30.11, 36.80, 42.40, 43.67, 113.21, 114.06, 116.57, 118.40, 119.97, 121.20, 121.69, 125.97, 128.71, 129.26, 129.78, 129.88, 130.33, 130.98, 131.15, 134.00, 135.00, 135.33, 135.41, 136.36, 136.41, 137.63, 137.91, 144.16, 147.10, 156.58, 159.91. FAB$^+$ m/z calcd. for

$C_{45}H_{50}N_4$: 646.40. Found: 647.4102 (M + 1), 511.2820 (M-Ad), 496.2632 (M-HNAd).

General procedure for kinetic runs with variable azidotrimethylsilane concentrations. In a glovebox, [^{Mes}NNN]Fe(THF) (82.7 mg, 133 μmol) and ferrocene (112.7 mg, 605.8 μmol) were dissolved in 7.00 mL of C_6D_6 via syringe. 3.60 mL of the solution were transferred to a Strauss flask. On a high vacuum line, THF (240 μL) was measured by vac. transfer from a sodium/benzophenone pot into a calibrated glass vessel. The THF was subsequently transferred into the Strauss flask. In a glovebox, 640 μL portions were syringed into 5 J-Young NMR tubes. C_6D_6 was added to each tube such that the amount of azidotrimethylsilane to be transferred would give a final volume of 740 μL.

For each sample, the solution was frozen and the appropriate amount of azidotrimethylsilane was vac. transferred onto the solution. The solutions were thawed immediately before ^{1}H NMR acquisition. Spectra were acquired at regular intervals at 25 °C. At the end of each reaction, diamagnetic parameters were employed and a ^{1}H NMR spectrum was obtained. This spectrum allowed for quantitative determination of the azidotrimethylsilane concentration by integration vs. the ferrocene standard.

Synthesis of [ONO]Fe(NC_5H_5)$_2$. In a glovebox, [ONO]H_2 (600.0 mg, 1.230 mmol) and trimethylsilylmethyllithium (231.7 mg, 2.460 mmol) were combined as solids in a 100 mL roundbottom flask equipped with a 180° teflon valve. 25 mL of toluene were vac. transferred onto the solids at -78° C. The mixture was warmed to room temperature, and stirred for approx. 1 hour. The yellow solution was

concentrated in vacuo. In the glovebox, ferrous chloride (187.0 mg, 1.475 mmol) was added to the roundbottom, which was then attached to a swivel frit apparatus. 25 mL of THF and pyridine (1.00 mL, 12.4 mmol) were sequentially vac. transferred onto the solids. The apparatus was put under 1 atmosphere of argon, and the solution was stirred and heated to 70° C. Upon heating, the solution turned red. After 2.5 hours, heating was discontinued and the volatiles were removed in vacuo. 50 mL of toluene were vac. transferred onto the solids. After stirring for ~10 minutes, the dark solid dissolved to give a red solution and white solid. The solution was filtered (medium frit), then concentrated in vacuo to give dark sludge. Pentane was vac. transferred onto the sludge, stirred briefly, and removed in vacuo to yield a powder. 840.5 mg of [ONO]Fe(NC_5H_5)$_2$ were isolated in 98% yield. ^{1}H NMR (300 MHz, d_8-toluene, 42 mM): δ 3.51, 10.02, 17.05, 30.66, 33.87, 36.26, 46.33, 107.10. ^{1}H NMR (300 MHz, d_8-toluene, 11 mM): δ 3.60, 10.13, 15.64, 28.79, 35.76, 37.89, 46.48, 99.72. Anal. Calcd. for $C_{43}H_{53}FeN_3O_2$: C, 73.81; H, 7.63; N, 6.01. Found: C, 72.77; H, 7.51; N, 5.22. X-ray quality crystals were grown by vapor diffusion of heptane into a saturated toluene solution. The crystal data is summarized as follows: formula, $C_{43}H_{53}N_3O_2Fe \cdot C_7H_8$; formula weight, 791.87; lattice system, monoclinic; space group P 2_1/c (No. 14); temperature 100(2) K; lattice parameters a = 15.8750(6) Å, b = 28.4782(10) Å, c = 9.7853(4) Å, β = 90.514(2)°; unit cell volume V = 4423.7(3) Å^3; calculated density D_{calc} = 1.189 g/cm^3; number of molecules in the unit cell Z = 4; linear absorption coefficient μ = 0.382 mm^{-1}; no empirical absorption correction; MoKα radiation recorded on a Bruker KAPPA APEX II diffractometer; 96663 reflections collected, 12036 unique

reflections, 9399 unique reflections used with $I > 2\sigma(I)$; $\theta_{max} = 29.74^{\circ}$; 749 parameters; 0 restraints; H atoms were located via a Difference Fourier map; all other atoms were refined anisotropically, full matrix least-squares on F^2 refinement method; reliability factor R for all data = 0.0614 (for data $I > 2\sigma(I) = 0.0444$), weighted reliability factor $R_w = 0.0621$ (for data $I > 2\sigma(I) = 0.0613$); goodness-of-fit on F^2, 2.235. Crystallographic data have been deposited at the CCDC, 12 Union Road, Cambridge CB2 1EZ, UK. Copies can be obtained on request, free of charge, by quoting the publication citation and the deposition number 785427 or by visiting http://www.ccdc.cam.ac.uk/data_request/cif.

Appendix A
Attempted Synthesis of Pyridine Bis(anilide) Scandium Complexes

Introduction

Organoscandium complexes have attracted widespread interest due to their ability to carry out a myriad of reactions: notably sigma bond metathesis, various insertion chemistry, and olefin polymerization. With regards to olefin polymerization, scandocene alkyls have provided valuable mechanistic insight; they are isoelectronic to cationic group IV metallocenes, the presumed active species in Ziegler-Natta olefin polymerization. Though the most well-studied scandium systems are undoubtedly metallocene-based, the past decade has seen a concerted effort to discover non-metallocene systems that incorporate the advantages of metallocenes but alleviate certain drawbacks.[1–5] Herein are described attempts at using ligands of the type in Figure A.1 for organoscandium chemistry. The possible conformations of these ligands mirror symmetries exhibited by ansa-metallocenes; it is well-established that the symmetries of ansa-metallocenes are strongly related to tacticity control in the polymerization of the α-olefins.[6]

Results and Discussion

Reaction of $[^{Mes}NNN]H_2$ with scandium alkyls was performed to obtain the

(1) Gromada, J.; Carpentier, J.; Mortreux, A. *Coord. Chem. Rev.* **2004**, *248*, 397–410.

(2) Gibson V. C.; Spitzmesser, S. K. *Chem. Rev.* **2003**, *103,* 283–315.

(3) Mountford, P.; Ward, B. D. *Chem. Commun.* **2003**, 1797–1803.

(4) Zeimentz, P. M.; Arndt, S.; Elvidge, B. R.; Okuda, J. *Chem. Rev.* **2006**, *106*, 2404–2433.

(5) Resconi, L.; Cavallo, L.; Fait, A.; Piemontesi, F. *Chem. Rev.* **2000**, *100,* 1253–1345.

(6) Coates, G. W. *Chem. Rev.* **2000**, *100*, 1223–1252, and references contained therein.

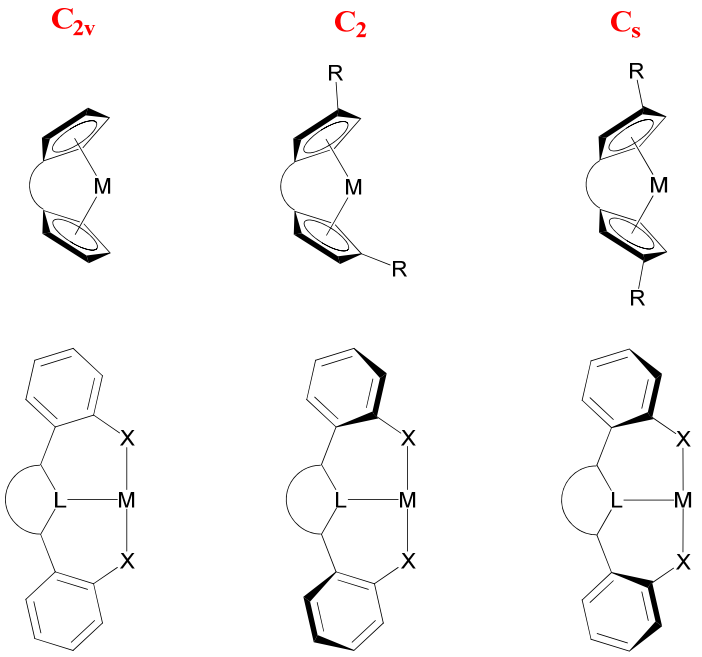

Figure A.1. Different symmetries exhibited by ansa-metallocenes (top), and analogous symmetries for the ligands herein (bottom).

desired monoalkylated product via double alkane elimination. Instead, triple alkane elimination was observed to form the scandium phenyl complex [^{Mes}NNN]ScPh(THF)$_n$ (Scheme A.1). Presumably, this reaction occurs via a transient scandium monoalkyl, which reacts via sigma bond metathesis with benzene to form the more stable scandium aryl linkage.[7] Also consistent with this explanation is the observation of the same product despite the use of different scandium alkyls. The three 6:6:6 singlets in the ^{1}H NMR spectrum of the compound were assigned as the mesityl methyl protons. This data is consistent with a structure exhibiting hindered bond rotation about the mesityl ipso carbon nitrogen bond, and

(7) Thompson, M. E.; Baxter, S. M.; Bulls, A. R.; Burger, B. J.; Nolan, M. C.; Santarsiero, B. D.; Schaefer, W. P.; Bercaw, J. E. *J. Am. Chem. Soc.* **1987**, *109*, 203–219.

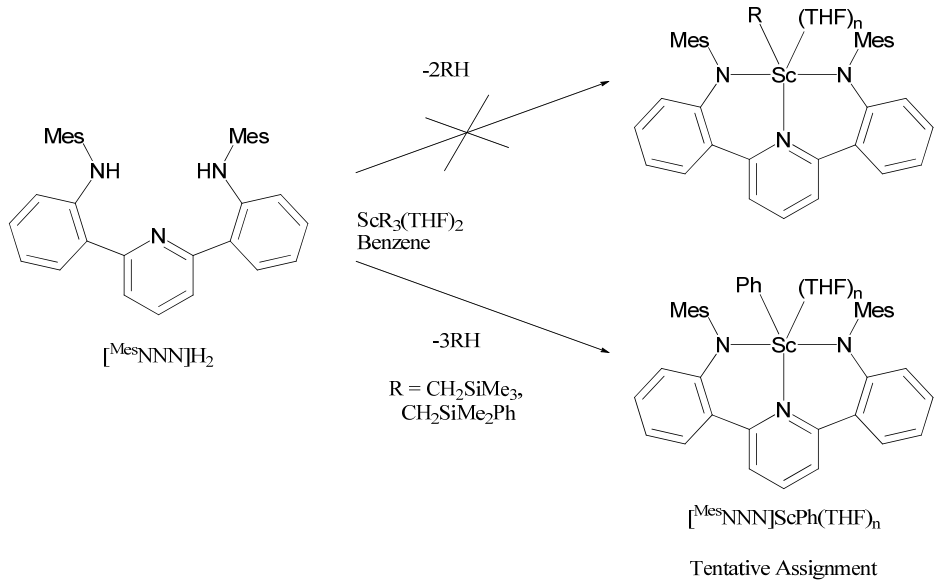

Scheme A.1. Reaction of $[^{Mes}NNN]H_2$ with scandium trialkyls.

an axial phenyl on scandium. Preparation of the scandium phenyl complex using protio benzene was undertaken in an effort to observe resonances corresponding to the phenyl protons. This attempt was probably precluded by fast sigma bond metathesis with the deuterated solvent; thus samples prepared in deutero or protio solvents produced identical NMR spectra.

Though initially a promising compound, several factors prevented the aforementioned complex from being a useful synthon for organoscandium chemistry. First, the scandium alkyl precursors used above typically require very short reaction times even at subambient temperatures for alkane elimination (~30 minutes to one hour).[8–10] This amount of time is small on the timescale of their

(8) Tredget, C. S.; Lawrence, S. C.; Ward, B. D.; Howe, R. G.; Cowley, A. R.; Mountford, P. *Organometallics* **2005**, *24*, 3136–3148.

(9) Ward, B. D.; Bellemin-Laponnaz, S.; Gade, L. H. *Angew. Chem. Int. Ed.* **2005**, *44*, 1668–1671.

decomposition reactions at room temperature. The metallation described herein, however, demands almost two weeks to reach completion at room temperature and high concentration. This implies that scandium alkyl decomposition competes with ligand metallation, and free ligand is invariably obtained even with greater than 1 equivalent of scandium alkyl. Mild heating of the reaction resulted in product decomposition and other unidentified products.

Second, the high reactivity of the product with solvents made its purification prohibitively difficult. Reactivity was observed even with titanocene dihydride dried solvents, so residual water content is an unlikely culprit. It has been observed that sufficiently reactive scandium alkyls and aryls undergo sigma bond metathesis with aryl and even primary C-H bonds, which is the likely explanation for the observed decomposition when solvents other than benzene were used. Despite the fact that benzene would itself fall into the aforementioned category, sigma bond metathesis would be degenerate and thus one species would be observed. Though there is some precedent for cyclohexane as a suitably inert solvent for such early metal hydrocarbyls,[7] attempted preparation of the scandium monoalkyl in C_6D_{12} led to complete decomposition, possibly due to the extremely low solubility of the reactants in cyclohexane.

In light of the challenges observed with alkane elimination, salt metathesis was explored as an alternative method of ligand metallation. Reaction of $[^{Mes}NNN]H_2$ with n-butyllithium in tetrahydrofuran led to the dilithium salt hexakis(THF)

---

(10) Estler, F.; Eickerling, G.; Herdtweck, E.; Anwander, R. *Organometallics* **2003**, *22*, 1212–1222.

adduct. The deprotonated ligand was then treated with $ScCl_3(THF)_3$ in toluene (Scheme A.2). In contrast to the scandium phenyl complex, only two ^1H resonances in a 12:6 ratio were observed, indicating either some degree of fluxionality on the NMR timescale, a chloride ligand in the plane of the ligand, or both. Unfortunately, the putative scandium chloride begins decomposing over the course of a day, in solution or the solid state, to a dark, insoluble solid. All attempts at obtaining

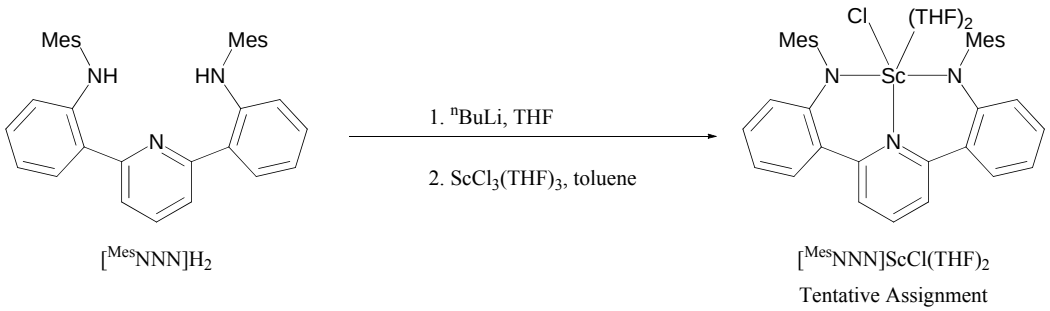

Scheme A.2. Deprotonation of $[^{Mes}NNN]H_2$ and subsequent salt metathesis with $ScCl_3(THF)_3$.

crystalline material inevitably led to precipitation of this solid. The preparation of the scandium chloride also suffered from reproducibility issues, the reasons for this problem are unclear. It is possible that the aforementioned decomposition results from loss of THF and subsequent dimerization or oligomerization. For that reason, preparation of the compound was attempted in deuterated THF. Unfortunately, formation of the complex was not observed. It is possible that THF loss from the scandium starting material is required for subsequent metallation, and thus the solvent inhibits the metallation. Additionally, the *in situ* generated scandium chloride was treated with excess trimethylphosphine. Surprisingly, this led to complete decomposition to many unidentified products.

Finally, amine elimination was attempted as an entry into scandium compounds of the ligand. Although less common than other methods for scandium installation, there is some precedent for its effectiveness.[11–13] Generation of the 3-coordinate tris(bis(trimethylsilyl)amide) scandium (III) was easily accomplished using a modified procedure from the original paper by Bradley.[14] This starting material has the advantage of being base free, and double amine elimination would be anticipated to lead to the four coordinate ligand scandium amide. A high degree of coordinative unsaturation has been shown to afford highly reactive complexes.[15] Unfortunately, refluxing a benzene solution of the tris(amide) with the ligand did not lead to a reaction. Additonally, refluxing a solution of the reactants in xylenes under an argon purge eventually led to decomposition of the scandium tris(amide). This result is surprising considering the large pK_a difference between amines and anilines, and the low kinetic barrier expected for a tricoordinate scandium center. The significant steric bulk of the ligand, however, may be the cause of this result.

In light of the apparent instability of the pyridine bis(aniline) system with scandium, a new strategy was employed to impart greater stability than the

---

(11) Skinner, M. E. G.; Mountford, P. *Dalton Trans*. **2002**, 1694–1703.

(12) Covert, K. J.; Neithamer, D. R.; Zonnevylle, M. C.; LaPointe, R. E.; Schaller, C. P.; Wolczanski, P. T. *Inorg. Chem.* **1991**, *30*, 2494–2508.

(13) Hitchcock, P. B.; Lappert, M. F.; Singh, A. *Chem. Comm.* **1983**, 1499–1501.

(14) Alyea, E. C.; Bradley, D. C.; Copperthwaite, R. G. *J. Chem. Soc., Dalton Trans.* **1972**, 1580–1584.

(15) Thompson, M. E.; Bercaw, J.E. *Pure Appl. Chem.* **1984**, *56*, 1–11.

previous system while still exploring a semi-rigid ligand as in Figure A.1. Specifically, the replacement of the anilines with phenols would be predicted to induce stability, as early metal oxygen bonds are known to be extremely strong. Additionally, the higher acidity of phenols compared to anilines could facilitate alkane and amine eliminations. Thus, the synthesis of the pyridine bis(phenol) $[ONO]H_2$ was undertaken using a known procedure (Scheme A.3).[16] Unfortunately, reaction of $[ONO]H_2$ with either $Sc(CH_2SiMe_3)_3(THF)_2$ or $Sc(N(SiMe_3)_2)_3$ led to unidentifiable mixtures. Reaction of the dilithium salt $[ONO]Li_2$ also resulted in decomposition, and the use of the bis(phenol) was not explored further.

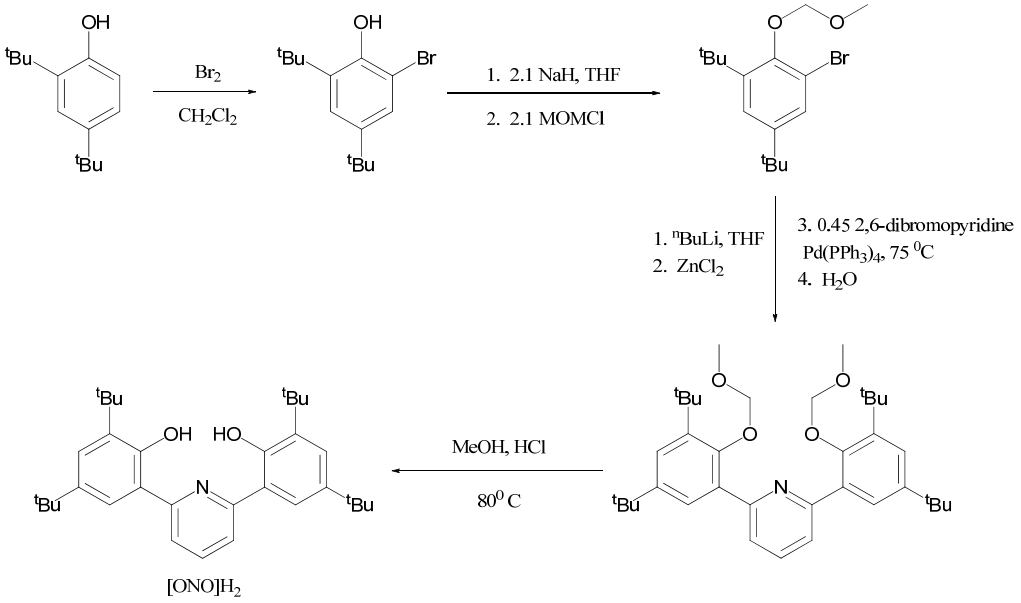

Scheme A.3. Synthesis of $[ONO]H_2$

(16) Agapie, T. Synthetic, Reactivity, and Mechanistic Studies Relevant to Olefin Oligomerization and Polymerization. PhD Thesis, California Institute of Technology, Pasadena, CA, January 2007.

Conclusions

The surprising instability of scandium complexes based on ^{Mes}NNN or ONO leads to the conclusion that they cannot provide useful entry points into organoscandium chemistry. This may be partially due to the small binding pocket of the ligand and relatively large size of scandium. Another factor is formation of six membered rings by the chelate, which might require severe distortion of the ligand framework to give favorable bond angles.

Experimental

General Methods: Unless otherwise specified, air exposed solids were dried under vacuum prior to use, liquids were degassed or bubbled with argon, reagents were used as received from the supplier, benzene, toluene, petroleum ether, xylenes, cyclohexane and diethyl ether were dried with titanocene dihydride for at least two days prior to use, and reactions were performed under inert atmosphere or vacuum. Tetrahydrofuran was dried via disodium benzophenone. Deuterated solvents were obtained from Cambridge Isotope Laboratories. Lithium granules, lithium bis(trimethylsilyl)amide, chloromethyldimethylphenylsilane, 2,4-ditertbutylphenol, bromine, methoxymethylchloride, zinc (II) chloride, and tetrakis(triphenylphosphine) palladium (0) were obtained from Aldrich. Chloromethyldimethylphenylsilane was exposed to the atmosphere, but degassed prior to use. [ONO]H_2 was prepared as reported previously.[16] Trichloro-tris(tetrahydrofuran) scandium (III) was prepared in an analogous manner to the

published procedure.[17,18] Dimethylphenylsilylmethyllithium and tris(dimethylphenylsilylmethyl)bis(tetrahydrofuran) scandium (III) were synthesized as described previously by Piers,[19] and the toluene used for these preparations was dried via Grubbs' method. Tris(bis(dimethylsilylamido)) scandium (III) was prepared in a similar manner to the reported procedure,[14] except $ScCl_3(THF)_3$ and $LiNSi(Me_3)_2$ were prepared beforehand and not generated *in situ*. NMR spectra were recorded on Varian Mercury 300 Megahertz NMR spectrometers, and referenced according to the solvent residual peak.

Synthesis of [^{Mes}NNN]ScPh(THF)$_n$. $Sc(CH_2SiMe_3)_3(THF)_2$ was generated *in situ* by allowing $LiCH_2SiMe_3$ (5 mg, 53 μmol) and $ScCl_3(THF)_3$ (6.5 mg, 17.7 μmol) to react in C_6D_6. After ~30 minutes, no $LiCH_2SiMe_3$ was detectable by ^{1}H NMR and the solution was cloudy. [^{Mes}NNN]H_2 (8.8 mg, 17.7 μmol) was added, and the reaction was complete after 13 days. ^{1}H NMR (C_6D_6): δ 1.21 (s, $OCH_2C\underline{H}_2$), 2.07 (s, 6H, $C\underline{H}_3$), 2.24 (s, 6H, $C\underline{H}_3$), 2.37 (s, 6H, $C\underline{H}_3$), 3.50 (s, $OC\underline{H}_2CH_2$), 6.5–7.6 (m, 13H, aryl-CH). The complexity of the aryl region precludes specific assignments.

Synthesis of [^{Mes}NNN]ScCl(THF)$_2$. A chilled solution of [^{Mes}NNN]H_2 (400 mg, 0.80 mmol) in 30 mL of THF was treated with 7.4 mL of a chilled THF/hexanes solution (6:1.4 THF:hexanes) of n-butyllithium (3.5 mmol, 0.49 M) over the course of five minutes. After 2 hours, the reaction was concentrated in vacuo. The

(17) Stotz, R. W.; Melson, G. A. *Inorg. Chem.* **1972**, *11*, 1720–1721.

(18) Atwood, J. L.; Smith, K. D. *Dalton Trans* **1974**, 921–923.

(19) David J. H. Emslie, D. J. H.; Piers, W. E.; Parvez, M.; McDonald, R. *Organometallics* **2002**, *21*, 4226–4240.

remaining solid was washed with 2 mL of cold petroleum ether, then dried in vacuo. A total of 477 mg were obtained. A solution of the deprotonated ligand (200 mg, 0.21 mmol) in 6 mL of toluene was added to solid $ScCl_3(THF)_3$ (78 mg, 0.21 mmol). The solution became very dark and white solid precipitated (presumably lithium chloride). After one hour, the reaction was filtered and the remaining white solid was washed with 1 mL of toluene. The filtrate was concentrated in vacuo, giving 141 mg of $[^{Mes}NNN]ScCl(THF)_2$.

^{1}H NMR (C_6D_6): δ 1.07(s, 4H $OCH_2C\underline{H}_2$), 1.93 (s, 12H, *o*-$C\underline{H}_3$), 2.38 (s, 6H, *p*-$C\underline{H}_3$), 3.08 (s, 4H, $OC\underline{H}_2CH_2$), 6.47 (t, $J_{H\text{-}H}$ = 7 Hz, 2H, C<u>H</u>), 6.56 (d, $J_{H\text{-}H}$ = 8.7 Hz, 2H, C<u>H</u>), 6.90 (s, 4H, mesityl aryl C<u>H</u>), 7.03 (t, $J_{H\text{-}H}$ = 7.6 Hz, 2H, C<u>H</u>), 7.24–7.36 (m, 3H, C<u>H</u>), 7.62 (d, $J_{H\text{-}H}$ = 8.4 Hz, 2H, C<u>H</u>).

Appendix B
Attempted Synthesis of other Transition Metal Pyridine Bis(anilide) Complexes

The application of the ONO pincer ligand has been realized for a variety of transition metals: Ti, Zr, Hf, V, Ta, Fe, and Ir. It was attempted to similarly expand the scope of the NNN ligand beyond iron chemistry. Additionally, metallations of ONO were tried for certain previously untested metals. A brief list of unsuccessful metallation reactions with Nb, Ta, Ru, Cu, Zn, and Cd is given in this appendix.

Given the successful application of the ONO ligand set to tantalum, it was desirable to investigate the analogous NNN complexes with group 5 metals. Both metathetical and methane elimination routes were tested (Table B.1), but inevitably led to decomposition.

Table B.1. Attempted group 5 metallations.

Ligand	Metal Source	Solvent, temp	Result
$[^{Mes}NNN]Li_2$	$NbCl_5$	C_6D_6, RT	Decomposition
$[^{Mes}NNN]Li_2$	$TaCl_5$	C_6D_6, RT	Decomposition
$[^{Mes}NNN]Li_2$	Me_3Ta Cl_2	C_6D_6, RT	Decomposition
$[^{Mes}NNN]H_2$	Me_3Ta Cl_2	C_6D_6, RT	No reaction, decomposition upon heating

Investigation of ruthenium pincer complexes was inspired by the ability of iron congeners to initiate intramolecular C-H activation via a high-valent iron imido species. It was thought that a high-valent ruthenium imide would be more stable, and thus more amenable to characterization and intermolecular reactivity. With the knowledge from the iron study, it was known that the $[^{Mes}NNN]H_2$ ligand decomposed via benzylic C-H activation. Thus, metallation focused on the 3,5-

ditbutylphenyl substituted ligand, [^{tBu}NNN]H_2, which contains no reactive benzylic C-H bonds (Table B.2). Ruthenium ONO complexes were also briefly investigated.

Copper metallation was briefly attempted because of its similarity to iron in terms of redox properties (Table B.3). Zinc and cadmium complexes of [^{Mes}NNN] were attempted to investigate the electrochemical properties of the NNN ligand with a redox-inactive metal. The results could then be compared the iron system, and the peaks observed for the iron complex could be assigned as primarily metal or ligand based. No attempts to make group 10 complexes of the [^{Mes}NNN] ligand were successful, however.

Table B.2. Attempted ligation of ruthenium.

Ligand	Metal Source (base)	Solvent, temp	Result
[^{tBu}NNN]Li_2	$[RuCl_2(C_6H_6)]_2$	d_8-THF, RT	Decomposition upon heating
[^{tBu}NNN]Li_2	(*p*-cymene)$RuCl_2(PCy_3)$	C_6D_6, RT	Decomposition
[^{tBu}NNN]Li_2	$(Ph_3P)_3RuCl_2$	C_6D_6, RT	2 major products
[^{tBu}NNN]Li_2	$(DMSO)_4RuCl_2$	C_6D_6,70 °C	No reaction, eventual ligand protonation
[^{tBu}NNN]Li_2	$RuCl_3$	d_8-THF, RT	Ligand protonation
[^{tBu}NNN]H_2	(*p*-cymene)$RuCl_2(PCy_3)$ (C_5H_5N)	C_6D_6, 90 °C	No reaction
[^{tBu}NNN]H_2	Ru metal	d_8-THF, 70 °C	No reaction
[^{tBu}NNN]H_2	$[RuCl_2(C_6H_6)]_2$ (NEt_3)	C_6D_6, 90 °C	No reaction
[^{tBu}NNN]H_2	(*p*-cymene)$RuCl_2(PCy_3)$ (NEt_3)	C_6D_6, RT	Decomposition upon heating
[ONO]Li_2	$(Ph_3P)_3RuCl_2$	C_6D_6, 80 °C	Metal source decomposition
[ONO]H_2	$(Ph_3P)_3RuCl_2$ (NEt_3)	d_8-isopropanol, 85 °C	No reaction

Table B.3. Attempted metallations with groups 9 and 10.

Ligand	Metal Source	Solvent, temp	Result
[^{Mes}NNN]Li_2	$CuCl_2$	d_8-THF, RT	Ligand protonation and decomposition
[^{Mes}NNN]H_2	$ZnMe_2$	C_6D_6, 90 °C	Inconclusive
[^{Mes}NNN]H_2	$ZnEt_2$	d_8-toluene, 120 °C	Decomposition
[^{Mes}NNN]Li_2	$ZnCl_2$	d_8-THF, RT	Mulitple products

$[^{Mes}NNN]Li_2$	$CdCl_2$	THF, RT	In solution, product decomposes to a gray solid over time. Crystallization attempts unsuccessful.
$[ONO]H_2$	$ZnMe_2$	Toluene/pyridine, RT	Successful metallation

An ONO zinc complex was accessible however, as the pyridine adduct (Scheme B.1). Mixing $[ONO]H_2$ and $ZnMe_2$ in toluene produces an

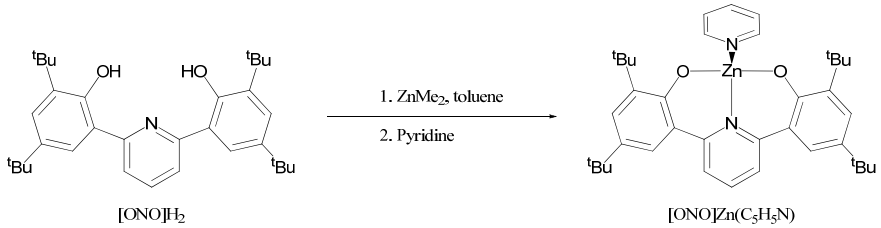

Scheme B.1. Synthesis of $[ONO]Zn(C_5H_5N)$.

intermediate complex. The intermediate is unlikely monomeric, in analogy to the known non-t-butyl substituted pyridine bis(phenoxide) zinc complex $([^{H}ONO]Zn)_n$, which is proposed to be a polymer.[1] Addition of pyridine produces a new complex by ^1H NMR, assigned as $[ONO]Zn(C_5H_5N)$. ^1H and ^{13}C NMR spectra confirm the 1:1 ratio of ONO ligand to pyridine. While $[^{H}ONO]Zn(C_5H_5N)$ is a tetramer, preliminary DOSY measurements indicated that $[ONO]Zn(C_5H_5N)$ is monomeric. Some caution must be taken with this statement however, as the standard for the DOSY solution was the solvent residual signal, whose hydrodynamic radius is significantly different from the product. The complex $[ONO]Zn(C_5H_5N)$ was not explored further.

(1) Zhang, H.-Y.; Ye, K.-Q.; Jing-Ying Zhang, J.-Y.; Liu, Y.; Wang, Y. *Inorg. Chem.* **2006**, *45*, 1745–1753.

Experimental

Synthesis of [ONO]Zn(C_5H_5N). 25 mL of toluene were vac. transferred from a Cp_2TiH_2 pot onto the solid $[ONO]H_2$ ligand (300.9 mg, 0.6170 mmol). Dimethylzinc (0.50 mL, 7.3 mmol) was vac. transferred onto the solution. Bubbling occurred for several minutes, and the solution was a golden yellow. ^{1}H NMR of "$([ONO]Zn)_n$" (C_6D_6, 300 MHz): 1.33 (s, 18H, $C(CH_3)_3$), 1.63 (s, 18H, $C(CH_3)_3$), 7.02–7.12 (m, 3H, CH), 7.41 (d, $J_{H\text{-}H}$ = 3 Hz, 2H, CH), 7.66 (d, $J_{H\text{-}H}$ = 3 Hz, 2H, CH). After two hours, the volatiles were removed in vacuo. To remove any residual dimethylzinc trapped in the solid, 25 mL of pentane were vac. transferred onto the solid. The solid dissolved upon warming to room temperature, and the pentane was removed in vacuo. 10 mL of pyridine were vac. transferred from a sodium pot onto the solid, giving an orange-brown solution. The solution was left stirring for 12 hours, then concentrated in vacuo. 30 mL of pentane were vac. transferred onto the solid, and the resulting suspension was left stirring for 30 minutes. The pentane was removed in vacuo. In a glovebox, the solid was dissolved in 10 mL of toluene. The solution was diluted with 30 mL of heptane, and cooled to -30 °C. After 2.5 hours, the cold solution was filtered, and the light solid was dried in vacuo. 148.8 mg of $[ONO]Zn(C_5H_5N)$ were obtained in 38% yield. ^{1}H NMR (C_6D_6, 400 MHz): δ 1.36 (s, 18H, $C(C\underline{H}_3)_3$), 1.42 (s, 18H, $C(C\underline{H}_3)_3$), 6.59 (t, $J_{H\text{-}H}$ = 6 Hz, 2H, *m*-$C_5\underline{H}_5N$), 6.89 (t, $J_{H\text{-}H}$ = 7 Hz, 1H, *p*-$C_5\underline{H}_5N$), 7.29 (m, 3H, overlap of *m*-$C_5\underline{H}_3Ar_2N$ and *p*-$C_5\underline{H}_3Ar_2N$), 7.54 (d, $J_{H\text{-}H}$ = 3 Hz, 2H, $C_6\underline{H}_2$), 7.66 (d, $J_{H\text{-}H}$ = 3 Hz, 2H, $C_6\underline{H}_2$), 8.64 (d, $J_{H\text{-}H}$ = 5 Hz, 2H, *o*-$C_5\underline{H}_5N$). ^{13}C NMR (C_6D_6, 101

MHz): δ 30.09, 31.41, 34.41, 35.53, 122.38, 124.53, 124.67, 124.84, 127.50, 138.79, 140.02, 140.09, 140.94, 149.64, 158.15, 159.79.

Appendix C
Crystallographic Tables

CALIFORNIA INSTITUTE OF TECHNOLOGY

BECKMAN INSTITUTE
X-RAY CRYSTALLOGRAPHY LABORATORY

Date 10 July 2007

Crystal Structure Analysis of:

[^{Mes}NNN]H_2 (ECW01)

(shown below)

For Investigator: Edward Weintrob ext. 6576

Advisor: J. E. Bercaw ext. 6577

Account Number: JEB.65152-1DOE.651520

By Michael W. Day 116 Beckman ext. 2734
e-mail: mikeday@caltech.edu

Contents

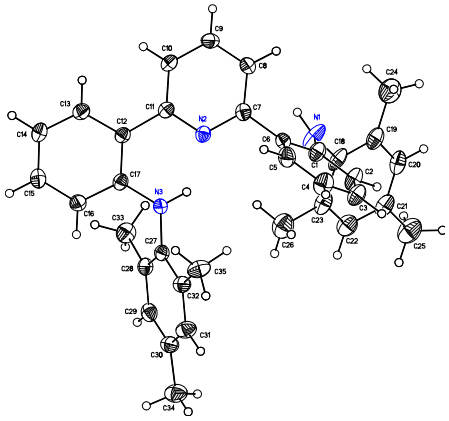

ECW01

Note: The crystallographic data have been deposited in the Cambridge Database (CCDC) and has been placed on hold pending further instructions from me. The deposition number is 653538. Ideally the CCDC would like the publication to contain a footnote of the type: "Crystallographic data have been deposited at the CCDC, 12 Union Road, Cambridge CB2 1EZ, UK and copies can be obtained on request, free of charge, by quoting the publication citation and the deposition number 653538."

Table 1. Crystal data and structure refinement for ECW01 (CCDC 653538).

Empirical formula	$C_{35}H_{35}N_3$
Formula weight	497.66
Crystallization Solvent	Diethyl ether
Crystal Habit	Blade
Crystal size	0.39 x 0.22 x 0.09 mm^3
Crystal color	Colorless

Data Collection

Type of diffractometer	Bruker SMART 1000
Wavelength	0.71073 Å MoKα
Data Collection Temperature	100(2) K
θ range for 8568 reflections used in lattice determination	2.54 to 27.95°
Unit cell dimensions	a = 12.1774(12) Å b = 8.3901(8) Å β= 93.803(2)° c = 27.039(3) Å
Volume	2756.5(5) $Å^3$
Z	4
Crystal system	Monoclinic
Space group	$P2_1/n$
Density (calculated)	1.199 Mg/m^3
F(000)	1064
Data collection program	Bruker SMART v5.630
θ range for data collection	1.51 to 28.41°
Completeness to θ = 28.41°	93.2 %
Index ranges	$-15 \le h \le 16$, $-10 \le k \le 11$, $-36 \le l \le 35$
Data collection scan type	ω scans at 5 ϕ settings
Data reduction program	Bruker SAINT v6.45A
Reflections collected	34841
Independent reflections	6474 [R_{int}= 0.0831]
Absorption coefficient	0.070 mm^{-1}
Absorption correction	None
Max. and min. transmission	0.9937 and 0.9732

Table 1 (cont.)

Structure solution and Refinement

Structure solution program	SHELXS-97 (Sheldrick, 1990)
Primary solution method	Direct methods
Secondary solution method	Difference Fourier map
Hydrogen placement	Geometric positions
Structure refinement program	SHELXL-97 (Sheldrick, 1997)
Refinement method	Full matrix least-squares on F^2
Data / restraints / parameters	6474 / 0 / 349
Treatment of hydrogen atoms	Riding
Goodness-of-fit on F^2	1.579
Final R indices [$I>2\sigma(I)$, 4122 reflections]	R1 = 0.0554, *w*R2 = 0.0907
R indices (all data)	R1 = 0.0900, *w*R2 = 0.0939
Type of weighting scheme used	Sigma
Weighting scheme used	$w=1/\sigma^2(Fo^2)$
Max shift/error	0.000
Average shift/error	0.000
Largest diff. peak and hole	0.387 and -0.364 e.Å^{-3}

Special Refinement Details

Refinement of F^2 against ALL reflections. The weighted R-factor (*w*R) and goodness of fit (S) are based on F^2, conventional R-factors (R) are based on F, with F set to zero for negative F^2. The threshold expression of $F^2 > 2\sigma(F^2)$ is used only for calculating R-factors(gt) etc. and is not relevant to the choice of reflections for refinement. R-factors based on F^2 are statistically about twice as large as those based on F, and R-factors based on ALL data will be even larger.

All esds (except the esd in the dihedral angle between two l.s. planes) are estimated using the full covariance matrix. The cell esds are taken into account individually in the estimation of esds in distances, angles and torsion angles; correlations between esds in cell parameters are only used when they are defined by crystal symmetry. An approximate (isotropic) treatment of cell esds is used for estimating esds involving l.s. planes.

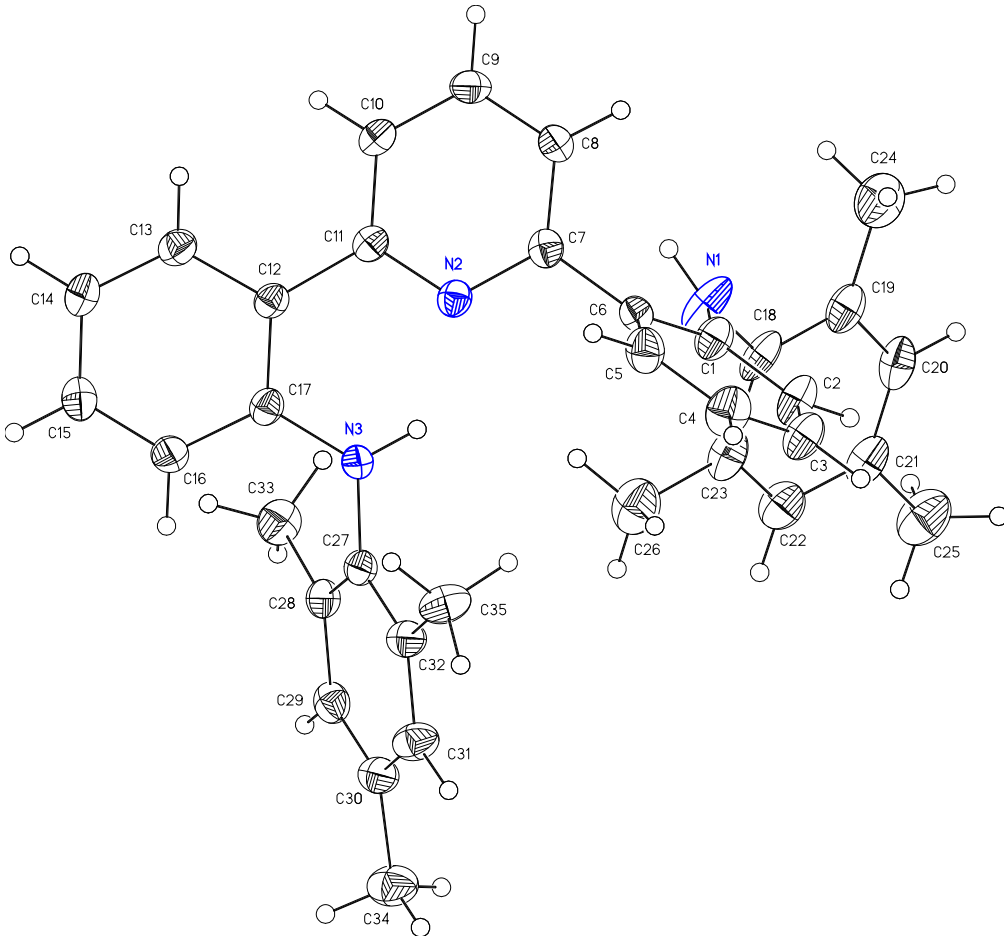
C9
C10
C8
C24
C13
C11
C7
N1
C12
N2
C19
C14
C6
C18
C20
C5
C1
C2
C17
C4
N3
C15
C3
C21
C16
C33
C23
C27
C26
C22
C25
C28
C35
C32
C29
C31
C30
C34

Table 2. Atomic coordinates (x 10^4) and equivalent isotropic displacement parameters ($Å^2$x 10^3) for ECW01 (CCDC 653538). U(eq) is defined as the trace of the orthogonalized U^{ij} tensor.

	x	y	z	U_{eq}
N(1)	1038(1)	3989(2)	1311(1)	39(1)
N(2)	3731(1)	5158(2)	1856(1)	21(1)
N(3)	4904(1)	2425(2)	1759(1)	24(1)
C(1)	1569(1)	5009(2)	998(1)	27(1)
C(2)	1265(1)	5049(2)	493(1)	33(1)
C(3)	1798(1)	6037(2)	181(1)	34(1)
C(4)	2639(1)	7005(2)	366(1)	36(1)
C(5)	2952(1)	6967(2)	866(1)	31(1)
C(6)	2434(1)	5978(2)	1186(1)	22(1)
C(7)	2781(1)	5934(2)	1727(1)	22(1)
C(8)	2159(1)	6639(2)	2073(1)	27(1)
C(9)	2504(1)	6534(2)	2570(1)	28(1)
C(10)	3462(1)	5726(2)	2705(1)	25(1)
C(11)	4076(1)	5057(2)	2340(1)	21(1)
C(12)	5122(1)	4202(2)	2469(1)	20(1)
C(13)	5747(1)	4626(2)	2903(1)	25(1)
C(14)	6718(1)	3870(2)	3052(1)	30(1)
C(15)	7103(1)	2667(2)	2758(1)	29(1)
C(16)	6516(1)	2220(2)	2327(1)	26(1)
C(17)	5517(1)	2946(2)	2180(1)	22(1)
C(18)	458(2)	2616(2)	1119(1)	31(1)
C(19)	-685(2)	2578(2)	1105(1)	31(1)
C(20)	-1216(2)	1243(2)	903(1)	34(1)
C(21)	-652(2)	-34(2)	722(1)	33(1)
C(22)	485(1)	30(2)	744(1)	36(1)
C(23)	1059(1)	1350(2)	938(1)	34(1)
C(24)	-1328(2)	3938(2)	1312(1)	45(1)
C(25)	-1250(2)	-1478(2)	512(1)	49(1)
C(26)	2300(1)	1393(2)	948(1)	45(1)
C(27)	5218(1)	1155(2)	1452(1)	22(1)
C(28)	5264(1)	-416(2)	1626(1)	25(1)
C(29)	5539(1)	-1613(2)	1302(1)	27(1)
C(30)	5737(1)	-1313(2)	812(1)	28(1)
C(31)	5673(1)	251(2)	649(1)	30(1)
C(32)	5430(1)	1503(2)	963(1)	25(1)
C(33)	4974(1)	-839(2)	2143(1)	34(1)
C(34)	5955(1)	-2667(2)	464(1)	37(1)
C(35)	5391(1)	3205(2)	784(1)	34(1)

Table 3. Bond lengths [Å] and angles [°] for ECW01 (CCDC 653538).

N(1)-C(1)	1.3935(19)	N(1)-C(1)-C(6)	120.22(14)
N(1)-C(18)	1.430(2)	C(3)-C(2)-C(1)	120.67(16)
N(2)-C(11)	1.3511(18)	C(4)-C(3)-C(2)	120.27(16)
N(2)-C(7)	1.3525(18)	C(3)-C(4)-C(5)	119.50(16)
N(3)-C(17)	1.3900(17)	C(6)-C(5)-C(4)	121.31(16)
N(3)-C(27)	1.4191(19)	C(5)-C(6)-C(1)	118.94(15)
C(1)-C(2)	1.390(2)	C(5)-C(6)-C(7)	121.10(14)
C(1)-C(6)	1.400(2)	C(1)-C(6)-C(7)	119.96(14)
C(2)-C(3)	1.376(2)	N(2)-C(7)-C(8)	122.15(14)
C(3)-C(4)	1.374(2)	N(2)-C(7)-C(6)	116.41(14)
C(4)-C(5)	1.383(2)	C(8)-C(7)-C(6)	121.44(14)
C(5)-C(6)	1.381(2)	C(7)-C(8)-C(9)	119.20(15)
C(6)-C(7)	1.496(2)	C(10)-C(9)-C(8)	119.07(15)
C(7)-C(8)	1.376(2)	C(9)-C(10)-C(11)	119.67(14)
C(8)-C(9)	1.383(2)	N(2)-C(11)-C(10)	120.90(14)
C(9)-C(10)	1.378(2)	N(2)-C(11)-C(12)	117.71(13)
C(10)-C(11)	1.395(2)	C(10)-C(11)-C(12)	121.39(14)
C(11)-C(12)	1.483(2)	C(13)-C(12)-C(17)	117.77(14)
C(12)-C(13)	1.4016(19)	C(13)-C(12)-C(11)	118.97(14)
C(12)-C(17)	1.416(2)	C(17)-C(12)-C(11)	123.25(13)
C(13)-C(14)	1.378(2)	C(14)-C(13)-C(12)	122.38(15)
C(14)-C(15)	1.386(2)	C(13)-C(14)-C(15)	118.92(15)
C(15)-C(16)	1.376(2)	C(16)-C(15)-C(14)	120.50(15)
C(16)-C(17)	1.395(2)	C(15)-C(16)-C(17)	121.12(15)
C(18)-C(19)	1.390(2)	N(3)-C(17)-C(16)	120.52(14)
C(18)-C(23)	1.396(2)	N(3)-C(17)-C(12)	120.20(13)
C(19)-C(20)	1.387(2)	C(16)-C(17)-C(12)	119.27(14)
C(19)-C(24)	1.512(2)	C(19)-C(18)-C(23)	121.33(16)
C(20)-C(21)	1.380(2)	C(19)-C(18)-N(1)	119.83(17)
C(21)-C(22)	1.384(2)	C(23)-C(18)-N(1)	118.83(16)
C(21)-C(25)	1.505(2)	C(20)-C(19)-C(18)	117.95(17)
C(22)-C(23)	1.393(2)	C(20)-C(19)-C(24)	121.01(16)
C(23)-C(26)	1.511(2)	C(18)-C(19)-C(24)	121.03(16)
C(27)-C(32)	1.394(2)	C(21)-C(20)-C(19)	122.48(17)
C(27)-C(28)	1.400(2)	C(20)-C(21)-C(22)	118.34(17)
C(28)-C(29)	1.390(2)	C(20)-C(21)-C(25)	121.32(17)
C(28)-C(33)	1.505(2)	C(22)-C(21)-C(25)	120.34(18)
C(29)-C(30)	1.385(2)	C(21)-C(22)-C(23)	121.50(18)
C(30)-C(31)	1.385(2)	C(22)-C(23)-C(18)	118.39(16)
C(30)-C(34)	1.509(2)	C(22)-C(23)-C(26)	120.14(18)
C(31)-C(32)	1.395(2)	C(18)-C(23)-C(26)	121.47(16)
C(32)-C(35)	1.507(2)	C(32)-C(27)-C(28)	120.76(15)
		C(32)-C(27)-N(3)	118.11(14)
C(1)-N(1)-C(18)	120.80(13)	C(28)-C(27)-N(3)	121.06(14)
C(11)-N(2)-C(7)	119.00(13)	C(29)-C(28)-C(27)	118.24(15)
C(17)-N(3)-C(27)	124.37(12)	C(29)-C(28)-C(33)	119.80(15)
C(2)-C(1)-N(1)	120.47(15)	C(27)-C(28)-C(33)	121.89(15)
C(2)-C(1)-C(6)	119.30(15)	C(30)-C(29)-C(28)	122.51(16)
		C(29)-C(30)-C(31)	117.83(15)

C(29)-C(30)-C(34)	120.51(1616)
C(31)-C(30)-C(34)	121.59(16)
C(30)-C(31)-C(32)	121.95(16)
C(27)-C(32)-C(31)	118.67(15)
C(27)-C(32)-C(35)	119.94(14)
C(31)-C(32)-C(35)	121.39(15)

Table 5. Hydrogen bonds for ECW01 (CCDC 653538) [Å and °].

D-H...A	d(D-H)	d(H...A)	d(D...A)	<(DHA)
N(3)-H(3)...N(2)	0.88	2.06	2.7235(18)	130.9

Symmetry transformations used to generate equivalent atoms:

CALIFORNIA INSTITUTE OF TECHNOLOGY

BECKMAN INSTITUTE

X-RAY CRYSTALLOGRAPHY LABORATORY

Date 15 February 2008

Crystal Structure Analysis of:

[^{Mes}NNN]Fe(THF) (ECW03)

(shown below)

For Investigator: Edward Weintrob ext. 6576

Advisor: J. E. Bercaw ext. 6577

Account Number: JEB.ENERGY-1.02-GRANT.MOOREJCP

By Michael W. Day 116 Beckman ext. 2734

e-mail: mikeday@caltech.edu

Contents

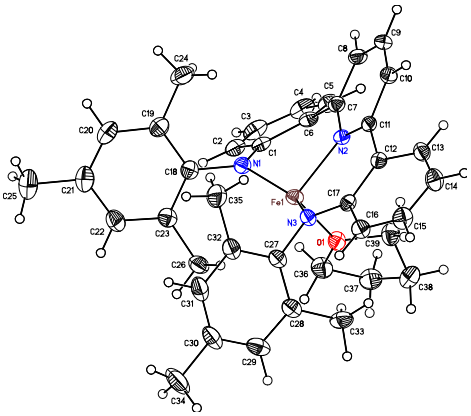

ECW03

Note: The crystallographic data have been deposited in the Cambridge Database (CCDC) and has been placed on hold pending further instructions from me. The deposition number is 678268. Ideally the CCDC would like the publication to contain a footnote of the type: "Crystallographic data have been deposited at the CCDC, 12 Union Road, Cambridge CB2 1EZ, UK and copies can be obtained on request, free of charge, by quoting the publication citation and the deposition number 678268."

Table 1. Crystal data and structure refinement for ECW03 (CCDC 678268).

Empirical formula	$C_{39}H_{41}N_3OFe$
Formula weight	623.60
Crystallization Solvent	Toluene/petroleumether
Crystal Habit	Block
Crystal size	0.26 x 0.25 x 0.21 mm^3
Crystal color	Dark red

Data Collection

Type of diffractometer	Bruker KAPPA APEX II
Wavelength	0.71073 Å MoKα
Data Collection Temperature	100(2) K
θ range for 9851 reflections used in lattice determination	2.48 to 35.69°
Unit cell dimensions	a = 14.5396(6) Å b = 13.5644(6) Å β= 98.247(2)° c = 16.6014(7) Å
Volume	3240.3(2) $Å^3$
Z	4
Crystal system	Monoclinic
Space group	$P2_1/c$
Density (calculated)	1.278 Mg/m^3
F(000)	1320
Data collection program	Bruker APEX2 v2.1-0
θ range for data collection	1.95 to 36.53°
Completeness to θ = 36.53°	93.3 %
Index ranges	$-24 \le h \le 22$, $-22 \le k \le 22$, $-26 \le l \le 27$
Data collection scan type	ω scans; 17 settings
Data reduction program	Bruker SAINT-Plus v7.34A
Reflections collected	97719
Independent reflections	14879 [R_{int}= 0.0486]
Absorption coefficient	0.501 mm^{-1}
Absorption correction	None

Table 1 (cont.)

Structure solution and Refinement

Structure solution program	SHELXS-97 (Sheldrick, 2008)
Primary solution method	Direct methods
Secondary solution method	Difference Fourier map
Hydrogen placement	Geometric positions
Structure refinement program	SHELXL-97 (Sheldrick, 2008)
Refinement method	Full matrix least-squares on F^2
Data / restraints / parameters	14879 / 0 / 403
Treatment of hydrogen atoms	Riding
Goodness-of-fit on F^2	2.823
Final R indices [$I>2\sigma(I)$, 10317 reflections]	R1 = 0.0501, *w*R2 = 0.0848
R indices (all data)	R1 = 0.0792, *w*R2 = 0.0860
Type of weighting scheme used	Sigma
Weighting scheme used	$w=1/\sigma^2(Fo^2)$
Max shift/error	0.003
Average shift/error	0.000
Largest diff. peak and hole	2.279 and -1.067 e.Å^{-3}

Special Refinement Details

Crystals were mounted on a glass fiber using Paratone oil then placed on the diffractometer under a nitrogen stream at 100K.

Refinement of F^2 against ALL reflections. The weighted R-factor (*w*R) and goodness of fit (S) are based on F^2, conventional R-factors (R) are based on F, with F set to zero for negative F^2. The threshold expression of $F^2 > 2\sigma(F^2)$ is used only for calculating R-factors(gt) etc. and is not relevant to the choice of reflections for refinement. R-factors based on F^2 are statistically about twice as large as those based on F, and R-factors based on ALL data will be even larger.

All esds (except the esd in the dihedral angle between two l.s. planes) are estimated using the full covariance matrix. The cell esds are taken into account individually in the estimation of esds in distances, angles and torsion angles; correlations between esds in cell parameters are only used when they are defined by crystal symmetry. An approximate (isotropic) treatment of cell esds is used for estimating esds involving l.s. planes.

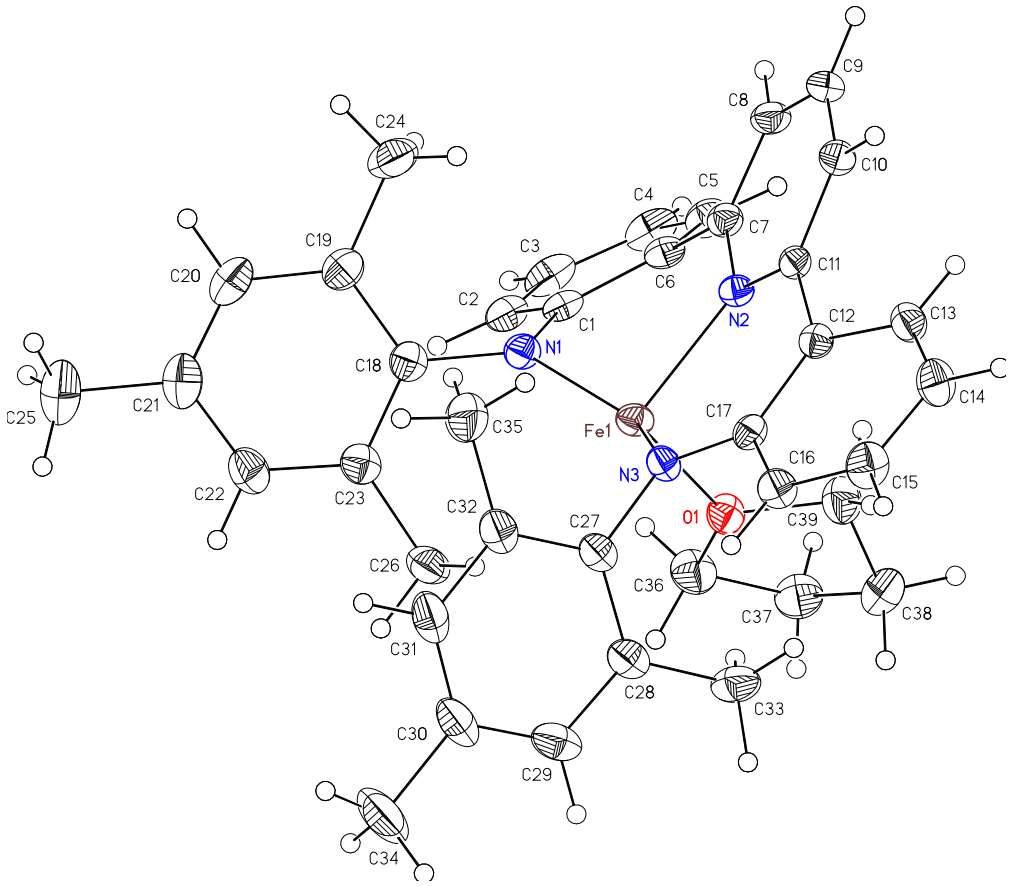
C9
C8
C24
C10
C4
C5
C19
C3
C7
C20
C6
C11
C2
N2
C1
C12
C13
N1
C18
C14
C21
C25
C35
Fe1
C17
N3
C16
C15
C22
C23
C32
C27
O1
C39
C26
C36
C37
C38
C31
C28
C33
C30
C29
C34

Table 2. Atomic coordinates (x 10^4) and equivalent isotropic displacement parameters ($Å^2$x 10^3) for ECW03 (CCDC 678268). U(eq) is defined as the trace of the orthogonalized U^{ij} tensor.

	x	y	z	U_{eq}
Fe(1)	2281(1)	2168(1)	8517(1)	19(1)
O(1)	2086(1)	2910(1)	7387(1)	24(1)
N(1)	1773(1)	860(1)	8316(1)	21(1)
N(2)	1160(1)	2750(1)	8954(1)	17(1)
N(3)	3188(1)	2847(1)	9282(1)	19(1)
C(1)	898(1)	889(1)	7846(1)	21(1)
C(2)	640(1)	204(1)	7222(1)	25(1)
C(3)	-198(1)	270(1)	6716(1)	30(1)
C(4)	-809(1)	1027(1)	6800(1)	30(1)
C(5)	-590(1)	1696(1)	7418(1)	27(1)
C(6)	244(1)	1635(1)	7966(1)	21(1)
C(7)	329(1)	2301(1)	8682(1)	20(1)
C(8)	-444(1)	2470(1)	9065(1)	24(1)
C(9)	-365(1)	3075(1)	9738(1)	26(1)
C(10)	466(1)	3530(1)	10008(1)	23(1)
C(11)	1234(1)	3388(1)	9596(1)	18(1)
C(12)	2101(1)	3946(1)	9852(1)	19(1)
C(13)	2009(1)	4838(1)	10263(1)	24(1)
C(14)	2748(1)	5410(1)	10593(1)	29(1)
C(15)	3637(1)	5083(1)	10530(1)	29(1)
C(16)	3769(1)	4231(1)	10121(1)	24(1)
C(17)	3023(1)	3652(1)	9734(1)	19(1)
C(18)	2226(1)	-67(1)	8422(1)	23(1)
C(19)	1844(1)	-829(1)	8840(1)	28(1)
C(20)	2299(1)	-1734(1)	8933(1)	34(1)
C(21)	3133(1)	-1905(1)	8648(1)	36(1)
C(22)	3521(1)	-1128(1)	8274(1)	31(1)
C(23)	3089(1)	-214(1)	8148(1)	25(1)
C(24)	955(1)	-666(1)	9191(1)	37(1)
C(25)	3616(1)	-2900(1)	8753(1)	49(1)
C(26)	3530(1)	588(1)	7708(1)	30(1)
C(27)	4129(1)	2569(1)	9221(1)	22(1)
C(28)	4607(1)	3015(1)	8642(1)	25(1)
C(29)	5484(1)	2647(1)	8549(1)	31(1)
C(30)	5884(1)	1864(1)	9001(1)	35(1)
C(31)	5406(1)	1449(1)	9574(1)	35(1)
C(32)	4530(1)	1782(1)	9694(1)	28(1)
C(33)	4194(1)	3870(1)	8130(1)	32(1)
C(34)	6839(1)	1497(1)	8872(1)	57(1)
C(35)	4025(1)	1312(1)	10322(1)	38(1)
C(36)	2090(1)	2548(1)	6570(1)	32(1)
C(37)	1640(1)	3365(1)	6009(1)	33(1)
C(38)	1787(1)	4274(1)	6540(1)	34(1)
C(39)	1653(1)	3871(1)	7358(1)	31(1)

Table 3. Selected bond lengths [Å] and angles [°] for ECW03 (CCDC 678268).

Fe(1)-N(3)	1.9278(10)	N(3)-Fe(1)-N(1)	139.52(4)
Fe(1)-N(1)	1.9319(10)	N(3)-Fe(1)-N(2)	94.97(4)
Fe(1)-N(2)	2.0356(10)	N(1)-Fe(1)-N(2)	96.44(4)
Fe(1)-O(1)	2.1126(9)	N(3)-Fe(1)-O(1)	110.45(4)
		N(1)-Fe(1)-O(1)	106.54(4)
		N(2)-Fe(1)-O(1)	96.85(4)

Table 4. Bond lengths [Å] and angles [°] for ECW03 (CCDC 678268).

Fe(1)-N(3)	1.9278(10)		
Fe(1)-N(1)	1.9319(10)	N(3)-Fe(1)-N(1)	139.52(4)
Fe(1)-N(2)	2.0356(10)	N(3)-Fe(1)-N(2)	94.97(4)
Fe(1)-O(1)	2.1126(9)	N(1)-Fe(1)-N(2)	96.44(4)
O(1)-C(36)	1.4435(15)	N(3)-Fe(1)-O(1)	110.45(4)
O(1)-C(39)	1.4453(15)	N(1)-Fe(1)-O(1)	106.54(4)
N(1)-C(1)	1.3950(15)	N(2)-Fe(1)-O(1)	96.85(4)
N(1)-C(18)	1.4184(16)	C(36)-O(1)-C(39)	109.65(10)
N(2)-C(11)	1.3654(15)	C(36)-O(1)-Fe(1)	130.90(8)
N(2)-C(7)	1.3706(14)	C(39)-O(1)-Fe(1)	117.46(7)
N(3)-C(17)	1.3656(15)	C(1)-N(1)-C(18)	117.65(10)
N(3)-C(27)	1.4373(15)	C(1)-N(1)-Fe(1)	111.48(8)
C(1)-C(2)	1.4027(17)	C(18)-N(1)-Fe(1)	129.32(8)
C(1)-C(6)	1.4218(17)	C(11)-N(2)-C(7)	120.38(10)
C(2)-C(3)	1.3797(18)	C(11)-N(2)-Fe(1)	123.15(8)
C(3)-C(4)	1.378(2)	C(7)-N(2)-Fe(1)	115.05(8)
C(4)-C(5)	1.3723(19)	C(17)-N(3)-C(27)	119.46(10)
C(5)-C(6)	1.4106(17)	C(17)-N(3)-Fe(1)	125.95(8)
C(6)-C(7)	1.4838(17)	C(27)-N(3)-Fe(1)	113.35(8)
C(7)-C(8)	1.3868(17)	N(1)-C(1)-C(2)	121.35(12)
C(8)-C(9)	1.3786(18)	N(1)-C(1)-C(6)	121.06(11)
C(9)-C(10)	1.3735(18)	C(2)-C(1)-C(6)	117.57(11)
C(10)-C(11)	1.4028(16)	C(3)-C(2)-C(1)	121.66(13)
C(11)-C(12)	1.4788(16)	C(4)-C(3)-C(2)	120.85(13)
C(12)-C(13)	1.4036(17)	C(5)-C(4)-C(3)	119.03(13)
C(12)-C(17)	1.4398(16)	C(4)-C(5)-C(6)	121.93(13)
C(13)-C(14)	1.3738(18)	C(5)-C(6)-C(1)	118.76(12)
C(14)-C(15)	1.3849(18)	C(5)-C(6)-C(7)	116.50(12)
C(15)-C(16)	1.3671(18)	C(1)-C(6)-C(7)	124.43(11)
C(16)-C(17)	1.4151(16)	N(2)-C(7)-C(8)	120.67(11)
C(18)-C(19)	1.4030(18)	N(2)-C(7)-C(6)	120.17(10)
C(18)-C(23)	1.4103(17)	C(8)-C(7)-C(6)	119.16(11)
C(19)-C(20)	1.3926(19)	C(9)-C(8)-C(7)	119.39(12)
C(19)-C(24)	1.5084(19)	C(10)-C(9)-C(8)	119.92(12)
C(20)-C(21)	1.382(2)	C(9)-C(10)-C(11)	120.29(12)
C(21)-C(22)	1.384(2)	N(2)-C(11)-C(10)	119.20(11)
C(21)-C(25)	1.520(2)	N(2)-C(11)-C(12)	121.14(10)
C(22)-C(23)	1.3905(19)	C(10)-C(11)-C(12)	119.64(11)
C(23)-C(26)	1.5049(18)	C(13)-C(12)-C(17)	117.37(11)
C(27)-C(32)	1.4007(18)	C(13)-C(12)-C(11)	116.38(11)
C(27)-C(28)	1.4020(18)	C(17)-C(12)-C(11)	126.24(11)
C(28)-C(29)	1.3982(18)	C(14)-C(13)-C(12)	123.88(12)
C(28)-C(33)	1.5114(19)	C(13)-C(14)-C(15)	118.24(12)
C(29)-C(30)	1.380(2)	C(16)-C(15)-C(14)	120.50(12)
C(30)-C(31)	1.376(2)	C(15)-C(16)-C(17)	122.76(12)
C(30)-C(34)	1.5190(19)	N(3)-C(17)-C(16)	120.67(11)
C(31)-C(32)	1.3919(18)	N(3)-C(17)-C(12)	122.43(11)
C(32)-C(35)	1.502(2)	C(16)-C(17)-C(12)	116.89(11)
C(36)-C(37)	1.5311(19)	C(19)-C(18)-C(23)	119.24(12)
C(37)-C(38)	1.513(2)	C(19)-C(18)-N(1)	120.38(11)
C(38)-C(39)	1.5034(19)	C(23)-C(18)-N(1)	120.30(12)

C(20)-C(19)-C(18)	119.27(13)
C(20)-C(19)-C(24)	120.45(13)
C(18)-C(19)-C(24)	120.28(12)
C(21)-C(20)-C(19)	122.43(14)
C(20)-C(21)-C(22)	117.34(14)
C(20)-C(21)-C(25)	121.52(15)
C(22)-C(21)-C(25)	121.13(14)
C(21)-C(22)-C(23)	122.83(13)
C(22)-C(23)-C(18)	118.77(13)
C(22)-C(23)-C(26)	120.19(12)
C(18)-C(23)-C(26)	121.02(12)
C(32)-C(27)-C(28)	120.32(11)
C(32)-C(27)-N(3)	119.01(11)
C(28)-C(27)-N(3)	120.39(12)
C(29)-C(28)-C(27)	118.17(13)
C(29)-C(28)-C(33)	120.43(13)
C(27)-C(28)-C(33)	121.40(11)
C(30)-C(29)-C(28)	122.26(14)
C(31)-C(30)-C(29)	118.40(13)
C(31)-C(30)-C(34)	121.75(15)
C(29)-C(30)-C(34)	119.83(15)
C(30)-C(31)-C(32)	121.93(14)
C(31)-C(32)-C(27)	118.90(13)
C(31)-C(32)-C(35)	120.65(13)
C(27)-C(32)-C(35)	120.45(12)
O(1)-C(36)-C(37)	105.45(11)
C(38)-C(37)-C(36)	102.94(11)
C(39)-C(38)-C(37)	101.77(11)
O(1)-C(39)-C(38)	104.19(11)

CALIFORNIA INSTITUTE OF TECHNOLOGY

BECKMAN INSTITUTE

X-RAY CRYSTALLOGRAPHY LABORATORY

Date 18 July 2008

Crystal Structure Analysis of:

[^{Mes}NNN]FeI (ECW04)

(shown below)

For Investigator: Edward Weintrob ext. 6576

Advisor: J. E. Bercaw ext. 6577

Account Number: JEB.ENERGY-1.02-GRANT.MOOREJCP

By Michael W. Day 116 Beckman ext. 2734

e-mail: mikeday@caltech.edu

Contents

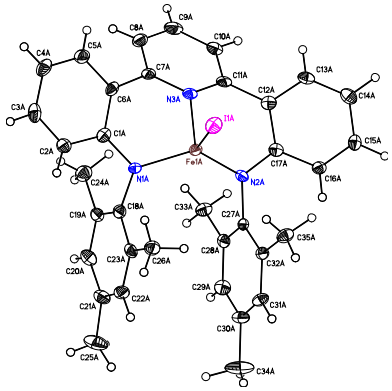

ECW04

Note: The crystallographic data have been deposited in the Cambridge Database (CCDC) and has been placed on hold pending further instructions from me. The deposition number is 695390. Ideally the CCDC would like the publication to contain a footnote of the type: "Crystallographic data have been deposited at the CCDC, 12 Union Road, Cambridge CB2 1EZ, UK and copies can be obtained on request, free of charge, by quoting the publication citation and the deposition number 695390."

Table 1. Crystal data and structure refinement for ECW04 (CCDC 695390).

Empirical formula	$2(C_{35}H_{33}N_3FeI)\ 1.5(C_6H_6)$	
Formula weight	736.97	
Crystallization Solvent	Benzene/petroleumether	
Crystal Habit	Flake	
Crystal size	0.16 x 0.10 x 0.06 mm^3	
Crystal color	Dark brown	

Data Collection

Type of diffractometer	Bruker KAPPA APEX II	
Wavelength	0.71073 Å MoKα	
Data Collection Temperature	100(2) K	
θ range for 9935 reflections used in lattice determination	2.54 to 31.80°	
Unit cell dimensions	a = 14.8740(7) Å b = 14.9489(7) Å c = 16.9750(8) Å	α= 69.528(3)° β= 72.061(3)° γ = 76.207(3)°
Volume	3327.7(3) $Å^3$	
Z	4	
Crystal system	Triclinic	
Space group	P-1	
Density (calculated)	1.471 Mg/m^3	
F(000)	1498	
Data collection program	Bruker APEX2 v2.1-0	
θ range for data collection	1.66 to 32.13°	
Completeness to θ = 32.13°	94.8 %	
Index ranges	$-21 \le h \le 20, -22 \le k \le 21, -25 \le l \le 24$	
Data collection scan type	ω scans; 17 settings	
Data reduction program	Bruker SAINT-Plus v7.34A	
Reflections collected	85468	
Independent reflections	22141 [R_{int}= 0.0607]	
Absorption coefficient	1.413 mm^{-1}	
Absorption correction	Semi-empirical from equivalents	
Max. and min. transmission	0.4344 and 0.3722	

Table 1 (cont.)

Structure solution and Refinement

Structure solution program	SHELXS-97 (Sheldrick, 2008)
Primary solution method	Direct methods
Secondary solution method	Difference Fourier map
Hydrogen placement	Difference Fourier map
Structure refinement program	SHELXL-97 (Sheldrick, 2008)
Refinement method	Full matrix least-squares on F^2
Data / restraints / parameters	22141 / 0 / 1102
Treatment of hydrogen atoms	Unrestrained
Goodness-of-fit on F^2	1.524
Final R indices [$I>2\sigma(I)$, 13476 reflections]	R1 = 0.0507, *w*R2 = 0.0602
R indices (all data)	R1 = 0.1132, *w*R2 = 0.0647
Type of weighting scheme used	Sigma
Weighting scheme used	$w=1/\sigma^2(Fo^2)$
Max shift/error	0.003
Average shift/error	0.000
Largest diff. peak and hole	1.916 and -1.795 e.Å^{-3}

Special Refinement Details

Crystals were mounted on a glass fiber using Paratone oil then placed on the diffractometer under a nitrogen stream at 100K.

Refinement of F^2 against ALL reflections. The weighted R-factor (*w*R) and goodness of fit (S) are based on F^2, conventional R-factors (R) are based on F, with F set to zero for negative F^2. The threshold expression of $F^2 > 2\sigma(F^2)$ is used only for calculating R-factors(gt) etc. and is not relevant to the choice of reflections for refinement. R-factors based on F^2 are statistically about twice as large as those based on F, and R-factors based on ALL data will be even larger.

All esds (except the esd in the dihedral angle between two l.s. planes) are estimated using the full covariance matrix. The cell esds are taken into account individually in the estimation of esds in distances, angles and torsion angles; correlations between esds in cell parameters are only used when they are defined by crystal symmetry. An approximate (isotropic) treatment of cell esds is used for estimating esds involving l.s. planes.

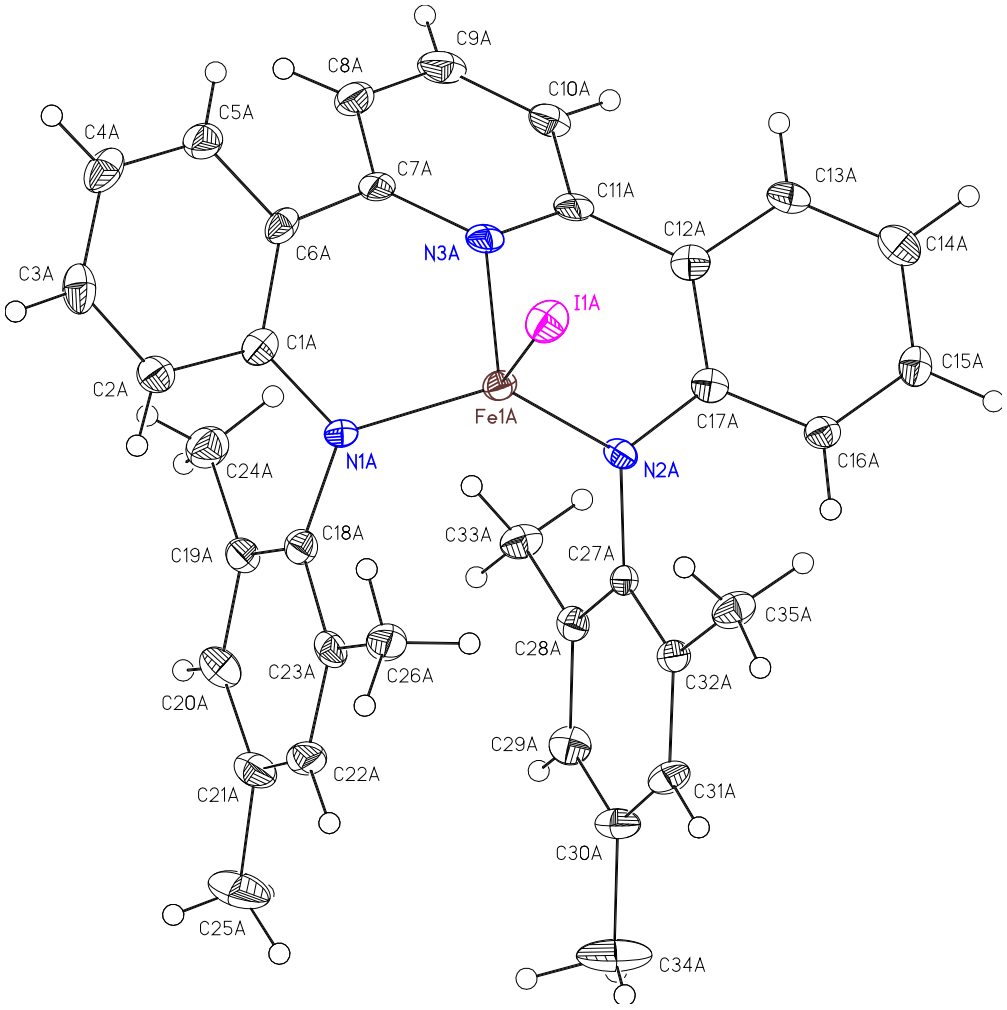
C9A
C8A
C10A
C5A
C4A
C7A
C11A
C13A
C6A
N3A
C12A
C14A
C3A
I1A
C1A
C15A
C2A
Fe1A
C17A
C24A
N1A
N2A
C16A
C18A
C33A
C27A
C19A
C35A
C28A
C23A
C26A
C32A
C20A
C29A
C22A
C31A
C21A
C30A
C25A
C34A

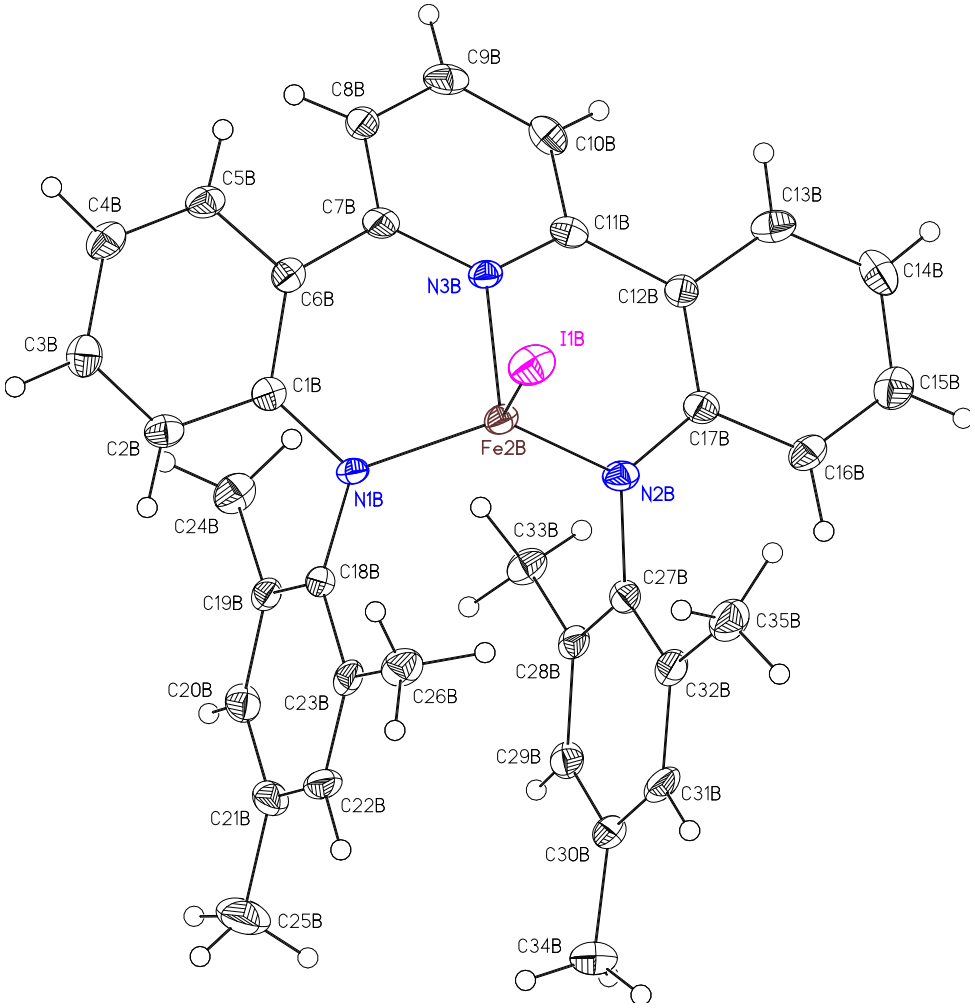
C9B
C8B
C10B
C5B
C4B
C7B
C11B
C13B
C14B
C6B
N3B
C12B
I1B
C3B
C1B
C15B
C2B
Fe2B
C17B
C16B
N1B
N2B
C24B
C33B
C18B
C27B
C19B
C35B
C28B
C32B
C20B
C23B
C26B
C29B
C31B
C22B
C21B
C30B
C25B
C34B

Table 2. Atomic coordinates (x 10^4) and equivalent isotropic displacement parameters ($Å^2$x 10^3) for ECW04 (CCDC 695390). U(eq) is defined as the trace of the orthogonalized U^{ij} tensor.

	x	y	z	U_{eq}
Fe(1A)	7733(1)	6797(1)	9594(1)	14(1)
I(1A)	9034(1)	6803(1)	10304(1)	22(1)
N(1A)	7164(2)	8029(2)	9000(1)	15(1)
N(2A)	6991(2)	5785(2)	10103(1)	14(1)
N(3A)	8373(2)	6424(2)	8490(1)	15(1)
C(1A)	7828(2)	8566(2)	8359(2)	16(1)
C(2A)	7785(2)	9546(2)	8240(2)	18(1)
C(3A)	8485(2)	10070(2)	7659(2)	23(1)
C(4A)	9263(2)	9626(2)	7158(2)	24(1)
C(5A)	9303(2)	8677(2)	7232(2)	22(1)
C(6A)	8601(2)	8124(2)	7809(2)	17(1)
C(7A)	8641(2)	7147(2)	7758(2)	17(1)
C(8A)	8926(2)	6978(2)	6952(2)	21(1)
C(9A)	8919(2)	6077(2)	6911(2)	24(1)
C(10A)	8649(2)	5360(2)	7654(2)	20(1)
C(11A)	8382(2)	5522(2)	8472(2)	16(1)
C(12A)	8097(2)	4739(2)	9261(2)	16(1)
C(13A)	8492(2)	3790(2)	9268(2)	19(1)
C(14A)	8181(2)	2995(2)	9922(2)	21(1)
C(15A)	7410(2)	3130(2)	10613(2)	17(1)
C(16A)	7027(2)	4047(2)	10647(2)	16(1)
C(17A)	7357(2)	4873(2)	10015(2)	14(1)
C(18A)	6176(2)	8444(2)	9186(2)	16(1)
C(19A)	5661(2)	8661(2)	8566(2)	18(1)
C(20A)	4674(2)	8922(2)	8799(2)	21(1)
C(21A)	4192(2)	8966(2)	9634(2)	22(1)
C(22A)	4737(2)	8802(2)	10216(2)	20(1)
C(23A)	5719(2)	8542(2)	10017(2)	17(1)
C(24A)	6135(3)	8585(3)	7663(2)	25(1)
C(25A)	3117(2)	9170(4)	9891(3)	35(1)
C(26A)	6268(2)	8374(3)	10677(2)	22(1)
C(27A)	6023(2)	5936(2)	10621(2)	13(1)
C(28A)	5287(2)	6171(2)	10211(2)	15(1)
C(29A)	4355(2)	6369(2)	10683(2)	19(1)
C(30A)	4150(2)	6325(2)	11550(2)	20(1)
C(31A)	4900(2)	6079(2)	11942(2)	18(1)
C(32A)	5846(2)	5879(2)	11494(2)	14(1)
C(33A)	5483(2)	6220(3)	9275(2)	20(1)
C(34A)	3127(2)	6531(4)	12043(3)	38(1)
C(35A)	6631(2)	5585(3)	11954(2)	21(1)
Fe(2B)	2563(1)	7908(1)	5601(1)	15(1)
I(1B)	1359(1)	9349(1)	5034(1)	25(1)
N(1B)	3345(2)	8156(2)	6179(1)	15(1)
N(2B)	3089(2)	6942(2)	5040(1)	16(1)
N(3B)	1832(2)	7032(2)	6682(1)	15(1)
C(1B)	2814(2)	8512(2)	6866(2)	15(1)

C(2B)	3128(2)	9216(2)	7047(2)	19(1)
C(3B)	2569(2)	9650(2)	7667(2)	21(1)
C(4B)	1679(2)	9394(2)	8131(2)	21(1)
C(5B)	1375(2)	8680(2)	7996(2)	19(1)
C(6B)	1930(2)	8195(2)	7384(2)	16(1)
C(7B)	1617(2)	7311(2)	7417(2)	17(1)
C(8B)	1126(2)	6738(2)	8196(2)	19(1)
C(9B)	895(2)	5884(2)	8233(2)	21(1)
C(10B)	1162(2)	5596(2)	7496(2)	20(1)
C(11B)	1613(2)	6185(2)	6707(2)	16(1)
C(12B)	1870(2)	5893(2)	5899(2)	17(1)
C(13B)	1373(2)	5194(2)	5910(2)	22(1)
C(14B)	1617(2)	4758(2)	5258(2)	25(1)
C(15B)	2389(2)	5023(2)	4563(2)	23(1)
C(16B)	2868(2)	5723(2)	4517(2)	19(1)
C(17B)	2615(2)	6199(2)	5156(2)	17(1)
C(18B)	4357(2)	8138(2)	5915(2)	15(1)
C(19B)	4925(2)	7499(2)	6459(2)	15(1)
C(20B)	5915(2)	7440(2)	6167(2)	20(1)
C(21B)	6348(2)	7993(2)	5361(2)	21(1)
C(22B)	5776(2)	8625(2)	4835(2)	21(1)
C(23B)	4783(2)	8722(2)	5090(2)	17(1)
C(24B)	4486(2)	6884(3)	7340(2)	23(1)
C(25B)	7428(2)	7925(3)	5055(3)	36(1)
C(26B)	4198(2)	9436(2)	4505(2)	23(1)
C(27B)	4033(2)	7003(2)	4476(2)	15(1)
C(28B)	4814(2)	6468(2)	4821(2)	16(1)
C(29B)	5733(2)	6607(2)	4304(2)	20(1)
C(30B)	5894(2)	7239(2)	3474(2)	20(1)
C(31B)	5110(2)	7738(2)	3144(2)	21(1)
C(32B)	4177(2)	7629(2)	3629(2)	19(1)
C(33B)	4662(2)	5779(2)	5719(2)	21(1)
C(34B)	6900(3)	7403(3)	2965(2)	31(1)
C(35B)	3349(2)	8191(3)	3241(2)	26(1)
C(41)	9959(2)	8043(2)	3955(2)	31(1)
C(42)	10483(3)	7138(3)	4013(2)	31(1)
C(43)	10445(2)	6636(3)	3490(2)	37(1)
C(44)	9886(2)	7032(3)	2909(2)	36(1)
C(45)	9370(2)	7937(3)	2841(2)	30(1)
C(46)	9411(2)	8439(2)	3367(2)	29(1)
C(51)	588(2)	421(2)	206(2)	26(1)
C(52)	117(2)	952(2)	-423(2)	25(1)
C(53)	488(2)	-534(3)	629(2)	26(1)

Table 3. Selected bond lengths [Å] and angles [°] for ECW04 (CCDC 695390).

Fe(1A)-N(2A)	1.883(2)	N(2A)-Fe(1A)-N(1A)	118.30(10)
Fe(1A)-N(1A)	1.899(2)	N(2A)-Fe(1A)-N(3A)	94.66(9)
Fe(1A)-N(3A)	2.0274(19)	N(1A)-Fe(1A)-N(3A)	93.44(9)
Fe(1A)-I(1A)	2.5784(4)	N(2A)-Fe(1A)-I(1A)	118.77(7)
Fe(2B)-N(2B)	1.888(2)	N(1A)-Fe(1A)-I(1A)	115.77(7)
Fe(2B)-N(1B)	1.902(2)	N(3A)-Fe(1A)-I(1A)	108.74(6)
Fe(2B)-N(3B)	2.008(2)	N(2B)-Fe(2B)-N(1B)	116.72(9)
Fe(2B)-I(1B)	2.5576(5)	N(2B)-Fe(2B)-N(3B)	94.66(9)
		N(1B)-Fe(2B)-N(3B)	94.36(9)
		N(2B)-Fe(2B)-I(1B)	121.38(7)
		N(1B)-Fe(2B)-I(1B)	115.03(7)
		N(3B)-Fe(2B)-I(1B)	107.04(6)

Table 4. Bond lengths [Å] and angles [°] for ECW04 (CCDC 695390).

Fe(1A)-N(2A)	1.883(2)	C(24A)-H(24B)	0.94(3)
Fe(1A)-N(1A)	1.899(2)	C(24A)-H(24C)	0.86(3)
Fe(1A)-N(3A)	2.0274(19)	C(25A)-H(25A)	0.88(3)
Fe(1A)-I(1A)	2.5784(4)	C(25A)-H(25B)	0.80(4)
N(1A)-C(1A)	1.381(3)	C(25A)-H(25C)	0.97(5)
N(1A)-C(18A)	1.435(3)	C(26A)-H(26A)	0.96(2)
N(2A)-C(17A)	1.385(3)	C(26A)-H(26B)	0.95(3)
N(2A)-C(27A)	1.449(3)	C(26A)-H(26C)	0.94(3)
N(3A)-C(7A)	1.354(3)	C(27A)-C(28A)	1.386(4)
N(3A)-C(11A)	1.356(3)	C(27A)-C(32A)	1.398(3)
C(1A)-C(2A)	1.396(4)	C(28A)-C(29A)	1.392(4)
C(1A)-C(6A)	1.426(3)	C(28A)-C(33A)	1.502(4)
C(2A)-C(3A)	1.373(4)	C(29A)-C(30A)	1.388(4)
C(2A)-H(2A)	0.85(2)	C(29A)-H(29A)	0.87(3)
C(3A)-C(4A)	1.388(4)	C(30A)-C(31A)	1.384(4)
C(3A)-H(3A)	0.89(2)	C(30A)-C(34A)	1.511(4)
C(4A)-C(5A)	1.369(4)	C(31A)-C(32A)	1.395(3)
C(4A)-H(4A)	0.91(3)	C(31A)-H(31A)	0.91(2)
C(5A)-C(6A)	1.396(4)	C(32A)-C(35A)	1.499(4)
C(5A)-H(5A)	0.82(3)	C(33A)-H(33A)	0.93(3)
C(6A)-C(7A)	1.479(4)	C(33A)-H(33B)	0.92(4)
C(7A)-C(8A)	1.398(3)	C(33A)-H(33C)	0.92(3)
C(8A)-C(9A)	1.374(4)	C(34A)-H(34A)	0.76(3)
C(8A)-H(8A)	0.87(2)	C(34A)-H(34B)	0.79(3)
C(9A)-C(10A)	1.359(4)	C(34A)-H(34C)	1.04(6)
C(9A)-H(9A)	0.90(2)	C(35A)-H(35A)	0.93(3)
C(10A)-C(11A)	1.412(3)	C(35A)-H(35B)	0.86(3)
C(10A)-H(10A)	0.90(2)	C(35A)-H(35C)	0.97(3)
C(11A)-C(12A)	1.462(4)	Fe(2B)-N(2B)	1.888(2)
C(12A)-C(13A)	1.396(4)	Fe(2B)-N(1B)	1.902(2)
C(12A)-C(17A)	1.448(3)	Fe(2B)-N(3B)	2.008(2)
C(13A)-C(14A)	1.372(4)	Fe(2B)-I(1B)	2.5576(5)
C(13A)-H(13A)	0.86(2)	N(1B)-C(1B)	1.391(3)
C(14A)-C(15A)	1.399(4)	N(1B)-C(18B)	1.430(3)
C(14A)-H(14A)	1.00(3)	N(2B)-C(17B)	1.381(3)
C(15A)-C(16A)	1.368(4)	N(2B)-C(27B)	1.438(3)
C(15A)-H(15A)	0.97(2)	N(3B)-C(11B)	1.364(3)
C(16A)-C(17A)	1.399(4)	N(3B)-C(7B)	1.374(3)
C(16A)-H(16A)	0.90(2)	C(1B)-C(2B)	1.403(4)
C(18A)-C(19A)	1.393(4)	C(1B)-C(6B)	1.422(4)
C(18A)-C(23A)	1.406(3)	C(2B)-C(3B)	1.379(3)
C(19A)-C(20A)	1.394(4)	C(2B)-H(2B)	0.93(2)
C(19A)-C(24A)	1.508(4)	C(3B)-C(4B)	1.381(4)
C(20A)-C(21A)	1.395(4)	C(3B)-H(3B)	0.95(2)
C(20A)-H(20A)	0.96(2)	C(4B)-C(5B)	1.364(4)
C(21A)-C(22A)	1.386(4)	C(4B)-H(4B)	0.96(2)
C(21A)-C(25A)	1.508(4)	C(5B)-C(6B)	1.414(3)
C(22A)-C(23A)	1.384(4)	C(5B)-H(5B)	0.88(3)
C(22A)-H(22A)	0.92(2)	C(6B)-C(7B)	1.480(4)
C(23A)-C(26A)	1.502(4)	C(7B)-C(8B)	1.388(4)
C(24A)-H(24A)	1.01(3)	C(8B)-C(9B)	1.375(4)

C(8B)-H(8B)	0.87(2)	C(35B)-H(35E)	0.98(3)
C(9B)-C(10B)	1.378(4)	C(35B)-H(35F)	0.94(3)
C(9B)-H(9B)	0.98(3)	C(41)-C(46)	1.367(4)
C(10B)-C(11B)	1.386(4)	C(41)-C(42)	1.378(4)
C(10B)-H(10B)	0.88(2)	C(41)-H(41)	0.86(2)
C(11B)-C(12B)	1.495(3)	C(42)-C(43)	1.368(4)
C(12B)-C(13B)	1.410(4)	C(42)-H(42)	0.88(3)
C(12B)-C(17B)	1.417(4)	C(43)-C(44)	1.371(5)
C(13B)-C(14B)	1.387(4)	C(43)-H(43)	1.00(3)
C(13B)-H(13B)	0.89(3)	C(44)-C(45)	1.372(5)
C(14B)-C(15B)	1.386(4)	C(44)-H(44)	0.93(3)
C(14B)-H(14B)	0.84(2)	C(45)-C(46)	1.373(4)
C(15B)-C(16B)	1.368(4)	C(45)-H(45)	0.97(3)
C(15B)-H(15B)	0.92(2)	C(46)-H(46)	0.90(2)
C(16B)-C(17B)	1.408(3)	C(51)-C(52)	1.364(4)
C(16B)-H(16B)	0.97(2)	C(51)-C(53)	1.377(4)
C(18B)-C(19B)	1.399(4)	C(51)-H(51)	0.93(3)
C(18B)-C(23B)	1.409(4)	C(52)-C(53)#1	1.392(4)
C(19B)-C(20B)	1.393(4)	C(52)-H(52)	0.91(2)
C(19B)-C(24B)	1.494(4)	C(53)-C(52)#1	1.392(4)
C(20B)-C(21B)	1.375(4)	C(53)-H(53)	0.87(3)
C(20B)-H(20B)	0.96(3)		
C(21B)-C(22B)	1.381(4)	N(2A)-Fe(1A)-N(1A)	118.30(10)
C(21B)-C(25B)	1.519(4)	N(2A)-Fe(1A)-N(3A)	94.66(9)
C(22B)-C(23B)	1.393(4)	N(1A)-Fe(1A)-N(3A)	93.44(9)
C(22B)-H(22B)	0.95(3)	N(2A)-Fe(1A)-I(1A)	118.77(7)
C(23B)-C(26B)	1.493(4)	N(1A)-Fe(1A)-I(1A)	115.77(7)
C(24B)-H(24D)	0.94(2)	N(3A)-Fe(1A)-I(1A)	108.74(6)
C(24B)-H(24E)	0.94(3)	C(1A)-N(1A)-C(18A)	120.0(2)
C(24B)-H(24F)	0.93(3)	C(1A)-N(1A)-Fe(1A)	112.52(18)
C(25B)-H(25D)	0.89(4)	C(18A)-N(1A)-Fe(1A)	127.38(18)
C(25B)-H(25E)	0.95(3)	C(17A)-N(2A)-C(27A)	118.0(2)
C(25B)-H(25F)	0.91(5)	C(17A)-N(2A)-Fe(1A)	121.37(17)
C(26B)-H(26D)	0.93(4)	C(27A)-N(2A)-Fe(1A)	120.59(16)
C(26B)-H(26E)	0.89(3)	C(7A)-N(3A)-C(11A)	122.0(2)
C(26B)-H(26F)	0.99(3)	C(7A)-N(3A)-Fe(1A)	116.75(17)
C(27B)-C(32B)	1.398(4)	C(11A)-N(3A)-Fe(1A)	120.33(18)
C(27B)-C(28B)	1.406(4)	N(1A)-C(1A)-C(2A)	121.6(2)
C(28B)-C(29B)	1.397(4)	N(1A)-C(1A)-C(6A)	120.7(2)
C(28B)-C(33B)	1.495(4)	C(2A)-C(1A)-C(6A)	117.7(3)
C(29B)-C(30B)	1.379(4)	C(3A)-C(2A)-C(1A)	122.4(3)
C(29B)-H(29B)	0.91(3)	C(3A)-C(2A)-H(2A)	117.3(18)
C(30B)-C(31B)	1.388(4)	C(1A)-C(2A)-H(2A)	120.3(18)
C(30B)-C(34B)	1.508(4)	C(2A)-C(3A)-C(4A)	119.8(3)
C(31B)-C(32B)	1.394(4)	C(2A)-C(3A)-H(3A)	118.4(16)
C(31B)-H(31B)	0.91(3)	C(4A)-C(3A)-H(3A)	121.8(16)
C(32B)-C(35B)	1.508(4)	C(5A)-C(4A)-C(3A)	119.1(3)
C(33B)-H(33D)	0.93(2)	C(5A)-C(4A)-H(4A)	123.2(16)
C(33B)-H(33E)	0.96(3)	C(3A)-C(4A)-H(4A)	117.6(16)
C(33B)-H(33F)	1.06(4)	C(4A)-C(5A)-C(6A)	122.6(3)
C(34B)-H(34D)	0.88(4)	C(4A)-C(5A)-H(5A)	121(2)
C(34B)-H(34E)	0.92(4)	C(6A)-C(5A)-H(5A)	117(2)
C(34B)-H(34F)	0.91(3)	C(5A)-C(6A)-C(1A)	118.2(3)
C(35B)-H(35D)	0.87(3)	C(5A)-C(6A)-C(7A)	118.4(2)

C(1A)-C(6A)-C(7A)	123.1(2)	H(24A)-C(24A)-H(24B)	106(2)
N(3A)-C(7A)-C(8A)	119.9(3)	C(19A)-C(24A)-H(24C)	108.4(18)
N(3A)-C(7A)-C(6A)	120.1(2)	H(24A)-C(24A)-H(24C)	107(3)
C(8A)-C(7A)-C(6A)	120.0(3)	H(24B)-C(24A)-H(24C)	113(3)
C(9A)-C(8A)-C(7A)	119.3(3)	C(21A)-C(25A)-H(25A)	115(2)
C(9A)-C(8A)-H(8A)	122.2(14)	C(21A)-C(25A)-H(25B)	115(3)
C(7A)-C(8A)-H(8A)	118.4(14)	H(25A)-C(25A)-H(25B)	107(4)
C(10A)-C(9A)-C(8A)	119.8(3)	C(21A)-C(25A)-H(25C)	114(3)
C(10A)-C(9A)-H(9A)	120.9(16)	H(25A)-C(25A)-H(25C)	105(4)
C(8A)-C(9A)-H(9A)	119.1(16)	H(25B)-C(25A)-H(25C)	99(4)
C(9A)-C(10A)-C(11A)	121.0(3)	C(23A)-C(26A)-H(26A)	114.4(16)
C(9A)-C(10A)-H(10A)	122.4(15)	C(23A)-C(26A)-H(26B)	110(2)
C(11A)-C(10A)-H(10A)	116.6(15)	H(26A)-C(26A)-H(26B)	109(2)
N(3A)-C(11A)-C(10A)	117.9(3)	C(23A)-C(26A)-H(26C)	113.7(19)
N(3A)-C(11A)-C(12A)	122.2(2)	H(26A)-C(26A)-H(26C)	105(2)
C(10A)-C(11A)-C(12A)	119.9(3)	H(26B)-C(26A)-H(26C)	105(3)
C(13A)-C(12A)-C(17A)	117.1(3)	C(28A)-C(27A)-C(32A)	121.5(2)
C(13A)-C(12A)-C(11A)	118.7(2)	C(28A)-C(27A)-N(2A)	117.6(2)
C(17A)-C(12A)-C(11A)	123.9(2)	C(32A)-C(27A)-N(2A)	120.9(2)
C(14A)-C(13A)-C(12A)	123.6(3)	C(27A)-C(28A)-C(29A)	118.6(2)
C(14A)-C(13A)-H(13A)	118.4(19)	C(27A)-C(28A)-C(33A)	121.1(2)
C(12A)-C(13A)-H(13A)	118.0(19)	C(29A)-C(28A)-C(33A)	120.2(3)
C(13A)-C(14A)-C(15A)	118.9(3)	C(30A)-C(29A)-C(28A)	121.6(3)
C(13A)-C(14A)-H(14A)	121.9(17)	C(30A)-C(29A)-H(29A)	121.1(17)
C(15A)-C(14A)-H(14A)	119.2(17)	C(28A)-C(29A)-H(29A)	117.2(17)
C(16A)-C(15A)-C(14A)	119.3(3)	C(31A)-C(30A)-C(29A)	118.3(3)
C(16A)-C(15A)-H(15A)	120.6(13)	C(31A)-C(30A)-C(34A)	121.7(3)
C(14A)-C(15A)-H(15A)	119.9(13)	C(29A)-C(30A)-C(34A)	120.0(3)
C(15A)-C(16A)-C(17A)	123.3(3)	C(30A)-C(31A)-C(32A)	122.1(2)
C(15A)-C(16A)-H(16A)	121.3(17)	C(30A)-C(31A)-H(31A)	119.4(15)
C(17A)-C(16A)-H(16A)	115.3(17)	C(32A)-C(31A)-H(31A)	118.5(15)
N(2A)-C(17A)-C(16A)	121.4(2)	C(31A)-C(32A)-C(27A)	117.8(3)
N(2A)-C(17A)-C(12A)	121.2(2)	C(31A)-C(32A)-C(35A)	120.2(2)
C(16A)-C(17A)-C(12A)	117.4(2)	C(27A)-C(32A)-C(35A)	122.0(2)
C(19A)-C(18A)-C(23A)	120.7(2)	C(28A)-C(33A)-H(33A)	110.7(16)
C(19A)-C(18A)-N(1A)	119.3(2)	C(28A)-C(33A)-H(33B)	116(2)
C(23A)-C(18A)-N(1A)	119.8(2)	H(33A)-C(33A)-H(33B)	106(3)
C(18A)-C(19A)-C(20A)	118.8(2)	C(28A)-C(33A)-H(33C)	108.1(17)
C(18A)-C(19A)-C(24A)	122.0(3)	H(33A)-C(33A)-H(33C)	106(2)
C(20A)-C(19A)-C(24A)	119.2(3)	H(33B)-C(33A)-H(33C)	110(3)
C(19A)-C(20A)-C(21A)	121.7(3)	C(30A)-C(34A)-H(34A)	116(3)
C(19A)-C(20A)-H(20A)	117.1(15)	C(30A)-C(34A)-H(34B)	113(2)
C(21A)-C(20A)-H(20A)	121.2(15)	H(34A)-C(34A)-H(34B)	129(4)
C(22A)-C(21A)-C(20A)	117.7(3)	C(30A)-C(34A)-H(34C)	108(3)
C(22A)-C(21A)-C(25A)	121.7(3)	H(34A)-C(34A)-H(34C)	98(4)
C(20A)-C(21A)-C(25A)	120.7(3)	H(34B)-C(34A)-H(34C)	78(4)
C(23A)-C(22A)-C(21A)	122.7(3)	C(32A)-C(35A)-H(35A)	114.9(19)
C(23A)-C(22A)-H(22A)	115.3(17)	C(32A)-C(35A)-H(35B)	109(2)
C(21A)-C(22A)-H(22A)	121.9(17)	H(35A)-C(35A)-H(35B)	106(2)
C(22A)-C(23A)-C(18A)	118.2(3)	C(32A)-C(35A)-H(35C)	111.9(17)
C(22A)-C(23A)-C(26A)	120.1(2)	H(35A)-C(35A)-H(35C)	105(3)
C(18A)-C(23A)-C(26A)	121.7(3)	H(35B)-C(35A)-H(35C)	109(2)
C(19A)-C(24A)-H(24A)	114.5(16)	N(2B)-Fe(2B)-N(1B)	116.72(9)
C(19A)-C(24A)-H(24B)	108.2(16)	N(2B)-Fe(2B)-N(3B)	94.66(9)

N(1B)-Fe(2B)-N(3B)	94.36(9)	C(13B)-C(14B)-H(14B)	119.8(18)
N(2B)-Fe(2B)-I(1B)	121.38(7)	C(16B)-C(15B)-C(14B)	120.1(3)
N(1B)-Fe(2B)-I(1B)	115.03(7)	C(16B)-C(15B)-H(15B)	122.5(18)
N(3B)-Fe(2B)-I(1B)	107.04(6)	C(14B)-C(15B)-H(15B)	117.4(18)
C(1B)-N(1B)-C(18B)	119.3(2)	C(15B)-C(16B)-C(17B)	122.8(3)
C(1B)-N(1B)-Fe(2B)	112.61(17)	C(15B)-C(16B)-H(16B)	117.8(13)
C(18B)-N(1B)-Fe(2B)	127.48(15)	C(17B)-C(16B)-H(16B)	119.2(13)
C(17B)-N(2B)-C(27B)	120.1(2)	N(2B)-C(17B)-C(16B)	119.7(2)
C(17B)-N(2B)-Fe(2B)	123.15(17)	N(2B)-C(17B)-C(12B)	122.3(2)
C(27B)-N(2B)-Fe(2B)	116.77(17)	C(16B)-C(17B)-C(12B)	118.0(3)
C(11B)-N(3B)-C(7B)	121.5(2)	C(19B)-C(18B)-C(23B)	120.3(2)
C(11B)-N(3B)-Fe(2B)	122.99(16)	C(19B)-C(18B)-N(1B)	119.6(2)
C(7B)-N(3B)-Fe(2B)	115.34(18)	C(23B)-C(18B)-N(1B)	120.0(3)
N(1B)-C(1B)-C(2B)	120.6(2)	C(20B)-C(19B)-C(18B)	118.9(3)
N(1B)-C(1B)-C(6B)	120.9(2)	C(20B)-C(19B)-C(24B)	120.0(3)
C(2B)-C(1B)-C(6B)	118.5(2)	C(18B)-C(19B)-C(24B)	121.1(3)
C(3B)-C(2B)-C(1B)	121.5(3)	C(21B)-C(20B)-C(19B)	121.9(3)
C(3B)-C(2B)-H(2B)	117.2(13)	C(21B)-C(20B)-H(20B)	118.0(17)
C(1B)-C(2B)-H(2B)	121.2(13)	C(19B)-C(20B)-H(20B)	120.1(17)
C(2B)-C(3B)-C(4B)	120.2(3)	C(20B)-C(21B)-C(22B)	118.4(3)
C(2B)-C(3B)-H(3B)	117.4(14)	C(20B)-C(21B)-C(25B)	121.2(3)
C(4B)-C(3B)-H(3B)	122.4(14)	C(22B)-C(21B)-C(25B)	120.4(3)
C(5B)-C(4B)-C(3B)	119.4(3)	C(21B)-C(22B)-C(23B)	122.5(3)
C(5B)-C(4B)-H(4B)	118.7(15)	C(21B)-C(22B)-H(22B)	118.3(18)
C(3B)-C(4B)-H(4B)	121.7(15)	C(23B)-C(22B)-H(22B)	119.2(18)
C(4B)-C(5B)-C(6B)	122.6(3)	C(22B)-C(23B)-C(18B)	117.9(3)
C(4B)-C(5B)-H(5B)	122.4(16)	C(22B)-C(23B)-C(26B)	120.3(3)
C(6B)-C(5B)-H(5B)	115.0(16)	C(18B)-C(23B)-C(26B)	121.7(3)
C(5B)-C(6B)-C(1B)	117.5(2)	C(19B)-C(24B)-H(24D)	111.5(17)
C(5B)-C(6B)-C(7B)	117.4(2)	C(19B)-C(24B)-H(24E)	114.8(18)
C(1B)-C(6B)-C(7B)	124.5(2)	H(24D)-C(24B)-H(24E)	109(2)
N(3B)-C(7B)-C(8B)	119.1(3)	C(19B)-C(24B)-H(24F)	110(2)
N(3B)-C(7B)-C(6B)	120.4(2)	H(24D)-C(24B)-H(24F)	110(2)
C(8B)-C(7B)-C(6B)	120.4(2)	H(24E)-C(24B)-H(24F)	101(3)
C(9B)-C(8B)-C(7B)	120.1(3)	C(21B)-C(25B)-H(25D)	113(2)
C(9B)-C(8B)-H(8B)	122.6(17)	C(21B)-C(25B)-H(25E)	114(2)
C(7B)-C(8B)-H(8B)	117.0(17)	H(25D)-C(25B)-H(25E)	112(3)
C(8B)-C(9B)-C(10B)	119.6(3)	C(21B)-C(25B)-H(25F)	113(3)
C(8B)-C(9B)-H(9B)	119.3(14)	H(25D)-C(25B)-H(25F)	97(4)
C(10B)-C(9B)-H(9B)	120.5(14)	H(25E)-C(25B)-H(25F)	106(3)
C(9B)-C(10B)-C(11B)	120.6(3)	C(23B)-C(26B)-H(26D)	116(2)
C(9B)-C(10B)-H(10B)	119.2(16)	C(23B)-C(26B)-H(26E)	115.2(19)
C(11B)-C(10B)-H(10B)	120.2(15)	H(26D)-C(26B)-H(26E)	103(3)
N(3B)-C(11B)-C(10B)	118.9(2)	C(23B)-C(26B)-H(26F)	115.6(17)
N(3B)-C(11B)-C(12B)	120.4(2)	H(26D)-C(26B)-H(26F)	103(2)
C(10B)-C(11B)-C(12B)	120.8(3)	H(26E)-C(26B)-H(26F)	103(2)
C(13B)-C(12B)-C(17B)	117.4(2)	C(32B)-C(27B)-C(28B)	120.8(2)
C(13B)-C(12B)-C(11B)	116.6(2)	C(32B)-C(27B)-N(2B)	120.9(2)
C(17B)-C(12B)-C(11B)	125.8(2)	C(28B)-C(27B)-N(2B)	118.2(2)
C(14B)-C(13B)-C(12B)	123.2(3)	C(29B)-C(28B)-C(27B)	118.1(3)
C(14B)-C(13B)-H(13B)	117.4(17)	C(29B)-C(28B)-C(33B)	121.0(3)
C(12B)-C(13B)-H(13B)	119.3(16)	C(27B)-C(28B)-C(33B)	120.8(3)
C(15B)-C(14B)-C(13B)	118.3(3)	C(30B)-C(29B)-C(28B)	122.2(3)
C(15B)-C(14B)-H(14B)	121.7(17)	C(30B)-C(29B)-H(29B)	119.4(18)

C(28B)-C(29B)-H(29B)	118.3(18)
C(29B)-C(30B)-C(31B)	118.3(3)
C(29B)-C(30B)-C(34B)	120.0(3)
C(31B)-C(30B)-C(34B)	121.7(3)
C(30B)-C(31B)-C(32B)	122.0(3)
C(30B)-C(31B)-H(31B)	119.6(18)
C(32B)-C(31B)-H(31B)	118.4(18)
C(31B)-C(32B)-C(27B)	118.5(3)
C(31B)-C(32B)-C(35B)	120.0(3)
C(27B)-C(32B)-C(35B)	121.5(3)
C(28B)-C(33B)-H(33D)	114.1(16)
C(28B)-C(33B)-H(33E)	111.9(17)
H(33D)-C(33B)-H(33E)	106(2)
C(28B)-C(33B)-H(33F)	114(2)
H(33D)-C(33B)-H(33F)	109(2)
H(33E)-C(33B)-H(33F)	101(2)
C(30B)-C(34B)-H(34D)	111(2)
C(30B)-C(34B)-H(34E)	107(3)
H(34D)-C(34B)-H(34E)	109(3)
C(30B)-C(34B)-H(34F)	111.0(19)
H(34D)-C(34B)-H(34F)	102(3)
H(34E)-C(34B)-H(34F)	117(3)
C(32B)-C(35B)-H(35D)	112(2)
C(32B)-C(35B)-H(35E)	108.9(19)
H(35D)-C(35B)-H(35E)	115(3)
C(32B)-C(35B)-H(35F)	111(2)
H(35D)-C(35B)-H(35F)	102(3)
H(35E)-C(35B)-H(35F)	109(3)
C(46)-C(41)-C(42)	119.8(3)
C(46)-C(41)-H(41)	117(2)
C(42)-C(41)-H(41)	123(2)
C(43)-C(42)-C(41)	120.0(4)
C(43)-C(42)-H(42)	118.9(19)
C(41)-C(42)-H(42)	121.0(19)
C(42)-C(43)-C(44)	120.0(3)
C(42)-C(43)-H(43)	120.9(18)
C(44)-C(43)-H(43)	118.9(18)
C(43)-C(44)-C(45)	120.3(3)
C(43)-C(44)-H(44)	118.9(19)
C(45)-C(44)-H(44)	120.8(19)
C(44)-C(45)-C(46)	119.5(3)
C(44)-C(45)-H(45)	118.0(15)
C(46)-C(45)-H(45)	122.4(15)
C(41)-C(46)-C(45)	120.5(3)
C(41)-C(46)-H(46)	120.6(17)
C(45)-C(46)-H(46)	118.9(17)
C(52)-C(51)-C(53)	120.7(3)
C(52)-C(51)-H(51)	121(2)
C(53)-C(51)-H(51)	118(2)
C(51)-C(52)-C(53)#1	120.0(3)
C(51)-C(52)-H(52)	119.3(16)
C(53)#1-C(52)-H(52)	120.6(16)
C(51)-C(53)-C(52)#1	119.2(3)
C(51)-C(53)-H(53)	121.0(19)
C(52)#1-C(53)-H(53)	119.6(19)

Symmetry transformations used to generate equivalent atoms: #1 -x,-y,-z

CALIFORNIA INSTITUTE OF TECHNOLOGY

BECKMAN INSTITUTE

X-RAY CRYSTALLOGRAPHY LABORATORY

Date 8 August 2008

Crystal Structure Analysis of:

([^{Mes}NNN]Fe)$_2$O (ECW05)

(shown below)

For Investigator: Edward Weintrob ext. 6576

Advisor: J. E. Bercaw ext. 6577

Account Number: JEB.ENERGY-1.02-GRANT.MOOREJCP

By Michael W. Day 116 Beckman ext. 2734

e-mail: mikeday@caltech.edu

Contents

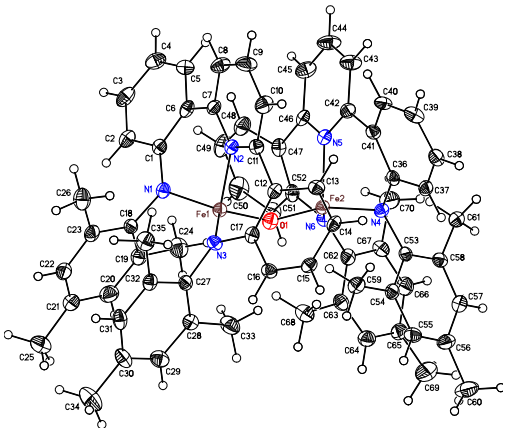

ECW05

Note: The crystallographic data have been deposited in the Cambridge Database (CCDC) and has been placed on hold pending further instructions from me. The deposition number is 697910. Ideally the CCDC would like the publication to contain a footnote of the type: "Crystallographic data have been deposited at the CCDC, 12 Union Road, Cambridge CB2 1EZ, UK and copies can be obtained on request, free of charge, by quoting the publication citation and the deposition number 697910."

Table 1. Crystal data and structure refinement for ECW05 (CCDC 697910).

Empirical formula	$C_{70}H_{66}N_6OFe_2 \bullet 0.5(C_7H_8)$
Formula weight	1165.05
Crystallization Solvent	Toluene
Crystal Habit	Plate
Crystal size	0.38 x 0.24 x 0.07 mm^3
Crystal color	Green

Data Collection

Type of diffractometer	Bruker KAPPA APEX II
Wavelength	0.71073 Å MoKα
Data Collection Temperature	100(2) K
θ range for 9283 reflections used in lattice determination	2.30 to 31.52°
Unit cell dimensions	a = 19.8707(9) Å b = 39.4031(19) Å c = 15.1038(6) Å
Volume	11825.8(9) $Å^3$
Z	8
Crystal system	Orthorhombic
Space group	I*ba*2
Density (calculated)	1.309 Mg/m^3
F(000)	4904
Data collection program	Bruker APEX2 v2.1-0
θ range for data collection	1.86 to 32.23°
Completeness to θ = 32.23°	93.8 %
Index ranges	$-29 \le h \le 29$, $-59 \le k \le 42$, $-19 \le l \le 22$
Data collection scan type	ω scans; 12 settings
Data reduction program	Bruker SAINT-Plus v7.34A
Reflections collected	121688
Independent reflections	18216 [R_{int}= 0.0571]
Absorption coefficient	0.542 mm^{-1}
Absorption correction	None
Max. and min. transmission	0.9630 and 0.8204

Table 1 (cont.)

Structure solution and Refinement

Structure solution program	SHELXS-97 (Sheldrick, 2008)
Primary solution method	Direct methods
Secondary solution method	Difference Fourier map
Hydrogen placement	Geometric positions
Structure refinement program	SHELXL-97 (Sheldrick, 2008)
Refinement method	Full matrix least-squares on F^2
Data / restraints / parameters	18216 / 10 / 757
Treatment of hydrogen atoms	Riding
Goodness-of-fit on F^2	1.792
Final R indices [$I>2\sigma(I)$, 14462 reflections]	R1 = 0.0416, *w*R2 = 0.0558
R indices (all data)	R1 = 0.0600, *w*R2 = 0.0567
Type of weighting scheme used	Sigma
Weighting scheme used	$w=1/\sigma^2(Fo^2)$
Max shift/error	0.003
Average shift/error	0.000
Absolute structure determination	Anomalous differences
Absolute structure parameter	-0.007(6)
Largest diff. peak and hole	1.372 and -0.704 e.$Å^{-3}$

Special Refinement Details

Crystals were mounted on a glass fiber using Paratone oil then placed on the diffractometer under a nitrogen stream at 100K.

Refinement of F^2 against ALL reflections. The weighted R-factor (*w*R) and goodness of fit (S) are based on F^2, conventional R-factors (R) are based on F, with F set to zero for negative F^2. The threshold expression of $F^2 > 2\sigma(F^2)$ is used only for calculating R-factors(gt) etc. and is not relevant to the choice of reflections for refinement. R-factors based on F^2 are statistically about twice as large as those based on F, and R-factors based on ALL data will be even larger.

All esds (except the esd in the dihedral angle between two l.s. planes) are estimated using the full covariance matrix. The cell esds are taken into account individually in the estimation of esds in distances, angles and torsion angles; correlations between esds in cell parameters are only used when they are defined by crystal symmetry. An approximate (isotropic) treatment of cell esds is used for estimating esds involving l.s. planes.

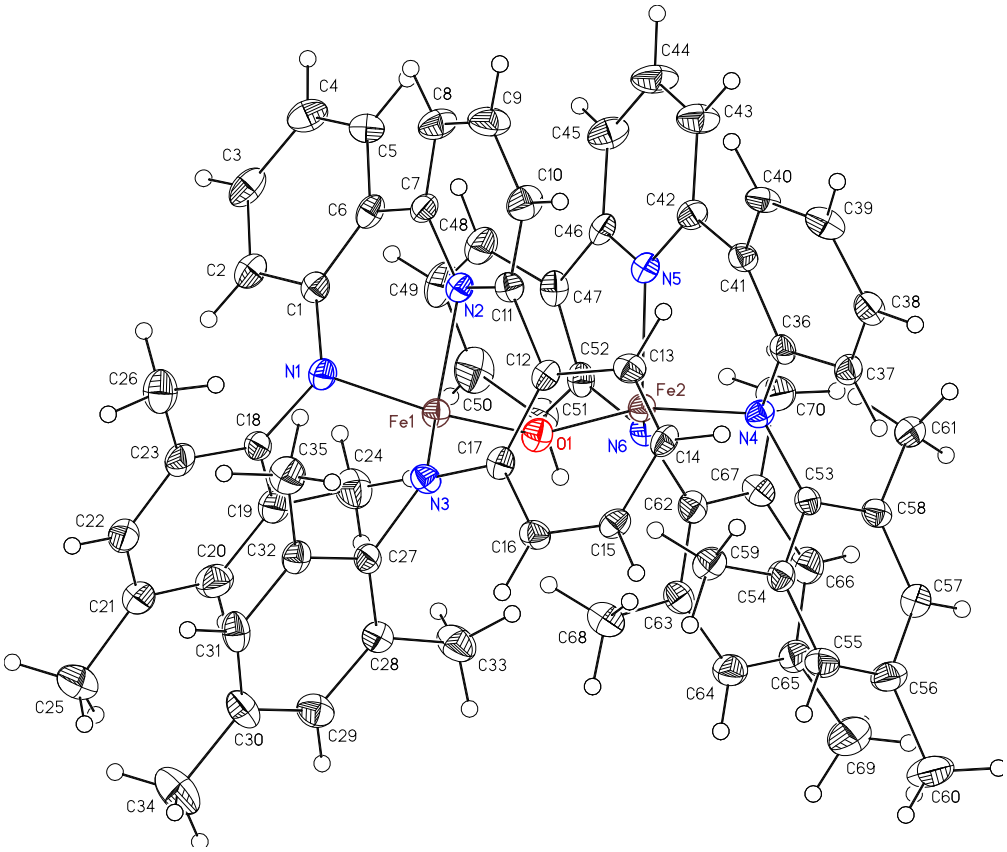
C44
C4
C8
C9
C43
C45
C5
C3
C10
C40
C7
C42
C39
C6
C48
C46
C2
N5
C41
C49
N2
C11
C47
C38
C1
C36
C52
C12
C13
N1
C26
C37
Fe2
C18
C50
C51
C70
C61
Fe1
O1
N6
N4
C23
C35
C24
C17
C14
C67
C53
N3
C62
C58
C22
C19
C16
C15
C59
C20
C32
C27
C66
C54
C57
C21
C63
C68
C31
C28
C33
C55
C25
C65
C56
C64
C30
C29
C69
C34
C60

Table 2. Atomic coordinates (x 10^4) and equivalent isotropic displacement parameters ($Å^2$x 10^3) for ECW05 (CCDC 697910). U(eq) is defined as the trace of the orthogonalized U^{ij} tensor.

	x	y	z	U_{eq}
Fe(1)	7380(1)	8495(1)	10926(1)	16(1)
Fe(2)	7526(1)	8565(1)	8636(1)	16(1)
O(1)	7402(1)	8618(1)	9792(1)	21(1)
N(1)	8180(1)	8518(1)	11632(1)	19(1)
N(2)	7370(1)	7983(1)	10897(1)	16(1)
N(3)	6529(1)	8538(1)	11526(1)	18(1)
N(4)	6787(1)	8425(1)	7895(1)	17(1)
N(5)	8028(1)	8124(1)	8483(1)	17(1)
N(6)	8206(1)	8840(1)	8083(1)	18(1)
C(1)	8708(1)	8299(1)	11484(1)	18(1)
C(2)	9373(1)	8391(1)	11729(1)	23(1)
C(3)	9912(1)	8190(1)	11523(1)	27(1)
C(4)	9823(1)	7887(1)	11070(1)	27(1)
C(5)	9181(1)	7785(1)	10874(1)	22(1)
C(6)	8607(1)	7975(1)	11101(1)	19(1)
C(7)	7949(1)	7801(1)	10999(1)	19(1)
C(8)	7909(1)	7449(1)	11032(1)	26(1)
C(9)	7294(1)	7289(1)	10922(2)	29(1)
C(10)	6722(1)	7481(1)	10808(1)	26(1)
C(11)	6760(1)	7832(1)	10801(1)	18(1)
C(12)	6139(1)	8040(1)	10700(1)	17(1)
C(13)	5624(1)	7897(1)	10185(1)	19(1)
C(14)	4989(1)	8035(1)	10140(1)	20(1)
C(15)	4850(1)	8326(1)	10626(1)	19(1)
C(16)	5349(1)	8483(1)	11104(1)	19(1)
C(17)	6014(1)	8356(1)	11122(1)	18(1)
C(18)	8271(1)	8820(1)	12134(1)	19(1)
C(19)	8463(1)	9122(1)	11722(1)	24(1)
C(20)	8476(1)	9417(1)	12220(1)	30(1)
C(21)	8305(1)	9422(1)	13118(1)	31(1)
C(22)	8132(1)	9116(1)	13510(1)	28(1)
C(23)	8118(1)	8816(1)	13049(1)	22(1)
C(24)	8664(1)	9124(1)	10762(1)	31(1)
C(25)	8297(1)	9749(1)	13633(2)	50(1)
C(26)	7947(1)	8485(1)	13498(1)	31(1)
C(27)	6372(1)	8808(1)	12120(1)	18(1)
C(28)	6424(1)	9147(1)	11842(1)	20(1)
C(29)	6325(1)	9406(1)	12450(1)	25(1)
C(30)	6169(1)	9340(1)	13334(1)	26(1)
C(31)	6107(1)	9004(1)	13585(1)	24(1)
C(32)	6199(1)	8739(1)	13004(1)	20(1)
C(33)	6572(1)	9232(1)	10887(1)	31(1)
C(34)	6062(1)	9631(1)	13968(1)	44(1)
C(35)	6107(1)	8376(1)	13307(1)	27(1)
C(36)	6541(1)	8101(1)	7933(1)	16(1)
C(37)	5878(1)	8026(1)	7672(1)	20(1)
C(38)	5605(1)	7708(1)	7745(1)	22(1)

C(39)	5979(1)	7445(1)	8100(1)	24(1)
C(40)	6632(1)	7506(1)	8338(1)	21(1)
C(41)	6948(1)	7821(1)	8226(1)	18(1)
C(42)	7693(1)	7830(1)	8310(1)	19(1)
C(43)	8061(1)	7535(1)	8154(1)	28(1)
C(44)	8756(1)	7544(1)	8191(1)	32(1)
C(45)	9081(1)	7842(1)	8362(1)	27(1)
C(46)	8716(1)	8137(1)	8517(1)	19(1)
C(47)	9071(1)	8461(1)	8678(1)	20(1)
C(48)	9712(1)	8436(1)	9075(1)	26(1)
C(49)	10152(1)	8702(1)	9122(1)	32(1)
C(50)	9958(1)	9011(1)	8760(1)	35(1)
C(51)	9326(1)	9055(1)	8419(1)	28(1)
C(52)	8853(1)	8785(1)	8390(1)	20(1)
C(53)	6399(1)	8693(1)	7508(1)	17(1)
C(54)	5914(1)	8866(1)	8008(1)	19(1)
C(55)	5601(1)	9149(1)	7644(1)	23(1)
C(56)	5755(1)	9263(1)	6801(1)	25(1)
C(57)	6228(1)	9085(1)	6307(1)	22(1)
C(58)	6548(1)	8800(1)	6647(1)	18(1)
C(59)	5729(1)	8747(1)	8924(1)	23(1)
C(60)	5417(1)	9575(1)	6434(1)	38(1)
C(61)	7040(1)	8606(1)	6082(1)	23(1)
C(62)	8065(1)	9128(1)	7541(1)	19(1)
C(63)	7634(1)	9382(1)	7838(1)	21(1)
C(64)	7468(1)	9649(1)	7285(1)	25(1)
C(65)	7724(1)	9677(1)	6439(1)	26(1)
C(66)	8157(1)	9422(1)	6157(1)	27(1)
C(67)	8334(1)	9149(1)	6676(1)	23(1)
C(68)	7356(1)	9380(1)	8775(1)	28(1)
C(69)	7543(1)	9972(1)	5848(1)	44(1)
C(70)	8796(1)	8877(1)	6331(1)	31(1)
C(81)	10000	10000	7764(3)	288(7)
C(82)	10000	10000	6753(3)	204(4)
C(83)	9909(2)	9699(1)	6290(3)	155(3)
C(84)	9909(2)	9699(1)	5371(3)	381(8)
C(85)	10000	10000	4906(3)	207(6)

Table 3. Selected bond lengths [Å] and angles [°] for ECW05 (CCDC 697910).

Fe(1)-O(1)	1.7802(14)	O(1)-Fe(1)-N(1)	120.08(6)
Fe(1)-N(1)	1.9174(15)	O(1)-Fe(1)-N(3)	116.84(6)
Fe(1)-N(3)	1.9262(14)	N(1)-Fe(1)-N(3)	117.50(6)
Fe(1)-N(2)	2.0161(14)	O(1)-Fe(1)-N(2)	104.57(6)
Fe(2)-O(1)	1.7761(14)	N(1)-Fe(1)-N(2)	93.86(6)
Fe(2)-N(6)	1.9234(15)	N(3)-Fe(1)-N(2)	95.14(6)
Fe(2)-N(4)	1.9262(15)	O(1)-Fe(2)-N(6)	117.27(6)
Fe(2)-N(5)	2.0153(15)	O(1)-Fe(2)-N(4)	119.97(6)
		N(6)-Fe(2)-N(4)	116.39(6)
		O(1)-Fe(2)-N(5)	106.37(6)
		N(6)-Fe(2)-N(5)	95.06(6)
		N(4)-Fe(2)-N(5)	93.67(6)

Table 4. Bond lengths [Å] and angles [°] for ECW05 (CCDC 697910).

Fe(1)-O(1)	1.7802(14)	C(29)-C(30)	1.396(3)
Fe(1)-N(1)	1.9174(15)	C(30)-C(31)	1.383(3)
Fe(1)-N(3)	1.9262(14)	C(30)-C(34)	1.508(3)
Fe(1)-N(2)	2.0161(14)	C(31)-C(32)	1.378(3)
Fe(2)-O(1)	1.7761(14)	C(32)-C(35)	1.513(3)
Fe(2)-N(6)	1.9234(15)	C(36)-C(37)	1.406(2)
Fe(2)-N(4)	1.9262(15)	C(36)-C(41)	1.437(3)
Fe(2)-N(5)	2.0153(15)	C(37)-C(38)	1.370(3)
N(1)-C(1)	1.378(2)	C(38)-C(39)	1.382(3)
N(1)-C(18)	1.421(2)	C(39)-C(40)	1.369(2)
N(2)-C(11)	1.358(2)	C(40)-C(41)	1.402(3)
N(2)-C(7)	1.365(2)	C(41)-C(42)	1.487(2)
N(3)-C(17)	1.391(2)	C(42)-C(43)	1.395(3)
N(3)-C(27)	1.428(2)	C(43)-C(44)	1.382(3)
N(4)-C(36)	1.370(2)	C(44)-C(45)	1.362(3)
N(4)-C(53)	1.431(2)	C(45)-C(46)	1.391(3)
N(5)-C(42)	1.361(2)	C(46)-C(47)	1.478(2)
N(5)-C(46)	1.371(2)	C(47)-C(48)	1.410(2)
N(6)-C(52)	1.384(2)	C(47)-C(52)	1.416(3)
N(6)-C(62)	1.427(2)	C(48)-C(49)	1.367(3)
C(1)-C(2)	1.419(2)	C(49)-C(50)	1.387(3)
C(1)-C(6)	1.414(3)	C(50)-C(51)	1.369(3)
C(2)-C(3)	1.370(3)	C(51)-C(52)	1.422(3)
C(3)-C(4)	1.386(3)	C(53)-C(58)	1.398(2)
C(4)-C(5)	1.370(2)	C(53)-C(54)	1.402(2)
C(5)-C(6)	1.408(2)	C(54)-C(55)	1.391(3)
C(6)-C(7)	1.486(2)	C(54)-C(59)	1.506(2)
C(7)-C(8)	1.389(3)	C(55)-C(56)	1.385(2)
C(8)-C(9)	1.384(2)	C(56)-C(57)	1.391(3)
C(9)-C(10)	1.376(3)	C(56)-C(60)	1.506(3)
C(10)-C(11)	1.385(3)	C(57)-C(58)	1.390(3)
C(11)-C(12)	1.487(2)	C(58)-C(61)	1.507(2)
C(12)-C(13)	1.403(2)	C(62)-C(63)	1.391(3)
C(12)-C(17)	1.421(3)	C(62)-C(67)	1.414(2)
C(13)-C(14)	1.376(2)	C(63)-C(64)	1.384(3)
C(14)-C(15)	1.387(2)	C(63)-C(68)	1.519(2)
C(15)-C(16)	1.374(2)	C(64)-C(65)	1.380(3)
C(16)-C(17)	1.413(2)	C(65)-C(66)	1.390(3)
C(18)-C(19)	1.397(3)	C(65)-C(69)	1.507(3)
C(18)-C(23)	1.415(2)	C(66)-C(67)	1.379(3)
C(19)-C(20)	1.385(3)	C(67)-C(70)	1.504(3)
C(19)-C(24)	1.503(3)	C(81)-C(82)	1.5266(9)
C(20)-C(21)	1.400(3)	C(82)-C(83)#1	1.3880(9)
C(21)-C(22)	1.384(3)	C(82)-C(83)	1.3881(9)
C(21)-C(25)	1.506(3)	C(83)-C(84)	1.3885(9)
C(22)-C(23)	1.374(3)	C(84)-C(85)	1.3897(10)
C(23)-C(26)	1.509(3)	C(85)-C(84)#1	1.3898(10)
C(27)-C(28)	1.402(3)		
C(27)-C(32)	1.406(2)	O(1)-Fe(1)-N(1)	120.08(6)
C(28)-C(29)	1.389(3)	O(1)-Fe(1)-N(3)	116.84(6)
C(28)-C(33)	1.509(2)	N(1)-Fe(1)-N(3)	117.50(6)

O(1)-Fe(1)-N(2)	104.57(6)	N(3)-C(17)-C(16)	120.89(17)
N(1)-Fe(1)-N(2)	93.86(6)	N(3)-C(17)-C(12)	121.30(16)
N(3)-Fe(1)-N(2)	95.14(6)	C(16)-C(17)-C(12)	117.80(16)
O(1)-Fe(2)-N(6)	117.27(6)	C(19)-C(18)-C(23)	120.15(19)
O(1)-Fe(2)-N(4)	119.97(6)	C(19)-C(18)-N(1)	120.67(16)
N(6)-Fe(2)-N(4)	116.39(6)	C(23)-C(18)-N(1)	119.04(18)
O(1)-Fe(2)-N(5)	106.37(6)	C(20)-C(19)-C(18)	118.61(18)
N(6)-Fe(2)-N(5)	95.06(6)	C(20)-C(19)-C(24)	120.88(19)
N(4)-Fe(2)-N(5)	93.67(6)	C(18)-C(19)-C(24)	120.51(19)
Fe(2)-O(1)-Fe(1)	156.60(7)	C(19)-C(20)-C(21)	122.3(2)
C(1)-N(1)-C(18)	120.93(15)	C(22)-C(21)-C(20)	117.6(2)
C(1)-N(1)-Fe(1)	120.81(12)	C(22)-C(21)-C(25)	121.43(19)
C(18)-N(1)-Fe(1)	116.21(12)	C(20)-C(21)-C(25)	121.0(2)
C(11)-N(2)-C(7)	122.30(15)	C(23)-C(22)-C(21)	122.49(19)
C(11)-N(2)-Fe(1)	116.62(12)	C(22)-C(23)-C(18)	118.85(19)
C(7)-N(2)-Fe(1)	121.04(12)	C(22)-C(23)-C(26)	121.44(18)
C(17)-N(3)-C(27)	120.01(14)	C(18)-C(23)-C(26)	119.71(18)
C(17)-N(3)-Fe(1)	113.20(11)	C(28)-C(27)-C(32)	119.27(18)
C(27)-N(3)-Fe(1)	123.58(12)	C(28)-C(27)-N(3)	120.36(16)
C(36)-N(4)-C(53)	120.80(15)	C(32)-C(27)-N(3)	120.28(18)
C(36)-N(4)-Fe(2)	120.97(12)	C(29)-C(28)-C(27)	119.46(17)
C(53)-N(4)-Fe(2)	115.93(12)	C(29)-C(28)-C(33)	119.71(18)
C(42)-N(5)-C(46)	121.72(16)	C(27)-C(28)-C(33)	120.81(17)
C(42)-N(5)-Fe(2)	120.95(12)	C(28)-C(29)-C(30)	121.74(19)
C(46)-N(5)-Fe(2)	117.25(12)	C(31)-C(30)-C(29)	117.50(18)
C(52)-N(6)-C(62)	120.02(15)	C(31)-C(30)-C(34)	122.66(18)
C(52)-N(6)-Fe(2)	114.75(12)	C(29)-C(30)-C(34)	119.83(19)
C(62)-N(6)-Fe(2)	123.96(12)	C(30)-C(31)-C(32)	122.70(18)
N(1)-C(1)-C(2)	120.41(17)	C(31)-C(32)-C(27)	119.28(19)
N(1)-C(1)-C(6)	121.52(16)	C(31)-C(32)-C(35)	120.62(17)
C(2)-C(1)-C(6)	118.07(17)	C(27)-C(32)-C(35)	120.09(18)
C(3)-C(2)-C(1)	121.34(19)	N(4)-C(36)-C(37)	121.31(17)
C(2)-C(3)-C(4)	120.65(18)	N(4)-C(36)-C(41)	121.83(16)
C(5)-C(4)-C(3)	118.70(18)	C(37)-C(36)-C(41)	116.85(18)
C(4)-C(5)-C(6)	122.93(18)	C(38)-C(37)-C(36)	122.77(18)
C(5)-C(6)-C(1)	117.77(16)	C(37)-C(38)-C(39)	120.26(18)
C(5)-C(6)-C(7)	116.14(17)	C(40)-C(39)-C(38)	118.66(19)
C(1)-C(6)-C(7)	125.76(16)	C(39)-C(40)-C(41)	123.27(19)
N(2)-C(7)-C(8)	118.77(16)	C(40)-C(41)-C(36)	117.70(17)
N(2)-C(7)-C(6)	120.70(16)	C(40)-C(41)-C(42)	117.14(17)
C(8)-C(7)-C(6)	120.51(16)	C(36)-C(41)-C(42)	124.69(17)
C(9)-C(8)-C(7)	120.01(17)	N(5)-C(42)-C(43)	119.14(17)
C(10)-C(9)-C(8)	119.52(18)	N(5)-C(42)-C(41)	121.49(17)
C(9)-C(10)-C(11)	120.43(18)	C(43)-C(42)-C(41)	119.24(18)
N(2)-C(11)-C(10)	118.91(16)	C(44)-C(43)-C(42)	119.6(2)
N(2)-C(11)-C(12)	120.75(16)	C(45)-C(44)-C(43)	120.3(2)
C(10)-C(11)-C(12)	120.34(16)	C(44)-C(45)-C(46)	120.32(18)
C(13)-C(12)-C(17)	118.16(16)	N(5)-C(46)-C(45)	118.86(17)
C(13)-C(12)-C(11)	116.22(17)	N(5)-C(46)-C(47)	120.98(16)
C(17)-C(12)-C(11)	125.50(16)	C(45)-C(46)-C(47)	120.10(17)
C(14)-C(13)-C(12)	122.53(18)	C(48)-C(47)-C(52)	117.91(17)
C(13)-C(14)-C(15)	118.88(17)	C(48)-C(47)-C(46)	116.22(17)
C(16)-C(15)-C(14)	120.42(17)	C(52)-C(47)-C(46)	125.57(16)
C(15)-C(16)-C(17)	121.63(17)	C(49)-C(48)-C(47)	123.2(2)

C(48)-C(49)-C(50)	118.32(18)
C(51)-C(50)-C(49)	120.99(19)
C(50)-C(51)-C(52)	121.45(19)
N(6)-C(52)-C(47)	121.93(17)
N(6)-C(52)-C(51)	120.39(18)
C(47)-C(52)-C(51)	117.68(17)
C(58)-C(53)-C(54)	120.03(17)
C(58)-C(53)-N(4)	119.14(16)
C(54)-C(53)-N(4)	120.60(16)
C(55)-C(54)-C(53)	119.01(17)
C(55)-C(54)-C(59)	120.24(17)
C(53)-C(54)-C(59)	120.74(17)
C(56)-C(55)-C(54)	121.66(18)
C(55)-C(56)-C(57)	118.59(18)
C(55)-C(56)-C(60)	120.29(18)
C(57)-C(56)-C(60)	121.12(18)
C(56)-C(57)-C(58)	121.36(18)
C(57)-C(58)-C(53)	119.32(17)
C(57)-C(58)-C(61)	119.89(17)
C(53)-C(58)-C(61)	120.78(17)
C(63)-C(62)-C(67)	119.28(18)
C(63)-C(62)-N(6)	120.59(16)
C(67)-C(62)-N(6)	120.04(17)
C(64)-C(63)-C(62)	119.96(18)
C(64)-C(63)-C(68)	118.63(17)
C(62)-C(63)-C(68)	121.39(17)
C(65)-C(64)-C(63)	122.15(19)
C(64)-C(65)-C(66)	117.03(19)
C(64)-C(65)-C(69)	121.48(19)
C(66)-C(65)-C(69)	121.49(19)
C(67)-C(66)-C(65)	123.23(18)
C(66)-C(67)-C(62)	118.35(18)
C(66)-C(67)-C(70)	120.91(17)
C(62)-C(67)-C(70)	120.73(18)
C(83)#1-C(82)-C(83)	119.49(17)
C(83)#1-C(82)-C(81)	120.26(8)
C(83)-C(82)-C(81)	120.25(8)
C(82)-C(83)-C(84)	120.28(11)
C(83)-C(84)-C(85)	120.30(11)
C(84)-C(85)-C(84)#1	119.36(18)

Symmetry transformations used to
generate equivalent atoms:
#1 -x+2,-y+2,z

CALIFORNIA INSTITUTE OF TECHNOLOGY

BECKMAN INSTITUTE

X-RAY CRYSTALLOGRAPHY LABORATORY

Date 23 July 2010

Crystal Structure Analysis of:

[^{Mes}NNN]FeCH$_2$PMe$_3$ (ECW09)

(shown below)

For Investigator: Ed Weintrob ext. 6576

Advisor: J. E. Bercaw ext. 6577

Account Number: JEB.ENERGY-1.02-GRANT.MOOREJCP

By Michael W. Day 116 Beckman ext. 2734

e-mail: mikeday@caltech.edu

Contents

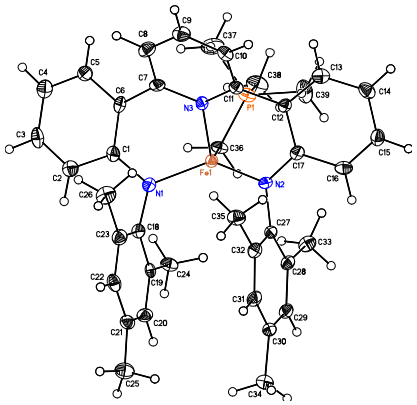

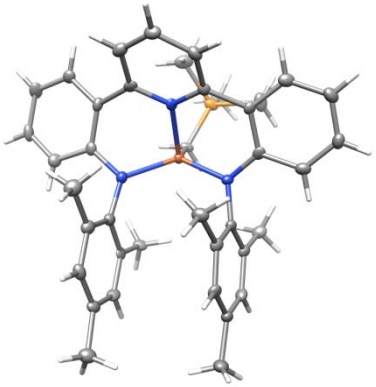

ECW09

Note: The crystallographic data have been deposited in the Cambridge Database (CCDC) and has been placed on hold pending further instructions from me. The deposition number is 785426. Ideally the CCDC would like the publication to contain a footnote of the type: "Crystallographic data have been deposited at the CCDC, 12 Union Road, Cambridge CB2 1EZ, UK and copies can be obtained on request, free of charge, by quoting the publication citation and the deposition number 785426."

Table 1. Crystal data and structure refinement for ECW09 (CCDC 785426).

Empirical formula	$C_{39}H_{44}N_3PFe \bullet 1.5(C_6H_6)$
Formula weight	758.75
Crystallization Solvent	Benzene/pentane
Crystal Habit	Blade
Crystal size	0.21 x 0.11 x 0.07 mm^3
Crystal color	Dark red

Data Collection

Type of diffractometer	Bruker KAPPA APEX II	
Wavelength	0.71073 Å MoKα	
Data Collection Temperature	100(2) K	
θ range for 6619 reflections used in lattice determination	2.32 to 27.47°	
Unit cell dimensions	a = 10.0318(4) Å b = 37.7399(15) Å c = 10.8356(4) Å	α= 90° β= 98.561(2)° γ = 90°
Volume	4056.6(3) $Å^3$	
Z	4	
Crystal system	Monoclinic	
Space group	P $2_1/n$	
Density (calculated)	1.242 Mg/m^3	
F(000)	1612	
Data collection program	Bruker APEX2 v2009.7-0	
θ range for data collection	1.08 to 28.31°	
Completeness to θ = 28.31°	94.4 %	
Index ranges	$-13 \le h \le 13$, $-49 \le k \le 50$, $-12 \le l \le 14$	
Data collection scan type	ω scans; 6 settings	
Data reduction program	Bruker SAINT-Plus v7.66A	
Reflections collected	32506	
Independent reflections	9557 [R_{int}= 0.1258]	
Absorption coefficient	0.448 mm^{-1}	
Absorption correction	None	
Max. and min. transmission	0.9693 and 0.9118	

Table 1 (cont.)

Structure solution and Refinement

Structure solution program	SHELXS-97 (Sheldrick, 2008)
Primary solution method	Direct methods
Secondary solution method	Difference Fourier map
Hydrogen placement	Geometric positions
Structure refinement program	SHELXL-97 (Sheldrick, 2008)
Refinement method	Full matrix least-squares on F^2
Data / restraints / parameters	9557 / 0 / 487
Treatment of hydrogen atoms	Riding
Goodness-of-fit on F^2	1.292
Final R indices [$I>2\sigma(I)$, 6045 reflections]	R1 = 0.0630, *w*R2 = 0.1094
R indices (all data)	R1 = 0.1102, *w*R2 = 0.1148
Type of weighting scheme used	Sigma
Weighting scheme used	$w=1/\sigma^2(Fo^2)$
Max shift/error	0.000
Average shift/error	0.000
Largest diff. peak and hole	0.775 and -0.798 e.Å^{-3}

Special Refinement Details

Crystals were mounted on a glass fiber using Paratone oil then placed on the diffractometer under a nitrogen stream at 100K.

Refinement of F^2 against ALL reflections. The weighted R-factor (*w*R) and goodness of fit (S) are based on F^2, conventional R-factors (R) are based on F, with F set to zero for negative F^2. The threshold expression of $F^2 > 2\sigma(F^2)$ is used only for calculating R-factors(gt) etc. and is not relevant to the choice of reflections for refinement. R-factors based on F^2 are statistically about twice as large as those based on F, and R-factors based on ALL data will be even larger.

All esds (except the esd in the dihedral angle between two l.s. planes) are estimated using the full covariance matrix. The cell esds are taken into account individually in the estimation of esds in distances, angles and torsion angles; correlations between esds in cell parameters are only used when they are defined by crystal symmetry. An approximate (isotropic) treatment of cell esds is used for estimating esds involving l.s. planes.

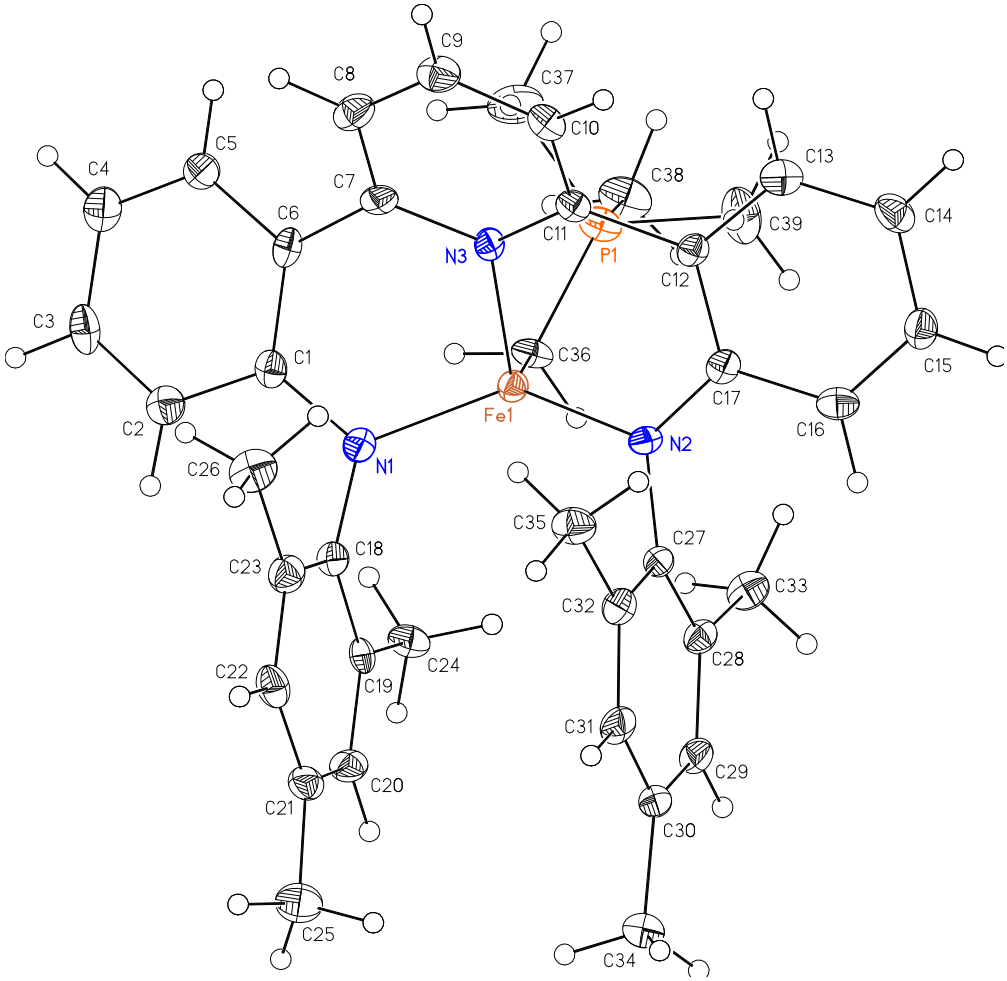
C9
C8
C37
C10
C5
C4
C7
C38
C13
C6
C11
C39
C14
N3
P1
C12
C3
C36
C15
C1
Fe1
C17
C2
C16
N2
C26
N1
C35
C27
C18
C23
C33
C32
C28
C24
C22
C19
C31
C29
C20
C21
C30
C25
C34

Table 2. Atomic coordinates (x 10^4) and equivalent isotropic displacement parameters ($Å^2$x 10^3) for ECW09 (CCDC 785426). U(eq) is defined as the trace of the orthogonalized U^{ij} tensor.

	x	y	z	U_{eq}
Fe(1)	5324(1)	1475(1)	6796(1)	14(1)
P(1)	3260(1)	1577(1)	8838(1)	19(1)
N(1)	5064(2)	1474(1)	4954(2)	17(1)
N(2)	7192(2)	1438(1)	7640(2)	14(1)
N(3)	5080(2)	932(1)	6784(2)	13(1)
C(1)	3828(3)	1337(1)	4439(3)	15(1)
C(2)	3026(3)	1493(1)	3413(3)	21(1)
C(3)	1743(3)	1384(1)	3007(3)	23(1)
C(4)	1175(3)	1101(1)	3590(3)	23(1)
C(5)	1964(3)	929(1)	4546(3)	18(1)
C(6)	3306(3)	1032(1)	4986(3)	16(1)
C(7)	4144(3)	794(1)	5850(3)	15(1)
C(8)	4025(3)	429(1)	5702(3)	21(1)
C(9)	4895(3)	207(1)	6454(3)	22(1)
C(10)	5861(3)	347(1)	7340(3)	18(1)
C(11)	5919(3)	716(1)	7539(3)	14(1)
C(12)	6917(3)	853(1)	8561(3)	14(1)
C(13)	7297(3)	637(1)	9589(3)	20(1)
C(14)	8352(3)	714(1)	10525(3)	22(1)
C(15)	9098(3)	1018(1)	10418(3)	20(1)
C(16)	8741(3)	1248(1)	9445(3)	19(1)
C(17)	7603(3)	1188(1)	8527(3)	15(1)
C(18)	5900(3)	1642(1)	4174(3)	16(1)
C(19)	6190(3)	2004(1)	4297(3)	15(1)
C(20)	7148(3)	2149(1)	3635(3)	18(1)
C(21)	7816(3)	1948(1)	2844(3)	18(1)
C(22)	7465(3)	1595(1)	2698(3)	19(1)
C(23)	6531(3)	1435(1)	3357(3)	20(1)
C(24)	5498(3)	2231(1)	5143(3)	20(1)
C(25)	8909(3)	2106(1)	2197(3)	25(1)
C(26)	6224(3)	1043(1)	3196(3)	26(1)
C(27)	8178(3)	1673(1)	7277(3)	15(1)
C(28)	8273(3)	2028(1)	7654(3)	17(1)
C(29)	9143(3)	2252(1)	7125(3)	20(1)
C(30)	9934(3)	2132(1)	6273(3)	20(1)
C(31)	9863(3)	1776(1)	5944(3)	20(1)
C(32)	9004(3)	1544(1)	6432(3)	17(1)
C(33)	7447(3)	2169(1)	8600(3)	21(1)
C(34)	10786(3)	2385(1)	5648(3)	28(1)
C(35)	8897(3)	1163(1)	6024(3)	22(1)
C(36)	3887(3)	1781(1)	7609(3)	18(1)
C(37)	2329(3)	1190(1)	8304(3)	30(1)
C(38)	2115(3)	1841(1)	9602(3)	28(1)
C(39)	4594(3)	1456(1)	10065(3)	32(1)
C(51)	4089(3)	472(1)	883(3)	28(1)
C(52)	3734(3)	341(1)	-300(3)	26(1)

C(53)	2404(3)	273(1)	-776(3)	30(1)
C(54)	1409(3)	337(1)	-44(4)	34(1)
C(55)	1771(3)	465(1)	1153(4)	31(1)
C(56)	3100(3)	538(1)	1608(3)	26(1)
C(61)	8996(5)	212(1)	5322(5)	53(1)
C(62)	9170(5)	181(1)	4103(5)	58(1)
C(63)	10180(5)	-26(1)	3789(4)	57(1)

Table 3. Selected bond lengths [Å] and angles [°] for ECW09 (CCDC 785426).

Fe(1)-N(2)	1.964(2)
Fe(1)-N(1)	1.974(2)
Fe(1)-N(3)	2.062(2)
Fe(1)-C(36)	2.137(3)
N(2)-Fe(1)-N(1)	116.38(9)
N(2)-Fe(1)-N(3)	92.16(10)
N(1)-Fe(1)-N(3)	89.71(10)
N(2)-Fe(1)-C(36)	120.06(11)
N(1)-Fe(1)-C(36)	114.93(11)
N(3)-Fe(1)-C(36)	116.94(10)

Table 4. Bond lengths [Å] and angles [°] for ECW09 (CCDC 785426).

Fe(1)-N(2)	1.964(2)	C(51)-C(56)	1.377(4)
Fe(1)-N(1)	1.974(2)	C(52)-C(53)	1.381(5)
Fe(1)-N(3)	2.062(2)	C(53)-C(54)	1.385(4)
Fe(1)-C(36)	2.137(3)	C(54)-C(55)	1.381(5)
P(1)-C(36)	1.735(3)	C(55)-C(56)	1.378(5)
P(1)-C(37)	1.784(3)	C(61)-C(62)	1.363(6)
P(1)-C(39)	1.800(3)	C(61)-C(63)#1	1.367(6)
P(1)-C(38)	1.809(3)	C(62)-C(63)	1.361(6)
N(1)-C(1)	1.383(4)	C(63)-C(61)#1	1.367(6)
N(1)-C(18)	1.425(4)		
N(2)-C(17)	1.368(4)	N(2)-Fe(1)-N(1)	116.38(9)
N(2)-C(27)	1.427(3)	N(2)-Fe(1)-N(3)	92.16(10)
N(3)-C(11)	1.356(4)	N(1)-Fe(1)-N(3)	89.71(10)
N(3)-C(7)	1.375(4)	N(2)-Fe(1)-C(36)	120.06(11)
C(1)-C(2)	1.402(4)	N(1)-Fe(1)-C(36)	114.93(11)
C(1)-C(6)	1.429(4)	N(3)-Fe(1)-C(36)	116.94(10)
C(2)-C(3)	1.360(4)	C(36)-P(1)-C(37)	110.23(16)
C(3)-C(4)	1.406(4)	C(36)-P(1)-C(39)	111.38(15)
C(4)-C(5)	1.369(4)	C(37)-P(1)-C(39)	109.05(18)
C(5)-C(6)	1.414(4)	C(36)-P(1)-C(38)	115.80(14)
C(6)-C(7)	1.467(4)	C(37)-P(1)-C(38)	105.18(15)
C(7)-C(8)	1.390(4)	C(39)-P(1)-C(38)	104.79(16)
C(8)-C(9)	1.385(4)	C(1)-N(1)-C(18)	119.9(2)
C(9)-C(10)	1.365(4)	C(1)-N(1)-Fe(1)	112.60(17)
C(10)-C(11)	1.408(4)	C(18)-N(1)-Fe(1)	126.80(19)
C(11)-C(12)	1.473(4)	C(17)-N(2)-C(27)	118.4(2)
C(12)-C(13)	1.387(4)	C(17)-N(2)-Fe(1)	122.85(18)
C(12)-C(17)	1.440(4)	C(27)-N(2)-Fe(1)	118.73(19)
C(13)-C(14)	1.383(4)	C(11)-N(3)-C(7)	120.7(2)
C(14)-C(15)	1.386(4)	C(11)-N(3)-Fe(1)	122.14(19)
C(15)-C(16)	1.370(4)	C(7)-N(3)-Fe(1)	116.54(19)
C(16)-C(17)	1.416(4)	N(1)-C(1)-C(2)	122.5(3)
C(18)-C(23)	1.400(4)	N(1)-C(1)-C(6)	119.7(3)
C(18)-C(19)	1.400(4)	C(2)-C(1)-C(6)	117.8(3)
C(19)-C(20)	1.394(4)	C(3)-C(2)-C(1)	122.2(3)
C(19)-C(24)	1.500(4)	C(2)-C(3)-C(4)	120.8(3)
C(20)-C(21)	1.390(4)	C(5)-C(4)-C(3)	118.2(3)
C(21)-C(22)	1.381(4)	C(4)-C(5)-C(6)	122.6(3)
C(21)-C(25)	1.510(4)	C(5)-C(6)-C(1)	118.0(3)
C(22)-C(23)	1.397(4)	C(5)-C(6)-C(7)	118.3(3)
C(23)-C(26)	1.514(4)	C(1)-C(6)-C(7)	123.1(3)
C(27)-C(28)	1.399(4)	N(3)-C(7)-C(8)	119.8(3)
C(27)-C(32)	1.410(4)	N(3)-C(7)-C(6)	120.2(3)
C(28)-C(29)	1.397(4)	C(8)-C(7)-C(6)	120.0(3)
C(28)-C(33)	1.507(4)	C(9)-C(8)-C(7)	119.8(3)
C(29)-C(30)	1.380(4)	C(10)-C(9)-C(8)	119.9(3)
C(30)-C(31)	1.389(4)	C(9)-C(10)-C(11)	119.9(3)
C(30)-C(34)	1.510(4)	N(3)-C(11)-C(10)	119.7(3)
C(31)-C(32)	1.386(4)	N(3)-C(11)-C(12)	122.2(3)
C(32)-C(35)	1.505(4)	C(10)-C(11)-C(12)	118.1(3)
C(51)-C(52)	1.372(5)	C(13)-C(12)-C(17)	117.4(3)

C(13)-C(12)-C(11)	118.1(3)	C(28)-C(27)-N(2)	122.3(2)
C(17)-C(12)-C(11)	124.3(3)	C(32)-C(27)-N(2)	117.5(3)
C(14)-C(13)-C(12)	123.7(3)	C(29)-C(28)-C(27)	118.6(3)
C(13)-C(14)-C(15)	118.4(3)	C(29)-C(28)-C(33)	120.5(3)
C(16)-C(15)-C(14)	120.4(3)	C(27)-C(28)-C(33)	121.0(3)
C(15)-C(16)-C(17)	122.0(3)	C(30)-C(29)-C(28)	122.2(3)
N(2)-C(17)-C(16)	120.6(3)	C(29)-C(30)-C(31)	118.5(3)
N(2)-C(17)-C(12)	121.9(3)	C(29)-C(30)-C(34)	120.8(3)
C(16)-C(17)-C(12)	117.4(3)	C(31)-C(30)-C(34)	120.6(3)
C(23)-C(18)-C(19)	119.9(3)	C(32)-C(31)-C(30)	121.5(3)
C(23)-C(18)-N(1)	119.3(3)	C(31)-C(32)-C(27)	119.3(3)
C(19)-C(18)-N(1)	120.6(2)	C(31)-C(32)-C(35)	120.8(3)
C(20)-C(19)-C(18)	119.0(3)	C(27)-C(32)-C(35)	119.9(2)
C(20)-C(19)-C(24)	120.5(3)	P(1)-C(36)-Fe(1)	114.92(15)
C(18)-C(19)-C(24)	120.6(2)	C(52)-C(51)-C(56)	119.3(3)
C(21)-C(20)-C(19)	122.3(3)	C(51)-C(52)-C(53)	121.2(3)
C(22)-C(21)-C(20)	117.4(3)	C(52)-C(53)-C(54)	119.5(3)
C(22)-C(21)-C(25)	121.3(3)	C(55)-C(54)-C(53)	119.2(3)
C(20)-C(21)-C(25)	121.3(3)	C(56)-C(55)-C(54)	120.7(3)
C(21)-C(22)-C(23)	122.5(3)	C(51)-C(56)-C(55)	120.0(3)
C(18)-C(23)-C(22)	118.9(3)	C(62)-C(61)-C(63)#1	119.2(4)
C(18)-C(23)-C(26)	120.9(3)	C(61)-C(62)-C(63)	119.9(5)
C(22)-C(23)-C(26)	120.2(3)	C(62)-C(63)-C(61)#1	120.9(4)
C(28)-C(27)-C(32)	119.9(3)		

Symmetry transformations used to generate equivalent atoms:
#1 -x+2,-y,-z+1

CALIFORNIA INSTITUTE OF TECHNOLOGY

BECKMAN INSTITUTE

X-RAY CRYSTALLOGRAPHY LABORATORY

Crystal Structure Analysis of:

[^{Mes}NNN-NHAd]Fe (ECW16)

(shown below)

For Investigator: Edward Weintrob ext. 6576

Advisor: J. E. Bercaw ext. 6577

Account Number: JEB.ENERGY-1.02-GRANT.MOOREJCP

By Edward Weintrob 204 Noyes ext. 6576

e-mail: tw288@caltech.edu

Contents

Table 1. Crystal data and structure refinement for ecw16.

Empirical formula	$C_{45}H_{47}N_4Fe$	
Formula weight	699.72	

Data Collection

Type of diffractometer	Synchrotron	
Wavelength	0.72930 Å	
Data Collection Temperature	100(2) K	
Unit cell dimensions	a = 11.579(2) Å b = 13.386(3) Å c = 24.019(5) Å	α= 83.94(3)° β= 76.78(3)° γ = 79.94(3)°
Volume	3560.1(12) $Å^3$	
Z	4	
Crystal system	Triclinic	
Space group	P-1	
Density (calculated)	1.305 Mg/m^3	
F(000)	1484	
θ range for data collection	0.90 to 21.94°	
Completeness to θ = 21.94°	90.8 %	
Index ranges	-11<=h<=11, -13<=k<=13, -24<=l<=24	
Reflections collected	23622	
Independent reflections	7300 [R_{int}= 0.0895]	

Structure solution and Refinement

Structure solution program	SHELXS-97 (Sheldrick, 2008)
Primary solution method	Direct methods
Secondary solution method	Difference Fourier map
Hydrogen placement	Geometric positions
Structure refinement program	SHELXL-97 (Sheldrick, 2008)
Refinement method	Full matrix least-squares on F^2
Data / restraints / parameters	7300 / 612 / 912
Treatment of hydrogen atoms	Riding
Goodness-of-fit on F^2	4.154
Final R indices [I>2σ(I), 5605 reflections]	R1 = 0.1499, *w*R2 = 0.3194
R indices (all data)	R1 = 0.1755, *w*R2 = 0.3221
Type of weighting scheme used	Sigma
Weighting scheme used	$w=1/\sigma^2(Fo^2)$
Max shift/error	4.790

Average shift/error	0.027
Largest diff. peak and hole	2.935 and -1.439 e.Å^{-3}

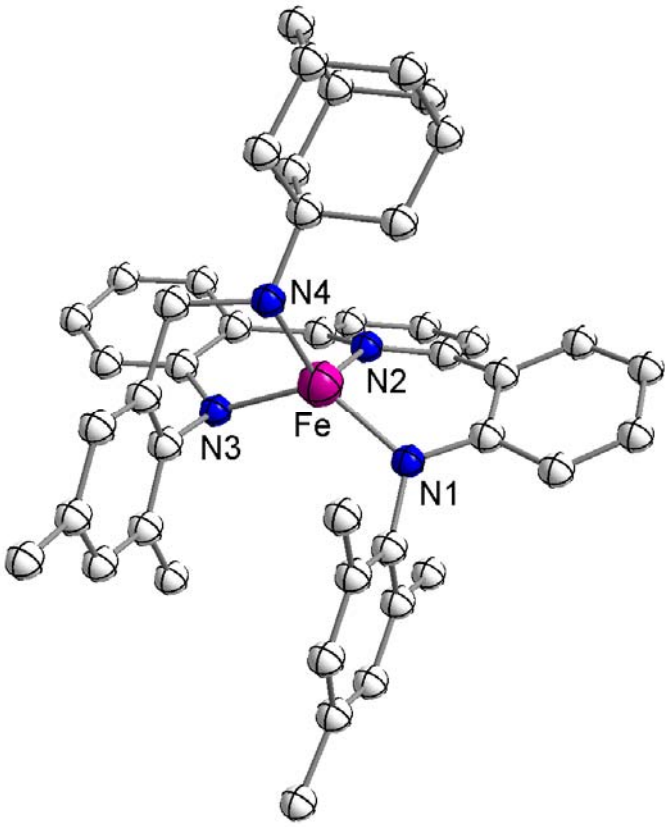

CALIFORNIA INSTITUTE OF TECHNOLOGY

BECKMAN INSTITUTE

X-RAY CRYSTALLOGRAPHY LABORATORY

Date 13 September 2010

Crystal Structure Analysis of:

[^{Mes}NNN-NH_2]H_2 (ECW13)

(shown below)

For Investigator: Edward Weintrob ext. 6576

Advisor: J. E. Bercaw ext. 6577

Account Number: JEB.ENERGY-1.02-GRANT.MOOREJCP

By Michael W. Day 116 Beckman ext. 2734

e-mail: mikeday@caltech.edu

Contents

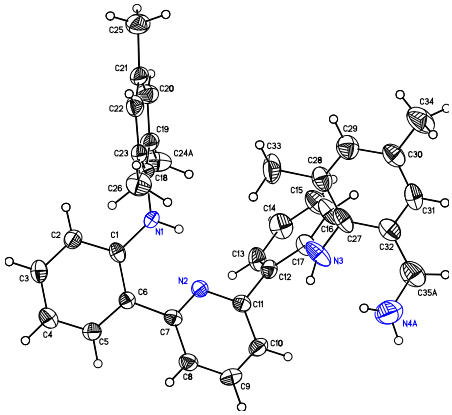

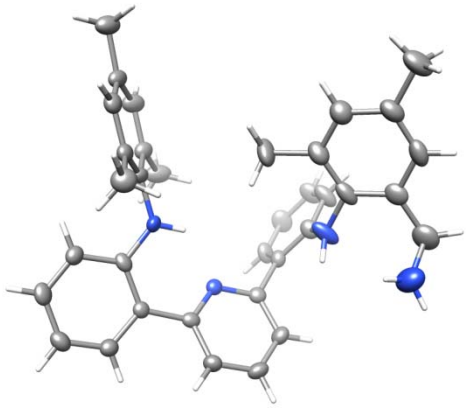

ECW13

Note: The crystallographic data have been deposited in the Cambridge Database (CCDC) and has been placed on hold pending further instructions from me. The deposition number is 793154. Ideally the CCDC would like the publication to contain a footnote of the type: "Crystallographic data have been deposited at the CCDC, 12 Union Road, Cambridge CB2 1EZ, UK and copies can be obtained on request, free of charge, by quoting the publication citation and the deposition number 793154."

Table 1. Crystal data and structure refinement for ECW13 (CCDC 793154).

Empirical formula	$C_{35}H_{36}N_4$
Formula weight	512.68
Crystallization Solvent	Dichloromethane/pentane
Crystal Habit	Fragment
Crystal size	0.24 x 0.15 x 0.12 mm^3
Crystal color	Colorless

Data Collection

Type of diffractometer	Bruker KAPPA APEX II	
Wavelength	0.71073 Å MoKα	
Data Collection Temperature	100(2) K	
θ range for 6446 reflections used in lattice determination	2.55 to 23.18°	
Unit cell dimensions	a = 12.1803(6) Å b = 8.3648(4) Å c = 27.4592(14) Å	α= 90° β= 94.852(3)° γ = 90°
Volume	2787.7(2) $Å^3$	
Z	4	
Crystal system	Monoclinic	
Space group	P $2_1/n$	
Density (calculated)	1.222 Mg/m^3	
F(000)	1096	
θ range for data collection	1.49 to 25.56°	
Completeness to θ = 25.56°	91.5 %	
Index ranges	$-13 \le h \le 13, -10 \le k \le 9, -32 \le l \le 33$	
Data collection scan type	ω scans; 8 settings	
Reflections collected	29589	
Independent reflections	4775 [R_{int}= 0.0438]	
Absorption coefficient	0.072 mm^{-1}	
Absorption correction	None	
Max. and min. transmission	0.9914 and 0.9829	

Table 1 (cont.)

Structure solution and Refinement

Structure solution program	SHELXS-97 (Sheldrick, 2008)
Primary solution method	Direct methods
Secondary solution method	Difference Fourier map
Hydrogen placement	Geometric positions
Structure refinement program	SHELXL-97 (Sheldrick, 2008)
Refinement method	Full matrix least-squares on F^2
Data / restraints / parameters	4775 / 1 / 361
Treatment of hydrogen atoms	Riding
Goodness-of-fit on F^2	2.495
Final R indices [$I>2\sigma(I)$, 3224 reflections]	R1 = 0.0574, *w*R2 = 0.0734
R indices (all data)	R1 = 0.0897, *w*R2 = 0.0748
Type of weighting scheme used	Sigma
Weighting scheme used	$w=1/\sigma^2(Fo^2)$
Max shift/error	0.015
Average shift/error	0.000
Largest diff. peak and hole	0.590 and -0.422 e.Å^{-3}

Special Refinement Details

Crystals were mounted on a glass fiber using Paratone oil then placed on the diffractometer under a nitrogen stream at 100K.

The sample appears to be multiple crystals with at least four discernable domains. The model presented here is the result of refinement against the major domain accounting for approximately 65% of the diffraction. Further problems rise from disorder in the NH_2 where it occupies two chemically equivalent positions.

Refinement of F^2 against ALL reflections. The weighted R-factor (*w*R) and goodness of fit (S) are based on F^2, conventional R-factors (R) are based on F, with F set to zero for negative F^2. The threshold expression of $F^2 > 2\sigma(F^2)$ is used only for calculating R-factors(gt) etc. and is not relevant to the choice of reflections for refinement. R-factors based on F^2 are statistically about twice as large as those based on F, and R-factors based on ALL data will be even larger.

All esds (except the esd in the dihedral angle between two l.s. planes) are estimated using the full covariance matrix. The cell esds are taken into account individually in the estimation of esds in distances, angles and torsion angles; correlations between esds in cell parameters are only used when they are defined by crystal symmetry. An approximate (isotropic) treatment of cell esds is used for estimating esds involving l.s. planes.

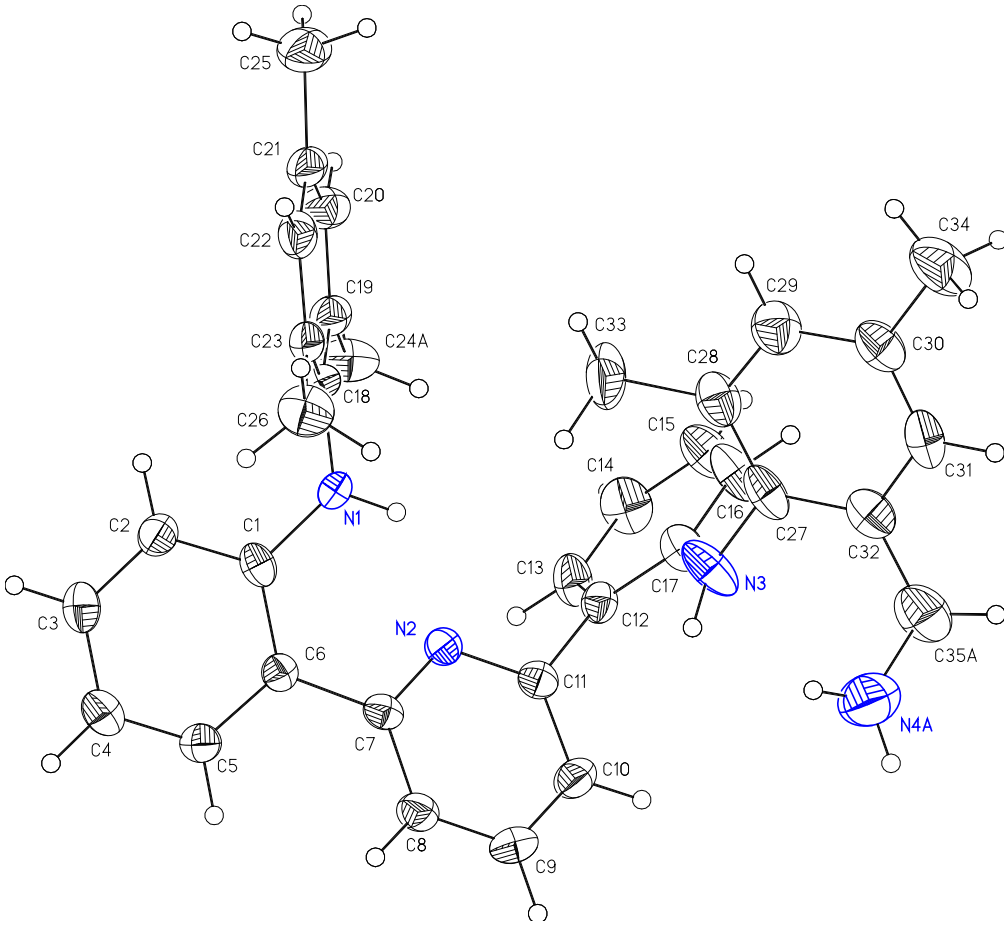
C25
C21
C20
C22
C19
C23
C24A
C18
C26
N1
C2
C1
C3
C6
N2
C11
C4
C5
C7
C10
C8
C9
C34
C29
C33
C28
C30
C15
C31
C14
C16
C27
C32
C13
C17
N3
C12
C35A
N4A

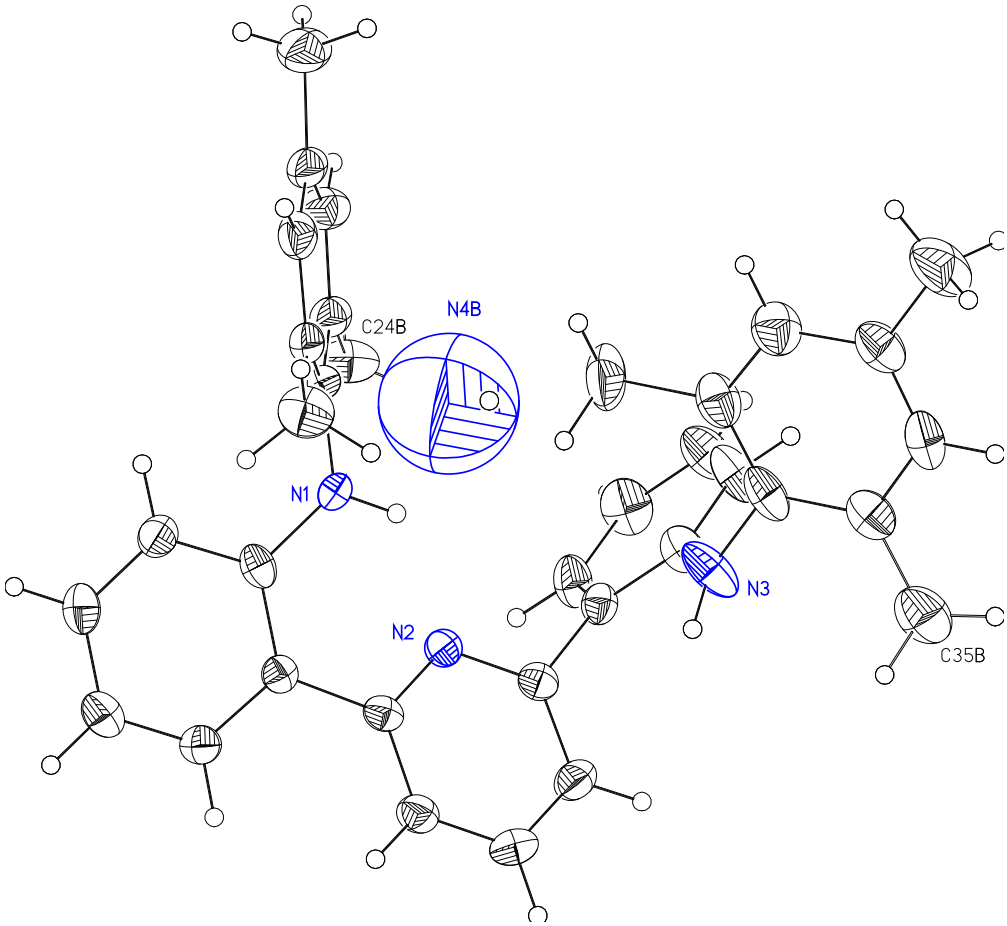
C24B
N4B
N1
N2
N3
C35B

Table 2. Atomic coordinates (x 10^4) and equivalent isotropic displacement parameters ($Å^2$x 10^3) for ECW13 (CCDC 793154). U(eq) is defined as the trace of the orthogonalized U^{ij} tensor.

	x	y	z	U_{eq}	Occ
N(1)	4914(1)	2590(2)	1735(1)	29(1)	1
N(2)	3702(2)	5238(2)	1848(1)	24(1)	1
N(3)	1028(2)	3989(2)	1295(1)	45(1)	1
N(4A)	-1033(2)	4282(3)	1739(1)	70(1)	0.806(3)
N(4B)	4307(8)	3930(30)	755(10)	342(19)	0.194(3)
C(1)	5519(2)	3083(3)	2158(1)	26(1)	1
C(2)	6529(2)	2361(3)	2303(1)	31(1)	1
C(3)	7121(2)	2779(3)	2732(1)	33(1)	1
C(4)	6724(2)	3943(3)	3030(1)	34(1)	1
C(5)	5744(2)	4688(3)	2885(1)	29(1)	1
C(6)	5120(2)	4304(3)	2455(1)	23(1)	1
C(7)	4066(2)	5162(3)	2326(1)	24(1)	1
C(8)	3471(2)	5867(3)	2682(1)	29(1)	1
C(9)	2507(2)	6667(3)	2542(1)	35(1)	1
C(10)	2134(2)	6741(3)	2053(1)	33(1)	1
C(11)	2745(2)	6014(3)	1717(1)	25(1)	1
C(12)	2400(2)	6030(3)	1182(1)	26(1)	1
C(13)	2929(2)	6999(3)	869(1)	36(1)	1
C(14)	2646(2)	6980(3)	371(1)	44(1)	1
C(15)	1839(2)	5963(3)	180(1)	44(1)	1
C(16)	1302(2)	4985(3)	484(1)	43(1)	1
C(17)	1568(2)	5007(3)	985(1)	32(1)	1
C(18)	5221(2)	1324(3)	1428(1)	28(1)	1
C(19)	5439(2)	1699(3)	954(1)	31(1)	1
C(20)	5673(2)	450(3)	637(1)	39(1)	1
C(21)	5724(2)	-1116(3)	792(1)	34(1)	1
C(22)	5516(2)	-1440(3)	1268(1)	35(1)	1
C(23)	5241(2)	-258(3)	1590(1)	30(1)	1
C(24A)	5404(2)	3412(3)	784(1)	46(1)	0.806(3)
C(24B)	5404(2)	3412(3)	784(1)	46(1)	0.194(3)
C(25)	5944(2)	-2455(3)	441(1)	49(1)	1
C(26)	4916(2)	-707(3)	2088(1)	46(1)	1
C(27)	479(2)	2600(3)	1102(1)	37(1)	1
C(28)	1088(2)	1328(3)	939(1)	41(1)	1
C(29)	519(2)	6(3)	752(1)	45(1)	1
C(30)	-631(2)	-92(3)	723(1)	42(1)	1
C(31)	-1204(2)	1181(3)	892(1)	41(1)	1
C(32)	-680(2)	2543(3)	1080(1)	36(1)	1
C(33)	2336(2)	1383(3)	960(1)	59(1)	1
C(34)	-1220(2)	-1561(3)	521(1)	63(1)	1
C(35A)	-1332(2)	3949(3)	1246(1)	54(1)	0.806(3)
C(35B)	-1332(2)	3949(3)	1246(1)	54(1)	0.194(3)

Table 3. Bond lengths [Å] and angles [°] for ECW13 (CCDC 793154).

N(1)-C(1)	1.385(2)	C(3)-C(2)-C(1)	121.4(2)
N(1)-C(18)	1.423(3)	C(2)-C(3)-C(4)	120.1(2)
N(2)-C(7)	1.351(3)	C(5)-C(4)-C(3)	119.0(2)
N(2)-C(11)	1.356(2)	C(4)-C(5)-C(6)	122.8(2)
N(3)-C(17)	1.404(3)	C(5)-C(6)-C(1)	117.8(2)
N(3)-C(27)	1.421(3)	C(5)-C(6)-C(7)	119.4(2)
N(4A)-C(35A)	1.400(3)	C(1)-C(6)-C(7)	122.8(2)
N(4B)-C(24B)	1.400(3)	N(2)-C(7)-C(8)	120.8(2)
C(1)-C(2)	1.398(3)	N(2)-C(7)-C(6)	117.4(2)
C(1)-C(6)	1.419(3)	C(8)-C(7)-C(6)	121.8(2)
C(2)-C(3)	1.373(3)	C(9)-C(8)-C(7)	119.4(2)
C(3)-C(4)	1.385(3)	C(8)-C(9)-C(10)	119.7(2)
C(4)-C(5)	1.375(3)	C(11)-C(10)-C(9)	118.7(2)
C(5)-C(6)	1.387(3)	N(2)-C(11)-C(10)	122.4(2)
C(6)-C(7)	1.486(3)	N(2)-C(11)-C(12)	115.4(2)
C(7)-C(8)	1.396(3)	C(10)-C(11)-C(12)	122.2(2)
C(8)-C(9)	1.378(3)	C(13)-C(12)-C(17)	118.6(2)
C(9)-C(10)	1.382(3)	C(13)-C(12)-C(11)	120.7(2)
C(10)-C(11)	1.375(3)	C(17)-C(12)-C(11)	120.6(2)
C(11)-C(12)	1.493(3)	C(12)-C(13)-C(14)	121.3(2)
C(12)-C(13)	1.380(3)	C(15)-C(14)-C(13)	119.7(2)
C(12)-C(17)	1.400(3)	C(14)-C(15)-C(16)	120.1(2)
C(13)-C(14)	1.383(3)	C(15)-C(16)-C(17)	120.8(2)
C(14)-C(15)	1.370(3)	C(16)-C(17)-C(12)	119.5(2)
C(15)-C(16)	1.373(3)	C(16)-C(17)-N(3)	120.6(2)
C(16)-C(17)	1.388(3)	C(12)-C(17)-N(3)	119.9(2)
C(18)-C(19)	1.386(3)	C(19)-C(18)-C(23)	121.0(2)
C(18)-C(23)	1.396(3)	C(19)-C(18)-N(1)	118.0(2)
C(19)-C(20)	1.404(3)	C(23)-C(18)-N(1)	121.0(2)
C(19)-C(24A)	1.506(3)	C(18)-C(19)-C(20)	118.6(2)
C(20)-C(21)	1.377(3)	C(18)-C(19)-C(24A)	120.1(2)
C(21)-C(22)	1.377(3)	C(20)-C(19)-C(24A)	121.3(2)
C(21)-C(25)	1.517(3)	C(21)-C(20)-C(19)	121.4(2)
C(22)-C(23)	1.387(3)	C(22)-C(21)-C(20)	118.3(2)
C(23)-C(26)	1.505(3)	C(22)-C(21)-C(25)	120.9(2)
C(27)-C(28)	1.392(3)	C(20)-C(21)-C(25)	120.7(2)
C(27)-C(32)	1.409(3)	C(21)-C(22)-C(23)	122.5(2)
C(28)-C(29)	1.381(3)	C(22)-C(23)-C(18)	118.1(2)
C(28)-C(33)	1.517(3)	C(22)-C(23)-C(26)	119.9(2)
C(29)-C(30)	1.398(3)	C(18)-C(23)-C(26)	121.9(2)
C(30)-C(31)	1.375(3)	N(4B)-C(24B)-C(19)	108(1)
C(30)-C(34)	1.506(3)	C(28)-C(27)-C(32)	121.3(2)
C(31)-C(32)	1.385(3)	C(28)-C(27)-N(3)	119.9(3)
C(32)-C(35A)	1.510(3)	C(32)-C(27)-N(3)	118.8(3)
		C(29)-C(28)-C(27)	117.9(3)
C(1)-N(1)-C(18)	124.8(2)	C(29)-C(28)-C(33)	120.6(3)
C(7)-N(2)-C(11)	119.0(2)	C(27)-C(28)-C(33)	121.5(2)
C(17)-N(3)-C(27)	120.0(2)	C(28)-C(29)-C(30)	122.4(3)
N(1)-C(1)-C(2)	120.2(2)	C(31)-C(30)-C(29)	118.1(3)
N(1)-C(1)-C(6)	120.9(2)	C(31)-C(30)-C(34)	121.0(3)
C(2)-C(1)-C(6)	118.9(2)	C(29)-C(30)-C(34)	120.8(3)

C(30)-C(31)-C(32)	122.1(3)
C(31)-C(32)-C(27)	118.1(3)
C(31)-C(32)-C(35A)	121.1(3)
C(27)-C(32)-C(35A)	120.8(3)
N(4A)-C(35A)-C(32)	110.2(2)

Table 5. Hydrogen bonds for ECW13 (CCDC 793154) [Å and °].

D-H...A	d(D-H)	d(H...A)	d(D...A)	<(DHA)
N(1)-H(1)...N(2)	0.88	2.02	2.695(2)	132.2

CALIFORNIA INSTITUTE OF TECHNOLOGY

BECKMAN INSTITUTE

X-RAY CRYSTALLOGRAPHY LABORATORY

Date 13 September 2010

Crystal Structure Analysis of:

[^{tBu}NNN]H_2 (ECW18)

(shown below)

For Investigator: Edward Weintrob ext. 6576

Advisor: J. E. Bercaw ext. 6577

Account Number: JEB.ENERGY-1.02-GRANT.MOOREJCP

By Michael W. Day 116 Beckman ext. 2734

e-mail: mikeday@caltech.edu

Contents

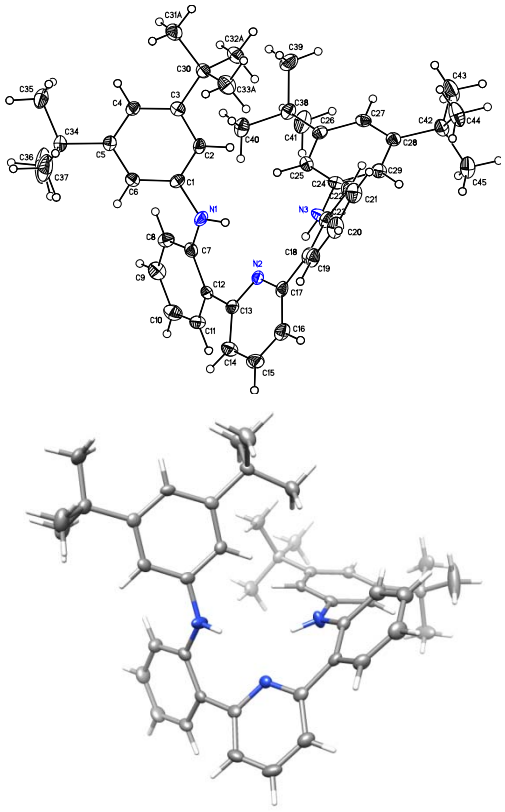

ECW18

Note: The crystallographic data have been deposited in the Cambridge Database (CCDC) and has been placed on hold pending further instructions from me. The deposition number is 793155. Ideally the CCDC would like the publication to contain a footnote of the type: "Crystallographic data have been deposited at the CCDC, 12 Union Road, Cambridge CB2 1EZ, UK and copies can be obtained on request, free of charge, by quoting the publication citation and the deposition number 793155."

Table 1. Crystal data and structure refinement for ECW18 (CCDC 793155).

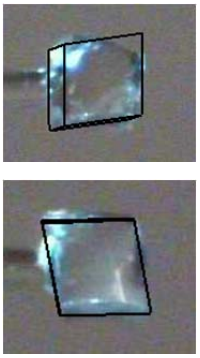

Empirical formula	$C_{45}H_{55}N_3 \bullet C_6H_{12}$
Formula weight	722.08
Crystallization Solvent	Hexanes
Crystal Habit	Block
Crystal size	0.19 x 0.17 x 0.16 mm^3
Crystal color	Colorless

Data Collection

Type of diffractometer	Bruker KAPPA APEX II	
Wavelength	0.71073 Å MoKα	
Data Collection Temperature	100(2) K	
θ range for 9933 reflections used in lattice determination	2.39 to 25.70°	
Unit cell dimensions	a = 13.2349(5) Å b = 17.6560(8) Å c = 19.0978(8) Å	α= 90° β= 102.355(2)° γ = 90°
Volume	4359.3(3) $Å^3$	
Z	4	
Crystal system	Monoclinic	
Space group	P $2_1/c$	
Density (calculated)	1.100 Mg/m^3	
F(000)	1576	
θ range for data collection	1.95 to 27.52°	
Completeness to θ = 27.52°	99.8 %	
Index ranges	$-17 \le h \le 16$, $-22 \le k \le 22$, $-24 \le l \le 24$	
Data collection scan type	ω scans; 8 settings	
Reflections collected	63493	
Independent reflections	10009 [R_{int}= 0.0554]	
Absorption coefficient	0.063 mm^{-1}	
Absorption correction	None	
Max. and min. transmission	0.9900 and 0.9881	

Table 1 (cont.)

Structure solution and Refinement

Structure solution program	SHELXS-97 (Sheldrick, 2008)
Primary solution method	Direct methods
Secondary solution method	Difference Fourier map
Hydrogen placement	Geometric positions
Structure refinement program	SHELXL-97 (Sheldrick, 2008)
Refinement method	Full matrix least-squares on F^2
Data / restraints / parameters	10009 / 0 / 537
Treatment of hydrogen atoms	Riding
Goodness-of-fit on F^2	2.513
Final R indices [$I>2\sigma(I)$, 6629 reflections]	R1 = 0.0641, *w*R2 = 0.0867
R indices (all data)	R1 = 0.0986, *w*R2 = 0.0886
Type of weighting scheme used	Sigma
Weighting scheme used	$w=1/\sigma^2(Fo^2)$
Max shift/error	0.000
Average shift/error	0.000
Largest diff. peak and hole	1.093 and -0.828 e.Å^{-3}

Special Refinement Details

Crystals were mounted on a glass fiber using Paratone oil then placed on the diffractometer under a nitrogen stream at 100K.

One of the t-butyl groups is disordered by rotation around the tertiary C-C bond as is common for t-butyl groups. Additional disorder occurs in the solvent of crystallization, methylcylcopentane, with the methyl group disordered over two carbon sites.

Refinement of F^2 against ALL reflections. The weighted R-factor (*w*R) and goodness of fit (S) are based on F^2, conventional R-factors (R) are based on F, with F set to zero for negative F^2. The threshold expression of $F^2 > 2\sigma(F^2)$ is used only for calculating R-factors(gt) etc. and is not relevant to the choice of reflections for refinement. R-factors based on F^2 are statistically about twice as large as those based on F, and R-factors based on ALL data will be even larger.

All esds (except the esd in the dihedral angle between two l.s. planes) are estimated using the full covariance matrix. The cell esds are taken into account individually in the estimation of esds in distances, angles and torsion angles; correlations between esds in cell parameters are only used when they are defined by crystal symmetry. An approximate (isotropic) treatment of cell esds is used for estimating esds involving l.s. planes.

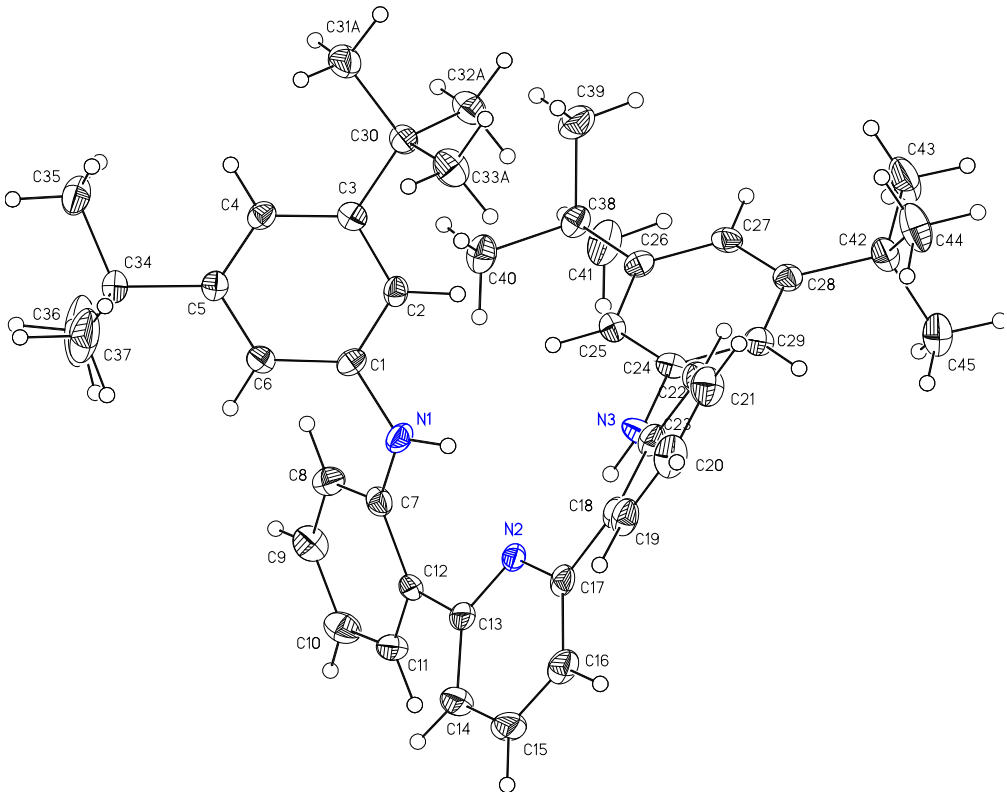
C31A
C32A
C39
C30
C33A
C43
C35
C4
C3
C38
C27
C42
C44
C34
C5
C2
C40
C41
C26
C28
C36
C37
C6
C1
C25
C24
C29
C45
C22
C21
N1
N3
C23
C20
C8
C7
C18
C19
N2
C9
C12
C17
C13
C10
C11
C16
C14
C15

Table 2. Atomic coordinates (x 10^4) and equivalent isotropic displacement parameters ($Å^2$x 10^3) for ECW18 (CCDC 793155). U(eq) is defined as the trace of the orthogonalized U^{ij} tensor.

	x	y	z	U_{eq}	Occ
N(1)	3974(1)	8271(1)	4141(1)	22(1)	1
N(2)	3363(1)	9602(1)	4650(1)	19(1)	1
N(3)	2370(1)	8733(1)	5492(1)	25(1)	1
C(1)	4677(1)	7661(1)	4308(1)	18(1)	1
C(2)	4719(1)	7273(1)	4946(1)	18(1)	1
C(3)	5436(2)	6695(1)	5167(1)	18(1)	1
C(4)	6113(1)	6524(1)	4722(1)	19(1)	1
C(5)	6104(2)	6910(1)	4085(1)	18(1)	1
C(6)	5372(1)	7482(1)	3879(1)	18(1)	1
C(7)	3521(2)	8552(1)	3468(1)	20(1)	1
C(8)	3363(2)	8084(1)	2864(1)	24(1)	1
C(9)	2885(2)	8353(1)	2194(1)	28(1)	1
C(10)	2544(2)	9099(1)	2112(1)	29(1)	1
C(11)	2696(2)	9559(1)	2705(1)	25(1)	1
C(12)	3192(2)	9318(1)	3388(1)	19(1)	1
C(13)	3352(2)	9866(1)	3987(1)	21(1)	1
C(14)	3500(2)	10632(1)	3869(1)	27(1)	1
C(15)	3600(2)	11128(1)	4437(1)	31(1)	1
C(16)	3585(2)	10860(1)	5114(1)	27(1)	1
C(17)	3496(2)	10079(1)	5214(1)	21(1)	1
C(18)	3558(2)	9757(1)	5939(1)	20(1)	1
C(19)	4210(2)	10096(1)	6522(1)	26(1)	1
C(20)	4336(2)	9830(1)	7213(1)	30(1)	1
C(21)	3793(2)	9191(1)	7334(1)	30(1)	1
C(22)	3141(2)	8833(1)	6771(1)	26(1)	1
C(23)	3011(2)	9095(1)	6067(1)	22(1)	1
C(24)	1772(2)	8074(1)	5509(1)	19(1)	1
C(25)	1853(1)	7499(1)	5024(1)	19(1)	1
C(26)	1253(1)	6847(1)	4986(1)	18(1)	1
C(27)	575(1)	6789(1)	5453(1)	19(1)	1
C(28)	470(2)	7356(1)	5936(1)	20(1)	1
C(29)	1081(2)	8007(1)	5957(1)	21(1)	1
C(30)	5452(2)	6275(1)	5869(1)	20(1)	1
C(31A)	6273(2)	5639(2)	6012(1)	30(1)	0.849(3)
C(32A)	4393(2)	5904(2)	5835(1)	27(1)	0.849(3)
C(33A)	5693(2)	6833(2)	6488(1)	31(1)	0.849(3)
C(31B)	6545(11)	6330(10)	6405(8)	44(5)	0.151(3)
C(32B)	5142(13)	5441(9)	5736(8)	43(5)	0.151(3)
C(33B)	4651(12)	6629(9)	6323(8)	39(5)	0.151(3)
C(34)	6925(2)	6765(1)	3642(1)	22(1)	1
C(35)	7413(2)	5985(1)	3780(1)	44(1)	1
C(36)	6456(2)	6806(2)	2840(1)	79(1)	1
C(37)	7762(2)	7364(1)	3841(2)	59(1)	1
C(38)	1318(2)	6211(1)	4453(1)	21(1)	1
C(39)	1588(2)	5459(1)	4857(1)	32(1)	1
C(40)	2134(1)	6362(1)	4005(1)	29(1)	1
C(41)	260(1)	6124(1)	3931(1)	34(1)	1

C(42)	-307(2)	7315(1)	6430(1)	25(1)	1
C(43)	-857(2)	6548(1)	6377(1)	42(1)	1
C(44)	250(2)	7437(1)	7213(1)	40(1)	1
C(45)	-1133(2)	7936(1)	6206(1)	42(1)	1
C(51)	1385(2)	4424(1)	1794(1)	45(1)	1
C(52)	1090(2)	4984(1)	2341(1)	49(1)	1
C(53)	-141(2)	4988(2)	2108(2)	82(1)	1
C(54)	-426(2)	4637(2)	1296(2)	69(1)	1
C(55)	633(2)	4593(2)	1085(1)	45(1)	1
C(56A)	639(2)	4039(2)	498(1)	50(1)	0.886(3)
C(56B)	-745(12)	3769(10)	1281(10)	21(5)	0.114(3)

Table 3. Bond lengths [Å] and angles [°] for ECW18 (CCDC 793155).

N(1)-C(7)	1.388(2)	C(38)-C(41)	1.543(3)
N(1)-C(1)	1.414(2)	C(42)-C(43)	1.530(3)
N(2)-C(13)	1.348(2)	C(42)-C(44)	1.535(3)
N(2)-C(17)	1.350(2)	C(42)-C(45)	1.544(3)
N(3)-C(23)	1.391(2)	C(51)-C(55)	1.529(3)
N(3)-C(24)	1.413(2)	C(51)-C(52)	1.548(3)
C(1)-C(2)	1.389(3)	C(52)-C(53)	1.595(3)
C(1)-C(6)	1.392(2)	C(53)-C(54)	1.638(4)
C(2)-C(3)	1.396(3)	C(54)-C(56B)	1.590(17)
C(3)-C(4)	1.393(3)	C(54)-C(55)	1.541(3)
C(3)-C(30)	1.529(3)	C(55)-C(56A)	1.489(3)
C(4)-C(5)	1.391(3)		
C(5)-C(6)	1.397(3)	C(7)-N(1)-C(1)	127.91(18)
C(5)-C(34)	1.534(3)	C(13)-N(2)-C(17)	120.47(19)
C(7)-C(8)	1.398(3)	C(23)-N(3)-C(24)	127.63(18)
C(7)-C(12)	1.417(3)	C(2)-C(1)-C(6)	119.75(19)
C(8)-C(9)	1.386(3)	C(2)-C(1)-N(1)	118.37(18)
C(9)-C(10)	1.390(3)	C(6)-C(1)-N(1)	121.71(19)
C(10)-C(11)	1.373(3)	C(1)-C(2)-C(3)	121.53(19)
C(11)-C(12)	1.396(3)	C(4)-C(3)-C(2)	117.3(2)
C(12)-C(13)	1.479(3)	C(4)-C(3)-C(30)	122.72(19)
C(13)-C(14)	1.391(3)	C(2)-C(3)-C(30)	120.00(19)
C(14)-C(15)	1.379(3)	C(5)-C(4)-C(3)	122.7(2)
C(15)-C(16)	1.381(3)	C(4)-C(5)-C(6)	118.43(19)
C(16)-C(17)	1.399(3)	C(4)-C(5)-C(34)	121.66(19)
C(17)-C(18)	1.483(3)	C(6)-C(5)-C(34)	119.74(19)
C(18)-C(19)	1.390(3)	C(1)-C(6)-C(5)	120.3(2)
C(18)-C(23)	1.422(3)	N(1)-C(7)-C(8)	120.7(2)
C(19)-C(20)	1.376(3)	N(1)-C(7)-C(12)	120.2(2)
C(20)-C(21)	1.384(3)	C(8)-C(7)-C(12)	119.1(2)
C(21)-C(22)	1.381(3)	C(9)-C(8)-C(7)	121.1(2)
C(22)-C(23)	1.398(3)	C(8)-C(9)-C(10)	120.2(2)
C(24)-C(29)	1.385(3)	C(11)-C(10)-C(9)	118.7(2)
C(24)-C(25)	1.393(3)	C(10)-C(11)-C(12)	123.2(2)
C(25)-C(26)	1.393(3)	C(11)-C(12)-C(7)	117.7(2)
C(26)-C(27)	1.397(3)	C(11)-C(12)-C(13)	118.93(19)
C(26)-C(38)	1.530(3)	C(7)-C(12)-C(13)	123.4(2)
C(27)-C(28)	1.388(3)	N(2)-C(13)-C(14)	121.0(2)
C(28)-C(29)	1.399(3)	N(2)-C(13)-C(12)	118.10(19)
C(28)-C(42)	1.539(3)	C(14)-C(13)-C(12)	120.9(2)
C(30)-C(33A)	1.520(3)	C(15)-C(14)-C(13)	118.9(2)
C(30)-C(32B)	1.536(15)	C(14)-C(15)-C(16)	120.0(2)
C(30)-C(32A)	1.536(3)	C(15)-C(16)-C(17)	119.0(2)
C(30)-C(31A)	1.546(3)	N(2)-C(17)-C(16)	120.4(2)
C(30)-C(31B)	1.586(15)	N(2)-C(17)-C(18)	118.45(19)
C(30)-C(33B)	1.631(14)	C(16)-C(17)-C(18)	121.1(2)
C(34)-C(35)	1.520(3)	C(19)-C(18)-C(23)	117.9(2)
C(34)-C(37)	1.520(3)	C(19)-C(18)-C(17)	118.87(19)
C(34)-C(36)	1.527(3)	C(23)-C(18)-C(17)	123.18(19)
C(38)-C(40)	1.538(2)	C(20)-C(19)-C(18)	123.2(2)
C(38)-C(39)	1.538(3)	C(19)-C(20)-C(21)	118.6(2)

C(22)-C(21)-C(20)	120.2(2)	C(44)-C(42)-C(45)	109.46(19)
C(21)-C(22)-C(23)	121.7(2)	C(28)-C(42)-C(45)	108.84(18)
N(3)-C(23)-C(22)	122.41(19)	C(55)-C(51)-C(52)	105.2(2)
N(3)-C(23)-C(18)	119.2(2)	C(51)-C(52)-C(53)	101.8(2)
C(22)-C(23)-C(18)	118.3(2)	C(52)-C(53)-C(54)	106.1(2)
C(29)-C(24)-C(25)	120.24(19)	C(56B)-C(54)-C(55)	101.5(6)
C(29)-C(24)-N(3)	122.17(19)	C(56B)-C(54)-C(53)	112.8(7)
C(25)-C(24)-N(3)	117.49(18)	C(55)-C(54)-C(53)	103.2(2)
C(26)-C(25)-C(24)	120.82(19)	C(56A)-C(55)-C(51)	115.6(2)
C(25)-C(26)-C(27)	117.6(2)	C(56A)-C(55)-C(54)	112.4(2)
C(25)-C(26)-C(38)	121.92(19)	C(51)-C(55)-C(54)	103.5(2)
C(27)-C(26)-C(38)	120.45(19)		
C(28)-C(27)-C(26)	122.7(2)		
C(27)-C(28)-C(29)	118.16(19)		
C(27)-C(28)-C(42)	123.18(19)		
C(29)-C(28)-C(42)	118.63(19)		
C(24)-C(29)-C(28)	120.4(2)		
C(33A)-C(30)-C(3)	109.25(19)		
C(33A)-C(30)-C(32B)	139.0(6)		
C(3)-C(30)-C(32B)	111.5(6)		
C(33A)-C(30)-C(32A)	110.32(19)		
C(3)-C(30)-C(32A)	109.19(18)		
C(32B)-C(30)-C(32A)	51.3(6)		
C(33A)-C(30)-C(31A)	108.1(2)		
C(3)-C(30)-C(31A)	112.62(18)		
C(32B)-C(30)-C(31A)	59.0(6)		
C(32A)-C(30)-C(31A)	107.4(2)		
C(33A)-C(30)-C(31B)	56.5(6)		
C(3)-C(30)-C(31B)	112.1(6)		
C(32B)-C(30)-C(31B)	109.9(9)		
C(32A)-C(30)-C(31B)	138.7(6)		
C(31A)-C(30)-C(31B)	54.6(6)		
C(33A)-C(30)-C(33B)	52.4(6)		
C(3)-C(30)-C(33B)	113.1(5)		
C(32B)-C(30)-C(33B)	105.9(8)		
C(32A)-C(30)-C(33B)	59.7(6)		
C(31A)-C(30)-C(33B)	134.1(5)		
C(31B)-C(30)-C(33B)	103.9(8)		
C(35)-C(34)-C(37)	109.08(18)		
C(35)-C(34)-C(36)	106.4(2)		
C(37)-C(34)-C(36)	109.6(2)		
C(35)-C(34)-C(5)	112.41(18)		
C(37)-C(34)-C(5)	108.10(18)		
C(36)-C(34)-C(5)	111.23(18)		
C(26)-C(38)-C(40)	112.91(17)		
C(26)-C(38)-C(39)	109.86(17)		
C(40)-C(38)-C(39)	108.26(17)		
C(26)-C(38)-C(41)	109.30(17)		
C(40)-C(38)-C(41)	107.81(18)		
C(39)-C(38)-C(41)	108.60(17)		
C(43)-C(42)-C(44)	108.1(2)		
C(43)-C(42)-C(28)	111.93(19)		
C(44)-C(42)-C(28)	110.26(17)		
C(43)-C(42)-C(45)	108.19(18)		

Table 5. Hydrogen bonds for ECW18 (CCDC 793155) [Å and °].

D-H...A	d(D-H)	d(H...A)	d(D...A)	<(DHA)
N(1)-H(1)...N(2)	0.88	2.06	2.730(2)	131.7
N(3)-H(3)...N(2)	0.88	2.08	2.750(2)	132.3

CALIFORNIA INSTITUTE OF TECHNOLOGY

BECKMAN INSTITUTE

X-RAY CRYSTALLOGRAPHY LABORATORY

Date 14 September 2010

Crystal Structure Analysis of:

[^{tBu}NNN]H_2 (ECW19)

(shown below)

For Investigator: Edward Weintrob ext. 6576

Advisor: J. E. Bercaw ext. 6577

Account Number: JEB.ENERGY-1.02-GRANT.MOOREJCP

By Michael W. Day 116 Beckman ext. 2734

e-mail: mikeday@caltech.edu

Contents

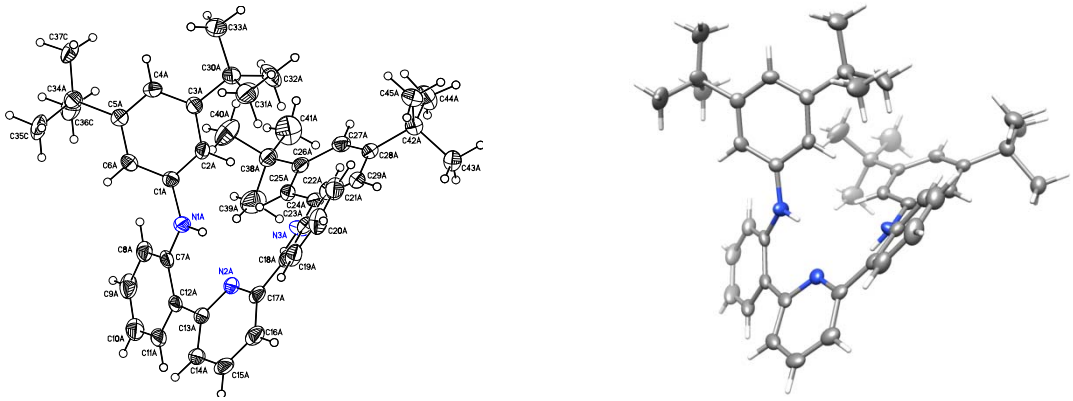

ECW19

Note: The crystallographic data have been deposited in the Cambridge Database (CCDC) and has been placed on hold pending further instructions from me. The deposition number is 793156. Ideally the CCDC would like the publication to contain a footnote of the type: "Crystallographic data have been deposited at the CCDC, 12 Union Road, Cambridge CB2 1EZ, UK and copies can be obtained on request, free of charge, by quoting the publication citation and the deposition number 793156."

Table 1. Crystal data and structure refinement for ECW19 (CCDC 793156).

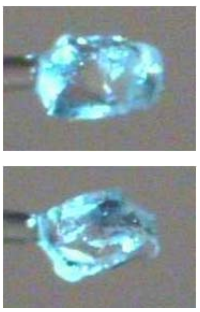

Empirical formula	$C_{45}H_{55}N_3$
Formula weight	637.92
Crystallization Solvent	Acetonitrile
Crystal Habit	Fragment
Crystal size	0.23 x 0.16 x 0.15 mm^3
Crystal color	Colorless

Data Collection

Type of diffractometer	Bruker KAPPA APEX II	
Wavelength	0.71073 Å MoKα	
Data Collection Temperature	100(2) K	
θ range for 9914 reflections used in lattice determination	2.19 to 24.21°	
Unit cell dimensions	a = 14.7469(5) Å b = 17.4293(6) Å c = 18.0411(7) Å	α= 64.238(2)° β= 76.593(2)° γ = 66.808(2)°
Volume	3828.4(2) $Å^3$	
Z	4	
Crystal system	Triclinic	
Space group	P-1	
Density (calculated)	1.107 Mg/m^3	
F(000)	1384	
θ range for data collection	1.89 to 27.51°	
Completeness to θ = 27.51°	93.4 %	
Index ranges	$-17 \le h \le 18, -22 \le k \le 22, -23 , l \le 22$	
Data collection scan type	ω scans; 11 settings	
Reflections collected	75730	
Independent reflections	16451 [R_{int}= 0.0496]	
Absorption coefficient	0.064 mm^{-1}	
Absorption correction	None	
Max. and min. transmission	0.9905 and 0.9855	

Table 1 (cont.)

Structure solution and Refinement

Structure solution program	SHELXS-97 (Sheldrick, 2008)
Primary solution method	Direct methods
Secondary solution method	Difference Fourier map
Hydrogen placement	Geometric positions
Structure refinement program	SHELXL-97 (Sheldrick, 2008)
Refinement method	Full matrix least-squares on F^2
Data / restraints / parameters	16451 / 0 / 976
Treatment of hydrogen atoms	Riding
Goodness-of-fit on F^2	1.817
Final R indices [$I>2\sigma(I)$, 9925 reflections]	R1 = 0.0528, *w*R2 = 0.0721
R indices (all data)	R1 = 0.0981, *w*R2 = 0.0743
Type of weighting scheme used	Sigma
Weighting scheme used	$w=1/\sigma^2(Fo^2)$
Max shift/error	0.001
Average shift/error	0.000
Largest diff. peak and hole	0.443 and -0.396 e.Å^{-3}

Special Refinement Details

Crystals were mounted on a glass fiber using Paratone oil then placed on the diffractometer under a nitrogen stream at 100K.

There are two molecules in the asymmetric unit and each contains disorder common to t-butyl groups. A fully labeled figure is shown for molecule A only and the overlap of A and B is shown

Refinement of F^2 against ALL reflections. The weighted R-factor (*w*R) and goodness of fit (S) are based on F^2, conventional R-factors (R) are based on F, with F set to zero for negative F^2. The threshold expression of $F^2 > 2\sigma(F^2)$ is used only for calculating R-factors(gt) etc. and is not relevant to the choice of reflections for refinement. R-factors based on F^2 are statistically about twice as large as those based on F, and R-factors based on ALL data will be even larger.

All esds (except the esd in the dihedral angle between two l.s. planes) are estimated using the full covariance matrix. The cell esds are taken into account individually in the estimation of esds in distances, angles and torsion angles; correlations between esds in cell parameters are only used when they are defined by crystal symmetry. An approximate (isotropic) treatment of cell esds is used for estimating esds involving l.s. planes.

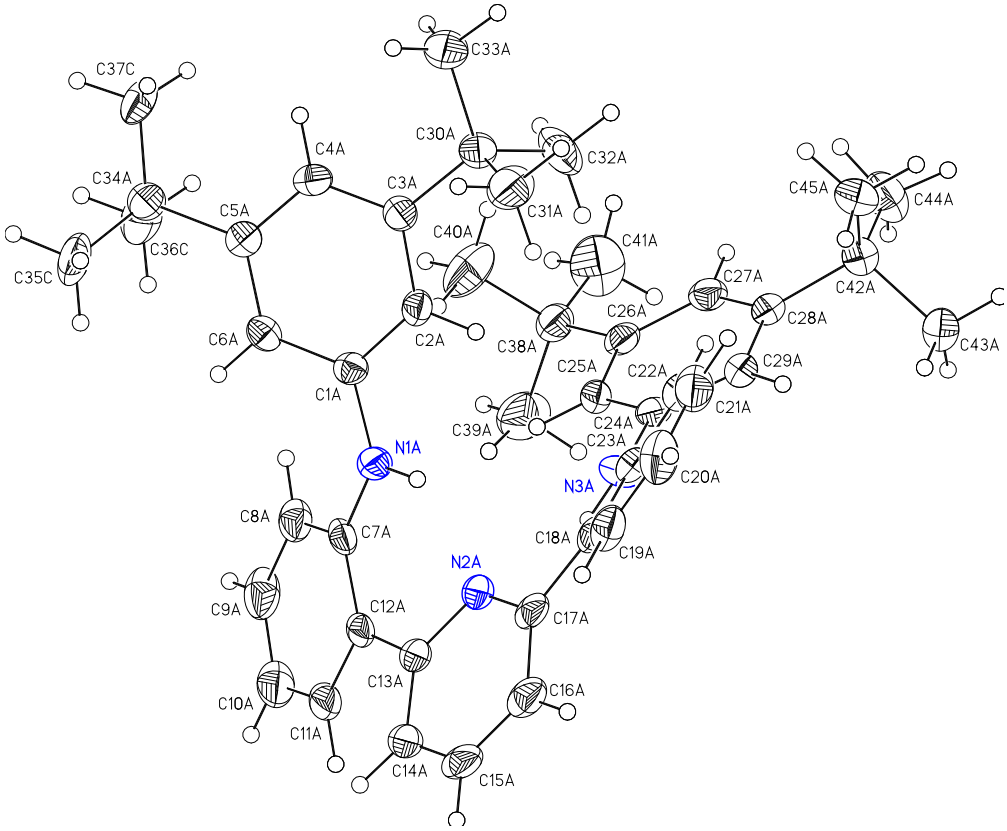
C33A
C37C
C30A
C4A
C32A
C34A
C3A
C31A
C45A
C44A
C5A
C40A
C41A
C27A
C36C
C35C
C42A
C26A
C28A
C6A
C2A
C38A
C43A
C25A
C22A
C29A
C1A
C24A
C21A
C39A
C23A
N1A
C20A
N3A
C8A
C7A
C18A
C19A
N2A
C9A
C12A
C17A
C13A
C16A
C10A
C11A
C14A
C15A

Table 2. Atomic coordinates (x 10^4) and equivalent isotropic displacement parameters ($Å^2$x 10^3) for ECW19 (CCDC 793156). U(eq) is defined as the trace of the orthogonalized U^{ij} tensor.

	x	y	z	U_{eq}	Occ
N(1A)	2376(1)	1612(1)	5813(1)	28(1)	1
N(2A)	3767(1)	32(1)	5856(1)	27(1)	1
N(3A)	4586(1)	322(1)	6898(1)	31(1)	1
C(1A)	1694(1)	2044(1)	6316(1)	24(1)	1
C(2A)	1932(1)	1728(1)	7122(1)	27(1)	1
C(3A)	1297(1)	2059(1)	7692(1)	26(1)	1
C(4A)	388(1)	2716(1)	7442(1)	27(1)	1
C(5A)	113(1)	3042(1)	6638(1)	26(1)	1
C(6A)	781(1)	2704(1)	6079(1)	25(1)	1
C(7A)	2550(1)	1907(1)	4962(1)	27(1)	1
C(8A)	2210(1)	2824(1)	4459(1)	34(1)	1
C(9A)	2368(1)	3112(1)	3612(1)	45(1)	1
C(10A)	2876(1)	2494(2)	3247(1)	50(1)	1
C(11A)	3248(1)	1592(1)	3738(1)	40(1)	1
C(12A)	3112(1)	1270(1)	4594(1)	28(1)	1
C(13A)	3566(1)	289(1)	5071(1)	29(1)	1
C(14A)	3797(1)	-365(1)	4740(1)	36(1)	1
C(15A)	4264(1)	-1261(1)	5206(1)	40(1)	1
C(16A)	4484(1)	-1509(1)	5998(1)	37(1)	1
C(17A)	4200(1)	-847(1)	6323(1)	29(1)	1
C(18A)	4317(1)	-1074(1)	7200(1)	28(1)	1
C(19A)	4229(1)	-1893(1)	7789(1)	37(1)	1
C(20A)	4273(1)	-2146(1)	8621(1)	44(1)	1
C(21A)	4376(1)	-1553(1)	8881(1)	41(1)	1
C(22A)	4468(1)	-733(1)	8318(1)	33(1)	1
C(23A)	4462(1)	-484(1)	7474(1)	27(1)	1
C(24A)	4744(1)	1004(1)	7023(1)	27(1)	1
C(25A)	4298(1)	1897(1)	6510(1)	28(1)	1
C(26A)	4411(1)	2615(1)	6587(1)	27(1)	1
C(27A)	4968(1)	2404(1)	7216(1)	30(1)	1
C(28A)	5439(1)	1521(1)	7729(1)	29(1)	1
C(29A)	5343(1)	821(1)	7611(1)	28(1)	1
C(30A)	1626(1)	1692(1)	8566(1)	36(1)	1
C(31A)	1911(1)	651(1)	8948(1)	57(1)	1
C(32A)	2528(1)	1949(1)	8513(1)	68(1)	1
C(33A)	817(1)	2070(1)	9138(1)	44(1)	1
C(34A)	-917(1)	3721(1)	6397(1)	39(1)	1
C(35A)	-1216(3)	4555(3)	6557(3)	40(1)	0.493(2)
C(36A)	-1735(2)	3184(2)	7025(2)	35(1)	0.493(2)
C(37A)	-1199(4)	3928(3)	5556(3)	41(1)	0.493(2)
C(35C)	-1378(3)	3455(3)	5973(3)	50(2)	0.507(2)
C(36C)	-642(3)	4634(2)	5677(2)	46(1)	0.507(2)
C(37C)	-1497(3)	4018(3)	7048(3)	51(1)	0.507(2)
C(38A)	3879(1)	3582(1)	6024(1)	32(1)	1
C(39A)	4132(1)	3696(1)	5116(1)	59(1)	1
C(40A)	2761(1)	3809(1)	6207(1)	59(1)	1
C(41A)	4159(2)	4289(1)	6125(1)	65(1)	1

C(42A)	6008(1)	1300(2)	8446(1)	38(1)	1
C(43A)	7066(3)	584(2)	8385(2)	40(1)	0.625(4)
C(44A)	6117(3)	2052(3)	8514(3)	50(1)	0.625(4)
C(45A)	5491(2)	758(3)	9284(2)	44(1)	0.625(4)
C(43C)	5181(4)	1729(5)	9038(3)	64(3)	0.375(4)
C(44C)	6562(6)	426(5)	8856(4)	60(2)	0.375(4)
C(45C)	6708(5)	1953(5)	8126(4)	53(2)	0.375(4)
N(1B)	2202(1)	7918(1)	6496(1)	29(1)	1
N(2B)	916(1)	9601(1)	5942(1)	27(1)	1
N(3B)	-349(1)	8848(1)	7182(1)	27(1)	1
C(1B)	2664(1)	7235(1)	7211(1)	26(1)	1
C(2B)	2167(1)	7260(1)	7958(1)	27(1)	1
C(3B)	2566(1)	6646(1)	8704(1)	31(1)	1
C(4B)	3492(1)	6004(1)	8675(1)	38(1)	1
C(5B)	4015(1)	5966(1)	7940(1)	34(1)	1
C(6B)	3595(1)	6590(1)	7204(1)	29(1)	1
C(7B)	2316(1)	7969(1)	5693(1)	28(1)	1
C(8B)	2770(1)	7199(1)	5508(1)	34(1)	1
C(9B)	2908(1)	7261(1)	4705(1)	42(1)	1
C(10B)	2587(1)	8088(1)	4066(1)	43(1)	1
C(11B)	2094(1)	8849(1)	4247(1)	36(1)	1
C(12B)	1934(1)	8825(1)	5047(1)	28(1)	1
C(13B)	1371(1)	9672(1)	5187(1)	27(1)	1
C(14B)	1307(1)	10525(1)	4570(1)	32(1)	1
C(15B)	733(1)	11285(1)	4735(1)	35(1)	1
C(16B)	253(1)	11204(1)	5508(1)	33(1)	1
C(17B)	376(1)	10339(1)	6115(1)	27(1)	1
C(18B)	-21(1)	10184(1)	6986(1)	27(1)	1
C(19B)	-44(1)	10777(1)	7319(1)	35(1)	1
C(20B)	-321(1)	10650(1)	8135(1)	43(1)	1
C(21B)	-564(1)	9884(1)	8656(1)	41(1)	1
C(22B)	-561(1)	9282(1)	8342(1)	33(1)	1
C(23B)	-317(1)	9425(1)	7514(1)	26(1)	1
C(24B)	-590(1)	8044(1)	7602(1)	24(1)	1
C(25B)	-8(1)	7308(1)	7394(1)	23(1)	1
C(26B)	-198(1)	6489(1)	7774(1)	23(1)	1
C(27B)	-975(1)	6439(1)	8378(1)	26(1)	1
C(28B)	-1586(1)	7173(1)	8591(1)	24(1)	1
C(29B)	-1396(1)	7987(1)	8176(1)	25(1)	1
C(30B)	5059(2)	5276(1)	7950(1)	45(1)	1
C(31B)	5098(6)	4366(5)	8479(5)	68(2)	0.708(9)
C(32B)	5750(5)	5608(5)	8207(4)	43(1)	0.708(9)
C(33B)	5498(3)	5328(4)	7052(3)	60(2)	0.708(9)
C(31D)	5140(9)	4773(10)	7365(7)	71(4)	0.292(9)
C(32D)	5140(14)	4357(12)	8859(9)	45(4)	0.292(9)
C(33D)	5822(13)	5554(13)	7868(14)	90(7)	0.292(9)
C(34B)	1969(1)	6710(1)	9506(1)	38(1)	1
C(35B)	2534(2)	6055(1)	10267(1)	69(1)	1
C(36B)	1007(1)	6532(1)	9586(1)	51(1)	1
C(37B)	1709(1)	7670(1)	9490(1)	53(1)	1
C(38B)	476(1)	5695(1)	7526(1)	26(1)	1
C(39B)	138(1)	4869(1)	7970(1)	41(1)	1
C(40B)	1534(1)	5420(1)	7745(1)	37(1)	1

C(41B)	479(1)	5977(1)	6593(1)	36(1)	1
C(42B)	-2401(1)	7060(1)	9292(1)	29(1)	1
C(43B)	-3081(1)	6664(1)	9156(1)	54(1)	1
C(44B)	-1906(1)	6412(1)	10104(1)	51(1)	1
C(45B)	-3042(1)	7941(1)	9394(1)	42(1)	1

Table 3. Bond lengths [Å] and angles [°] for ECW19 (CCDC 793156).

N(1A)-C(7A)	1.3864(19)	C(38A)-C(39A)	1.534(2)
N(1A)-C(1A)	1.405(2)	C(42A)-C(44C)	1.362(6)
N(2A)-C(17A)	1.3500(19)	C(42A)-C(44A)	1.439(4)
N(2A)-C(13A)	1.3535(19)	C(42A)-C(43A)	1.584(4)
N(3A)-C(23A)	1.3896(18)	C(42A)-C(45A)	1.598(3)
N(3A)-C(24A)	1.4117(18)	C(42A)-C(43C)	1.600(6)
C(1A)-C(2A)	1.390(2)	C(42A)-C(45C)	1.664(6)
C(1A)-C(6A)	1.393(2)	N(1B)-C(7B)	1.3850(19)
C(2A)-C(3A)	1.382(2)	N(1B)-C(1B)	1.4076(19)
C(3A)-C(4A)	1.392(2)	N(2B)-C(17B)	1.347(2)
C(3A)-C(30A)	1.537(2)	N(2B)-C(13B)	1.3471(19)
C(4A)-C(5A)	1.401(2)	N(3B)-C(23B)	1.3933(18)
C(5A)-C(6A)	1.390(2)	N(3B)-C(24B)	1.4173(17)
C(5A)-C(34A)	1.530(2)	C(1B)-C(2B)	1.387(2)
C(7A)-C(8A)	1.396(2)	C(1B)-C(6B)	1.393(2)
C(7A)-C(12A)	1.421(2)	C(2B)-C(3B)	1.386(2)
C(8A)-C(9A)	1.379(2)	C(3B)-C(4B)	1.391(2)
C(9A)-C(10A)	1.380(3)	C(3B)-C(34B)	1.534(2)
C(10A)-C(11A)	1.376(2)	C(4B)-C(5B)	1.385(2)
C(11A)-C(12A)	1.392(2)	C(5B)-C(6B)	1.388(2)
C(12A)-C(13A)	1.483(2)	C(5B)-C(30B)	1.533(2)
C(13A)-C(14A)	1.401(2)	C(7B)-C(8B)	1.394(2)
C(14A)-C(15A)	1.378(2)	C(7B)-C(12B)	1.426(2)
C(15A)-C(16A)	1.379(2)	C(8B)-C(9B)	1.377(2)
C(16A)-C(17A)	1.394(2)	C(9B)-C(10B)	1.380(2)
C(17A)-C(18A)	1.489(2)	C(10B)-C(11B)	1.378(2)
C(18A)-C(19A)	1.396(2)	C(11B)-C(12B)	1.391(2)
C(18A)-C(23A)	1.419(2)	C(12B)-C(13B)	1.482(2)
C(19A)-C(20A)	1.378(2)	C(13B)-C(14B)	1.399(2)
C(20A)-C(21A)	1.376(2)	C(14B)-C(15B)	1.380(2)
C(21A)-C(22A)	1.386(2)	C(15B)-C(16B)	1.385(2)
C(22A)-C(23A)	1.392(2)	C(16B)-C(17B)	1.395(2)
C(24A)-C(29A)	1.387(2)	C(17B)-C(18B)	1.488(2)
C(24A)-C(25A)	1.392(2)	C(18B)-C(19B)	1.390(2)
C(25A)-C(26A)	1.392(2)	C(18B)-C(23B)	1.419(2)
C(26A)-C(27A)	1.389(2)	C(19B)-C(20B)	1.376(2)
C(26A)-C(38A)	1.526(2)	C(20B)-C(21B)	1.386(2)
C(27A)-C(28A)	1.388(2)	C(21B)-C(22B)	1.390(2)
C(28A)-C(29A)	1.389(2)	C(22B)-C(23B)	1.387(2)
C(28A)-C(42A)	1.530(2)	C(24B)-C(25B)	1.387(2)
C(30A)-C(33A)	1.525(2)	C(24B)-C(29B)	1.389(2)
C(30A)-C(32A)	1.534(2)	C(25B)-C(26B)	1.4015(19)
C(30A)-C(31A)	1.546(2)	C(26B)-C(27B)	1.387(2)
C(34A)-C(35C)	1.436(5)	C(26B)-C(38B)	1.533(2)
C(34A)-C(37C)	1.447(4)	C(27B)-C(28B)	1.398(2)
C(34A)-C(35A)	1.481(4)	C(28B)-C(29B)	1.3946(19)
C(34A)-C(37A)	1.517(5)	C(28B)-C(42B)	1.532(2)
C(34A)-C(36C)	1.688(4)	C(30B)-C(33D)	1.35(2)
C(34A)-C(36A)	1.718(3)	C(30B)-C(31B)	1.437(8)
C(38A)-C(40A)	1.527(2)	C(30B)-C(33B)	1.575(4)
C(38A)-C(41A)	1.533(2)	C(30B)-C(32B)	1.586(8)

C(30B)-C(31D)	1.599(10)
C(30B)-C(32D)	1.711(17)
C(34B)-C(35B)	1.516(2)
C(34B)-C(36B)	1.531(2)
C(34B)-C(37B)	1.550(2)
C(38B)-C(39B)	1.5300(19)
C(38B)-C(40B)	1.534(2)
C(38B)-C(41B)	1.535(2)
C(42B)-C(45B)	1.518(2)
C(42B)-C(43B)	1.533(2)
C(42B)-C(44B)	1.537(2)

C(7A)-N(1A)-C(1A)	130.97(15)
C(17A)-N(2A)-C(13A)	120.85(16)
C(23A)-N(3A)-C(24A)	129.37(14)
C(2A)-C(1A)-C(6A)	118.90(17)
C(2A)-C(1A)-N(1A)	116.36(16)
C(6A)-C(1A)-N(1A)	124.54(16)
C(3A)-C(2A)-C(1A)	122.07(17)
C(2A)-C(3A)-C(4A)	117.96(16)
C(2A)-C(3A)-C(30A)	118.92(16)
C(4A)-C(3A)-C(30A)	123.12(16)
C(3A)-C(4A)-C(5A)	121.75(17)
C(6A)-C(5A)-C(4A)	118.50(16)
C(6A)-C(5A)-C(34A)	120.91(16)
C(4A)-C(5A)-C(34A)	120.53(17)
C(5A)-C(6A)-C(1A)	120.81(16)
N(1A)-C(7A)-C(8A)	121.19(17)
N(1A)-C(7A)-C(12A)	119.64(16)
C(8A)-C(7A)-C(12A)	119.14(17)
C(9A)-C(8A)-C(7A)	120.95(19)
C(8A)-C(9A)-C(10A)	120.3(2)
C(11A)-C(10A)-C(9A)	119.34(19)
C(10A)-C(11A)-C(12A)	122.44(19)
C(11A)-C(12A)-C(7A)	117.74(18)
C(11A)-C(12A)-C(13A)	118.47(17)
C(7A)-C(12A)-C(13A)	123.79(16)
N(2A)-C(13A)-C(14A)	119.82(18)
N(2A)-C(13A)-C(12A)	117.37(16)
C(14A)-C(13A)-C(12A)	122.81(17)
C(15A)-C(14A)-C(13A)	119.54(18)
C(14A)-C(15A)-C(16A)	119.95(18)
C(15A)-C(16A)-C(17A)	118.99(19)
N(2A)-C(17A)-C(16A)	120.72(17)
N(2A)-C(17A)-C(18A)	117.09(16)
C(16A)-C(17A)-C(18A)	122.14(18)
C(19A)-C(18A)-C(23A)	118.26(17)
C(19A)-C(18A)-C(17A)	118.06(16)
C(23A)-C(18A)-C(17A)	123.59(16)
C(20A)-C(19A)-C(18A)	122.66(17)
C(21A)-C(20A)-C(19A)	118.49(18)
C(20A)-C(21A)-C(22A)	120.81(18)
C(21A)-C(22A)-C(23A)	121.27(17)
N(3A)-C(23A)-C(22A)	122.17(16)
N(3A)-C(23A)-C(18A)	119.42(16)
C(22A)-C(23A)-C(18A)	118.41(16)
C(29A)-C(24A)-C(25A)	119.11(15)
C(29A)-C(24A)-N(3A)	123.20(16)
C(25A)-C(24A)-N(3A)	117.66(15)
C(24A)-C(25A)-C(26A)	121.83(16)
C(27A)-C(26A)-C(25A)	117.10(16)
C(27A)-C(26A)-C(38A)	123.27(16)
C(25A)-C(26A)-C(38A)	119.53(16)
C(28A)-C(27A)-C(26A)	122.62(16)
C(27A)-C(28A)-C(29A)	118.56(16)
C(27A)-C(28A)-C(42A)	122.02(16)
C(29A)-C(28A)-C(42A)	119.33(17)
C(24A)-C(29A)-C(28A)	120.59(16)
C(33A)-C(30A)-C(32A)	108.37(15)
C(33A)-C(30A)-C(3A)	112.52(15)
C(32A)-C(30A)-C(3A)	109.03(14)
C(33A)-C(30A)-C(31A)	108.04(15)
C(32A)-C(30A)-C(31A)	109.29(16)
C(3A)-C(30A)-C(31A)	109.53(15)
C(35C)-C(34A)-C(37C)	118.2(3)
C(35C)-C(34A)-C(35A)	131.7(3)
C(37C)-C(34A)-C(35A)	44.82(19)
C(35C)-C(34A)-C(37A)	36.40(19)
C(37C)-C(34A)-C(37A)	130.1(3)
C(35A)-C(34A)-C(37A)	111.3(3)
C(35C)-C(34A)-C(5A)	111.7(2)
C(37C)-C(34A)-C(5A)	113.1(2)
C(35A)-C(34A)-C(5A)	116.4(2)
C(37A)-C(34A)-C(5A)	116.6(2)
C(35C)-C(34A)-C(36C)	105.7(3)
C(37C)-C(34A)-C(36C)	104.6(3)
C(35A)-C(34A)-C(36C)	59.9(2)
C(37A)-C(34A)-C(36C)	69.3(2)
C(5A)-C(34A)-C(36C)	101.57(18)
C(35C)-C(34A)-C(36A)	66.6(2)
C(37C)-C(34A)-C(36A)	61.9(2)
C(35A)-C(34A)-C(36A)	104.3(2)
C(37A)-C(34A)-C(36A)	100.2(2)
C(5A)-C(34A)-C(36A)	105.75(17)
C(36C)-C(34A)-C(36A)	152.5(2)
C(26A)-C(38A)-C(40A)	110.15(14)
C(26A)-C(38A)-C(41A)	113.23(15)
C(40A)-C(38A)-C(41A)	107.33(16)
C(26A)-C(38A)-C(39A)	110.36(15)
C(40A)-C(38A)-C(39A)	108.57(15)
C(41A)-C(38A)-C(39A)	107.03(15)
C(44C)-C(42A)-C(44A)	122.6(3)
C(44C)-C(42A)-C(28A)	119.0(3)
C(44A)-C(42A)-C(28A)	116.6(2)
C(44C)-C(42A)-C(43A)	39.1(3)
C(44A)-C(42A)-C(43A)	109.5(2)
C(28A)-C(42A)-C(43A)	108.32(19)
C(44C)-C(42A)-C(45A)	64.4(3)

C(44A)-C(42A)-C(45A)	109.9(2)	C(23B)-C(22B)-C(21B)	121.58(16)
C(28A)-C(42A)-C(45A)	108.18(16)	C(22B)-C(23B)-N(3B)	122.36(15)
C(43A)-C(42A)-C(45A)	103.5(2)	C(22B)-C(23B)-C(18B)	118.73(16)
C(44C)-C(42A)-C(43C)	112.9(4)	N(3B)-C(23B)-C(18B)	118.92(16)
C(44A)-C(42A)-C(43C)	64.7(2)	C(25B)-C(24B)-C(29B)	120.06(14)
C(28A)-C(42A)-C(43C)	103.8(2)	C(25B)-C(24B)-N(3B)	117.35(15)
C(43A)-C(42A)-C(43C)	145.6(3)	C(29B)-C(24B)-N(3B)	122.53(15)
C(45A)-C(42A)-C(43C)	54.0(2)	C(24B)-C(25B)-C(26B)	121.12(16)
C(44C)-C(42A)-C(45C)	109.4(4)	C(27B)-C(26B)-C(25B)	117.29(16)
C(44A)-C(42A)-C(45C)	36.3(2)	C(27B)-C(26B)-C(38B)	123.79(14)
C(28A)-C(42A)-C(45C)	109.2(3)	C(25B)-C(26B)-C(38B)	118.89(15)
C(43A)-C(42A)-C(45C)	79.8(3)	C(26B)-C(27B)-C(28B)	122.99(15)
C(45A)-C(42A)-C(45C)	139.2(3)	C(29B)-C(28B)-C(27B)	117.92(16)
C(43C)-C(42A)-C(45C)	101.0(3)	C(29B)-C(28B)-C(42B)	121.63(15)
C(7B)-N(1B)-C(1B)	131.55(15)	C(27B)-C(28B)-C(42B)	120.37(14)
C(17B)-N(2B)-C(13B)	121.33(15)	C(24B)-C(29B)-C(28B)	120.45(16)
C(23B)-N(3B)-C(24B)	127.92(14)	C(33D)-C(30B)-C(31B)	120.6(9)
C(2B)-C(1B)-C(6B)	119.57(16)	C(33D)-C(30B)-C(5B)	117.1(7)
C(2B)-C(1B)-N(1B)	116.25(16)	C(31B)-C(30B)-C(5B)	112.8(4)
C(6B)-C(1B)-N(1B)	124.07(17)	C(33D)-C(30B)-C(33B)	79.6(8)
C(3B)-C(2B)-C(1B)	121.63(17)	C(31B)-C(30B)-C(33B)	110.2(3)
C(2B)-C(3B)-C(4B)	117.32(18)	C(5B)-C(30B)-C(33B)	111.37(19)
C(2B)-C(3B)-C(34B)	118.73(16)	C(33D)-C(30B)-C(32B)	23.4(9)
C(4B)-C(3B)-C(34B)	123.94(17)	C(31B)-C(30B)-C(32B)	112.9(4)
C(5B)-C(4B)-C(3B)	122.63(17)	C(5B)-C(30B)-C(32B)	106.2(3)
C(4B)-C(5B)-C(6B)	118.65(17)	C(33B)-C(30B)-C(32B)	102.9(3)
C(4B)-C(5B)-C(30B)	119.99(17)	C(33D)-C(30B)-C(31D)	116.0(7)
C(6B)-C(5B)-C(30B)	121.29(18)	C(31B)-C(30B)-C(31D)	73.1(5)
C(5B)-C(6B)-C(1B)	120.18(17)	C(5B)-C(30B)-C(31D)	109.1(4)
N(1B)-C(7B)-C(8B)	121.45(17)	C(33B)-C(30B)-C(31D)	42.5(5)
N(1B)-C(7B)-C(12B)	119.25(17)	C(32B)-C(30B)-C(31D)	137.9(5)
C(8B)-C(7B)-C(12B)	119.27(17)	C(33D)-C(30B)-C(32D)	107.6(11)
C(9B)-C(8B)-C(7B)	120.94(18)	C(31B)-C(30B)-C(32D)	23.6(6)
C(8B)-C(9B)-C(10B)	120.58(19)	C(5B)-C(30B)-C(32D)	108.4(6)
C(11B)-C(10B)-C(9B)	118.88(19)	C(33B)-C(30B)-C(32D)	130.1(5)
C(10B)-C(11B)-C(12B)	122.90(19)	C(32B)-C(30B)-C(32D)	93.5(6)
C(11B)-C(12B)-C(7B)	117.26(18)	C(31D)-C(30B)-C(32D)	96.5(6)
C(11B)-C(12B)-C(13B)	119.23(17)	C(35B)-C(34B)-C(36B)	109.44(16)
C(7B)-C(12B)-C(13B)	123.50(17)	C(35B)-C(34B)-C(3B)	112.94(16)
N(2B)-C(13B)-C(14B)	120.03(17)	C(36B)-C(34B)-C(3B)	109.22(15)
N(2B)-C(13B)-C(12B)	117.70(15)	C(35B)-C(34B)-C(37B)	106.41(16)
C(14B)-C(13B)-C(12B)	122.27(17)	C(36B)-C(34B)-C(37B)	108.71(15)
C(15B)-C(14B)-C(13B)	118.97(18)	C(3B)-C(34B)-C(37B)	110.01(14)
C(14B)-C(15B)-C(16B)	120.47(17)	C(39B)-C(38B)-C(26B)	112.10(14)
C(15B)-C(16B)-C(17B)	118.40(18)	C(39B)-C(38B)-C(40B)	108.19(13)
N(2B)-C(17B)-C(16B)	120.71(17)	C(26B)-C(38B)-C(40B)	109.43(13)
N(2B)-C(17B)-C(18B)	116.88(15)	C(39B)-C(38B)-C(41B)	108.30(13)
C(16B)-C(17B)-C(18B)	122.30(17)	C(26B)-C(38B)-C(41B)	109.79(14)
C(19B)-C(18B)-C(23B)	118.00(16)	C(40B)-C(38B)-C(41B)	108.96(13)
C(19B)-C(18B)-C(17B)	118.60(15)	C(45B)-C(42B)-C(28B)	113.12(13)
C(23B)-C(18B)-C(17B)	123.26(16)	C(45B)-C(42B)-C(43B)	107.85(15)
C(20B)-C(19B)-C(18B)	122.99(16)	C(28B)-C(42B)-C(43B)	111.15(14)
C(19B)-C(20B)-C(21B)	118.66(17)	C(45B)-C(42B)-C(44B)	107.41(15)
C(20B)-C(21B)-C(22B)	119.92(18)	C(28B)-C(42B)-C(44B)	108.22(14)

C(43B)-C(42B)-C(44B)	108.97(14)

Table 5. Hydrogen bonds for ECW19 (CCDC 793156) [Å and °].

D-H...A	d(D-H)	d(H...A)	d(D...A)	<(DHA)
N(1A)-H(1A)...N(2A)	0.88	1.96	2.690(2)	139.0
N(3A)-H(3A)...N(2A)	0.88	2.10	2.7575(18)	130.4
N(1B)-H(1B)...N(2B)	0.88	1.94	2.6732(19)	139.9
N(3B)-H(3B)...N(2B)	0.88	2.16	2.7660(18)	125.8

CALIFORNIA INSTITUTE OF TECHNOLOGY

BECKMAN INSTITUTE

X-RAY CRYSTALLOGRAPHY LABORATORY

Date 23 July 2010

Crystal Structure Analysis of:

[ONO]Fe(NC_5H_5)$_2$ (ECW17)

(shown below)

For Investigator: Ed Weintrob ext. 6576

Advisor: J. E. Bercaw ext. 6577

Account Number: JEB.ENERGY-1.02-GRANT.MOOREJCP

By Michael W. Day 116 Beckman ext. 2734

e-mail: mikeday@caltech.edu

Contents

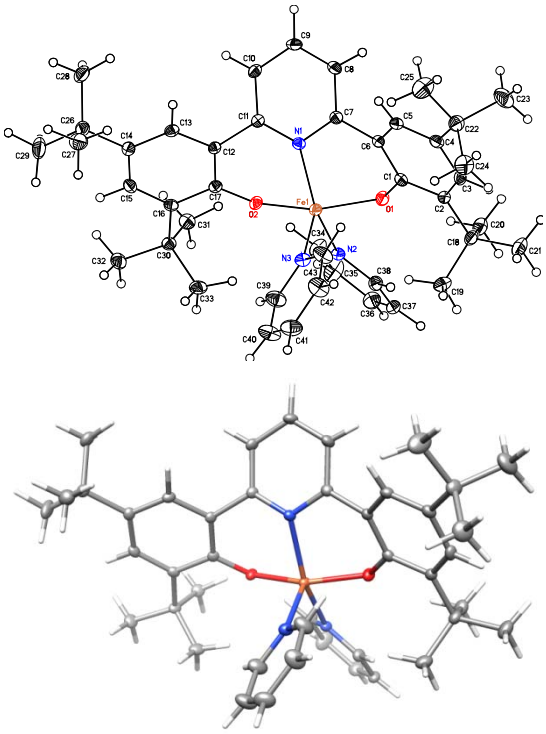

ECW17

Note: The crystallographic data have been deposited in the Cambridge Database (CCDC) and has been placed on hold pending further instructions from me. The deposition number is 785427. Ideally the CCDC would like the publication to contain a footnote of the type: "Crystallographic data have been deposited at the CCDC, 12 Union Road, Cambridge CB2 1EZ, UK and copies can be obtained on request, free of charge, by quoting the publication citation and the deposition number 785427."

Table 1. Crystal data and structure refinement for ECW17 (CCDC 785427).

Empirical formula	$C_{43}H_{53}N_3O_2Fe \bullet C_7H_8$
Formula weight	791.87
Crystallization Solvent	Toluene/*n*-heptane
Crystal Habit	Chunk
Crystal size	0.22 x 0.21 x 0.18 mm^3
Crystal color	Dark brown

Data Collection

Type of diffractometer	Bruker KAPPA APEX II	
Wavelength	0.71073 Å MoKα	
Data Collection Temperature	100(2) K	
θ range for 9221 reflections used in lattice determination	2.50 to 27.94°	
Unit cell dimensions	a = 15.8750(6) Å b = 28.4782(10) Å c = 9.7853(4) Å	α= 90° β= 90.514(2)° γ = 90°
Volume	4423.7(3) $Å^3$	
Z	4	
Crystal system	Monoclinic	
Space group	P $2_1/c$	
Density (calculated)	1.189 Mg/m^3	
F(000)	1696	
Data collection program	Bruker APEX2 v2009.7-0	
θ range for data collection	1.92 to 29.74°	
Completeness to θ = 29.74°	95.6 %	
Index ranges	$-21 \le h \le 22$, $-39 \le k \le 38$, $-12 \le l \le 13$	
Data collection scan type	ω scans; 12 settings	
Data reduction program	Bruker SAINT-Plus v7.66A	
Reflections collected	96663	
Independent reflections	12036 [R_{int}= 0.0514]	
Absorption coefficient	0.382 mm^{-1}	
Absorption correction	None	
Max. and min. transmission	0.9344 and 0.9206	

Table 1 (cont.)

Structure solution and Refinement

Structure solution program	SHELXS-97 (Sheldrick, 2008)
Primary solution method	Direct methods
Secondary solution method	Difference Fourier map
Hydrogen placement	Difference Fourier map
Structure refinement program	SHELXL-97 (Sheldrick, 2008)
Refinement method	Full matrix least-squares on F^2
Data / restraints / parameters	12036 / 0 / 749
Treatment of hydrogen atoms	Unrestrained
Goodness-of-fit on F^2	2.235
Final R indices [$I>2\sigma(I)$, 9399 reflections]	R1 = 0.0444, *w*R2 = 0.0613
R indices (all data)	R1 = 0.0614, *w*R2 = 0.0621
Type of weighting scheme used	Sigma
Weighting scheme used	$w=1/\sigma^2(Fo^2)$
Max shift/error	0.001
Average shift/error	0.000
Largest diff. peak and hole	0.804 and -0.672 e.Å^{-3}

Special Refinement Details

Crystals were mounted on a glass fiber using Paratone oil then placed on the diffractometer under a nitrogen stream at 100K.

Refinement of F^2 against ALL reflections. The weighted R-factor (*w*R) and goodness of fit (S) are based on F^2, conventional R-factors (R) are based on F, with F set to zero for negative F^2. The threshold expression of $F^2 > 2\sigma(F^2)$ is used only for calculating R-factors(gt) etc. and is not relevant to the choice of reflections for refinement. R-factors based on F^2 are statistically about twice as large as those based on F, and R-factors based on ALL data will be even larger.

All esds (except the esd in the dihedral angle between two l.s. planes) are estimated using the full covariance matrix. The cell esds are taken into account individually in the estimation of esds in distances, angles and torsion angles; correlations between esds in cell parameters are only used when they are defined by crystal symmetry. An approximate (isotropic) treatment of cell esds is used for estimating esds involving l.s. planes.

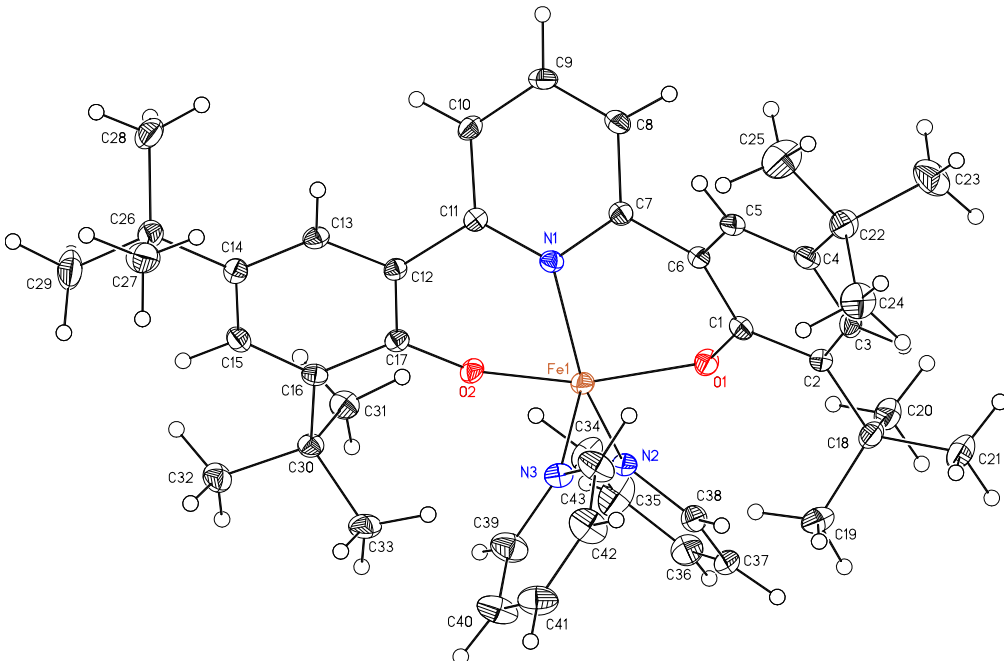
C9
C10
C8
C28
C25
C23
C26
C11
C7
C5
C22
C13
N1
C14
C6
C4
C29
C27
C12
C24
C1
C3
C15
C17
Fe1
O1
C2
C16
O2
C31
C34
C20
C18
N2
N3
C21
C32
C30
C43
C35
C38
C39
C33
C42
C19
C36
C37
C40
C41

Table 2. Atomic coordinates (x 10^4) and equivalent isotropic displacement parameters ($Å^2$x 10^3) for ECW17 (CCDC 785427). U(eq) is defined as the trace of the orthogonalized U^{ij} tensor.

	x	y	z	U_{eq}
Fe(1)	4229(1)	6372(1)	5559(1)	13(1)
O(1)	3041(1)	6269(1)	5136(1)	16(1)
O(2)	5275(1)	6724(1)	5651(1)	15(1)
N(1)	4539(1)	6184(1)	3431(1)	13(1)
N(2)	3797(1)	6837(1)	7263(1)	15(1)
N(3)	4495(1)	5708(1)	6507(1)	17(1)
C(1)	2725(1)	5940(1)	4309(1)	14(1)
C(2)	1969(1)	5694(1)	4627(1)	14(1)
C(3)	1705(1)	5340(1)	3748(2)	17(1)
C(4)	2132(1)	5206(1)	2562(1)	16(1)
C(5)	2837(1)	5462(1)	2239(2)	16(1)
C(6)	3140(1)	5830(1)	3072(1)	13(1)
C(7)	3876(1)	6088(1)	2575(1)	13(1)
C(8)	3901(1)	6217(1)	1196(2)	17(1)
C(9)	4608(1)	6422(1)	670(2)	18(1)
C(10)	5309(1)	6479(1)	1512(2)	15(1)
C(11)	5262(1)	6356(1)	2894(1)	12(1)
C(12)	6032(1)	6416(1)	3751(1)	12(1)
C(13)	6802(1)	6311(1)	3152(1)	14(1)
C(14)	7572(1)	6410(1)	3774(1)	14(1)
C(15)	7529(1)	6624(1)	5060(2)	16(1)
C(16)	6790(1)	6733(1)	5723(1)	13(1)
C(17)	6005(1)	6620(1)	5076(1)	12(1)
C(18)	1480(1)	5807(1)	5930(2)	18(1)
C(19)	2006(1)	5639(1)	7172(2)	22(1)
C(20)	1292(1)	6336(1)	6029(2)	22(1)
C(21)	632(1)	5552(1)	5999(2)	26(1)
C(22)	1802(1)	4798(1)	1683(2)	20(1)
C(23)	950(1)	4936(1)	1042(2)	32(1)
C(24)	1691(1)	4359(1)	2562(2)	27(1)
C(25)	2410(1)	4676(1)	528(2)	34(1)
C(26)	8399(1)	6289(1)	3072(1)	19(1)
C(27)	8502(1)	5756(1)	3020(2)	27(1)
C(28)	8401(1)	6487(1)	1610(2)	24(1)
C(29)	9165(1)	6498(1)	3828(2)	33(1)
C(30)	6813(1)	7003(1)	7091(1)	15(1)
C(31)	6460(1)	7497(1)	6842(2)	19(1)
C(32)	7711(1)	7061(1)	7661(2)	21(1)
C(33)	6305(1)	6751(1)	8193(2)	21(1)
C(34)	4135(1)	7264(1)	7435(2)	23(1)
C(35)	3834(1)	7586(1)	8369(2)	31(1)
C(36)	3159(1)	7471(1)	9169(2)	23(1)
C(37)	2801(1)	7033(1)	9008(2)	20(1)
C(38)	3134(1)	6730(1)	8049(2)	18(1)
C(39)	4977(1)	5672(1)	7646(2)	26(1)
C(40)	5114(1)	5254(1)	8309(2)	30(1)
C(41)	4746(1)	4851(1)	7827(2)	27(1)

C(42)	4260(1)	4879(1)	6644(2)	27(1)
C(43)	4159(1)	5308(1)	6033(2)	25(1)
C(51)	463(1)	6917(1)	7(2)	21(1)
C(52)	740(1)	6479(1)	417(2)	24(1)
C(53)	1305(1)	6427(1)	1509(2)	26(1)
C(54)	1600(1)	6819(1)	2178(2)	26(1)
C(55)	1335(1)	7260(1)	1778(2)	28(1)
C(56)	773(1)	7309(1)	689(2)	25(1)
C(57)	-171(1)	6973(1)	-1147(2)	31(1)

Table 3. Selected bond lengths [Å] and angles [°] for ECW17 (CCDC 785427).

Fe(1)-O(2)	1.9413(10)	O(2)-Fe(1)-O(1)	155.92(4)
Fe(1)-O(1)	1.9490(9)	O(2)-Fe(1)-N(3)	105.65(4)
Fe(1)-N(3)	2.1450(12)	O(1)-Fe(1)-N(3)	98.40(4)
Fe(1)-N(1)	2.2091(12)	O(2)-Fe(1)-N(1)	88.36(4)
Fe(1)-N(2)	2.2433(12)	O(1)-Fe(1)-N(1)	89.26(4)
		N(3)-Fe(1)-N(1)	98.64(4)
		O(2)-Fe(1)-N(2)	85.82(4)
		O(1)-Fe(1)-N(2)	86.82(4)
		N(3)-Fe(1)-N(2)	105.02(4)
		N(1)-Fe(1)-N(2)	156.33(4)

Table 4. Bond lengths [Å] and angles [°] for ECW17 (CCDC 785427).

Fe(1)-O(2)	1.9413(10)	C(21)-H(21A)	0.975(15)
Fe(1)-O(1)	1.9490(9)	C(21)-H(21B)	0.985(17)
Fe(1)-N(3)	2.1450(12)	C(21)-H(21C)	0.975(15)
Fe(1)-N(1)	2.2091(12)	C(22)-C(25)	1.532(2)
Fe(1)-N(2)	2.2433(12)	C(22)-C(24)	1.528(2)
O(1)-C(1)	1.3336(15)	C(22)-C(23)	1.536(2)
O(2)-C(17)	1.3255(16)	C(23)-H(23A)	0.992(17)
N(1)-C(11)	1.3589(17)	C(23)-H(23B)	1.011(16)
N(1)-C(7)	1.3659(15)	C(23)-H(23C)	0.968(15)
N(2)-C(34)	1.3386(19)	C(24)-H(24A)	0.958(16)
N(2)-C(38)	1.3442(19)	C(24)-H(24B)	0.996(16)
N(3)-C(43)	1.3402(18)	C(24)-H(24C)	0.972(15)
N(3)-C(39)	1.3493(17)	C(25)-H(25A)	0.995(15)
C(1)-C(6)	1.418(2)	C(25)-H(25B)	0.967(16)
C(1)-C(2)	1.4260(19)	C(25)-H(25C)	1.002(18)
C(2)-C(3)	1.3883(19)	C(26)-C(27)	1.528(2)
C(2)-C(18)	1.533(2)	C(26)-C(29)	1.538(2)
C(3)-C(4)	1.402(2)	C(26)-C(28)	1.538(2)
C(3)-H(3)	0.953(13)	C(27)-H(27A)	1.002(16)
C(4)-C(5)	1.375(2)	C(27)-H(27B)	1.021(14)
C(4)-C(22)	1.5369(19)	C(27)-H(27C)	0.951(16)
C(5)-C(6)	1.4081(19)	C(28)-H(28A)	0.975(16)
C(5)-H(5)	0.910(13)	C(28)-H(28B)	1.027(13)
C(6)-C(7)	1.468(2)	C(28)-H(28C)	0.941(15)
C(7)-C(8)	1.3989(19)	C(29)-H(29A)	0.972(16)
C(8)-C(9)	1.370(2)	C(29)-H(29B)	1.005(16)
C(8)-H(8)	0.931(13)	C(29)-H(29C)	1.047(17)
C(9)-C(10)	1.3870(18)	C(30)-C(32)	1.5343(19)
C(9)-H(9)	0.990(14)	C(30)-C(31)	1.532(2)
C(10)-C(11)	1.4000(19)	C(30)-C(33)	1.531(2)
C(10)-H(10)	0.967(13)	C(31)-H(31A)	1.063(15)
C(11)-C(12)	1.4854(16)	C(31)-H(31B)	0.952(15)
C(12)-C(13)	1.3932(19)	C(31)-H(31C)	0.988(14)
C(12)-C(17)	1.4213(18)	C(32)-H(32A)	1.020(15)
C(13)-C(14)	1.3892(17)	C(32)-H(32B)	0.982(15)
C(13)-H(13)	0.974(12)	C(32)-H(32C)	1.017(16)
C(14)-C(15)	1.3996(19)	C(33)-H(33A)	0.989(13)
C(14)-C(26)	1.527(2)	C(33)-H(33B)	0.941(16)
C(15)-C(16)	1.382(2)	C(33)-H(33C)	1.014(14)
C(15)-H(15)	0.954(12)	C(34)-C(35)	1.383(2)
C(16)-C(17)	1.4309(17)	C(34)-H(34)	0.976(16)
C(16)-C(30)	1.5437(19)	C(35)-C(36)	1.372(2)
C(18)-C(21)	1.532(2)	C(35)-H(35)	0.912(17)
C(18)-C(20)	1.539(2)	C(36)-C(37)	1.378(2)
C(18)-C(19)	1.544(2)	C(36)-H(36)	0.975(15)
C(19)-H(19A)	1.022(15)	C(37)-C(38)	1.382(2)
C(19)-H(19B)	0.980(16)	C(37)-H(37)	0.941(16)
C(19)-H(19C)	0.997(14)	C(38)-H(38)	0.968(14)
C(20)-H(20A)	0.975(14)	C(39)-C(40)	1.374(2)
C(20)-H(20B)	1.011(16)	C(39)-H(39)	1.005(14)
C(20)-H(20C)	0.986(15)	C(40)-C(41)	1.369(2)

C(40)-H(40)	0.926(15)	C(3)-C(4)-C(22)	120.27(13)
C(41)-C(42)	1.388(2)	C(4)-C(5)-C(6)	122.42(15)
C(41)-H(41)	0.966(15)	C(4)-C(5)-H(5)	121.5(9)
C(42)-C(43)	1.369(2)	C(6)-C(5)-H(5)	115.9(9)
C(42)-H(42)	0.918(15)	C(5)-C(6)-C(1)	119.92(14)
C(43)-H(43)	0.934(14)	C(5)-C(6)-C(7)	116.76(13)
C(51)-C(52)	1.380(2)	C(1)-C(6)-C(7)	123.31(13)
C(51)-C(56)	1.389(2)	N(1)-C(7)-C(8)	120.75(13)
C(51)-C(57)	1.515(2)	N(1)-C(7)-C(6)	120.54(12)
C(52)-C(53)	1.397(2)	C(8)-C(7)-C(6)	118.65(12)
C(52)-H(52)	0.938(14)	C(9)-C(8)-C(7)	120.24(13)
C(53)-C(54)	1.376(2)	C(9)-C(8)-H(8)	124.0(9)
C(53)-H(53)	0.961(15)	C(7)-C(8)-H(8)	115.7(9)
C(54)-C(55)	1.379(2)	C(8)-C(9)-C(10)	118.87(14)
C(54)-H(54)	0.920(14)	C(8)-C(9)-H(9)	119.9(8)
C(55)-C(56)	1.391(2)	C(10)-C(9)-H(9)	121.2(8)
C(55)-H(55)	0.936(14)	C(9)-C(10)-C(11)	119.67(14)
C(56)-H(56)	0.937(14)	C(9)-C(10)-H(10)	120.4(7)
C(57)-H(57A)	0.991(19)	C(11)-C(10)-H(10)	119.8(7)
C(57)-H(57B)	0.95(2)	N(1)-C(11)-C(10)	121.05(12)
C(57)-H(57C)	0.965(19)	N(1)-C(11)-C(12)	121.14(12)
		C(10)-C(11)-C(12)	117.80(12)
O(2)-Fe(1)-O(1)	155.92(4)	C(13)-C(12)-C(17)	120.38(12)
O(2)-Fe(1)-N(3)	105.65(4)	C(13)-C(12)-C(11)	117.27(12)
O(1)-Fe(1)-N(3)	98.40(4)	C(17)-C(12)-C(11)	122.02(13)
O(2)-Fe(1)-N(1)	88.36(4)	C(14)-C(13)-C(12)	122.92(13)
O(1)-Fe(1)-N(1)	89.26(4)	C(14)-C(13)-H(13)	119.1(8)
N(3)-Fe(1)-N(1)	98.64(4)	C(12)-C(13)-H(13)	118.0(8)
O(2)-Fe(1)-N(2)	85.82(4)	C(13)-C(14)-C(15)	115.67(13)
O(1)-Fe(1)-N(2)	86.82(4)	C(13)-C(14)-C(26)	120.89(13)
N(3)-Fe(1)-N(2)	105.02(4)	C(15)-C(14)-C(26)	123.44(12)
N(1)-Fe(1)-N(2)	156.33(4)	C(16)-C(15)-C(14)	124.64(13)
C(1)-O(1)-Fe(1)	126.31(9)	C(16)-C(15)-H(15)	120.4(8)
C(17)-O(2)-Fe(1)	127.98(9)	C(14)-C(15)-H(15)	115.0(8)
C(11)-N(1)-C(7)	118.94(11)	C(15)-C(16)-C(17)	118.78(13)
C(11)-N(1)-Fe(1)	118.23(8)	C(15)-C(16)-C(30)	120.44(12)
C(7)-N(1)-Fe(1)	116.69(9)	C(17)-C(16)-C(30)	120.65(13)
C(34)-N(2)-C(38)	116.65(14)	O(2)-C(17)-C(12)	120.81(12)
C(34)-N(2)-Fe(1)	120.36(11)	O(2)-C(17)-C(16)	121.55(12)
C(38)-N(2)-Fe(1)	122.55(10)	C(12)-C(17)-C(16)	117.54(13)
C(43)-N(3)-C(39)	116.24(13)	C(21)-C(18)-C(2)	112.85(13)
C(43)-N(3)-Fe(1)	121.55(10)	C(21)-C(18)-C(20)	106.88(14)
C(39)-N(3)-Fe(1)	122.15(11)	C(2)-C(18)-C(20)	110.95(13)
O(1)-C(1)-C(6)	119.87(13)	C(21)-C(18)-C(19)	106.64(14)
O(1)-C(1)-C(2)	121.69(13)	C(2)-C(18)-C(19)	108.41(13)
C(6)-C(1)-C(2)	118.44(13)	C(20)-C(18)-C(19)	111.04(13)
C(3)-C(2)-C(1)	118.12(14)	C(18)-C(19)-H(19A)	110.6(8)
C(3)-C(2)-C(18)	121.06(13)	C(18)-C(19)-H(19B)	109.6(9)
C(1)-C(2)-C(18)	120.78(12)	H(19A)-C(19)-H(19B)	106.2(12)
C(2)-C(3)-C(4)	124.36(14)	C(18)-C(19)-H(19C)	111.7(8)
C(2)-C(3)-H(3)	118.4(8)	H(19A)-C(19)-H(19C)	108.9(11)
C(4)-C(3)-H(3)	117.3(8)	H(19B)-C(19)-H(19C)	109.6(12)
C(5)-C(4)-C(3)	116.54(14)	C(18)-C(20)-H(20A)	111.9(8)
C(5)-C(4)-C(22)	123.18(14)	C(18)-C(20)-H(20B)	109.2(9)

H(20A)-C(20)-H(20B)	110.4(11)	H(29A)-C(29)-H(29B)	112.0(14)
C(18)-C(20)-H(20C)	110.8(9)	C(26)-C(29)-H(29C)	109.9(8)
H(20A)-C(20)-H(20C)	110.4(12)	H(29A)-C(29)-H(29C)	106.5(13)
H(20B)-C(20)-H(20C)	103.8(12)	H(29B)-C(29)-H(29C)	106.0(13)
C(18)-C(21)-H(21A)	112.7(9)	C(32)-C(30)-C(31)	107.27(13)
C(18)-C(21)-H(21B)	109.7(9)	C(32)-C(30)-C(33)	106.76(12)
H(21A)-C(21)-H(21B)	103.4(12)	C(31)-C(30)-C(33)	110.35(14)
C(18)-C(21)-H(21C)	112.3(9)	C(32)-C(30)-C(16)	112.52(13)
H(21A)-C(21)-H(21C)	110.9(12)	C(31)-C(30)-C(16)	108.24(11)
H(21B)-C(21)-H(21C)	107.2(13)	C(33)-C(30)-C(16)	111.62(12)
C(25)-C(22)-C(24)	107.86(16)	C(30)-C(31)-H(31A)	110.9(8)
C(25)-C(22)-C(4)	111.77(13)	C(30)-C(31)-H(31B)	113.0(9)
C(24)-C(22)-C(4)	110.13(12)	H(31A)-C(31)-H(31B)	106.6(12)
C(25)-C(22)-C(23)	108.36(14)	C(30)-C(31)-H(31C)	112.0(8)
C(24)-C(22)-C(23)	109.48(14)	H(31A)-C(31)-H(31C)	108.2(11)
C(4)-C(22)-C(23)	109.19(14)	H(31B)-C(31)-H(31C)	105.8(12)
C(22)-C(23)-H(23A)	111.6(9)	C(30)-C(32)-H(32A)	110.7(8)
C(22)-C(23)-H(23B)	112.8(8)	C(30)-C(32)-H(32B)	105.5(9)
H(23A)-C(23)-H(23B)	104.0(13)	H(32A)-C(32)-H(32B)	114.3(12)
C(22)-C(23)-H(23C)	108.9(9)	C(30)-C(32)-H(32C)	113.1(8)
H(23A)-C(23)-H(23C)	112.0(12)	H(32A)-C(32)-H(32C)	107.2(12)
H(23B)-C(23)-H(23C)	107.5(13)	H(32B)-C(32)-H(32C)	106.1(12)
C(22)-C(24)-H(24A)	113.4(9)	C(30)-C(33)-H(33A)	114.2(8)
C(22)-C(24)-H(24B)	110.7(9)	C(30)-C(33)-H(33B)	108.5(10)
H(24A)-C(24)-H(24B)	104.7(13)	H(33A)-C(33)-H(33B)	105.2(13)
C(22)-C(24)-H(24C)	111.5(10)	C(30)-C(33)-H(33C)	108.1(8)
H(24A)-C(24)-H(24C)	104.1(13)	H(33A)-C(33)-H(33C)	109.0(11)
H(24B)-C(24)-H(24C)	112.1(12)	H(33B)-C(33)-H(33C)	111.9(12)
C(22)-C(25)-H(25A)	112.6(9)	N(2)-C(34)-C(35)	122.97(17)
C(22)-C(25)-H(25B)	111.1(10)	N(2)-C(34)-H(34)	117.2(9)
H(25A)-C(25)-H(25B)	105.8(13)	C(35)-C(34)-H(34)	119.8(9)
C(22)-C(25)-H(25C)	106.9(10)	C(36)-C(35)-C(34)	119.68(18)
H(25A)-C(25)-H(25C)	106.9(13)	C(36)-C(35)-H(35)	123.9(11)
H(25B)-C(25)-H(25C)	113.6(13)	C(34)-C(35)-H(35)	116.4(12)
C(14)-C(26)-C(27)	109.41(14)	C(35)-C(36)-C(37)	118.31(17)
C(14)-C(26)-C(29)	112.06(13)	C(35)-C(36)-H(36)	120.4(10)
C(27)-C(26)-C(29)	108.45(14)	C(37)-C(36)-H(36)	121.3(10)
C(14)-C(26)-C(28)	110.11(12)	C(36)-C(37)-C(38)	118.76(17)
C(27)-C(26)-C(28)	109.43(14)	C(36)-C(37)-H(37)	122.8(10)
C(29)-C(26)-C(28)	107.33(14)	C(38)-C(37)-H(37)	118.3(10)
C(26)-C(27)-H(27A)	109.8(9)	N(2)-C(38)-C(37)	123.63(16)
C(26)-C(27)-H(27B)	111.4(8)	N(2)-C(38)-H(38)	116.2(9)
H(27A)-C(27)-H(27B)	113.4(12)	C(37)-C(38)-H(38)	120.1(9)
C(26)-C(27)-H(27C)	114.8(10)	N(3)-C(39)-C(40)	122.85(15)
H(27A)-C(27)-H(27C)	105.1(13)	N(3)-C(39)-H(39)	115.5(8)
H(27B)-C(27)-H(27C)	102.2(13)	C(40)-C(39)-H(39)	121.7(8)
C(26)-C(28)-H(28A)	110.7(9)	C(39)-C(40)-C(41)	119.93(15)
C(26)-C(28)-H(28B)	111.8(8)	C(39)-C(40)-H(40)	118.6(11)
H(28A)-C(28)-H(28B)	108.4(11)	C(41)-C(40)-H(40)	121.4(11)
C(26)-C(28)-H(28C)	108.7(9)	C(40)-C(41)-C(42)	118.13(16)
H(28A)-C(28)-H(28C)	106.4(13)	C(40)-C(41)-H(41)	123.4(9)
H(28B)-C(28)-H(28C)	110.7(11)	C(42)-C(41)-H(41)	118.4(9)
C(26)-C(29)-H(29A)	111.4(10)	C(43)-C(42)-C(41)	118.53(16)
C(26)-C(29)-H(29B)	110.9(9)	C(43)-C(42)-H(42)	122.9(9)

C(41)-C(42)-H(42)	118.6(9)
N(3)-C(43)-C(42)	124.29(14)
N(3)-C(43)-H(43)	114.9(10)
C(42)-C(43)-H(43)	120.8(10)
C(52)-C(51)-C(56)	118.42(14)
C(52)-C(51)-C(57)	121.40(16)
C(56)-C(51)-C(57)	120.18(16)
C(51)-C(52)-C(53)	121.25(16)
C(51)-C(52)-H(52)	119.9(9)
C(53)-C(52)-H(52)	118.7(9)
C(54)-C(53)-C(52)	119.49(16)
C(54)-C(53)-H(53)	122.1(9)
C(52)-C(53)-H(53)	118.4(9)
C(53)-C(54)-C(55)	120.12(15)
C(53)-C(54)-H(54)	117.7(10)
C(55)-C(54)-H(54)	122.1(10)
C(54)-C(55)-C(56)	120.06(17)
C(54)-C(55)-H(55)	121.9(9)
C(56)-C(55)-H(55)	118.0(9)
C(51)-C(56)-C(55)	120.64(16)
C(51)-C(56)-H(56)	121.0(8)
C(55)-C(56)-H(56)	118.4(8)
C(51)-C(57)-H(57A)	110.1(10)
C(51)-C(57)-H(57B)	110.1(12)
H(57A)-C(57)-H(57B)	110.9(16)
C(51)-C(57)-H(57C)	111.1(10)
H(57A)-C(57)-H(57C)	107.0(15)
H(57B)-C(57)-H(57C)	107.6(16)